DOCTOR OF PHILOSOPHY

Mapping protein-protein interactions in the Escherichia coli Twin Arginine Translocase

Moore, Kristoffer

Award date:
2016

Mapping protein-protein interactions in the *Escherichia coli* Twin Arginine Translocase

by

Kristoffer Moore

School of Life Sciences

August 2016

Thesis submitted to the University of Dundee in partial fulfilment of the requirements for the degree of Doctor of Philosophy

Declaration

I declare that I am the author of this thesis and that, unless otherwise stated, all references cited have been consulted; that the work of which this thesis is a record of has been performed by me, and that it has not been previously accepted for a higher degree: where the thesis is based upon joint research, the nature and extent of my individual contribution is defined.

Kristoffer Moore

Abstract

The Twin Arginine Translocase (Tat) system is a membrane-bound transport system present in plants and bacteria that has the remarkable ability to export fully folded proteins across a lipid bilayer, powered by the protonmotive force. In *Escherichia coli* the Tat system is composed of only three essential membrane proteins, the homologous TatA and TatB proteins, and the highly hydrophobic TatC core subunit. The transport mechanism involves a TatBC recognition complex which binds substrates through their signal peptides, with TatA being recruited to form an oligomeric structure that facilitates protein transport. Current models suggest that TatA oligomers locally disrupt membrane lipids allowing the substrate to move from the cytoplasm to the periplasm. Here, biochemical methods were used to further understand interactions between these components.

Affinity purification experiments in detergent solution, using a His-tagged TatC variant, resulted in co-purification of TatB along with a small amount of associated TatA. The amount of co-purifying TatA was notably increased when TatB was absent, suggesting that the proteins may compete for the same binding site on TatC.

Disulphide crosslinking experiments performed *in vivo* identified a binding site for TatA at the sixth transmembrane helix of TatC occupied in the resting state, indicating that TatA interacts constitutively with the TatBC recognition complex. Further crosslinking experiments found that the protonmotive force was required for TatA to occupy this constitutive site, explaining the poor yields of TatA co-purifying with TatC in detergent solution.

In response to increased substrate flux through the Tat pathway, disulphide crosslinking demonstrated that TatA no longer occupied its constitutive site, instead binding at the fifth transmembrane helix of TatC, a site previously shown to be occupied by TatB. This supports the proposition that TatA and TatB occupy this site differentially, with TatB potentially acting as a “gatekeeper” to modulate TatA polymerisation. Interaction sites were identified between the transmembrane regions of TatA and TatB when substrate was overexpressed.

Using these crosslinking data, a model was produced which presented interfaces between TatA, TatB and TatC in the resting state and how these change during interaction with a Tat substrate.

Table of Contents

Chapter 1: Introduction 1

1.1 *Escherichia coli* as a model organism 2

1.1.1 The *E. coli* cell envelope 2

1.1.2 Protein transport in *E. coli* 4

1.2 The Sec system 4

1.2.3 The SecB chaperone 5

1.2.4 The SecA ATPase 5

1.2.5 The SecYEG machinery: structures and mode of translocation 7

1.2.6 Powering movement of the Sec substrate across the membrane 11

1.3 Signal recognition particle (SRP) dependent protein transport 12

1.4 YidC-dependent membrane protein insertion 12

1.5 The discovery of the Tat protein transport system 13

1.6 Tat signal peptide 14

1.7 Tat Substrates 16

1.8 Tat proofreading 22

1.9 Tat quality control 24

1.10 The Tat machinery 25

1.10.1 The homologous TatA, TatB and TatE proteins 26

1.10.2 TatA and TatE 27

1.10.3 TatB 29

1.10.4 The TatC core 30

1.10.5 The TatBC recognition complex 33

1.10.6 The role of TatA 40

1.10.7 TatAC interactions 45

1.11 The Role of PMF 47

1.12 The Tat Transport Cycle 49

1.13 Aims of this Thesis 49

Chapter 2: Materials and methods 51

2.1 Bacterial strains 52

2.2 Materials 52

2.2.1 Growth Conditions 52

2.2.2 Scoring Tat-dependent anaerobic growth on TMAO/glycerol media 52
2.2.3 Scoring Tat-dependent growth on media containing 2% SDS 53
2.3 Molecular Biology Techniques 55
2.3.1 Preparation of component cells 55
2.3.2 Transformation of competent cells 55
2.3.4 Plasmid DNA preparation 56
2.3.5 DNA Quantification 65
2.3.6 DNA amplification using Polymerase Chain Reaction (PCR) 65
2.3.7 QuikChange site directed mutagenesis 66
2.3.8 Agarose gel electrophoresis of DNA 66
2.3.9 DNA Digestion 67
2.3.10 DNA ligation 68
2.4 Protein methods 69
2.4.1 SDS PAGE 69
2.4.2 Western Blotting 70
2.4.3 Cell fractionation and isolation of membranes 71
2.4.4 Periplasmic preparation of *E. coli* 72
2.4.5 Determining protein concentration of membrane fractions 72
2.4.6 Detergent solubilisation of membrane fractions 72
2.4.7 Nickel affinity co-purification assay 73
2.4.8 *In vivo* disulphide crosslinking of proteins from a medium copy number construct 74
2.4.9 *In vivo* disulphide crosslinking from a medium copy number construct with overexpressed substrate 74
2.4.10 *In vivo* disulphide crosslinking at very low copy number with and without overexpressed substrate 75
2.4.11 *In vivo* disulphide crosslinking with indole as an uncoupler 75

Chapter 3: TatA is loosely associated with the TatBC recognition complex 77
3.1 Introduction 78
3.1.1 Proposed interactions between TatA and TatBC 78
3.1.2 Previous purification of Tat complexes 78
3.1.3 Detergents used in this work 80
3.2 Aims 82
3.3 Results 83

3.3.1 A Tat(A)BC$_{His}$ complex can be purified after solubilisation in 1% digitonin 83
3.3.2 TatA-TatC$_{His}$ interactions are potentially enhanced in the absence of TatB when analysed using digitonin as detergent 84
3.3.3 A TatB and TatC$_{His}$ complex can be purified after solubilisation in 1% $C_{12}E_9$, with no associated TatA 85
3.3.4 Trace amounts of TatA can be co-purified with TatC$_{His}$ after $C_{12}E_9$ solubilisation when TatB is absent 86
3.3.5 Using the TatC D211A substitution as a tool to examine TatA-TatC interactions 87
3.3.6 The TatC$_{His}$ D211A substitution impairs Tat transport 87
3.3.7 The TatC$_{His}$ D211A substitution causes detergent-dependent dissociation of TatB and stabilisation of TatA-TatC interactions 89
3.3.8 Tat(A)BC$_{His}$ can be purified using 1% digitonin but not 1% $C_{12}E_9$ when proteins are expressed from a very low copy number vector 91
3.4 Discussion 93
3.4.1 TatA is weakly associated with TatC in the Tat(A)BC complex 93
3.4.2 Choice of detergent is important: A Tat(A)BC complex can be purified with but digitonin not $C_{12}E_9$ 93
3.4.3 A potential step in the Tat cycle: TatB dissociation from TatC promotes TatA-TatC interactions 94
3.4.4 The D211A substitution in TatC destabilises TatB-TatC interactions but still supports TatA-TatC interactions 95

Chapter 4: TatA interacts with TatC at the periplasmic facing region of TM6 *in vivo* 97

4.1 Introduction 98
4.1.1 Utilising crosslinking to dissect protein interactions in the Tat system 98
4.1.2 Crosslinking the *E. coli* Tat subunits *in vitro* and *in vivo* 102
4.1.3 TatA and TatC Cys substitutions chosen in this work 103
4.2 Aims 105
4.3 Results 106
4.3.1 The *in vivo* disulphide cross-linking protocol used in this study is not lethal to *E. coli* cells 106
4.3.2 Cys substitutions used in this work do not abolish Tat activity 107
4.3.3 TatA-TatC disulphide crosslinking *in vivo* 108

4.3.3.1 TatA L9C crosslinks TatC F213C at TM6 *in vivo* 108
4.3.3.2 TatA L10C crosslinks TatC V212C *in vivo* 113
4.3.3.3 TatA I11C crosslinks with TatC V212C and F213C *in vivo* 117
4.4 Discussion 121
4.4.1 TatA interacts with TatC TM6 and the extreme N-terminus of the P3 loop *in vivo* 121

Chapter 5: TatA occupies a constitutive binding site at TatC TM6, moving to occupy TatC TM5 in response to substrate overexpression 124

5.1 Introduction 124
5.1.1 Identifying further TatA interaction sites on TatC 125
5.1.2 Potential changes in TatA-TatC interactions in the absence of TatB 125
5.1.3 The influence of substrate expression and PMF on TatA-TatC interactions 126
5.2 Aims 127
5.3 Results 128
5.3.1 TatA L9C crosslinks both TatC TM5 and TM6 *in vivo* in the absence of TatB, with weaker interactions at P210C in the P3 loop 128
5.3.2 TatA L10C interacts with TatC TM5 in the absence of TatB 132
5.3.3 TatA I11C crosslinks TatC TM5, V213C and F213C in the absence of TatB *in vivo* 136
5.3.4 Mapping TatA-TatC interactions in the absence of TatB *in vivo* 139
5.3.5 The TatA interaction site at TatC TM6 *in vivo* is occupied in the absence of substrate binding 141
5.3.6 TatA-TatC interactions during substrate binding/translocation 143
5.3.7 TatA moves from its constitutive site at TM6 to the TatB constitutive site at TM5 in response to overexpressed substrate 144
5.3.7.1 Induction of substrate expression with L-arabinose does not impair cell growth during 20 min incubation phase 145
5.3.7.2 TatA L9C crosslinks to TatC F213C at the proposed constitutive interactions site for TatA decrease with substrate overexpression 145
5.3.7.3 TatA L9C crosslinks to TatC M205C at the TatB constitutive interactions site at TatC TM5 increase with substrate overexpression 147
5.3.7.4 TatA homodimerisation through TatA L9C increases in

response to overexpressed substrate 148
5.3.7.5 The presence of substrate is linked to the decreased TatA interactions through L9C with TatC F213C 149
5.3.8 TatA-TatC crosslinks at TatC TM6 are not detected *in vivo* when the PMF is dissipated 150
5.3.9 TatA-TatC crosslinks at TatC TM6 are disrupted *in vitro* in isolated membrane fractions 154
5.4 Discussion 156
5.4.1 TatA has constitutive binding site at TatC TM6 *in vivo* 156
5.4.2 TatA is able to occupy the TatB constitutive site when TatB is absent and during substrate binding and/or transport 157
5.4.3 Elucidating the role of PMF in the Tat system 160
5.4.4 Linking the role of TatA to the TatA-TatC disulphide crosslinks observed in this Chapter 161

Chapter 6: TatA crosslinks to TatC are validated with low copy number expression, with TatA and TatB interactions observed in the presence of substrate 163

6.1 Introduction 164
6.1.1 TatA-TatC crosslinks identified from disulphide crosslinking of TatA to a Cys scanning region of TatC 164
6.1.2 Copy number and substrate overexpression in studying the Tat system 165
6.1.3 Identifying TatA-TatB interactions 166
6.2 Aims 167
6.3 Results 168
6.3.1 Cys substitutions used in this work do not abolish Tat activity 168
6.3.2 TatA maintains interactions at TatC TM6 with protein expression at a low copy number 169
6.3.2.1 TatA L9C interacts with TatC F213C at TatC TM6 *in vivo* with expression from low copy number constructs 169
6.3.2.2 No crosslinks are observed through TatA L9C, L10C or I11C to TatC V212C *in vivo* with expression from low copy number constructs 172

6.3.3 TatA L9, L10 and I11 do not associate with M205C or L206C in TatC TM5 *in vivo* at low copy number expression 173

6.3.4 TatA interacts constitutively with TatC TM6 with low copy number expression 175

6.3.4.1 TatA L9C crosslinks TatC F213C the TM6 in the resting state *in vivo* 176

6.3.4.2 TatA L9C does not crosslink TatC M205C in TM5 *in vivo* in the resting state 177

6.3.5 TatA vacates its constitutive site at TatC TM6 and moves to TM5 at low copy number expression in the presence of overexpressed substrate 178

6.3.5.1 TatA L9C crosslinks to TatC F213C at TatC TM6 are greatly decreased with low copy number protein expression and overexpressed substrate 179

6.3.5.2 TatA L9C, L10C and I11C do not crosslink TatC V212C with low copy number in the presence of overexpressed substrate 181

6.3.5.3 TatA crosslinks through L9C, L10C and I11C to M205C appear at low copy number in the presence of overexpressed substrate 181

6.3.5.4 TatA does not crosslink through L9C, L10C or I11C to L206C with low copy number expression and overexpressed substrate 184

6.3.6 TatA vacates its constitutive binding site on TatC in response to PMF dissipation with indole with expression from low copy number vectors 185

6.3.6.1 The TatA L9C crosslink to TatC F213C at TM6 is greatly diminished after PMF dissipation *in vivo* 186

6.3.6.2 TatA L9C does not crosslink TatC M205C after PMF dissipation *in vivo* 187

6.3.7 Assessing TatA-TatB interactions by disulphide crosslinking *in vivo* 188

6.3.7.1 TatA L9C does not crosslink to TatB L9C, L10C or L11C *in vivo* with endogenous substrate levels 189

6.3.7.2 TatA L10C does not crosslink to TatB L9C, L10C or L11C *in vivo* with endogenous substrate levels 190

6.3.7.3 TatA I11C does not crosslink to TatB L9C, L10C or L11C *in vivo* with endogenous substrate levels 192

6.3.7.4 Summary of TatA-TatB crosslinks *in vivo* with low copy number expression and endogenous substrate 193

6.3.8 TatA-TatB interactions are observed *in vivo* with overexpressed substrate 193

6.3.8.1 TatA L9C crosslinks TatB L11C *in vivo* with overexpressed CueOH substrate 195
6.3.8.2 TatA L10C does not crosslink TatB L9C, L10C or L11C *in vivo* with overexpressed CueOH substrate 197
6.3.8.3 TatA I11C crosslinks TatB L11C *in vivo* with overexpressed CueOH substrate 197
6.3.9 TatA and TatB are able to interact following PMF dissipation, suggesting that TatA does not leave the Tat complex 199
6.4 Discussion 201
6.4.1 Mapping constitutive interactions between TatA and TatB with TatC informed by crosslinking proteins at low copy number expression 201
6.4.2 TatA and TatB swap sites during transport 203
6.4.3 PMF dissipation and the effect of Tat interactions 211
Chapter 7: Conclusion and perspectives 213
7.1 Building a model of the membrane-bound resting Tat complex 214
7.2 Subunit rearrangement during Tat export 219
7.3 An updated Tat cycle 220
7.4 Perspectives 222

Table of Figures

Figure 1.1) The typical cell envelope of a Gram-negative bacterium 2
Figure 1.2) Crystal structure of the open conformation of *Thermotoga maritima* SecA 5
Figure 1.3) Crystal structures of SecYEG/SecYEβ complexes showing helix rearrangements proposed to occur during substrate translocation 7
Figure 1.4) Crystal structure of *E. coli* SecA bound to the SecYE complex, with a translocating peptide 9
Figure 1.5) A comparison of the powerstroke and ratcheted diffusion model of polypeptide translocation 10
Figure 1.6) A schematic comparison of the Sec and Tat signal peptides 14
Figure 1.7) Diagram showing chaperone binding to a Tat substrate 22
Figure 1.8) *E. coli tat* genes 24
Figure 1.9) Solution NMR structures of homologous TatA and TatB with alignment of *E. coli* TatA family proteins 26
Figure 1.10) Solution NMR structures of TatA with transport-defective residues highlighted 27
Figure 1.11) Solution NMR ensemble structures TatB 28
Figure 1.12) Crystal structure of *Aquifex aeolicus* TatC 30
Figure 1.13) 3D maps of $TatBC_{His}$ recognition complex from single-particle electron microscopy 33
Figure 1.14) Homology structures of *E. coli* TatC highlighting residues important for signal peptide and TatB binding 35
Figure 1.15) Summary of proposed TatB-C interactions in the recognition complex 38
Figure 1.16) Low resolution electron microscopy structures of TatA oligomer 41
Figure 1.17) Higher resolution proposed arrangements of the TatA complex 42
Figure 1.18) Diagram of proposed TatA orientations that cause membrane thinning and subsequent substrate translocation 44
Figure 1.19) Proposed TatA-TatC interactions in bacteria and plants 45
Figure 1.20) Model of Tat transport 48
Fig. 3.1) Detergents used in this work 81
Figure 3.2) Western blot analysis of Ni affinity-purified $TatABC_{His}$ 82
Figure 3.3) Western blot analysis of Ni affinity-purified $TatAC_{His}$ and $TatBC_{His}$ 83
Figure 3.4) Western blot analysis of Ni affinity-purified $TatABC_{His}$ 84
Figure 3.5) Western blot analysis of Ni affinity-purified $TatAC_{His}$ and $TatBC_{His}$ 85
Figure 3.6) Growth assays to test for the presence of an active Tat system with the TatC substitution D211A 87
Figure 3.7) Western blot analysis of Ni affinity-purified $TatABC_{His}$ 88
Figure 3.8) Western blot analysis of Ni affinity-purified $TatABC_{His}$D211A 89
Figure 3.9) Western blot analysis of Ni affinity-purified $TatABC_{His}$ produced at a very low copy number 91
Fig. 4.1) Mechanisms behind maleimide, DSS and formaldehyde crosslinking 98
Fig. 4.2) Mechanisms behind disulphide and photo-crosslinking 100

Figure 4.3) Residues substituted to Cys in TatA and TatC 103
Figure 4.4) Colony forming units of *E. coli* recovered with and without copper phenanthroline exposure 105
Figure. 4.5) TatA L9C interacts with TatC F213C *in vivo* 108
Figure. 4.6) TatA L10C interacts with TatC V212C *in vivo* 113
Figure. 4.7) TatA I11C interacts with TatC V212C and F213C *in vivo* 117
Figure 4.8) Diagram showing crosslinks between TatA and TatC in this work, along with the proposed placement of TatB from previous studies 120
Figure 5.1) TatA L9C interacts with TatC TM5/TM6 and weakly at P3 in the absence of TatB *in vivo* 128
Figure 5.2) TatA-TatC heterodimer through TatA L9C and TatC TM5/TM6 can be detected on anti-TatA Western blots in the absence of TatB 131
Figure 5.3) TatA L10C interacts with TatC TM5 and weakly at P3 in the absence of TatB *in vivo* 133
Fig. 5.4) TatA-TatC heterodimer formed through TatA L10C and TatC TM5 cannot be detected on anti-TatA Western blots in the absence of TatB 135
Figure 5.5) TatA I11C interacts with TatC TM5/TM6 and weakly at P3 in the absence of TatB *in vivo* 137
Fig. 5.6) TatA-TatC heterodimer through TatA I11C and TatC TM5 can be detected on anti-TatA Western blots in the absence of TatB 139
Figure 5.7) Diagram showing crosslinks between TatA and TatC in the absence of TatB 140
Figure 5.8) TatA L9C interacts with TatC F213C in the absence of substrate binding 142
Figure 5.9) Growth of DADE-P is not affected during incubation with L-arabinose 145
Figure 5.10) The TatA-TatC heterodimer intensity at TatC TM6 decreases as Tat substrate level is increased 146
Figure 5.11) The TatA-TatC heterodimer intensity increases at TM5 as Tat substrate level is increased 148
Figure 5.12) TatA homodimerisation through TatA L9C increases as Tat substrate level is increased 149
Figure 5.13) L-arabinose alone does not affect the TatA L9C TatC F213C crosslink 150
Figure 5.14) TatA vacates its constitutive site at TatC TM6 in response to PMF dissipation 151
Figure 5.15) TatA L9C does not crosslink with TatC M205C when the PMF is dissipated 153
Figure 5.16) TatA L9C crosslinks to TatC M205C but not F213C *in vitro* 155
Figure 5.17) Proposed conformational change of TatA as it moves from TatC TM6 to TM5 159
Figure 5.18) Proposed movements of TatA in response to substrate overexpression 160
Figure 6.1) Residues on TatC proposed to interact with TatA through two different sites 165
Figure 6.2) TatA and TatB residues which will be examined for interactions *via* disulphide crosslinking 167

Figure 6.3) TatA L9C interacts with F213C *in vivo* 170
Figure 6.4) TatA L9C, L10 and I11 do not interact with V212C *in vivo* 172
Figure 6.5) TatA L9C, L10 and I11 do not interact withM205C *in vivo* 174
Figure 6.6) TatA L9C, L10 and I11 do not interact with L206C *in vivo* 175
Figure 6.7) TatA L9C crosslinks with TatC F94A, E103A, F213C when expressed from low copy number vectors 177
Figure 6.8) TatA L9C does not crosslink with TatC F94A, E103A, F213C at low copy number expression 178
Figure 6.9) TatA L9C, L10 and I11 do not interact with F213C *in vivo* with overexpressed CueOH 180
Figure 6.10) TatA L9C, L10 and I11 do not interact with V212C *in vivo* with overexpressed CueOH 182
Figure 6.11) TatA L9C and I11 interact favourably with TatC M205C while TatA L10C interacts weakly *in vivo* with overexpressed CueOH 183
Figure 6.12) TatA L9C, L10 and I11 do not interact with TatCL206C *in vivo* with overexpressed CueOH 185
Figure 6.13) TatA vacates its constitutive site at TatC TM6 in response to PMF dissipation with 5 mM indole 187
Figure 6.14) TatA does not interact with TatC TM5 in response to PMF dissipation with 5 mM indole 188
Figure 6.15) TatA L9C does not interact with TatB L9C, L10C or L11C *in vivo* with endogenous substrate 189
Figure 6.16) TatA L10C does not interact with TatB L9C, L10C or L11C *in vivo* with endogenous substrate 191
Figure 6.17) TatA I11C does not interact with TatB L9C, L10C or L11C *in vivo* with endogenous substrate 192
Figure 6.18) TatA L9C interacts with TatB L11C *in vivo* with overexpressed substrate 194
Figure 6.19) TatA L10C does not interact with TatB L9C, L10C or L11C *in vivo* with overexpressed substrate 196
Figure 6.20) TatA I11C interacts with TatB L11C *in vivo* with overexpressed substrate 198
Figure 6.21) TatA L9C interacts with TatB L11C in response to PMF dissipation with 5 mM indole 200
Figure 6.22) Crosslinking data from Johann Habersetzer shows TatB interacting with TatC TM5 in the resting state 202
Figure 6.23) Proposed TatA and TatB interactions with TatC in the resting state based on crosslinking 203
Figure 6.24) Western blots to show movement of TatB from TatC TM5 to TM6 in response to Tat substrate overexpression 204
Fig. 6.25) A proposed arrangement of Tat subunits to satisfy heterodimerisation of Tat subunits through *in vivo* crosslinking experiments performed with overexpressed substrate 208

Fig. 6.26) A proposed arrangement of Tat subunits to satisfy heterodimerisation of Tat subunits through *in vivo* crosslinking experiments performed with overexpressed substrate 209
Figure 6.27) TatB occupies both TatC TM5 and TM6 after PMF dissipation with chemical uncouplers 212
Figure 7.1) Schematic organisation of tetrameric and trimeric Tat complexes viewed from the periplasm 215
Figure 7.2) Model of tetrameric resting state Tat system 217
Figure 7.3) Model of trimeric resting state Tat system 218
Figure 7.4) Updated Model of Tat transport 221

Table of Tables

Table 1.1) Substrates of the Tat system in *E. coli* 18
Table 2.1) *E. coli* strains used in this work 51
Table 2.2) Composition of growth media used in this work 52
Table 2.3) List of antibiotics used in this study 53
Table 2.4) List of growth supplements used in this work 53
Table 2.5) Composition of buffers and solutions utilised in this work 53
Table 2.6) Plasmids used and constructed in this study 56
Table 2.7) The steps programmed in the PCR cycle during the QuikChange experiment 64
Table 2.8) The composition of the QuikChange PCR mix used 64
Table 2.9) Primers used in this work 66
Table 2.10) Components of the resolving and stacking gel used to produce polyacrylamide gels for SDS-PAGE 68
Table 2.11) List of antibodies in this study used for Western blots 70
Table 4.1) Cys substitutions in TatA and TatC do not abolish Tat activity 106
Table 6.1) Cys substitutions in TatA, TatB and TatC do not abolish Tat activity 168
Table 6.2) Cys positions of residues which form heterodimers between TatA, Tat and TatC 207

Abbreviations

Å	ångström (10^{-10} m; 0.1 nm)
aa	amino acids
ADP	adenosine diphosphate
Amp	ampicillin
AMS	4-acetamido-4'-maleimidylstilbene-2,2'-disulfonic acid
AP/H	amphipathic/helix
APS	ammonium persulfate
ATP	adenosine triphosphate
bp	base pair(s)
BN	blue native
Bpa	*p*-benzoyl-phenylalanine
BSA	bovine serum albumine
C	cytoplasmic domain
CCCP	carbonylcyanide m-chlorophenylhydrazone
Cml	chloramphenicol
C-terminal	carboxy terminal
C-terminus	caboxy terminus
CuP	copper phenanthroline
Da	Dalton
DMSO	dimethyl sulphoxide
DNA	deoxyribonucleic acid
DNase	deoxyribonuclease
dNTP	deoxynucleoside triphosphate
DTT	dithiotreitol
EDTA	ethylenediamine tetraacetate
Ffh	forty-four homologue
x *g*	relative centrifugal force in multiples of standard gravity
g	gram
GFP	green fluorescent protein
GTP	guanosine triphosphate
HRP	horse radish peroxidase
HSD	helical scaffold domain
HWD	helical wing domain
IM	inner membrane
IMAC	immobilised metal affinity chromatography
INV	inner membrane vesicle
IPTG	Isopropyl β-D-1-thiogalactopyranoside
Kan	Kanamycin
kb	kilobase pairs (1000 bp)
kDa	kilo Daltons
l	litre
LB	Luria and Bertani (medium)
LMNG	lauryl maltose neopentyl glycol
LPS	lipopolysaccharide
µ	micro
M	molar
m	milli
MALLS	multi-angle laser light scattering
mTT	membrane targeting and translocation
NBD	nucleotide binding domain
NEM	*N*-ethyl maleimide
PAGE	polyacrylamide gel electrophoresis
PEG-Mal	methoxypolyethylene glycol maleimide

min	minute
mRNA	messenger ribonucleic acid
Ni	nickel
nm	nanometre
NMR	nuclear magnetic resonance
nt	nucleotide(s)
N-terminal	amino terminal
N-terminus	amino terminus
OD	optical density
OM	outer membrane
ONPG	*ortho*-Nitrophenyl-β-galactoside
P	periplasmic domain
PAGE	polyacrylamide gel electrophoresis
PCR	polymerase chain reaction
PhoA	alkaline phosphatase
PMF	protonmotive force
PPXD	polypeptide crosslinking domain
RNC	ribosome nascent chain
rpm	rotations per minute
SA	signal anchor
SAXS	small-angle X-ray scattering
SDS	sodium dodecyl sulphate
Sec	secretory
SRP	signal recognition particle
Tat	twin-arginine translocase
TEMED	*N*,*N*,*N*′,*N*′-tetramethylethylenediamine
TM	transmembrane domain
TMAO	trimethylamine *N*-oxide
TM/H	transmembrane/helix
Tris	tris(hydroxymethyl) aminomethane
UV	ultra violet
v/v	volume per volume
w/v	weight per volume
YFP	yellow fluorescent protein
ΔpH	pH gradient
Δψ	electrical field gradient
3D	three dimensional

Amino Acid Abbreviations

Amino acid	Three-letter abbreviation	One-letter abbreviation
Alanine	Ala	A
Arginine	Arg	R
Asparagine	Asn	N
Aspartate	Asp	D
Cysteine	Cys	C
Glutamate	Glu	E
Glutamine	Gln	Q
Glycine	Gly	G
Histidine	His	H
Isoleucine	Ile	I
Leucine	Leu	L
Lysine	Lys	K
Methionine	Met	M
Phenylalanine	Phe	F
Proline	Pro	P
Serine	Ser	S
Threonine	Thr	T
Tryptophan	Trp	W
Tyrosine	Tyr	Y
Valine	Val	V
Any amino acid	Xaa	X

Acknowledgements

First and foremost, I would like to thank my supervisor, Prof. Tracy Palmer, for giving me the opportunity to join her laboratory. A PhD is not known for being an easy undertaking to say the least, especially when you work on membrane proteins, but Tracy's scientific and personal support over the years means I am able to successfully produce a thesis I am very proud of, and for that I will always be grateful.

In the laboratory I would like to thank Dr. Rebecca Keller, who helped me find my bearings in the initial stages of my PhD. Dr. Holger Kneuper for the extensive Tat advice he has given me, even though he moved on to work on Type VII secretion a long time ago, and Dr. Grant Buchanan for his assistance working on the Tat system and for all the constructs he made for me.

A big thank you also to everyone who worked with me in the Tat sub-group also- Dr. Johann Habersetzer, who I shared much of my time with in the lab with no doubt hours of abstract Tat discussions. Also thanks to Qi Huang, Dr. Francois Cleon and Dr. Marion Babot, Dr. Frank Sargent, Dr. Guillermina Casabona and Fiona Tooke for their constructive chats and exchange of Tat ideas. In addition a thank you to our Tat collaborators in Oxford, in particular Prof. Ben Berks, Dr. Fliss Alcock and Dr. Phill Standsfeld.

I would also like to express my gratitude everyone in MMB for providing an excellent, supportive work environment, in particular Dr. Jackie Heilbronn and Erin Stanbridge in MMB admin for making everything run smoothly.

I am also very grateful to Lucia and Ken, who started out as board game and poker buddies, for their close friendship and support over the years and all the favours they have done for me and Josh. A big thanks also to Ju, Rich, Triin, Alex and Giusy. I think now is an appropriate time to tell you all I let you win at poker all along.

Finally I would like to thank my family for all their support over the years, I would not be where I am today without them. Of course a big thank you to Josh as well- you are always there for me after a tough day in the lab.

Chapter 1: Introduction

1.1 *Escherichia coli* as a model organism

E. coli is a bacterial model organism used to study a great number of biological processes. The relatively simple and cheap requirements for laboratory-based culturing, its short multiplication time and well-characterised genetics mean it is well suited to this role and is often a host for the production of recombinant proteins.

Specifically, *E. coli* belongs to the family *Enterobacteriacae* and is facultatively anaerobic, rod-shaped and found naturally in the gastrointestinal tract of endothermic organisms where, with the exception of some pathogenic strains (such as *E. coli* O157:H7), it lives commensally. Indeed, the ability of some *E. coli* strains to cause disease, such as gastroenteritis, provides another dimension to research using this organism.

1.1.1 The *E. coli* cell envelope

Gram-negative bacteria, such as *E. coli* are bounded by two membranes, a cytoplasmic (or inner), membrane and an outer membrane. The space between the inner and outer membranes is the periplasm (Fig. 1.1), which is the site of a number of important cellular processes, such as electron transfer reactions involved in respiration, the acquisition of nutrients and the synthesis of peptidoglycan, composed of *N*-acetylglucosamine and *N*-acetylmuramic acid, which forms a layer in the periplasm that assists in maintaining the cell shape (Fig. 1.1) (Vollmer & Holtje, 2004).

The outer membrane of Gram-negative bacteria is asymmetric and mainly consists of lipopolysaccharide (LPS) in the outer leaflet. LPS is composed of lipid A, a hydrophobic part of the molecule which allows it to anchor in the outer membrane. This is linked *via* an inner and outer core region to the O-antigen, an oligosaccharide with a repeating pattern which can be modified across strains upon the addition of hexose, heptose and phosphate groups. Indeed, the O-antigen as a whole serves a protective role in bacteria defending against harmful agents such as antibiotics and bile salts, and is known to promote immune responses in animals (Raetz & Whitfield, 2002). The O-

antigen tends to be missing in laboratory strains of *E. coli*, which therefore display decreased virulence; such is the case in this work.

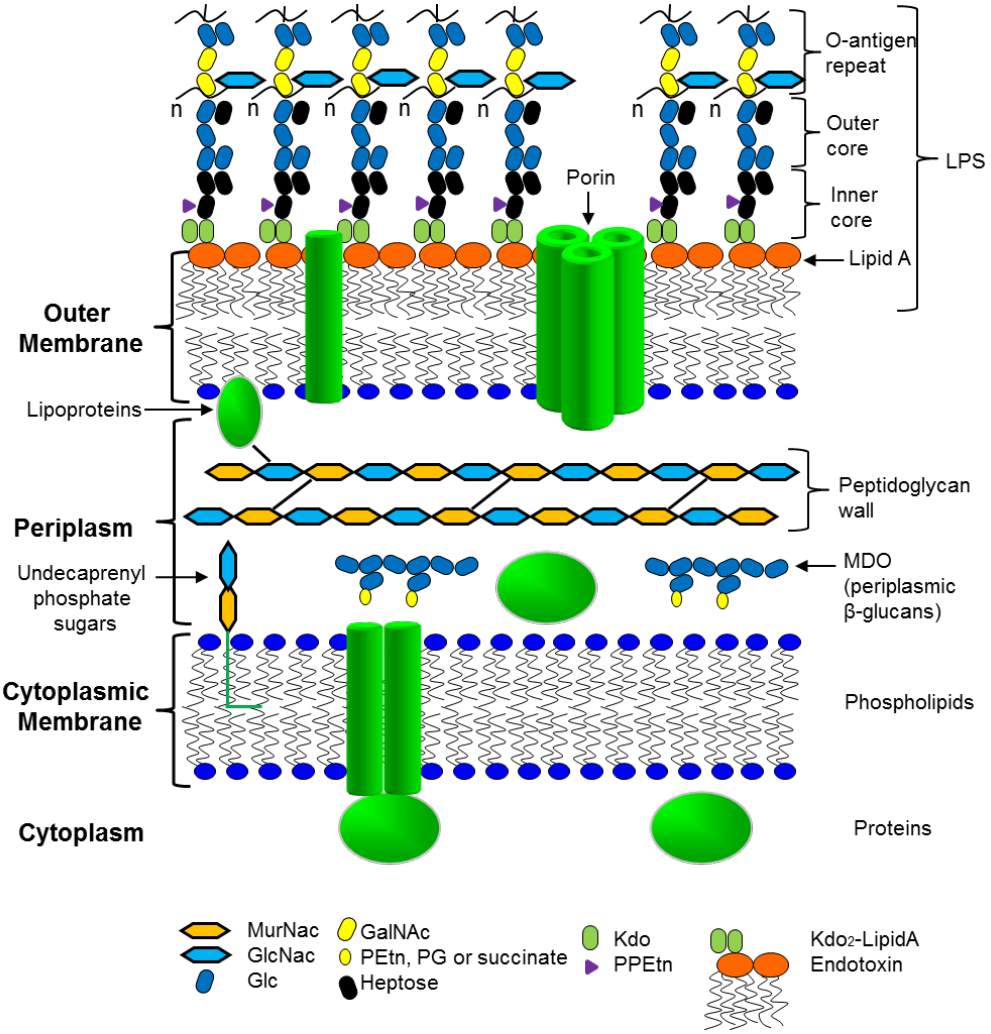

Figure 1.1) The typical cell envelope of a Gram-negative bacterium- The outer lipopolysaccharides are shown, with lipid A in orange in the outer membrane. Porins embedded in the outer membrane are shown as green cylinders, along with a green oval represening lipoproteins, some of which link the peptidoglycan to the outer wall. The cytoplasmic membrane is shown with green cylinders representing transport systems that facilitate movement of susbtrates across this bilayer. *N*- acetylglucosamine acid is represented by "MurNac", and *N*-acetylmuramic acid "GlcNac" in the peptidoglycan. Pyrophosphoethanolamine is represented by "PPEtn", 3-deoxy-D-manno-octulosonic acid is represented by "Kdo". "n" represents repeats in the O-antigen (Esko J. D., 2009)

Porins in the outer membrane allow passive diffusion of small molecules into the periplasm, while the inner membrane is much less permeable. Indeed, the inner membrane of bacteria is reminiscent of the mitochondrial equivalent, with lipid compositions of both showing a high phosphatidylglycerol:phosphatidylcholine ratio, likely required for oxidative phosphorylation, and the presence of ~20% cardiolipin, which exists in no other eukaryotic membrane (Osman *et al.*, 2011, Mileykovskaya &

Dowhan, 2000, Nishibori *et al.*, 2005). This is consistent with the endosymbiotic theory of mitochondrial origin, with the membrane composition of mitochondria being similar to that from the bacteria they descended from.

1.1.2 Protein transport in *E. coli*

Compartmentalisation of biochemical processes *via* the formation of lipid membranes was critical for the evolution of cellular organisms. For example, in *E. coli* such biochemical processes can occur in the cytoplasm, periplasm or indeed either the inner or outer membranes themselves, all of which have discrete chemistries. While many small molecules are able to traverse in and out of cells across the membranes, generally speaking protein translocation across, or insertion into, a membrane has required the evolution of transport systems.

Four generally conserved mechanisms to facilitate this have been discovered to date, these are: The general secretory (Sec) system, YidC dependent membrane insertion, the signal recognition partical (SRP) dependent pathway and the twin arginine translocase (Tat system).

This introduction will discuss all these transport mechanisms, but particular emphasis is placed on the Tat system, which is the subject of this work.

1.2 The Sec system

In *E. coli* most proteins are transported across the inner membrane as unfolded polypeptides *via* the Sec pathway. The core membrane-bound Sec machinery is composed of SecY, SecE and SecG, and the substrate traverses the membrane by a threading mechanism through the SecY channel. The substrate is targeted to Sec *via* a signal peptide at the N-terminus of the protein composed of an n-domain region, followed by a hydrophobic section and ending in a c-domain, which contains the signal peptidase cleavage site (this will be discussed in detail in the context of the Tat signal peptide in Section 1.6). Targeting can happen after translation or co-translationally (see

section 1.3), and post-translational targeting involves cytoplasmic proteins SecA and SecB, with the translocation event powered primarily by ATP hydrolysis. Non-essential accessory proteins SecD, SecF and YajC are also thought to be in involved in Sec translocation and will be discussed in Section 1.2.5.

1.2.3 The SecB chaperone

Once a Sec substrate has been translated in the cytoplasm, it must be prevented from folding. The cytoplasmic protein, SecB, has been shown to form a tetramer (Xu *et al.*, 2000) and to bind precursor Sec substrates (Gannon *et al.*, 1989, Liu *et al.*, 1989), preventing their folding prior to transport across the cytoplasmic membrane (Collier *et al.*, 1988, Bechtluft *et al.*, 2010). This binding of the substrate is thought to be mediated through hydrophobic patches of SecB seen in the crystal structure of the *E. coli* and *Haemophilus influenzae* proteins (Xu *et al*., 2000, Dekker *et al*., 2003). After binding the substrate, SecB targets the substrate to the Sec machinery *via* an interaction with the C-terminus of SecA (Zhou & Xu, 2003).

1.2.4 The SecA ATPase

Essentially SecA is a superfamily 2 helicase which has adapted to translocate proteins, (Koonin & Gorbalenya, 1992) containing a DEAD helicase motor domain in the N-terminal region of the protein, required for protein export (Sianidis *et al.*, 2001). A Walker A and B motif form a high affinity nucleotide binding site which is essential for SecA function (Schmidt *et al*., 1988, Lill *et al*., 1989). In bacteria, SecA is cytoplasmic and associates with the membrane-bound SecYEG complex to mediate post-translational export of proteins across the cytoplasmic membrane (Brundage *et al.*, 1990).

Overall SecA is composed of a number of domains, including the polypeptide cross-linking domain (PPXD), the helical wing domain (HWD), the helical scaffold domain (HSD) and nucleotide binding domains 1 and 2 (See Fig. 1.2). The crystal structure of SecA has been obtained from a number of organisms and when crystallised in the

absence of SecYEG it is usually in an “open” conformation (Osborne *et al.*, 2004, Zimmer *et al.*, 2006, Papanikolau *et al.*, 2007) with structures of the “closed”

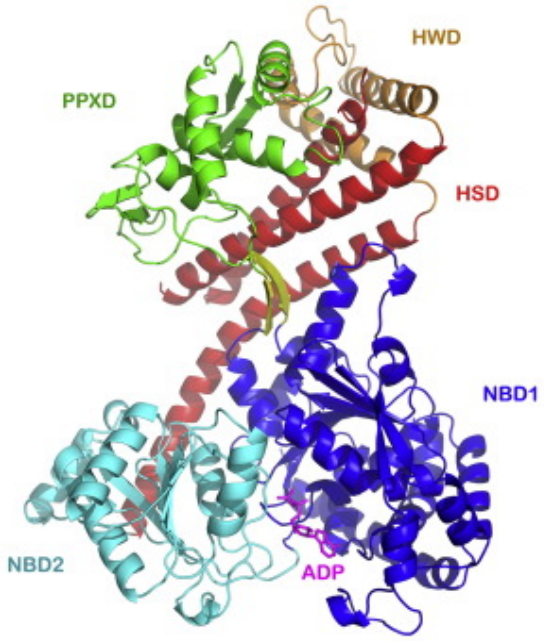

Figure 1.2) Crystal structure of the open conformation of *Thermotoga maritima* SecA- Solved to 1.9 Å resolution, the *T. maritima* SecA is shown in an open conformation with each domain labelled separately. ADP is shown bound at the nucleotide binding site 1 (NBD1 in blue and NBD2 in cyan). The polypeptide crosslinking domain (PPXD) is shown in green, the helical wing domain (HWD) is shown in orange, the helical scaffold domain (HSD) is shown in red and ADP is show in magenta. Taken from Chen *et al.* (2015).

conformation also observed with SecYE (Zimmer *et al.*, 2008). Molecular dynamics simulations, free-energy calculations and structural analysis of SecA from *Thermotoga maritima* have demonstrated that the protein may behave in a clamp-like manner, with large scale conformational changes holding the substrate in place as it traverses through SecYEG. The energy barrier in closing SecA is potentially overcome by insertion of the TM6/7 cytoplasmic loop of SecY into the region separating PPXD and HSD/HWD (Chen *et al.*, 2015). Specifically, it is proposed that in the first step of clamp closure PPXD, HSD and HWD move towards NBD2 with the second step involving a separation of PPXD from HSD and HSW as it moves further towards NBD2.

A controversy exists regarding the oligomeric state of SecA with crystal structures suggesting both monomeric (Osborne et al., 2004) and dimeric (Hunt *et al.*, 2002, Sharma *et al.*, 2003) forms. The latter studies are supported by crosslinking showing that a SecA dimer can support Sec transport (de Keyzer *et al.*, 2005, Jilaveanu &

Oliver, 2006) while conversely other work shows a monomeric derivative of SecA can also support transport. (Or *et al.*, 2002, Or *et al.*, 2005).

Two domains on SecA have been found to interact with the pre-protein *via* crosslinking the PPXD and the 2 helix finger (2HF) domain in the HSD (Bauer & Rapoport, 2009). Further details on how SecA may mediate transport through the SecY channel will be discussed in Section 1.2.5.

1.2.5 The SecYEG machinery: structures and mode of translocation

The structure of the *Methanococcus jannaschii* Sec translocon (SecYEβ, homologous to *E. coli* SecYEG) was obtained in the resting state, showing SecY, composed of 10 transmembrane (TM) helices, forming a channel with two halves of the protein in similar folds (one half, TM1-5 and the other, TM6-10 linked with a hinge region between TM5-6 giving the overall shape of a crab claw). The SecY channel was found to have an hourglass shape, with a ring of hydrophobic amino acids at its narrowest point and a short "plug" helix blocking the channel. At the cytoplasmic side, this cavity is 2-2.5 nm in diameter, gradually narrowing to a close at the centre of the membrane. Helices 2 and 7 at the end of each half of SecY can move apart, exposing the channel of SecY to the membrane - this is referred to as the lateral gate (LG) (Van den Berg *et al.*, 2004) (Fig. 1.3). Once a secreted protein engages with the Sec machinery, the signal sequence is inserted into the membrane near the SecY LG (Gold *et al.*, 2013, Briggs *et al.*, 1986). It is proposed that this interaction leads to a conformational change within SecY, whereby the TM7 straightens to contact TM10, displacing the plug which blocks the channel to unlock the complex (Hizlan *et al.*, 2012).

Experiments examining mutations in SecY found the $SecY_{F286Y/I408N}$ substitution was "hyperactive" due to its ability to facilitate translocation of substrates with defective signal peptides. This was thought to be due to complex destabilisation which leads to the two halves of SecY separating (Duong and Wickner 1999). To build on this, more recent work was able to generate a mutant of SecY which formed a disulphide bridge

between TM7 and TM10 through introduction of Cys-substitutions in these regions, holding the complex in an “unlocked” conformation. Strikingly, when this “unlocked” mutant was compared to the $SecY_{F286Y/I408N}EG$ complex, it was found that they both displayed this hyperactive behaviour in transporting substrates, compared to a wild-type Sec system. This supports the hypothesis that TM7 straightening towards TM10 unlocks the complex allowing translocation (Corey *et al*., 2016), this is outlined in detail in Fig. 1.3.

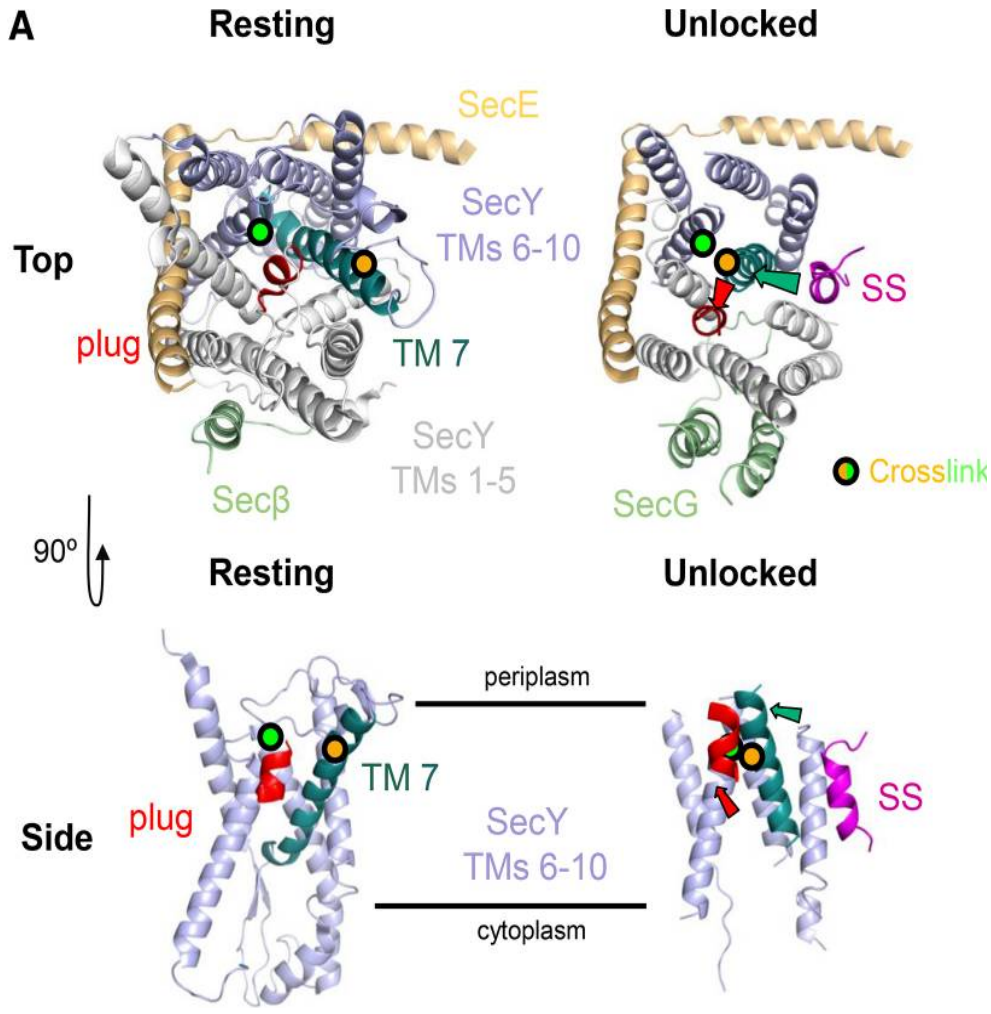

Figure 1.3) Crystal structures of SecYEG/SecYEβ complexes showing helix rearrangements proposed to occur during substrate translocation: Top left shows the structure of *M. jannaschii* SecYEβ viewing from the equivalent of the periplasm, with SecY helices TM1-5 shown in white and TM6-10 shown in blue, indicating the two domains. SecE is show in yellow bracing SecY with Secβ (equivalent to *E. coli* SecG) also associated with SecY. TM7 of SecY is shown in turquoise, with the plug shown in red. The plug is blocking the channel, with positions I284 and T404, shown as orange and green circles far apart in this proposed resting conformation. Top right shows the *E. coli* SecYEG bound to a Sec signal sequence (magenta) (Hislan *et al*., 2012) with the SecY residues I284 and T404 moving to a close proximity- forming a disulphide linkage which holds the channel in an unlocked conformation. Arrows denote the proposed movement of helices moving the plug to open the SecY channel. Bottom right and left both show more clearly TM6-10 of SecY with movement of TM7 displacing the plug. Taken from Corey *et al*. (2016).

SecE is an integral membrane protein that stabilises SecY *in vivo* (Kihara *et al.*, 1999). Within the SecYEG complex, SecE braces SecY, with a TM lying diagonally across the membrane and an amphipathic helix at the cytoplasmic side (Van den Berg *et al.*, 2004). It is thought that this arrangement of SecE holds together the two domains of SecY, whereby it relaxes its conformation to allow SecY to open. Studies observing disulphide crosslinked SecY and SecE showed that even when they are linked covalently transport is still facilitated, indicating that the SecY-E interaction is stable (Lycklama a Nijeholt *et al.*, 2013). The latter work also observed decreased Sec transport upon cleavage of SecE, suggesting that it holds the two domains of SecY together.

SecG is located peripherally in the *E. coli* SecYEG complex, with fewer contacts to SecY than those found for SecE (Van den Berg *et al.*, 2004). Although SecG is not essential for transport, it may play a role in promoting transport efficiency (Hanada *et al.*, 1994). In addition to this, it has been shown that SecG can facilitate transport at low temperatures in the absence of PMF (Hanada *et al.*, 1996).

Very recently, a crystal structure of the SecA-SecYE complex was solved with a translocating protein segment; here it was observed that the substrate peptide displaced the plug domain in SecY, with the complex presumably in the unlocked form (Fig. 1.4). Contacts between SecA and SecY were at the cytoplasmic loop between SecY TM8 and TM9, along with the C-terminal tail. The hydrophobic section of the signal sequence was found to form an alpha helix which sits outside the SecY lateral gate with the successive section of polypeptide intercalating with the gate itself (Li *et al.*, 2016). The substrate in the structure was derived from OmpA, and fused to the 2 helix finger (2HF) of SecA, which was informed by a previous structure of SecA from *Thermotoga maritima* which noted that the 2 helix finger (2HF) of SecA inserted into the cytoplasmic section of the SecY channel (Zimmer et al., 2008). In this recent structure SecA is in its closed conformation with the 2HF at the cytoplasmic side of the SecY channel (see Fig. 1.4).

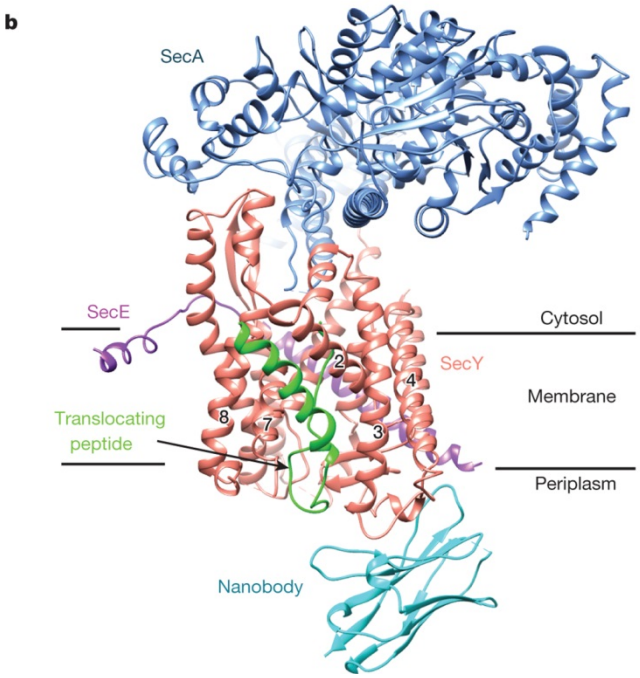

Figure 1.4) Crystal structure of *E. coli* SecA bound to the SecYE complex, with a translocating peptide- The core structure of Sec during translocation was solved to a 3.70 Å resolution. SecA (shown in blue) is bound to SecY (shown in pink) within the SecYE complex - helices in SecY are labelled, with helices 2 and 7 forming the lateral gate. SecE (purple) is shown bracing SecY and a translocating peptide (green) is shown within the SecY channel. The nanobody used during crystallisation is shown in cyan. Taken from Li *et al*. (2016).

SecD, SecF and YajC have been shown to form a trimeric complex which can interact with SecYEG in a transient fashion (Duong & Wickner, 1997). While not essential for Sec secretion, their absence at cold temperatures has a strong negative effect on translocation (Pogliano & Beckwith, 1994). All three subunits are integral membrane proteins, with the periplasmic domains proposed to play a role in releasing substrates from the Sec channel (Nouwen & Driessen, 2005, Matsuyama *et al.*, 1993). The role of these accessory proteins, along with YidC, will be detailed in section 1.4.

1.2.6 Powering movement of the Sec substrate across the membrane

How the polypeptide chain moves through the Sec machinery complex is contentious, with two different models being proposed. The “power stroke” model in which the polypeptide chain is bound and pulled forward in sequential steps of ATP hydrolysis and a diffusion based model, whereby ATP hydrolysis biases a forward movement of diffusing substrate polypeptide through the channel (Collinson *et al.*, 2015). These are demonstrated in Fig 1.5. The power stroke model is supported by translocation intermediates of the Sec system being observed, thought to be reflection of successive movement of a disordered polypeptide through the SecYEG pore (Schiebel *et al.*, 1991, Tani *et al.*, 1989). The ratcheted diffusion model relies on the Brownian diffusion of the polypeptide at physiological temperatures- a key advantage being that it would not require sequence specificity of the transported polypeptide.

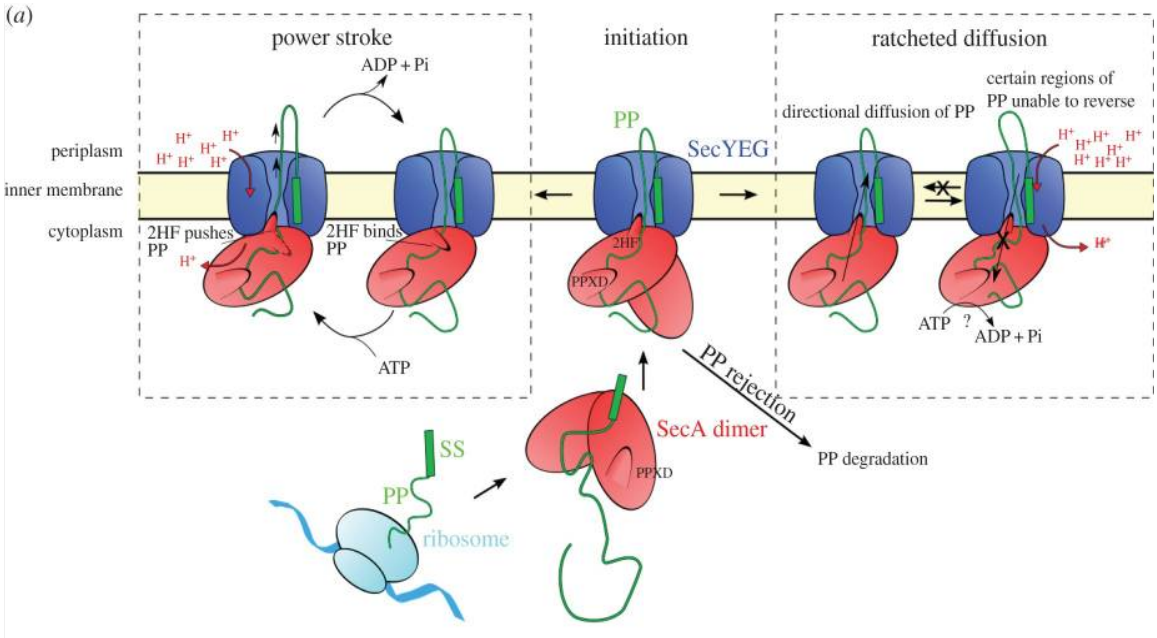

Figure 1.5) A comparison of the powerstroke and ratcheted diffusion model of polypeptide translocation- SecA, shown in red, binds the substrate after translation (SecB chaperone not shown) and delivers it to SecYEG. On the left the power stroke model is shown where the two helix finger (2HF) of SecA pushes the substrate polypeptide through the SecYEG channel in cycles of ATP hydrolysis. Conversely the ratcheted diffusion model shows SecA facilitating forward diffusion of the PP through SecYEG and disallowing backsliding, thereby allowing the entirety of the substrate to pass through- taken from Collinson *et. al.* (2015).

Aside from ATP hydrolysis, the protonmotive force (PMF) seems to play a role in the stages of Sec translocation where it can complete the translocation of trapped substrates and may be used in re-orientating the signal sequence (Schiebel et al., 1991, van Dalen *et al.*, 1999). In addition to this, Ismail and co-workers observed recently that charged residues in a nascent chain (co-translation transport is covered in section 1.3) were subject to a biphasic electrical force during translocation, this force could be modified by dissipating the PMF using indole as an uncoupler (Ismail *et al.*, 2015).

1.3 Signal recognition particle (SRP) dependent protein transport

Proteins can be transported co-translationally *via* a pathway dependent on the signal recognition particle (SRP) which consists of a GTP binding Ffh (fifty-four homologue) protein in complex with a 4.5S RNA (Bernstein *et al.*, 1993). Most of the substrates targeted to this system are inner membrane proteins (de Gier & Luirink, 2001) where the SRP binds the hydrophobic signal sequences of the nascent chains as they exit the ribosome, preventing further translation. A ribosome nascent chain complex is formed, which is targeted to the FtsY receptor protein. FtsY is a GTPase which associates with the SecYEG complex (Angelini *et al.*, 2005, Kuhn *et al.*, 2011), upon which the SRP and FtsY subunits dissociate and the nascent chain is fed through the Sec machinery as translation is restored (Luirink *et al.*, 2005).

1.4 YidC-dependent membrane protein insertion

In *E. coli*, YidC is essential for growth, and is composed of three domains, with a P1 (periplasmic) domain, a TM (transmembrane) region and a small cytoplasmic region (Kumazaki *et al.*, 2014). A hydrophilic groove was observed in the transmembrane domain, which has been implicated in binding of some substrates.

In *E. coli*, YidC is essential for growth (Samuelson *et al.*, 2000) and has been shown to co-purify with SecYEG (Scotti *et al.*, 2000). Indeed while YidC can act with the Sec YEG forming a holo-translocon complex for the insertion of membrane proteins

(Samuelson et al., 2000, Schulze *et al.*, 2014), it has been shown to work alone in some cases (Facey *et al.*, 2007). Interactions between the P1 (periplasmic) domain of YidC and SecF have also been observed, which implied an interface between YidC, SecYEG and SecDFYajC when the substrate is delivered into the membrane.

It has been shown that the lateral gate of SecY opens to release hydrophobic helices into the membrane (Luirink et al., 2005, Dalbey *et al.*, 2011) with YidC being involved in this release process (Urbanus *et al.*, 2001, Beck *et al.*, 2001). Furthermore, crosslinking data has shown interactions between YidC and the lateral gate region of SecY (Sachelaru *et al.*, 2015).

1.5 The discovery of the Tat protein transport system

The origins of the Tat system as a protein translocase existing independent of the universal ATP-driven Sec system were conceived in 1991 when Mould and Robinson identified subunits of the photosynthetic oxygen-evolving complex from wheat plants, which necessitated a proton gradient (ΔpH) for transport across the thylakoid membrane (Mould & Robinson, 1991). This was supported by data published shortly after showing similar thylakoid proteins which not only depended on ΔpH for translocation, but could also be localised in the complete absence of ATP (Cline *et al.*, 1992). Chaddock and co-workers that discovered a motif common to all the proposed substrates. While similar to the Sec targeting motif, it had the distinctive presence of two arginines near the N-terminus (Chaddock *et al.*, 1995).

The pertinence of this system in prokaryotes was recognised when signal sequences containing this “double-arginine” were identified in bacterial periplasmic proteins, providing an indication that this pathway was conserved (Berks, 1996). Notably, many of these bacterial proteins contained oxygen-sensitive cofactors, which may present a problem for insertion in the periplasm. Coupled with the inability of the Sec “pore” to accommodate folded proteins, this led to the proposition that these cofactor-containing

proteins were transported in a folded state, requiring a specialised translocation pathway.

The concept that a prokaryotic homologue exists for the plant ∆pH pathway was furthered by the discovery of a bacterial gene related to the plant *hcf106*. In plants, a mutation of the *hcf106* gene was shown to impair protein export *via* the ∆pH dependent pathway and analysis of bacterial genomes identified homologues to *hcf106*, further strengthening the premise of conserved export pathway in bacterial and plants (Settles *et al.*, 1997). A specific gene in *E. coli*, homologous to the plant *hcf106* was later identified by Weiner and co-workers. Designated *mttA* (membrane targeting and translocation) in the *mttABC* operon, mutations in this gene were found to prevent export of twin arginine redox enzymes to the periplasm (Weiner *et al.*, 1998).

Further analysis of these *mttABC* genes by Sargent and co-workers led to correction of the genome sequence, and the identification of a four cistron operon, *tatABCD* (*tat* standing for twin arginine translocase) along with an unlinked gene, *tatE* (Sargent *et al.*, 1998).

1.6 Tat signal peptide

The structural organisation of the Tat signal peptide is broadly similar to that of the Sec signal, containing n-, h- and c-regions with a cleavage site for leader peptidase LepB. Though a key difference, and where the Tat system acquires its name, is the presence of two usually invariant arginine residues in the n-region (Fig. 1.6).

While almost consistently present, a double arginine is not always part of the Tat consensus sequence in nature, with examples of “KR”, “RN” and “RQ” (Widdick *et al.*, 2008) motifs sometimes being found. Additionally, laboratory manipulation of the signal peptide of SufI in *E. coli* demonstrated that conservatively exchanging of either one of the twin arginine residues with lysine still supported low level export into the periplasm, with dual arginine to lysine mutations abolishing transport altogether (Stanley *et al.*, 2000). In addition exogenous green fluorescent protein (GFP) fused to a Tat signal

peptide was successfully exported to the periplasm with signal sequences containing a substitution of the first arginine with basic lysine and the second arginine with either lysine, glutamine or asparagine (DeLisa *et al.*, 2002).

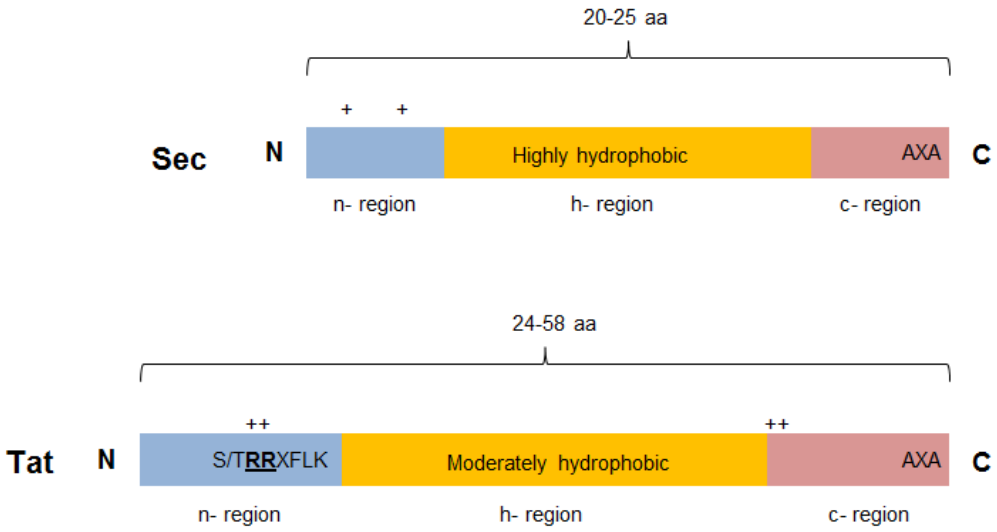

Figure 1.6) A schematic comparison of the Sec and Tat signal peptides- The N-terminal region is shown in blue, with the Tat consensus sequence and Twin arginines noted. The hydrophobic region of each signal peptide is shown in orange, ending in the pink C-terminal region with the LepB cleavage site noted on for both Tat and Sec. "+" denotes regions of positively charged residues and "X" denotes any amino acid.

Much of the work examining the importance of individual residues in the Tat signal sequence involves mutagenesis and subsequent analysis of translocation efficiency. The position of the first arginine residue in the consensus sequence is often referred to as position +1, with other residues numbered relative to this. Position -1, before the first arginine, is very often either a threonine or serine (Berks, 1996), the significance of which is unclear since its substitution has a detrimental effect on the translocation of some substrates but not others. It has been proposed that this residue stabilises a potential alpha helix formed by the h-region (Mendel *et al.*, 2008, Stanley *et al.*, 2002). The residue at +3 is very poorly conserved (Stanley et al., 2002) (noted as "X" in the consensus sequence) and as a consequence is thought to be a linker residue just after the twin arginines (Buchanan *et al.*, 2001). A phenylalanine residue at position +4 occurs fairly frequently (up to 70% of signal peptides (Berks, 1996)) with substitutions to less hydrophobic residues impairing the transport of *E. coli* SufI (Stanley et al.,

2000). Furthermore, secretion of the Tat substrate, Xylanase C in *Streptomyces lividans*, was reduced by 75% when the phenylalanine at +4 was replaced with any amino acid except tryptophan, which had a more modest effect at 50% reduction (Li *et al.*, 2006). Similar experiments observing the effect on Tat transport in response to substitution of amino acids a position +5 indicate that hydrophobicity is also important for this position (Stanley et al., 2000). Position +6 is most frequently occupied by a lysine residue (Berks, 1996) and is thought to act as a boundary before the hydrophobic stretch of the signal peptide.

The h-region of the Tat signal peptide starts after the Tat consensus sequence and has been found to be less hydrophobic than its Sec counterpart. This important distinction is highlighted by experiments showing that Tat substrates can be re-targeted to the Sec machinery if the h- region hydrophobicity is increased (Cristobal *et al.*, 1999).

The final section of the Tat signal peptide, and the part furthest from the N-terminus, is the c-region. In Tat signal peptides this region often contains positively charged residues, thought to act as a Sec avoidance signal (Bogsch *et al.*, 1997, Cristobal et al., 1999). Both Tat and Sec c-regions contain a LepB cleavage site, where the signal peptide is removed subsequent to translocation (Yahr & Wickner, 2001).

1.7 Tat Substrates

The requirement for a specialised Tat transport system to work alongside the universal Sec system reflects the need for a protein export system to accommodate substrates not compatible with transport as an unfolded polypeptide. There are a number of reasons behind this, for example, hydrolysis of cytoplasmic nucleotides may be needed for the cofactor insertion step, as in the case of GTP hydrolysis coupled to nickel insertion into *E. coli* hydrogenases (Maier *et al.*, 1995). Additionally, highly oxygen sensitive metallo-cofactors may require insertion in the reducing conditions of the cytoplasm prior to export (Berks, 1996). Even if substrates are able to fold prior to cofactor insertion in the periplasm, competition from other cofactors outside the

cytoplasmic membrane is also a factor. For instance the Mn^{2+} binding protein MncA in the cyanobacterium *Synechocystis* PCC 6803 requires cofactor insertion prior to transport outside the cell, where erroneous metallo-cofactors such as $Cu^{2+}$and Zn^{2+} can compete for binding (Tottey *et al.*, 2008).

It should be noted, however, that cofactor-containing proteins being exported *via* Tat is not a stringent rule, with exceptions including the *c*-type cytochromes in *E. coli*, which are transported *via* Sec prior to haem cofactor insertion in the periplasm (Thony-Meyer & Kunzler, 1997). Conversely, proteins such as the cell wall amidases AmiA and AmiC contain no cofactors but also utilise the Tat system for transport across the cytoplasmic membrane (Ize *et al.*, 2003).

Aside from cofactor insertion, some Tat substrates have been demonstrated to be exported as a heterodimeric complexes whereby only one of the constituent proteins contains a signal peptide. This is known as “hitchhiking” or “piggy-backing” and is exemplified by protein subunits HybO and HybC of Hydrogenase-2 in *E. coli*. These proteins are exported as a heterodimer and if either subunit is expressed without the other, they accumulate in the cytoplasm. Of the two subunits, only HybO contains a Tat signal peptide, with HybC devoid of any signal peptide at all, suggesting HybO and HybC are exported as a complex, with the Tat machinery recognising HybO (Rodrigue *et al.*, 1999).

With regard to *E. coli*, there are approximately 27 predicted Tat substrates, shown in Table 1.1 (Palmer *et al*., 2010) (not including proteins which are co-translocated with Tat signal peptide containing proteins) involved in a host of processes such as anaerobic respiration, cell wall metabolism, iron uptake and copper resistance. Though the complete absence of a Tat system in *E. coli* is not fatal, loss of Tat activity causes cells to exhibit a number of detrimental phenotypes such as cell chaining and increased sensitivity to detergents, with both of these phenotypes due to the mislocalisation of cell wall amidases (Ize et al., 2003). This characteristic has been exploited to identify

strains expressing a damaged Tat system, through the impaired or absence of growth on media containing SDS, as Δ*tat* cells are less able to cope with envelope stress

Table 1.1) Substrates of the Tat system in *E. coli* -showing physiological role, cofactors which are inserted and co-exported partners, if any. The twin arginines are highlighted within the signal sequence ((Palmer *et al.*, 2010)

Protein	Physiological role	Cofactor/s	Co-exported partner	Signal peptide sequence
HyaA	Hydrogen oxidation	3 x Fe-S clusters	HyaB	MNNEETFYQAMRRQG**RR**SFLKYCSLAATSLGLGAGMAPKIAW A
HybO	Hydrogen oxidation	3 x Fe-S clusters	HybC	MTGDNTLIHSHGIN**RR**DFMKLCAALAATMGLSSKAAA
HybA	Hydrogen oxidation	4 x Fe-S clusters	Unknown	MN**RR**NFIKAASCGALLTGALPSVSHA
NapG	Nitrate reduction	4 x Fe-S clusters	Unknown	MSRSAKPQNG**RR**RFLRDVVRTAGGLAAVGVALGLQQQTARA
NrfC	Nitrate reduction	4 x Fe-S clusters	Unknown	MTWS**RR**QFLTGVGVLAAVSGTAGRVVA
YagT	Aldehyde oxidoreductase	2 x Fe-S clusters	YagR (MCD) and YagS (FAD)	MSNQGEYPEDNRVGKHEPHDLSLT**RR**DLIKVSAATAVVYPHST LAASVPA
YdhX	Potential Component of aldehyde ferredoxin oxidoreductase	4 x Fe-S clusters	Potentially YdhV (tungsten)	MSWIGWTVAATALGDNQMSFT**RR**KFVLGMGTVIFFTGSASSLL A
TorA	TMAO reduction	MGD	None	MNNNDLFQAS**RR**RFLAQLGGLTVAGMLGPSLLTPRRATAAQA
TorZ	TMAO reduction	MGD	None	MTLT**RR**EFIKHSGIAAGALVVTSAAPLPAWA
NapA	Nitrate reduction	MGD, 1 FE-S cluster	None	MKLS**RR**SFMKANAVAAAAAAAGLSVPGVA
DmsA	DMSO reduction	MGD, 1 FE-S cluster	DmsB	MKTKIPDAVLAAEVS**RR**GLVKTTAIGGLAMASSALTLPFSRIAHA
YnfE	Selenate reduction	MGD, 1 FE-S cluster	YnfG	MSKNERMVGIS**RR**TLVKSTAIGSLALAAGGFSLPFTLRNAAA
YnfF	Potentially DMSO reduction	MGD, 1 FE-S cluster	YnfG	MMKIHTTEALMKAEIS**RR**SLMKTSALGSLALASSAFTLPFSQMV RA

FdnG	Formate oxidation	MGD, 1 FE-S cluster	FdnH	MDVS**RR**QFFKICAGGMAGTTVAALGFAPKQALA
FdoG	Formate oxidation	MGD, 1 FE-S cluster	FdoH	MQVS**RR**QFFKICAGGMAGTTAAALGFAPSVALA
YedY	Potentially TMAO/DMSO reduction	MPT	None	MK**RR**QVLKALGISATALSLPHAAHA
CueO	Cu(I) oxidation	4 x Cu ions	None	MQ**RR**DFLKYSVALGVASALPLWSRAVFA
PcoA	Copper resistance	4 x Cu ions	None	MLLKTS**RR**TFLKGLTLSGVAGSLGVWSFNARSSLSLPVAA
SufI	Cell division	None	Unknown	MSLS**RR**QFIQASGIALCAGAVPLKASA
YahJ	Putative deamidase	1 X Fe ion	Unknown	MKESNS**RR**EFLSQSGKMVTAAALFGTSVPLAHA
WcaM	Colanic acid biosynthesis	Unknown	Unknown	MPFKKLS**RR**TFLTASSALAFLHTPFARA
MdoD	Glucan biosyntheisis	Unknown	Unknown	MD**RR**RFIKGSMAMAAVCGTSGIASLFSQAAFA
EfeB	Iron extraction from heme	Heme	None	MQYKDENGVNEPS**RR**RLLKVIGALALAGSCPVAHA
YaeI	Potential phosphodiesterase	Unknown	Unknown	MIS**RR**RFLQATAATIATSSGFGYMHYC
AmiA	Cell wall amidase	1 x Zn^{2+}	Unknown	MSTFKPLKTLTS**RR**QVLKAGLAALTLSGMSQAIA
AmiC	Cell wall amidase	Potentially 1 x Zn^{2+}	Unknown	MSGSNTAIS**RR**RLLQGAGAMWLLSVSQVSLA
FhuD	Ferrichrome binding	None	Unknown	MSGLPLIS**RR**RLLTAMALSPLLWQMNTAHA

YcbK	Peptidase M15 superfamily	Unknown	Unknown	MDKFDAN**RR**KLLALGGVALGAAILPTPAFA
Pac	Penicillin amidase	Ca^{2+}	None	MKN**RN**RMIVNCVTASLMYYWSLPALA
C3736	Potential diene lactone hydrolase	Unknown	Unknown	MP**R**TAKDFPQELLDYYDYYAHGKIS**KR**EFLNLAAKYAVGGMTALA

brought about by detergents. Likewise, a lack of growth anaerobically with DMSO or TMAO as the sole electron acceptor identifies strains unable to export Tat-dependent substrates TMAO/DMSO reductase (Buchanan et al., 2001).

The Tat system is essential for viability in a number of other organisms, such as the nitrogen-fixing *Sinorhizobium meliloti,* the predator bacterium *Bdellovibrio bacteriovorus* and some Halophiles (Pickering & Oresnik, 2010, Chang *et al.*, 2011, Dilks *et al.*, 2005, Thomas & Bolhuis, 2006). Notably however, with regard to antimicrobial drug development, is the reliance of the human pathogens *Mycobacterium tuberculosis* and *Helicobacter pylori* on the Tat system for viability (Saint-Joanis et al., 2006, Benoit & Maier, 2011). In addition, it was found that deletion of the Tat substrate *cj0379c* (homologous to *E. coli* YedY) in zoonotic pathogen *Campylobacter jejuni* impaired the organism's ability to colonise chickens and conferred increased sensitivity to reactive nitrogen species (Hitchcock *et al.*, 2010).

This presents a potential avenue for antibiotic development, given the absence of a Tat system, or indeed any homologues in humans. Viability aside, the Tat system is usually required for virulence of those bacterial pathogens found to possess it (De Buck *et al.*, 2008).

1.8 Tat proofreading

While no chaperones have been found which are common to all Tat substrates, individual substrates have been found to be associated with discrete chaperones in the cytoplasm. These "proofreading chaperones" are able to bind the Tat signal peptide and in some cases the mature domain of co-factor-containing proteins, preventing targeting to the membrane before folding and cofactor insertion is completed (Fig. 1.7).

Examples of this include the chaperone DsmD which binds to the Tat substrate, dimethyl sulfoxide (DMSO) reductase (DmsA), a molybdopterin cofactor-containing protein. Typically *E. coli* is able to grow anaerobically with DMSO as the terminal electron acceptor due to the effective export of functional DmsA, however when DmsA

is expressed in the absence of DmsD, growth is prevented (Oresnik *et al.*, 2001). This is complemented with data showing a direct interaction between DmsD and the signal peptide of DsmA (Winstone *et al.*, 2006). A similar relationship has been identified between TorD and the molybdenum-containing Tat substrate, TorA. A binding site at the C-terminus of TorA was identified for TorD (Jack *et al.*, 2004, Hatzixanthis *et al.*, 2005) and further to this a direct interaction has been shown through two high affinity sites characterised using SAXS (small angle X-ray scattering) (Dow *et al.*, 2013). Notably, TorD is still able to interact with cofactor-free TorA even in the absence of the signal peptide. It is proposed that once the C-terminal domain of TorA is correctly folded, TorD is displaced prior to transport through Tat. Likewise the chaperone NapD is thought to bind nitrate reductase NapA at the Tat signal peptide in a similar manner to TorA (Grahl *et al.*, 2012), with SAXS data showing NapD bound to NapA in a partially folded state (Dow *et al.*, 2014).

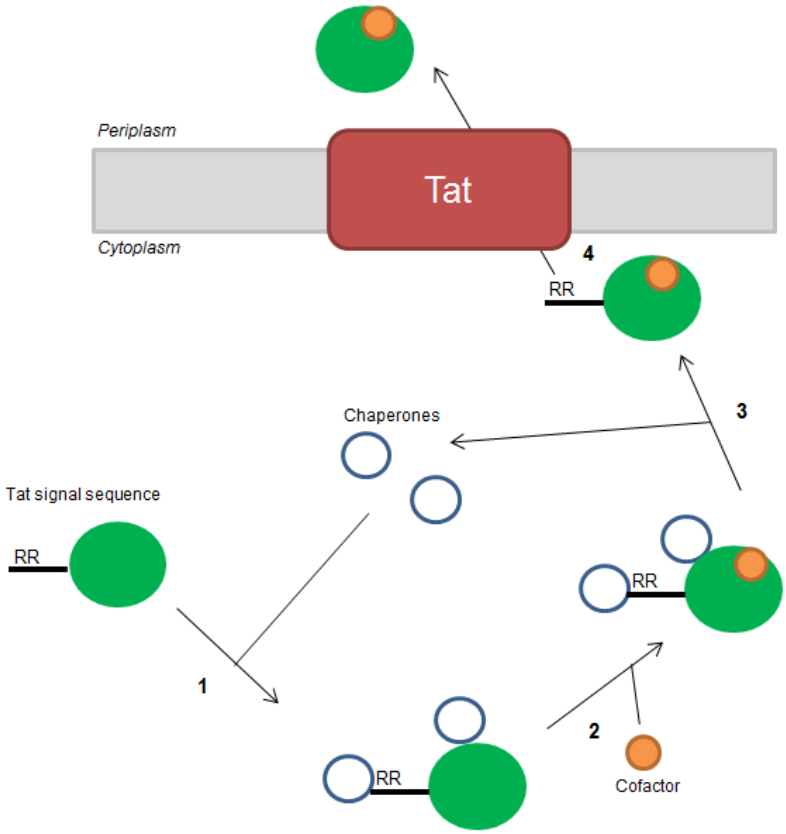

Figure 1.7) Diagram showing chaperone binding to a Tat substrate- 1) Bespoke protein chaperones (blue) bind to the Tat signal peptide (black) and the passenger domain (green) to prevent translocation until cofactor insertion occurs as in step 2). Once correctly folded with the cofactor the chaperones are released and the substrate is translocated by the Tat system into the periplasm. Adapted from (Palmer & Berks, 2012).

1.9 Tat quality control

The ability of the Tat system to distinguish between folded and unfolded protein substrates (i.e. quality control) has been demonstrated through experiments studying the transport of PhoA. Normally PhoA is a Sec substrate which is exported as a disordered polypeptide, whereby structural disulphide bonds, catalysed by the DsbAB system, drive its folding in the periplasm (Akiyama & Ito, 1993). Replacing the native signal peptide with a Tat signal does not result in export to the periplasm, presumably because it is incapable of forming disulphide bonds in the cytoplasm and is therefore not fully folded. Indeed, when PhoA is expressed with the Tat signal peptide in an *E. coli* strain engineered to have an oxidising cytoplasm (an environment that accommodates disulphide bond formation), it is exported to the periplasm indicating that the Tat system recognises folded PhoA (Panahandeh *et al.*, 2008, Stanley et al., 2002). A similar situation was encountered when Tat signal peptides were fused to antibody fragments, where transport to the periplasm was only observed with prior heterodimerisation of antibody fragments in the cytoplasm (DeLisa *et al.*, 2003).

The mechanism behind Tat's ability to discriminate unfolded and folded proteins in these instances has not been identified and is complicated somewhat by the Tat system's ability to transport some unfolded proteins, as long as they are small and hydrophilic (Richter *et al.*, 2007, Cline & McCaffery, 2007). It has been shown that long hydrophobic stretches in Tat substrates hinder their export, though this may be due to the hydrophobic residues interacting with the lipid bilayer directly, stalling movement through the Tat translocase (Richter et al., 2007). This may account for the lack of transport for unfolded proteins which have their hydrophobic core exposed. More recently, however, mutations in the Tat translocase have been identified which allow misfolded substrates to be translocated, indicating a potential role in recognising folded substrates which is intrinsic to the Tat system (Rocco *et al.*, 2012).

1.10 The Tat machinery

In *E. coli* two separate loci encode Tat components, with a four cistron operon at 86 min on the chromosome encoding *tatABCD* along with an unlinked *tatE* gene at 14 minutes (Sargent *et al.*, 1998) (Fig. 1.8). Due to the presence of a stem loop on the mRNA between *tatC* and *tatD*, the major transcript from the *tatABCD* operon is *tatABC*. Expression studies using transcriptional and translational fusions show *tatA* is produced greatly in excess of the other subunits, with a predicted ratio for TatA:TatB:TatC of 50:2:1 (Jack *et al.*, 2001). It was also observed that *tatA* was expressed at levels 50-200 times in excess of that seen for the unlinked gene, *tatE* (Jack et al., 2001). This TatA:TatE ratio, coupled to the homology between the two proteins, and presence of *tatE* on a separate locus has led to the proposition that *tatE* is a functional duplication of *tatA* (Sargent *et al.*, 1998). Indeed, deletion of *tatA* has a much more drastic effect on transport than deletion of *tatE*. The *tatA*, *tatB* and *tatC* were genes found to be critical for Tat transport, demonstrating that the core gene components for the system are *tatA*, *tatB* and *tatC* (Sargent *et al.,* 1998*,* Sargent *et al.,* 1999, Weiner *et al.,* 1998*,* Bogsch *et al.,* 1998).

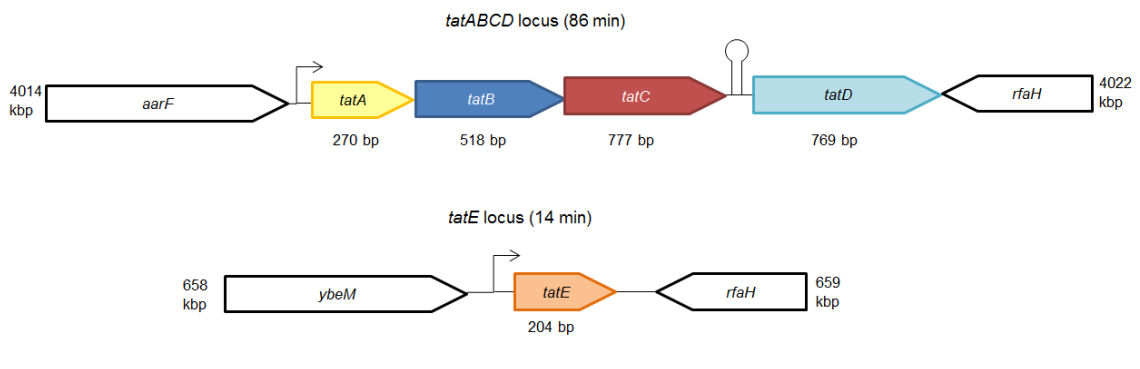

Figure 1.8) *E. coli tat* genes- The polycistronic *tatABCD* locus is at 86 min on the *E. coli* chromosome, with a predicted RNA step loop separating *tatC* and *tatD*. Monocistronic *tatE* is located at 14 min. Neighbouring genes are shown in white.

Generally, plant chloroplasts and Gram-negative organisms, such as *E. coli*, harbour a Tat system containing three core subunits, TatA and TatB which belong to the TatA family and a third subunit belonging to the TatC family. In Gram-positive bacteria (with the exception of the actinobacteria) and archaea a separate TatB is not usually found.

However these organisms frequently code for more than one copy of TatA and TatC, for example the Tat system in Gram-positive *Bacillus subtilis* is encoded by *tatCd* and *tatCy* and three *tatA* paralogues (*tatAd*, *tatAy* and *tatAc*) (Jongbloed *et al.*, 2004). Though it appears that TatA and TatB share a common ancestor, which accounts for their structural and sequence similarities (Yen *et al.*, 2002), where present they have been found to serve functionally distinct roles in the Tat translocase (Sargent *et al.*, 1999). Indeed, while deletion of *tatB* is extremely detrimental to the function of the *E. coli* Tat system, single amino acid substitutions in the N-terminal region of TatA can compensate for the loss of TatB (Sargent *et al.*, 1999, Blaudeck *et al.*, 2005). This has led to the proposition that TatA and TatB are functionally distinct and TatA subunits found in Gram-positive and archaeal TatAC systems are “bifunctional”, able to fulfil the roles of both TatA and TatB. To further substantiate this, TatA from the TatAC system of *Bacillus subtilis* has been shown to substitute for both TatA and TatB in the *E. coli* TatABC system (Barnett *et al.*, 2008). Finally, it should be noted that deletion of *tatB* from TatABC-based translocase systems does not always prevent Tat activity, with Gram-negative bacterium *Helicobacter pylori* able to carry out Tat transport without TatB (but not TatC) (Benoit & Maier, 2003).

1.10.1 The homologous TatA, TatB and TatE proteins

E. coli encodes three components of the TatA family; TatA itself, TatB and TatE. All three proteins have a similar topology, with a periplasmic-facing N-terminus followed by a short transmembrane helix linked *via* a hinge region to a longer, perpendicular amphipathic helix at the cytoplasmic side of the inner membrane. Each protein is also thought to have a C-terminal disordered region which protrudes into the cytoplasm (Koch *et al.*, 2012) (Fig 1.9A). Truncation experiments with TatA and TatB show that this C-terminal disordered region is not essential for Tat function (Lee *et al.*, 2002).

The *E. coli* TatA and TatE proteins share 53% sequence identity, and are more closely related to each other than to TatB. TatE itself is thought to function in a similar manner

to TatA, but is present at much lower levels (Sargent *et al.*, 1998, Jack *et al.*, 2001) (Fig. 1.9B). TatB has both a larger amphipathic helix and C-terminal disordered region than both TatA/E with its N-terminal region sharing 20% identity with TatA (Sargent et al., 1999, Hicks *et al.*, 2003). The notable presence of polar amino acids in the TM of TatA family proteins, such as Q8 in TatA, will be discussed in Section 1.11.

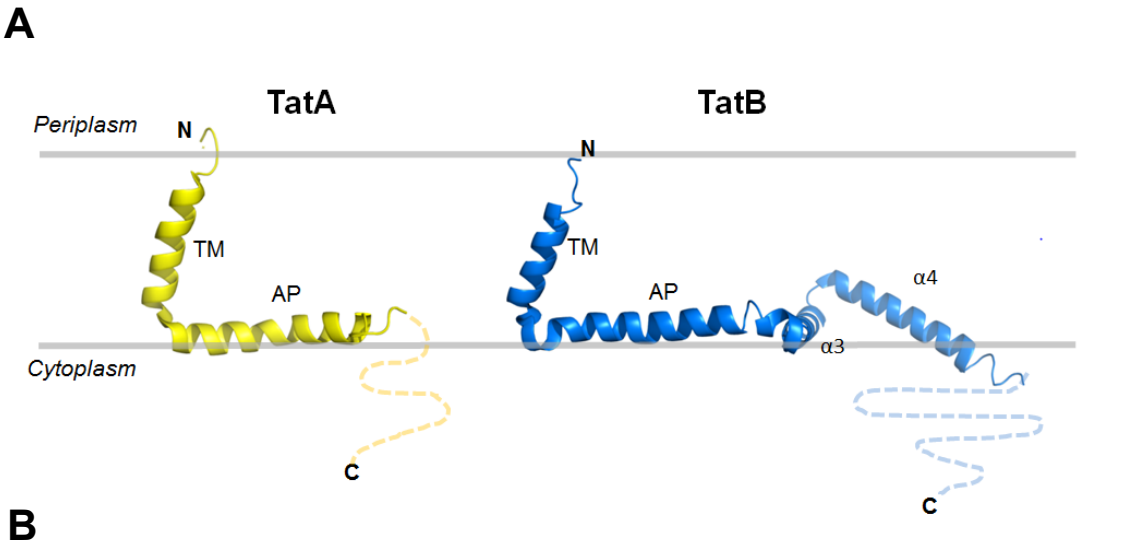

Figure 1.9) Solution NMR structures of homologous TatA and TatB with alignment of *E. coli* TatA family proteins- A- Amino acid number and region of each protein is noted above the sequences and grey cylinders denote alpha helical regions of the protein- adapted from Frobel *et al.*, 2012b **B-** Sequence alignment of TatA family proteins transmembrane (TM) and amphipathic (AP) helices of each protein are noted, along with a dashed region at the C-terminus representing the non-essential disordered region of each protein. TatA structure: Rodriguez *et al.* (2013), PDB: 2LZR and TatB structure: Zhang *et al.* (2014). PDB: 2MI2. (PDB- Protein Data Bank ID)

1.10.2 TatA and TatE

E. coli TatA is a small protein with a molecular mass of 8.9 kDa. The NMR structure of TatA was obtained in 2013, showing the transmembrane helix (TM) perpendicular to the amphipathic helix (AP) linked by a hinge region holding them at around 90 degrees to each other (further conformations will be outlined in section 1.10.6). The flexible

region at the N- and C- terminus of the protein was observed (Fig. 1.10A). The last 40 non-conserved amino acids in the disordered C-terminal region were removed to aid in structure derivation. TatA is known to self-interact, which will be expanded on in detail in Section 1.10.6.

Residues in the AP of TatA have been found to be more sensitive to substitution than in the TM (Hicks et al., 2003, Greene *et al.*, 2007). Highly conserved residues in the hinge/amphipathic region include F39, G21, F20 and a charged amino acid at position 41 (Hicks et al., 2003) (Fig. 1.10B). The F39A substitution was found to abolish transport completely and to show dominant negative behaviour. Additionally, screening random mutant libraries for defective TatA proteins highlighted a number of residues important for Tat transport, all located in the amphipathic or hinge region. In particular mutations T22A in the hinge region and D31G, A42T and G33S/G33D in the AP were all found to prevent self-interaction when TatA self-crosslinking experiments were performed (Fig.1.10B) (Hicks et al., 2003, Hicks *et al.*, 2005).

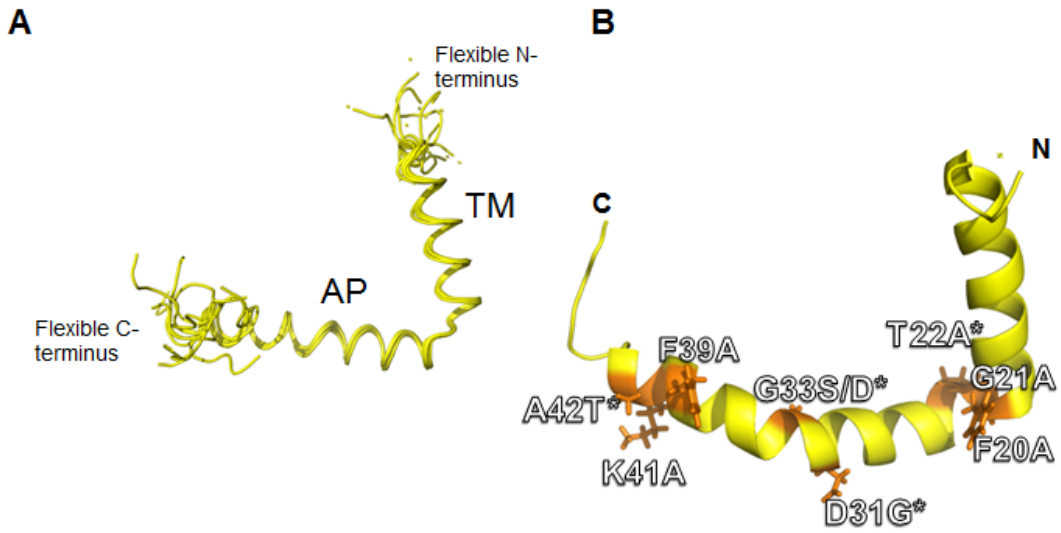

Figure 1.10) Solution NMR structures of TatA with transport-defective residues highlighted- A- shows structure ensemble of TatA with the 10 lowest energy states derived from solution NMR, demonstrating flexibility in the C and N-terminal regions, note- Tat was truncated, removing the longer, disordered, nonessential C-terminal tail not displayed in the structure (Rodriguez *et al.,* 2013, **B-** Notes amino acids in orange found to negatively impact Tat function from Hicks *et al.* (2003; 2005) mapped onto solution NMR structure for TatA. Residues with * were demonstrated to prevent TatA self-interaction *via* crosslinking (Hicks *et al*., 2005). TM- transmembrane helix, AP- amphipathic helix, PDB: 2LZR

Data concerning the function of TatE is scarce, likely due to TatE being regarded as a lower abundance, non-essential, functional duplication of TatA (Sargent *et al.*, 1998). TatE has been found to substitute for TatA in restoring transport of some substrates when overexpressed (Sargent *et al.,* 1999, Baglieri *et al.,* 2011) and restore activity to a transport-defective TatA-YFP fusion when they are co-expressed (Alcock *et al.*, 2013). Indeed very recently it has been proposed to be a regular constituent of the Tat complex in *E. coli* based on crosslinking experiments (Eimer *et al.*, 2015). Though whether these data show that TatE occasionally substitutes for TatA in the Tat machinery or it has a discrete function of its own is not fully understood.

1.10.3 TatB

TatB is the largest member of *E. coli* TatA protein family with a molecular mass of 18.5 kDa. While it has a larger amphipathic helix (AP) and C-terminal disordered region, TatB is oriented in the membrane in a similar manner to TatA (Koch et al., 2012, Zhang *et al.*, 2014). From the NMR structure, TatB has the two additional helices (α3 and α4) in the C-terminal region. Flexibility was pronounced in the C-terminal region with the α4 helix in particular found to be floppy (Zhang et al., 2014) (Fig. 1.11).

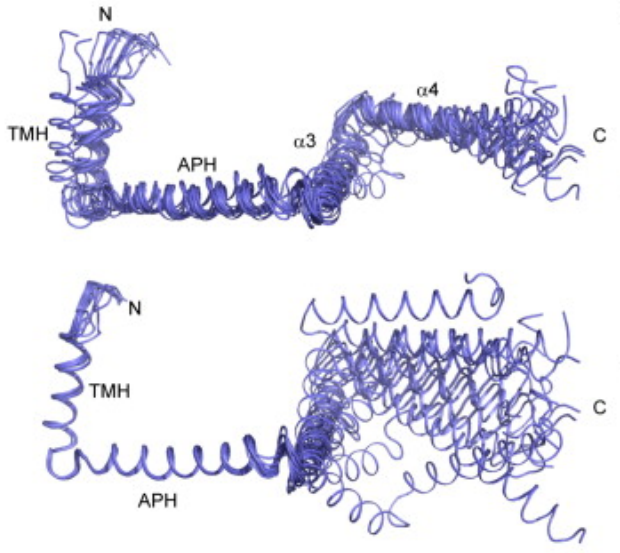

Figure 1.11) Solution NMR ensemble structures TatB- upper- 15 lowest energy conformers of TatB aligned to backbone residues 1-100 and **lower-** aligned to backbone atoms of residues 6-47. Taken from Zhang *et al.* (2014), TMH- Transmembrane helix, APH- Amphipathic helix.

As with the solution NMR experiments for TatA, TatB is truncated in the structure derivation, with non-conserved amino acids at the C-terminal region (the last 70 on TatB) not present.

In *E. coli* membrane fractions, chemical crosslinking demonstrated that TatB self-associated into at least homodimers (De Leeuw *et al.*, 2001), with site-specific crosslinking later identifying oligomers of up to six TatB units under similar conditions (Lee *et al.*, 2006a). The latter study observed one self-interacting face of TatB in the transmembrane helix through residues involving residues in the TM (Lee et al., 2006a) TatB multimerisation within the TatBC complex will be discussed in section 1.10.5.

1.10.4 The TatC core

TatC is the largest component of the Tat system, at 28.9 kDa in *E. coli*, and is essential for Tat function (Bogsch *et al.*, 1998). Topologically, TatC has six transmembrane helices with the N- and C- termini both located in the cytoplasm (Drew *et al.*, 2002, Behrendt *et al.*, 2004, Punginelli *et al.*, 2007a)). The crystal structure of TatC from thermophile, *Aquifex aeolicus* was obtained in 2012, and used to build a homology model for the structure of *E. coli* TatC, shown in Fig. 1.12A. This presents the predicted six transmembrane helices (TMs) forming a concave arrangement centred around TM4, with a short TM5 and 6 causing a pinching effect on the membrane lipids. The periplasmic loops 1 and 2 were found to form a cap, referred to as the “periplasmic cap”, which overhung the concave face of TatC (Rollauer *et al.*, 2012).

One of the most notable features of *A. aeolicus* TatC is the conserved residue E165 which appears to protrude out of the concave face into the hydrophobic lipid bilayer. The significance of this ionisable amino acid was supported by molecular dynamic simulations which observed bilayer perturbations as E165 attracted the lipid head groups. Due to this it was proposed that the E165 is likely buried through interactions with another component with candidates and is explored in Section 1.10.6 (Rollauer et al., 2012, Ramasamy *et al.*, 2013). In *E. coli* the equivalent residue is located at

position 170 (see Fig. 1.12A). A map of conserved residues in TatC is presented in Fig. 1.12B, with regions at the cytoplasmic side of TM1 and TM2, along with residues at the top of TM5 forming patches of conservation (Rollauer *et. al.*, 2012).

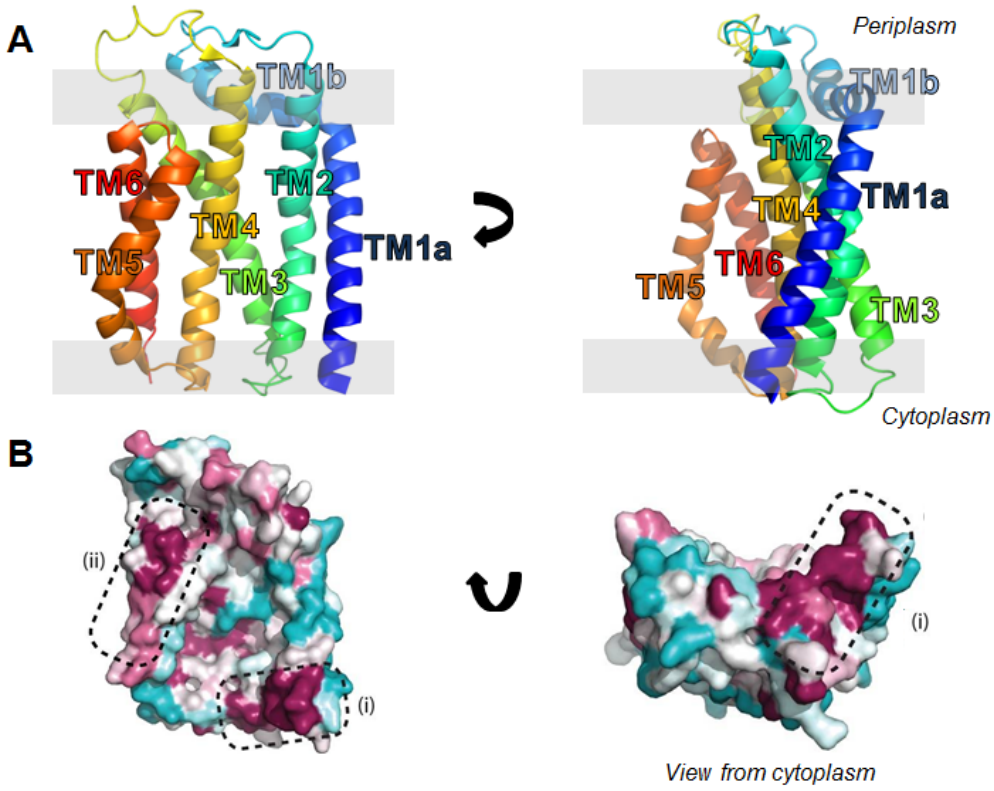

Figure 1.12) Crystal structure of *Aquifex aeolicus* TatC- A- Ribbon diagram of the *A. aeolicus* TatC crystal structure solved at a 3.5 Å resolution with transmembrane helices labelled TM 1-6 superimposed on a lipid bilayer representation (grey). Adapted from Rollauer *et al.* (2012). **B-** Surface diagram of TatC with conserved residues identified with maroon representing high and cyan representing low conservation. Areas of high conservation are labelled (i) and (ii). Consurf model taken from Rollauer *et al.* (2012).

Although TatC from *A. aeolicus* crystallised as a dimer, with contacts observed through two TM5 regions, the orientation is not considered topologically reasonable given that one monomer was flipped vertically (Rollauer et al., 2012). Self-contacts were also observed in the crystal structure between the TM1 however with the lack of conservation in this region (Fig. 1.12A and B) it was considered unlikely to be a native interaction site (Rollauer et al., 2012). TatC is able to support Tat transport when expressed as a fused dimer (Maldonado *et al.*, 2011) and in *E. coli* membrane fractions, was found to self-interact *via* disulphide crosslinks across all six helices (Punginelli *et al.*, 2007b, Kneuper *et al.*, 2012, Rollauer et al., 2012, Lee et al., 2006a).

This is supported by photo-crosslinking experiments in *E. coli* inside-out inner membrane vesicles (INVs), where similar extensive self-interaction of TatC was found, specifically in the first periplasmic loop (Zoufaly *et al.*, 2012), TM5, TM4 and TM2, with weaker associations at TM3 (Blummel *et al.*, 2015). This extensive self-crosslinking across the whole protein makes it difficult to identify an exact interaction face of TatC.

Of the self-crosslinks seen in TatC, the body of literature so far has consistently identified a TM5-TM5 self-interaction, which has been frequently observed *in vitro* (with the two monomers presumed to be in the same orientation as opposed to the crystal structure packing) (Kneuper *et al*., 2012, Rollauer *et al*., 2012, Punginelli *et al*., 2007, Blummel *et al*., 2015) however a recent study showed that in living *E. coli* cells, with Tat subunits expressed from low copy vector, self-interaction in this region was only detected in the presence of an overexpressed substrate (Cleon *et al.*, 2015). From this it appears that protein amount and experimental conditions (i.e. membrane fractions and INVs as opposed to living cells) may have a bearing on the crosslinks seen, perhaps suggesting that while TatC can self-interact at many positions, at least some may be specific to certain circumstances. TatC TM5 is of particular interest because it has also been shown to crosslink TatB and the Tat signal peptide, which will be explored further in section 1.10.5.

The periplasmic cap, composed of periplasmic loops 1 and 2, is also a candidate site for TatC self-interaction based on disulphide crosslinking in *E. coli* membrane fractions (Punginelli et al., 2007b) and photo-crosslinking in INVs from the same organism (Zoufaly *et al.*, 2012). Unlike self-crosslinks in the TM5, crosslinks in this region were also seen in living cells from a low copy number vector (Cleon et al., 2015). Furthermore, the latter study also identified dominant negative mutations in the periplasmic cap which ostensibly abolished the TM5-TM5 self-interaction site, while maintaining periplasmic loop contacts. These substitutions included P48L, M59K, S66P, V145E and D150Y. Indeed, it appears that there is more than one self-contact site on TatC that may be relevant at different points during transport of substrate.

Support for the *E. coli* TatC self-interactions is provided by self-crosslinks observed in the plant homologue, cpTatC, at helix 5, and luminal (analogous to periplasmic) loops 1 and 2 (Aldridge *et al.*, 2014) with co-purification experiments suggesting the plant equivalent to the periplasmic cap was important for self-interaction (Aldridge et al., 2014, Ma & Cline, 2013).

Thus TatC likely acts as an obligate oligomer, with multiple self-contact sites within the TatBC recognition complex. Higher order oligomers of TatC will be discussed as part of the TatBC complex in section 1.10.5.

1.10.5 The TatBC recognition complex

Affinity purification and BN-PAGE (blue native-polyacrylamide gel electrophoresis) analysis of Tat subunits shows that TatB and TatC interact as a stable hetero-oligomer with a stoichiometry of 1:1 (Bolhuis *et al.*, 2001, Orriss *et al.*, 2007, Tarry *et al.*, 2009, Oates *et al.*, 2005), with an analogous complex also detected in plants (Cline & Mori, 2001). TatA has been found to be weakly associated with this complex in numerous co-purification experiments (Bolhuis et al., 2001, Oates *et al.*, 2003, Porcelli *et al.*, 2002, de Leeuw *et al.*, 2002), and has been found to co-purify with TatC in the absence of TatB (Fritsch *et al.*, 2012). The culmination of this data has led to the alternate designation of the TatBC complex as Tat(A)BC. The molecular weight estimation of this Tat(A)BC complex varies depending on the purification method used, with approximations of 370-700 kDa derived (Bolhuis et al., 2001, Cline & Mori, 2001, Oates et al., 2005, McDevitt *et al.*, 2006).

It has been demonstrated that in the absence of TatA, this discrete TatBC complex is still able to form, with no detectable size change on BN-PAGE (Orriss et al., 2007). Indeed, immunoprecipitation of native level Tat subunits failed to detect any association of TatA with TatBC (McDevitt et al., 2006). However it should be noted that the presence of TatA has been found to modulate TatBC-substrate interactions in

fluorescence-based experiments (Whitaker *et al*., 2012). Therefore when this study refers to the TatBC complex, this potential role of TatA is taken into account.

The TatBC complex, purified without TatA, has been visualised directly by single particle electron microscopy- yielding a low resolution structure with a hollow hemicircular arrangement containing an estimated 6-8 copies of each subunit (Fig. 1.13). Up to two bound SufI substrates were also observed at adjacent sites- leading to the hypothesis that the complex is multivalent and that there are stronger and weaker binding sites on the complex (Tarry et al., 2009).

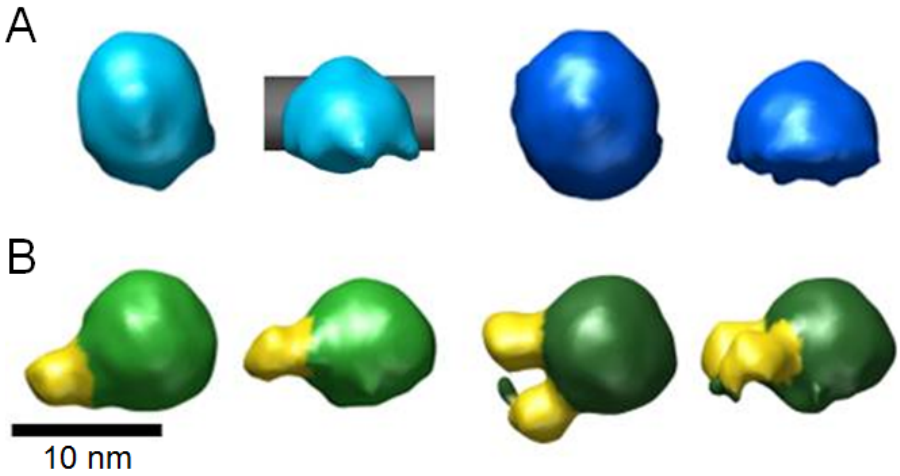

Figure 1.13) 3D maps of $TatBC_{His}$ recognition complex from single-particle electron microscopy, A- Smaller (light blue) and larger (blue) $TatBC_{His}$ complexes, with lipid bilayer representation in gray added on the small complex. **B-** TatBC complex (green) bound to 1 (left) and 2 (right) $SufI_{His}$ substrates. Taken from Tarry *et al*. (2009).

More recently, *in vivo* experiments with TatB-YFP and TatC-YFP protein fusions have been able to probe associations using fluorescence microscopy. Here, as in detergent solution, it was observed that TatBC forms a stable complex (Alcock *et al*., 2013). Further to this the same study found that TatB formed lower order oligomers (outlined in section 1.10.3) in the absence of TatC, with the oligomerisation state of TatC unaffected by the absence of TatB, consistent with previous data (Orriss *et al*., 2007, Behrendt *et al*., 2007). Other fluorescence-based studies observed fluorescence resonance energy transfer (FRET) between substrate, pre-SufI, and both TatB and TatC, which was reversible upon the addition of non-fluorescent pre-SufI, further

supporting the TatBC complex's role in recognising substrate and suggesting a reversible binding step to TatBC (Whitaker et al., 2012).

A host of genetic studies in *E. coli* have been able to isolate mutations in *tatB* and *tatC* which can rescue binding of defective signal peptides. From these it was discovered that amino acid substitutions in the first and second cytoplasmic loops of TatC and the N-terminal region of TatB could successfully facilitate transport of a passenger domain attached to a defective Tat signal peptide (Fig. 1.14A) (Kreutzenbeck *et al.*, 2007, Strauch & Georgiou, 2007, Lausberg *et al.*, 2012).

Mutations in TatC have been found that prevent the recognition of Tat signal peptides. Specifically it was found that amino acid substitutions P48A in TM1 at the periplasmic facing side, F94A, Y100A and E103A at the cytoplasmic facing region at TM1 and TM2 including the cytoplasmic loop 2 and Y126A at the top of TM3 prevented substrate binding (Holzapfel *et al.*, 2007). Of these mutations P48A, F94A and E103A had identified previously to independently have a negative impact on Tat function (Allen *et al.*, 2002, Barrett *et al.*, 2005, Buchanan *et al.*, 2002). Indeed Buchanan and co-workers noticed that F94A and E103A mutations in *E. coli* were able to block transport of both TorA and SufI substrates (Fig. 1.14A). A more recent fluorescence study was able to expand on the effect of some of these substitutions by showing that signal peptide binding and transport was blocked when TatC contained the F94A and E103A substitutions (Alcock et al., 2013). Indeed it appears that the regions of TatC that have been found to mediate signal peptide binding overlap when using various genetic studies, solidifying the importance of the TatBC complex itself in recognising signal peptides and particularly residues in or near the cytoplasmic loops of TatC.

In agreement with the genetic data, interactions have been observed between the signal peptide and TatBC. Photo-crosslinks, whereby a Bpa residue (benzoylphenylalanine) is engineered into TatC which can crosslink nearby molecules upon exposure to UV light, have demonstrated that regions in TatC interact directly

with the signal peptide in *E. coli* INVs at the cytoplasmic facing regions of TM1 and the first cytoplasmic loop (Zoufaly *et al.* 2012) and at a distal site at TatC helix five (Blummel et al., 2015). The observation of separate signal peptide binding sites at TM1 and cytoplasmic loops 1 and 2 with a distal site at TM5 are also in agreement with plant Tat models, which observed crosslinks between the stromal (analogous to cytoplasmic)

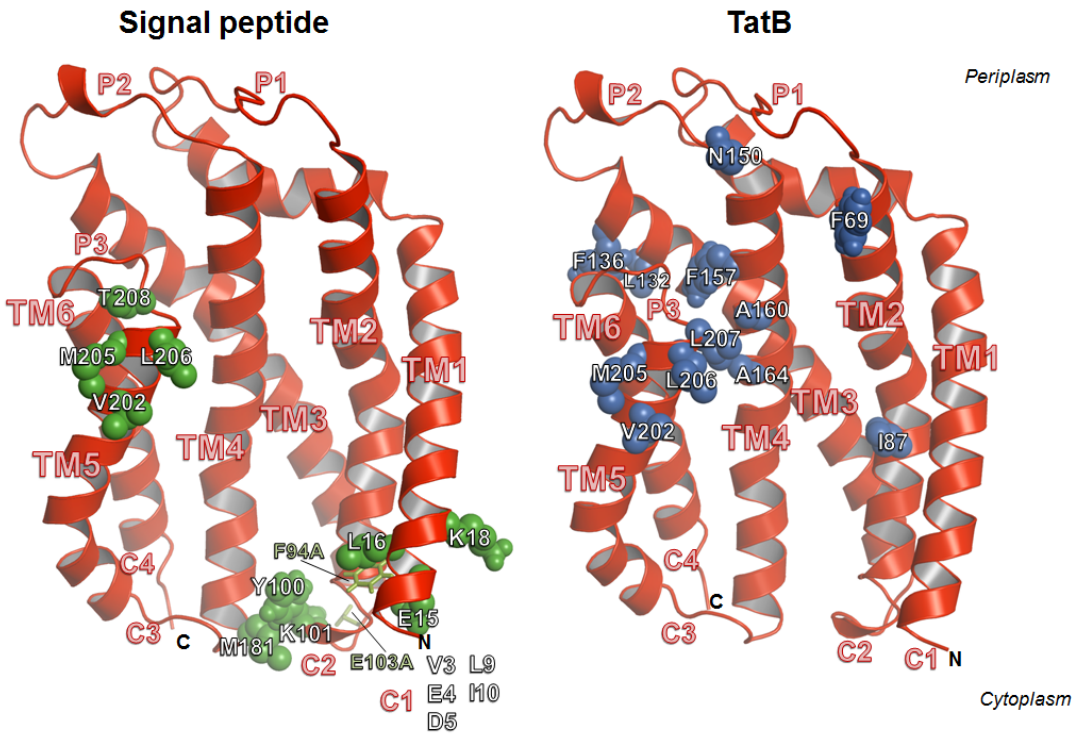

Figure 1.14) Homology structures of *E. coli* TatC highlighting residues important for signal peptide and TatB binding- A- Residues shown as green spheres are shown to photo-crosslink the Tat signal peptide, with residues shown as sticks shown to be important in signal peptide binding directly in fluorescence based (Alcock *et al.*, 2013) and genetic studies (Holzapfel *et al.,* 2007) **–** amino acids in the N-terminus but not in the structure are listed- which were all shown to crosslink signal peptide. **B-** TatC as on the left with residues as blue spheres shown to be in the proximity of TatB *via* photo and disulphide crosslinking (Kneuper *et al.,* 2012, Rollauer *et al.,* 2012, Zoufaly *et al*., 2012, Blummel *et al*., 2015) with TM1-6 denoting transmembrane helices, P1-3 periplasmic loops and C1-4 cytoplasmic loops. Figures created using PyMol.

regions 1 and 2 and the substrate RR sequence (Ma & Cline, 2010) with subsequent data showing crosslinks between cpTatC TM5 and the hydrophobic region of the signal peptide (Fig. 14A) (Aldridge et al., 2014).

Identifying interactions from the perspective of the signal peptide, it has been shown that the consensus sequence in the n-region of the Tat signal peptide binds TatC, while the hydrophobic h-region and precursor protein are in the vicinity of TatB (Alami *et al.*,

2003, Gerard & Cline, 2006, Maurer *et al.*, 2010). The signal peptide binding site on TatC at TM5 may reflect the deep insertion of the signal peptide into the recognition complex that was previously proposed in plant and bacterial models (Gerard & Cline, 2007, Frobel *et al.*, 2012). Further to this, molecular dynamics simulations have suggested that the signal peptide may interact within the concave face of TatC, involving the *E. coli* E170 residue at TM4 (Ramasamy *et al.,* 2013) with further studies proposing that the signal peptide binds deeply in the TatBC complex as a hairpin loop in the concave face of TatC (Blummel *et al.,* 2015).

When expressed as a single fusion protein, TatBC is able to support Tat transport, suggesting that TatB and TatC act together as an individual unit within the TatBC complex (Bolhuis *et al*., 2001). Photo-crosslinking in INVs show that a Bpa residue in TM5 of TatC was able to crosslink with TatB (Zoufaly *et al*., 2012), while Bpa incorporation at positions in the flexible N-terminal region of TatB (see Fig. 14B) formed crosslinks with TatC (and TatA, which will be discussed in section 1.10.6) (Blummel et al., 2015). Disulphide crosslinks between the TM of TatB and the TM5 of TatC have also been observed in *E. coli* membrane fractions (Rollauer *et al.,* 2012, Kneuper *et al.,* 2012) whereas a D211A substitution in TatC at the nearby P3 loop abolished TatB co-purification with TatC (Buchanan *et al.*, 2002) providing further biochemical evidence for the importance of this region on TatC for TatB-C interactions.

More recently however, a second binding site for the TatB TM was proposed around the TM2/4 of TatC based on photo-crosslinks (Blummel et al., 2015), with TatB simultaneously in the proximity of another TatC TM5 (see Fig. 14B and 15A). As mentioned in section 1.10.3 TatB is able to form oligomers in *E. coli* membrane fractions (Lee et al., 2006a) and when the crosslinking pattern is combined with self-crosslinking observed with TatC in similar conditions (Punginelli et al., 2007b) it seems likely that TatB forms an oligomer in the TatBC complex with TatC on the outside. Further to this multiple TatB units have been shown to form adducts which crosslink one Tat substrate which suggests, in the context of a TatBC complex, that the

substrate may localise to the TatB oligomer at the centre prior to transport (Maurer et al., 2010).

Taking into account the two sites for TatB on TatC, a recent model for the TatBC recognition complex has been presented, with an adapted version presented in Fig. 15B and C, showing a tetramer of TatB within a tetramer of TatC (Blummel et al., 2015). Blummel *et al.* (2015) acknowledge in their work that tetramerisation was merely based on the tetramer units of TatB in their photocrosslinking and the TatBC units in the model could be accommodated to incorporate further TatBC units. Indeed, photo-crosslinked TatC oligomers up to hexamers have been observed proposed to be joined *via* a bifunctional linker through Cys residues incorporated at D63 (in the first periplasmic loop) and A163 (at the periplasmic region of TM3) (Blummel et al., 2015) (Fig. 1.15A and C). Furthermore this arrangement of TatC subunits does not account for all the self-interaction of TatC residues outlined in section 1.10.4, given that the TatC TM5-TM5 interaction was only observed in the presence of increased substrate flux through the Tat pathway (Cleon et al., 2015). While this model is presumed to represent the resting Tat system, it seems more information is required as to the stage of Tat transport associated with each self-interacting site before they can be mapped directly onto a model.

Disulphide-crosslinking studies between plant homologue cpTatC and Tha4 (TatA) draw similar conclusions to that observed in *E. coli*, with Hcf106 positioned at the cpTatC TM5 in close proximity to a nearby Tha4 which will be discussed in section 1.10.6. The signal peptide of the substrate has the consensus twin arginine motif interacting near the thylakoid (stromal) regions at the bottom of cpTAtC TM1 and TM2 with the rest of the signal peptide in the proximity of Hcf106 and the TM5 of another cpTatC forming as dimer (Aldridge *et al*., 2014). Although Aldridge *et al.* present a dimeric cpTatC-cpTatC they acknowledge that questions still need to be answered regarding higher order states (Aldridge et al., 2014). The Tat signal peptide interacts with TM5 of TatC even in the presence of TatB, and this appears to be accounted for in

the model presented in Blummel *et al.* (2015) with TM5 near the centre of the TatBC complex (Fig. 1.15C). Additional accessibility studies of a Tat substrate precursor protein signal peptide in *E. coli* INVs using the membrane-impermeable probe, PEGMAL, suggested that the peptide was inserted into the TatBC complex in a hairpin

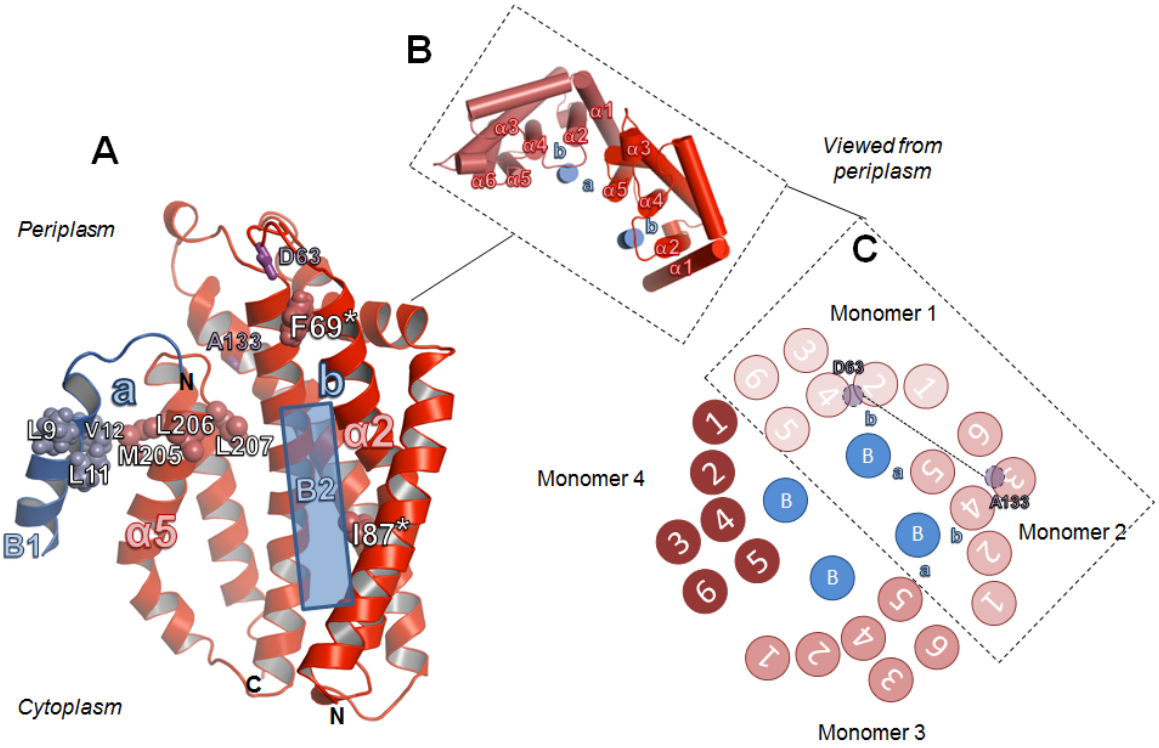

Figure 1.15) Summary of proposed TatB-C interactions in the recognition complex-A- Diagram representing proposed TatB-C interaction sites on a monomer of TatC, "a" represents a proposed TatB site on TatC (in red) at transmembrane helix 5 (TM5) with the TatB transmembrane helix shown as a blue ribbon. Residues shown as spheres in TatB and TatC TM5 were demonstrated to interact *via* disulphide crosslinking in *E. coli* membrane fractions (Kneuper *et al.*, 2012, Rollauer *et al.*, 2012). "b" represents the more recent proposed TatB site with residues noted by * shown to photo-crosslink TatB but be too far from the "a" site be accounted for by one TatB interacting at both sites. A second TatB is shown as a blue rectangle. Residue A133 was found to crosslink to D63 of another TatC (Blummel *et al.,* 2015) using a bifunctional linker, these are both shown as magenta sticks. **B-** Viewed from the periplasm, a dimer of TatC showing the arrangement of TatC TM helices and the positioning of sites "a" and "b". **C-** A schematic diagram of the TatBC complex adapted from Blummel *et al.* (2015), with the tetrameric state of TatB and TatC and self-crosslinking residues from A- shown as purple circles.

conformation (Blummel *et al.*, 2015). This is consistent with data suggesting a deep-insertion of the signal peptide into the recognition complex (Gerard & Cline, 2007, Frobel et al., 2012). Indeed, it seems that the Tat signal peptide interact initially at the cytoplasmic facing side of TatC TM1 and TM2 before moving deeper into the complex at TM5.

1.10.6 The role of TatA

Detergent-solubilised *E. coli* TatA has been observed to form ladders on BN-PAGE with bands separated by a step size of around 34 kDa. This size difference works out as units of tetramers, taking into account the monomeric size of TatA (8.9 kDa) (Oates et al., 2005) and the scale of these oligomers ranges from ~100 kDa to over 700 kDa. (Gohlke *et al.*, 2005, McDevitt et al., 2006, Oates et al., 2005, Porcelli et al., 2002, Bolhuis et al., 2001, Sargent *et al.*, 2001, de Leeuw et al., 2002).

This tetrameric state of TatA was further supported by disulphide crosslinking experiments of Tha4 (TatA) in plants (Dabney-Smith & Cline, 2009) and fluorescence data in *E. coli* tracking a TatA-YFP fusion at native level expression, which found assembly of the protein into average units of four when expressed in the absence of TatBC, with larger TatA complexes of varied size only forming in the *E. coli* membrane only when TatBC was present, (Leake *et al.*, 2008). Interestingly, it appears that in detergent solution TatA can still self-associate into larger oligomers both in the absence of TatBC and with transport-blocking mutations in TatC (Porcelli et al., 2002, Oates et al., 2005), suggesting differential behaviour of TatA in native membranes and detergent solution.

It is likely that TatA exists in a tetrameric state when free in the membrane, to be recruited to the TatBC complex in response to substrate binding the latter (Leake *et al*., 2008), though it should be noted that solid state NMR diffusion measurements of *Bacillus subtilis* TatAd in a bicellular environment are at odds with this, suggesting a monomeric state prior to oligomerisation (White *et al*., 2010).

Crosslinking studies in *E. coli* INVs have suggested that TatA is only in the proximity of substrate when a PMF is present (Frobel *et al.*, 2011). TatA oligomerisation has been observed directly in living cells using TatA fused to fluorescent proteins, with bright fluorescent foci being observed (Leake *et al*., 2008, Rose *et al*., 2013, Alcock *et al*., 2013). Alcock and co-workers found that when TatA-YFP was expressed in the

absence of TatBC it showed diffuse fluorescence around the edge of the *E. coli* cell, only concentrating into the characteristic bright foci in response to the presence of both TatBC and overexpressed substrate. TatA was unable to form oligomers when the overexpressed substrate contained a signal peptide with “RR” substituted for non-functional “KK”. The dependence of TatA oligomerisation on PMF was also probed through the use of the uncoupler carbonyl cyanide *m*-chlorophenyl hydrazone (CCCP), whereby the dissipation of PMF blocked TatA oligomerisation in a reversible manner. Notably, TatA oligomerisation was also prevented when TatC was mutated to prevent substrate binding (TatC F94A in combination with E103A, as outlined in section 1.10.5) providing a direct link between substrate and TatA recruitment. Rose and co-workers also observed the TatA oligomerisation dependence on TatBC, PMF and functional substrate using a TatA-GFP fusion and overexpressed substrate, with co-localisation of TatA-GFP and TatB-mCherry also reported in the bright foci/clusters (Rose *et al.,* 2013).

Studies with plants support these *E. coli* studies as the TatA homologue, Tha4, was shown to associate with Hcf106-cpTatC (TatBC) after the latter is triggered by substrate binding (Mori & Cline, 2002, Cline & McCaffery, 2007). This was also demonstrated by increased self-crosslinks between Tha4 that have been observed upon recruitment to the recognition complex indicating it undergoes large-scale reorganisation (Dabney-Smith *et al*., 2006, Dabney-Smith & Cline, 2009).

Negative stain electron microscopy images of the TatA complex have been observed, which have a cylindrical shape, proposed to constitute protein-conducting channel of the Tat system (Sargent et al., 2001) (Fig 1.16). This study was expanded by further electron microscopy experiments which presented a more detailed low resolution set of structures of ring purified ring-shaped TatA oligomers of varying sizes. In these structures the ring was apparently sealed with a “lid”, presumed to be formed by the TatA amphipathic helices (Gohlke et al., 2005). It was proposed that TatA was recruited to the TatBC complex, whereby it formed a ring shape to mediate transport of

the substrate by acting as a “trap door” through the membrane, with the amphipathic helices bending inwards allowing the substrate to translocate through the lipid bilayer. More recent data, however, has shed further light on the TatA behaviour, challenging this trap-door hypothesis. Indeed, the NMR structures for both *E. coli* TatA and *B. subtilis* TatAd show that the hinge region that links the transmembrane and amphipathic helices in TatAd is highly rigid, precluding such a conformational change (Hu *et al.*, 2010, Rodriguez *et al.*, 2013). Furthermore, accessibility studies of *E. coli* TatA found no periplasmic exposure to support the amphipathic helix flipping in whole cells which are able to transport Tat substrates (Koch et al., 2012).

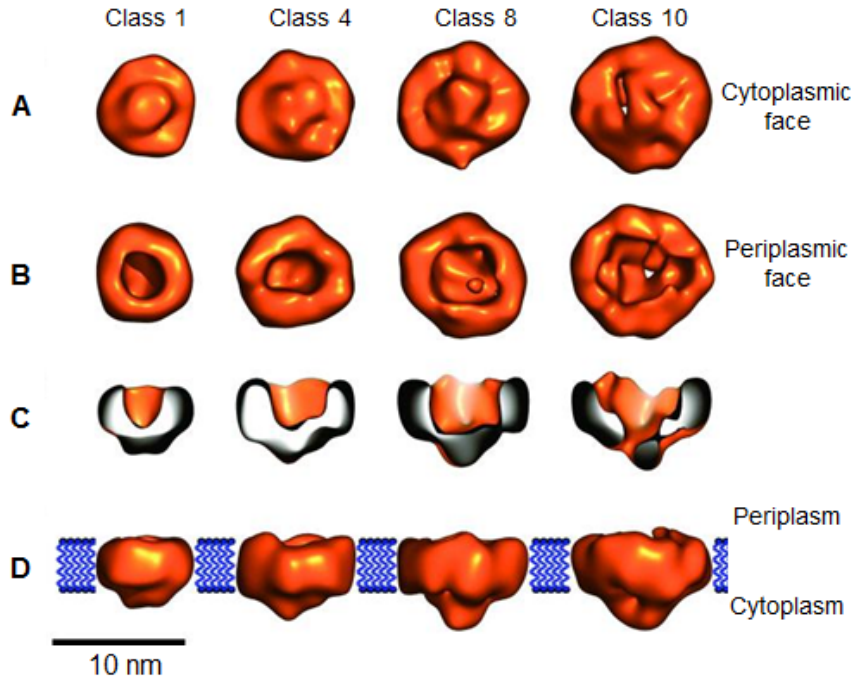

Figure 1.16) Low resolution electron microscopy structures of TatA oligomer- The electron microscopy structures obtained in Gohlke *et al.* (2005) showing varying sizes of the TatA oligomeric complex, from smaller “class 1” through to larger “class 10”, proposed to accommodate differently size substrates, **A-** View of the complex from the cytoplasm, showing the ring shape formed by TatA oligomers is sealed, **B-** The complex from the periplasmic face, **C**- Cross-section through the complex and **D-** with lipid bilayer represented diagrammatically.

A more recent study of TatA self-interaction has modelled the NMR structure of an *E. coli* oligomeric conformer of TatA (Rodriguez *et al.*, 2013) (Fig. 1.17A, B and C). This proposes a ring-like arrangement of subunits, as in the EM structure (Gohlke et al., 2005) with interactions between the transmembrane helices forming a wall. In this case

the amphipathic helices were positioned facing outwards from the centre of the ring (consistent with electron spin resonance distance measurements) with the polar Q8 residue in the transmembrane helix (TM) is facing inwards towards the centre of the ring (Hu et al., 2010, Rodriguez et al., 2013). This arrangement was supported by EPR measurements which show that detergent solubilised TatA oligomers interact through the TM *via* V14 with the I12 of another TatA as a repeating unit (Fig. 17B) (White *et al.*, 2010) but seemingly contradicted crosslinking data from Greene and co-workers that showed self-interactions of TatA *via* L9 and I12 on one face of the TM, and L10 and I11 on the other face (Greene et al., 2007). As White *et al.* (2010) notes, however, this could be due to the fact the Greene *et al.* (2007) crosslinks were performed in native membrane fractions and not solubilised in detergent where the large scale oligomers are found – leading tothe proposition that some crosslinks may be found in the free un-recruited TatA (perhaps as tetramers) and others in the large oligomeric ring.

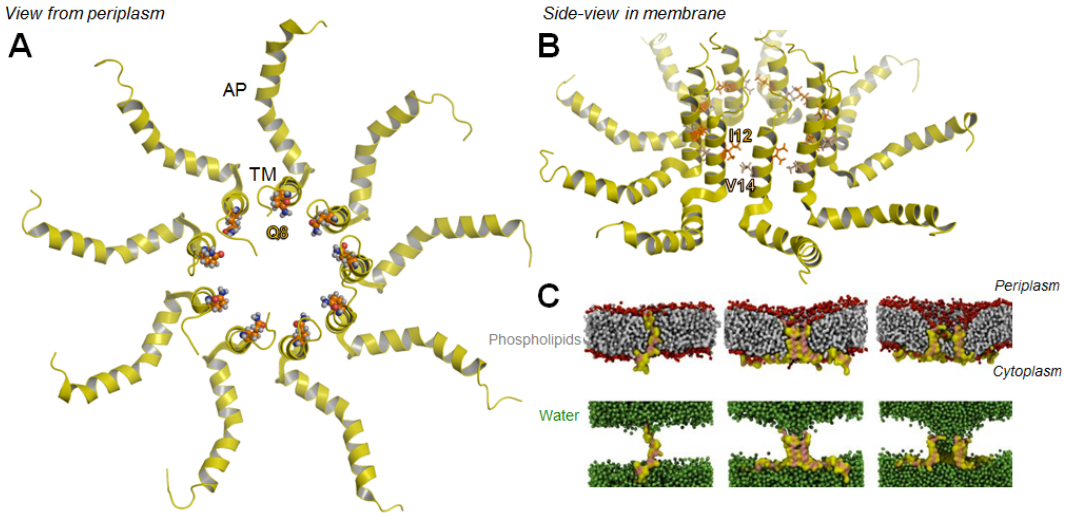

Figure 1.17) Higher resolution proposed arrangements of the TatA complex- A- shows an oligomer created *in silico* using the NMR structure of *E. coli* TatA (Rodriguez *et al*. (2013), PDB: 2LZs) showing a ring of transmembrane (TM) helices with the polar residue, Q8 facing inwards towards the and the amphipathic helices (AP) pointing outwards. This complex is shown viewed from the periplasm (Rodriguez *et al.*, 2013). **B-** As with A- viewed side-on in the membrane with residues I12 and V14 in the TM, which are shown to interact *via* EPR, in the oligomer (White *et al.,* 2010), C- Course-grain molecular dynamics simulations adapted from Rodriguez *et al.* (2013) which show TatA (yellow) making complexes of increasing size from left to right, showing the membrane thinning effect of the complex pulling on the phospholipids (gray) and water (green) accessibility that happened during this process. A- and B- were created in Pymol.

Rodriguez and co-workers also proposed a mechanism for the transport of substrate through the TatA ring. From chemical shift perturbations derived from solving the TatA solution NMR structure in oligomeric and monomeric states, it was suggested that TatA can adopt two conformations. In the resting state, where TatA is not part of any higher order oligomers, the transmembrane helix (TM), which is barely long enough to span the membrane itself, is moved upwards as the hinge widens slightly and angle between the TM and the amphipathic helix (AP) increases, with a tilt allowing TatA to comfortably span the bilayer (Fig. 1.18A). Upon oligomerisation, TatA changes to a second conformation with the transmembrane helix pulled down into the membrane, at ~90 degrees to the amphipathic helix, causing it to "pinch" the lipid bilayer (Fig. 1.18B). This orientation is thought to be shared by all the monomers within the oligomer, having a membrane thinning effect on the localised area within the TatA ring. Coarse grain molecular dynamic simulations shows that this membrane thinning allows water accessibility across the bilayer, thus facilitating substrate transport through the oligomer (Fig. 1.17C and 1.18C) (Hu et al., 2010, Rodriguez et al., 2013). Furthermore, Rodriguez and co-workers found that a T22P in the hinge region of TatA (note an alanine substitution here has already been shown to impair TatA oligomerisation, Hicks *et. al.,* 2005) caused TatA to adopt the oligomer conformation when it was in a monomeric state.

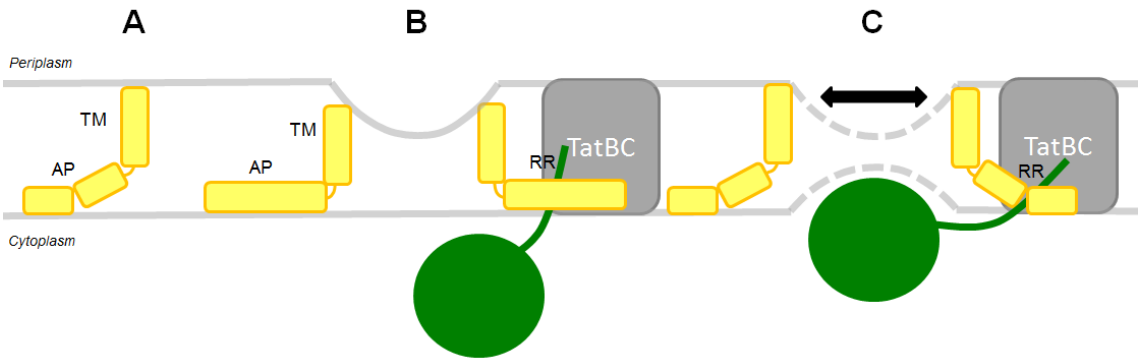

Figure 1.18) Diagram of proposed TatA orientations that cause membrane thinning and subsequent substrate translocation- A- Represents TatA in its monomeric form, spanning the entire bilayer, **B-** shows the proposed orientation of TatA in the oligomeric state, and the pulling downwards of the lipid bilayer that accompanies it, the substrate (green) is shown bound to the TatBC complex, a step which is thought to regulated the oligomerisation of TatA, **C-** A pulling effect of the substrate forces it into the bilayer as the TatA subunits in the oligomer break apart. Adapted from Rodriguez *et al.* (2013).

1.10.7 TatAC interactions

TatA has been shown to directly interact with TatC through photo-crosslinking experiments that demonstrated the transmembrane helix (TM) of TatA is able to associate with TatC directly within *E. coli* inner membrane vesicles (INVs) (Frobel *et al.,* 2011, Blummel *et al.,* 2015). Additionally, plant Tha4 (TatA) was found to transiently interact with cpTatC and Hcf106 *via* chemical crosslinking in the presence of a functional precursor and a proton gradient (Mori and Cline 2002)

To expand on the TatA-C photo-crosslinks in *E. coli* INVs, residues substituted with Bpa at positions in the TM5 and the P3 loop (including residues in TM3 and 4 that face the P3 loop) in TatC were shown to crosslink to both TatA and TatB, which would indicate an interaction with TatA in the vicinity of the TatB binding site (Fig. 1.19A and 1.15A in Section 1.10.5) (Blummel *et al.*, 2015). This is supported by disulphide crosslinking in the plants showing that Tha4 is able to interact at cpTatC TM5 and luminal loop L3 (analogous of *E. coli* periplasmic loop P3) (Aldridge *et al*., 2014). The latter study expanded these potential TatA sites by characterising them in the presence of overexpressed Tat substrate, and found that Tha4 interacted with cpTatC P3/TM5 (near the proposed TatB binding site) in a manner that was unchanged with overexpressed substrate and therefore proposed to be constitutive (Aldridge et al., 2014). Aldridge *et al.* (2014) also presented a model showing Hcf106 (analogous to *E.*

coli TatB) interacting at TatC TM5, with Tha4 interacting nearby with the L3 (P3) loop in a constitutive manner (Fig. 19B). Interestingly, photo-crosslinking in the *E. coli* P3 loop, identified a Bpa at TatC D211 as able to crosslink with TatA, but critically not with TatB, supporting the presence of a TatA/Tha4 binding site near the TatB site at TM5 but further towards the P3 loop region in both plant and bacterial models (Zoufaly *et al.* 2012)

Other interaction sites have been identified in the concave face of TatC in both plants and bacteria (Aldridge *et al.*, 2014), Blummel *et al.,* 2015) with plant studies identifying interactions at cpTatC TM4 being enhanced by substrate overexpression, as with the TM5 interaction (Aldridge et al., 2014). This may reflect TatA polymerisation in the concave face of TatC, triggered in response to substrate. Indeed when the crystal structure of *A. aeolicus* TatC was published, it was proposed that TatA may polymerise with its transmembrane helices arranging in the cup of TatC, around TM4/2 near the conserved E165 (*E. coli* E170) (Rollauer *et* al., 2012).

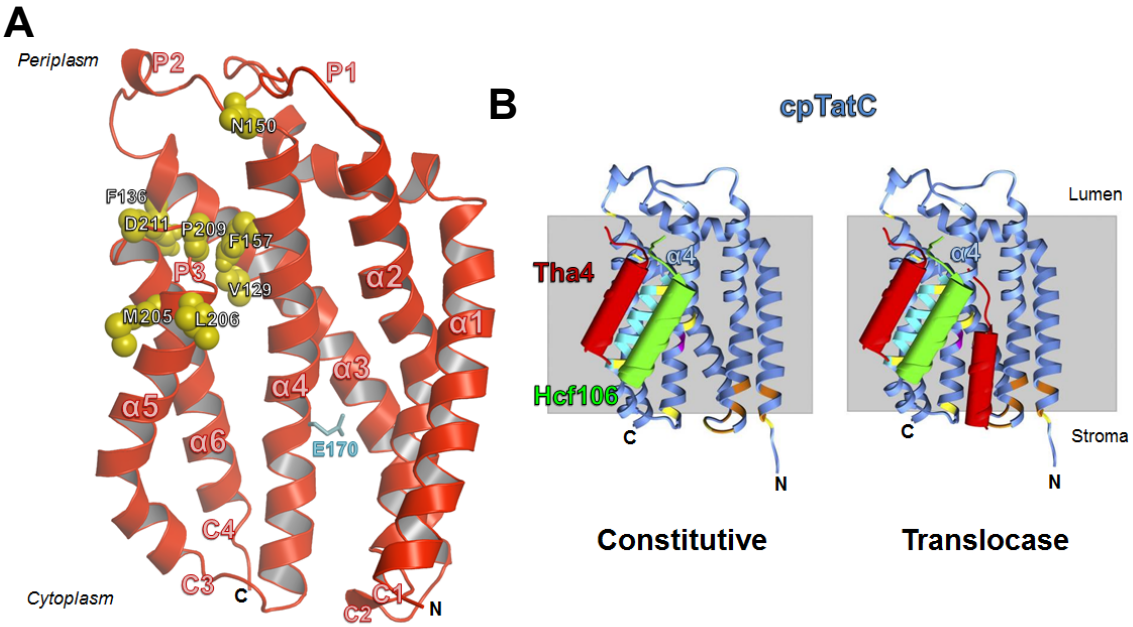

Figure 1.19) Proposed TatA-TatC interactions in bacteria and plants- **A-** demonstrates *E. coli* TatC with residues shown as yellow spheres shown to photo-crosslink to TatA, E170, a residue which may be important for subsequent TatA interactions in the face of TatC is highlighted. **B-** Proposed Tat interactions in the plant homologous Tat system, with the constitutive arrangement having Hcf106 (analogous to *E. coli* TatB) at TM5, shown in cyan, along with nearby interacting Tha4 (analogous to *E. coli* TatA), with Tha4 moving to the concave face of cpTatC during transport. Residues on cpTatC coloured orange are found to be important in signal peptide binding, with yellow residues mutated to Cys in the crosslinking to Hcf106 and Tha4 and the Q234 (equivalent to *E. coli* E170) shown in magenta- adapted from Aldridge *et al.* (2013).

Aldridge *et al.* (2014) were also able to demonstrate a PMF dependence of some of the Tha4 binding sites on cpTatC, with crosslinks reduced at cpTatC TM5 and TM4 in response to dissipation of PMF with ionophore combination nigericin/valinomycin, which will be discussed in detail in section 1.11.

1.11 The Role of PMF

In plants, the twin arginine translocase was discovered as a ΔpH dependent system, distinguishing it from the ATP-dependent Sec system as outlined in detail in Section 1.6. Specifically, it was found that the PMF was required for deep insertion of the Tat signal peptide (Gerard & Cline, 2007, Frobel *et al*., 2012) and also to promote large scale Tha4 self-interaction, as with TatA in *E. coli,* this was discussed extensively in Section 1.10. With regard to signal peptide binding, while substrate has been demonstrated to bind the Tat receptor complex in the absence of PMF in plants (Ma & Cline, 2013) and bacteria (Zoufaly *et al*. 2012), there is evidence to support a deeper binding site for the signal peptide in the TatBC complex, specifically in the concave face of TatC, which may require an intact PMF (Gerard & Cline, 2007, Blummel *et al.,* 2015, Ramasamy *et al*., 2013).

Evidence using an *in vitro* Tat transport system with *E. coli* INV has suggested that the Δψ (electrical potential) of the PMF is more important than the proton gradient for driving Tat transport. From this study it was proposed that Tat transport needed two PMF dependent steps, one with a larger magnitude Δψ for a shorter time and a later step with a smaller Δψ for a longer time (Bageshwar & Musser, 2007). It should be noted in this context that PMF powered Tat transport in thylakoids has been demonstrated to require around 80,000 protons per substrate (Alder & Theg, 2003).

With regard to TatA, there is evidence suggesting a PMF requirement for Tha4 (TatA) recruitment to the recognition complex in plants (Dabney-Smith et al., 2006, Mori & Cline, 2002) and bacteria (Rose *et al.*, 2013, Alcock *et al.*, 2013) along with data showing TatA crosslinking to substrate only in the presence of substrate (Frobel *et al.*,

2012). However, with regard to specific amino acids in TatA, it has been suggested that the N-terminal region and hydrophilic acids in the transmembrane helix could facilitate proton movements from the periplasm during the oligomerisation step, based on molecular dynamics simulations (Rodriguez *et al.*, 2013). It is should be noted here that plant studies have observed that Tha4 interactions at TM5 and TM4 of TatC were reduced in response to PMF dissipation with ionophores nigericin and valinomycin, suggesting the oligomerisation step may occur in the face of cpTatC (Aldridge *et al.*, 2014).

The E165 residue in *A. aeolicus* TatC (equivalent to E170 in *E. coli*) has been identified as a candidate for a protonable amino acid which may play a role in an aqueous channel forming in the cavity of TatC (Rollauer *et al.*, 2012, Ramasamy *et al*., 2013).

1.12 The Tat Transport Cycle

In the current model for Tat transport, 1) TatB and TatC for a recognition complex which is able to bind the signal peptide of a Tat substrate from the cytoplasmic side of the membrane. 2) TatA is then recruited to the recognition complex in a PMF-dependent step whereby it forms an oligomer in the membrane which facilitates transport of the substrate across the membrane. 3) Once the substrate reached the periplasm the signal peptide is cleaved by peptidase, LepB. 4) The processed substrate is then released into the periplasm. 5) The Tat system goes back to its resting state (Fig. 1.20).

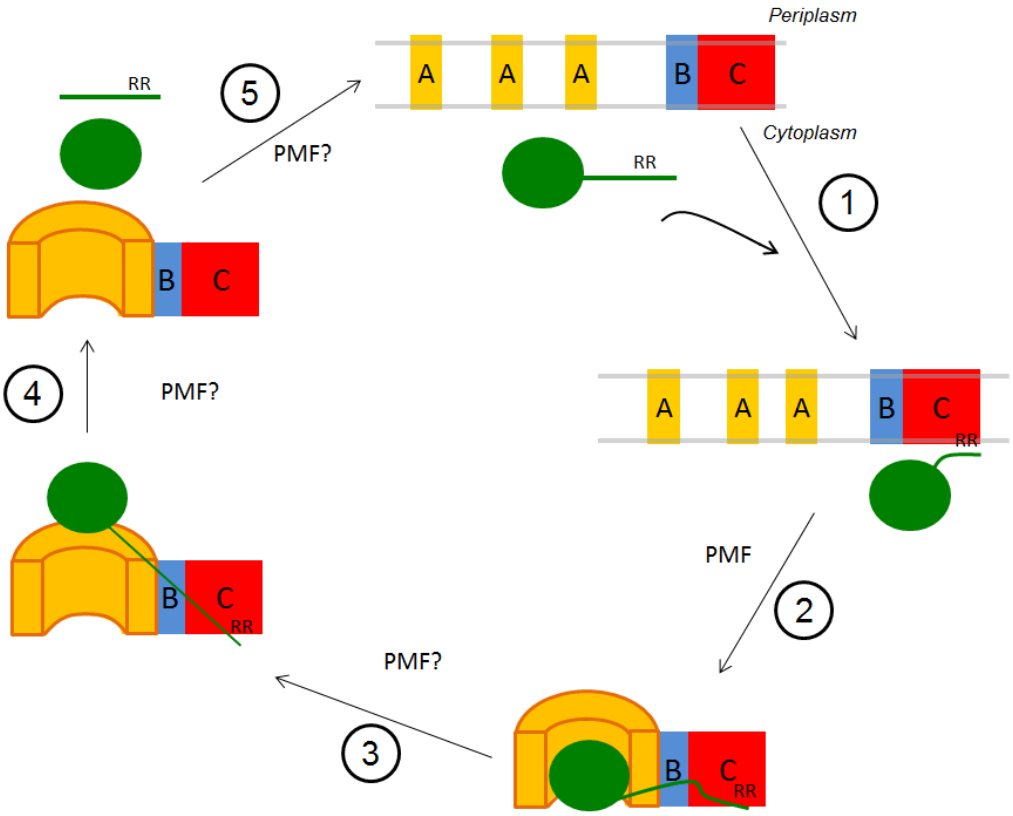

Figure 1.20) Model of Tat transport- TatA (yellow), TatB (blue) and TatC (red) are shown in the membrane, with substrate (green) containing the twin arginine (RR) signal peptide.

1.13 Aims of this Thesis:

The overall aim of this work is to build upon the literature showing interactions between TatA and TatB with TatC, by focussing specifically on the role of TatA and identifying how it associates with TatC, and how these interactions change under various conditions of the Tat cycle (*i.e.* in the resting state, in the presence of overexpressed substrate, and in the absence of *tatB*). Co-purification data showing TatA/B interactions with TatC will be used to complement disulphide crosslinking, which can identify specific residues involved in interfaces between TatA and TatC. Specifically this thesis aims to:

- Further decipher TatA, TatB and TatC subunit interactions using Ni-affinity co-purification experiments with His-Tagged TatC

- Characterise changes in co-purification of TatA/B with $TatC_{His}$ from constructs expressing either TatA or TatB only with $TatC_{His}$
- Map protein-protein interactions between TatA and TatC TM5, P3 and TM6 through disulphide crosslinking a Cys scanning region in TatC in living *E. coli* cells
- Identify sites occupied on TatC by TatA when TatB is absent
- Identify sites occupied on TatC by TatA in the resting state of the Tat system, using uncouplers and TatC substitutions that prevent substrate binding
- Monitor any changes in crosslinking patterns with overexpressed Tat substrates
- Confirm observed crosslinks with expression of protein from low copy number vectors

Chapter 2: Materials and methods

2.1 Bacterial strains

The *E. coli* strains used in this work are derived from strain K12. DH5α was used for all cloning applications, Experiments studying plasmid-borne *tatABC* operon were carried out in the chromosomal *tat* deletion strains DADE and DADE-P. A full list of strains is given in Table 2.1.

Table 2.1) *E. coli* strains used in this work.

Strain	Genotype	Resistance	Reference
DH5α	F^-, *endA1, glnV44, thi-1, recA1, relA1, gyrA96, deoR, nupG, Φ80dlacZΔM15,* Δ(*lacZYA-argF*)*U169, hsdR17*(r_K^- m_K^+), λ^-	None	Promega; Grant *et al.* (1990)
DADE	MC4100, Δ*tatABCD,* Δ*tatE*	None	Wexler *et al.* (2000)
DADE-P	MC4100, Δ*tatABCD,* Δ*tatE, pcn*B1 *zad-*981::Tn*10*d	Kan^R	Lee *et al.* (2006b)

2.2 Materials

2.2.1 Growth Conditions

Standard growth media was prepared by Central Technical Services at the School of Life Sciences, University of Dundee. Cultures were grown aerobically at 37°C with shaking at 200 rpm in Luria-Bertani (LB) broth, or on solid LB-Agar plates, both containing appropriate antibiotics (Table 2.3), unless otherwise stated. A comprehensive list of additives and media are shown in Table 2.2 and Table 2.4.

2.2.2 Scoring Tat-dependent anaerobic growth on TMAO/glycerol media

To identify whether cells harboured a functional Tat system, a stationary phase culture of the strain of interest was diluted in 1x M9 minimal medium salts (diluted from 10x stock with sterile water) to OD_{600} 0.01 before spotting on M9 agar plates supplemented with TMAO and glycerol (Table 2.2). Plates were incubated in an anaerobic jar (BBL GasPak System) for three days at 37°C. AnaeroGen sachets were used to purge oxygen from the jar. Anaerobic test strips (Merck) were used to confirm anaerobic conditions within the anaerobic jar.

2.2.3 Scoring Tat-dependent growth on media containing 2% SDS

As a further test to identify whether cells harboured a functional Tat system, growth in the presence of SDS was assessed – this depends on the ability of the strain to export Tat-dependent amidases. A stationary phase culture of the strain of interest was diluted in LB to OD_{600} 0.01 before spotting on LB agar containing 2% SDS (w/v) (Table 2.4) and incubating overnight at 37^{o}C.

Table 2.2) Composition of growth media used in this work-Media was autoclaved at 121^{o}C for 20 mins prior to use, with the exception of those marked with an asterisk, which were filter sterilised before

Growth Media	Components
Luria-Bertani (LB)	1% (w/v) tryptone 1% (w/v) NaCl, 0.5% (w/v) yeast extract
TSB Transformation buffer	1% (w/v) tryptone 1% (w/v) NaCl 0.5% (w/v) yeast extract 10 mM $MgSO_4$* 5% (v/v) dimethyl sulfoxide 10% (w/v) polyethylene glycol 6000
10x M9 minimal medium salts	3% (w/v) KH_2PO_4 6% (w/v) Na_2HPO_4 1% (w/v) NH_4Cl 0.5% (w/v) NaCl
MoSe salts	2 mM $MgSO_4$ 1 mM K_2SeO_3 1 mM $(NH_4)_6Mo_7O_{24}.4H_2O$
TMAO/glycerol agar	10% (v/v) 10x M9 minimal medium salts 1.2% (w/v) Bacto agar 0.1 mM $CaCl_2$* 0.5% (v/v) glycerol* 2 mM $MgSO_4$* 0.1% (v/v) MoSe salts 0.002% (w/v) thiamine* 0.4% (v/v) Trimethylamine N-oxide (TMAO)*

Table 2.3) List of antibiotics used in this study- Ampicillin and kanamycin were dissolved in distilled H_2O and chloramphenicol in 80% ethanol. All antibiotics were filter sterilised prior to use.

Antibiotic	Concentration in growth media
Ampicillin	100 µg/ µL
Chloramphenicol	25 µg/ µL
Kanamycin	50 µg/ µL

Table 2.4) List of growth supplements used in this work- All chemicals were dissolved in distilled H_2O and filter sterilised prior to use.

Supplement	Concentration in growth media
Isopropyl β-D-1 thiogalactopyranoside (IPTG)	1 mM
L-arabinose	Ranges between 0.001%-0.02%
Sodium dodecyl sulfate (SDS)	2% (w/v)

Buffers and Solutions

All buffers and solutions were prepared in distilled H_2O, with a comprehensive list of is shown in Table 2.5, along with the components.

Table 2.5) Composition of buffers and solutions utilised in this work

Solution	Components
2x Laemmli buffer, pH 6.8 (BioRad)	65.8 mM Tris-HCl 2.1% SDS 26.3% (v/v) glycerol 0.01% (w/v) bromophenol blue
Buffer 1, pH 7.5	50 mM Tris/HCl 5 mM $MgCl_2$ 10% (v/v) glycerol
Elution Buffer	20 mM MOPS 200 mM NaCl 10 mM EDTA 0.01% (w/v) digitonin/$C_{12}E_9$/Triton X-100
HEPES/$MgCl_2$ buffer, pH 6.8	50 mM HEPES 5 mM $MgCl_2$
Resuspension buffer, pH 7.5	20 mM Tris/HCl 200 mM NaCl
SDS-PAGE running buffer	25 mM Tris 192 mM glycine 0.1% (w/v) SDS
Sucrose Buffer	50 mM Tris.HCl pH 7.4 1 mM EDTA, 20% sucrose w/v
TAE buffer	40 mM Tris 1.142% (v/v) acetic acid 1 mM EDTA

TBS, pH 7.5	20 mM Tris/HCl 137 mM NaCl
TBS Tween, pH 7.5	20 mM Tris/HCl 137 mM NaCl 0.1 % (v/v) Tween-20
Transfer buffer	25 mM Tris 192 mM glycine 10% (v/v) methanol
Wash Buffer, pH 7.2	20 mM MOPS 200 mM NaCl 50 mM imidazole 0.01% (w/v) digitonin/$C_{12}E_9$/Triton X-100

2.3 Molecular Biology Techniques

2.3.1 Preparation of competant cells

The host strain was grown overnight in 5 mL LB and from this, 100 µL was used to inoculate 10 mL of LB containing appropriate antibiotics as necessary, which was cultured until an OD_{600} of 0.3 was reached. Cells were then harvested by centrifugation at 3000 x *g* for 10 minutes and resuspended in 1 mL ice cold TBS transformation buffer (see Table 2.2). After incubation for 30 mins on ice, cells were competent and ready for use in transformation experiments directly, or were snap frozen in liquid nitrogen and stored at -80^{o}C.

2.3.2 Transformation of competent cells

Competent cells of the strain of interest were thawed on ice, and 100 µL of cells per transformation were mixed with 1 µL (50 ng-1 µg) of plasmid DNA before incubation on ice for 30 mins. Cells were subsequently subjected to heat shock at 42^{o}C for 90 seconds before transferring onto ice for 2 mins. For the recovery step, 1 mL of LB was added to the cells before incubation at 37^{o}C for 1 hour. The cells then harvested by centrifugation at 16000 x *g* for 1 minute and resuspended in 100 µL LB before spreading on LB agar plates containing appropriate antibiotics and incubating overnight.

2.3.4 Plasmid DNA preparation

Cells harbouring the plasmid of interest was grown overnight in 5 mL LB and harvested by centrifugation at 3000 x *g* for 15 mins. Plasmid extraction was performed using a QIAprep spin miniprep kit (Qiagen), firstly resuspending the cell pellet in a buffer containing RNase before lysing the cells with NaOH and detergent. The reaction was quenched with sodium acetate before centrifugation at 16000 x *g* for 10 mins to remove cell debris. The supernatant was applied to a silica membrane before centrifugation at 16000 x *g* to bind the DNA selectively to the column. The column was washed with a buffer containing guanidine hydrochloride and isopropanol, then with a buffer containing ethanol and a high salt concentration to remove contaminants from the DNA, using the centrifugation step as previously. The plasmid DNA was finally eluted using 50 µL of ultra-pure water. A list of all the plasmids used in this work is given in Table 2.6.

Table 2.6) Plasmids used and constructed in this study

Construct	Description	Resistance	Reference
pQE60	Medium copy number expression vector with *T5* promoter	Amp^R	Qiagen
$pTH19K^R$	Very low copy number expression vector with P*lac* promoter	Kan^R	T. Hashimoto-Gotoh
$pBAD_{33}$	High copy number vector with P*araBAD* promoter	$Chlor^R$	Guzman *et al.* 1995
pQE80	Medium copy number expression vector with *T5* promoter	Amp^R	Qiagen
pUNITATCC4	*tatABC* operon with cysteine-less *tatC* in pQE60 vector	Amp^R	Lee *et al.,* 2006
pQE60 AΔBCC-	*tatABC* operon with cysteine-less *tatC* and a deletion of *tatB*	Amp^R	G. Buchanan
pTat101 Cysless	*tatABC* operon with cysteine-less *TatC* in $pTH19K^R$ vector	Kan^R	Cleon *et al.,*l 2015
pRep4	Encodes *lacI* repressor	Kan^R	Zamenhof and Villarejo (1972)
pQE80 CueOH	pQE80 encoding Tat substrate *cueO* with an C-terminal hexa-histidine tag	Amp^R	Alcock *et al.* 2013
pTGS	$pBAD_{33}$ encoding *gfp* with a C-terminal ssrA tag fused to the TorA Tat signal sequence	$Chlor^R$	DeLisa *et al.*, 2002
pUNITATCC4TatA L9C	pUNITATCC4with *tatA* L9 substituted with cysteine	Amp^R	F. Cleon
pUNITATCC4TatA L10C	pUNITATCC4with *tatA* L10 substituted with cysteine	Amp^R	F. Cleon
pUNITATCC4TatA I11C	pUNITATCC4with *tatA* I11 substituted with cysteine	Amp^R	F. Cleon
pUNITATCC4TatC M205C	pUNITATCC4with *tatC* M205 substituted with cysteine	Amp^R	Cleon *et al* 2015
pUNITATCC4TatC L206C	pUNITATCC4with *tatC* L206 substituted with cysteine	Amp^R	F. Cleon
pUNITATCC4TatC L207C	pUNITATCC4with *tatC* L207 substituted with cysteine	Amp^R	F. Cleon
pUNITATCC4TatC T208C	pUNITATCC4with *tatC* T208 substituted with cysteine	Amp^R	F. Cleon
pUNITATCC4TatC P209C	pUNITATCC4with *tatC* P209 substituted with cysteine	Amp^R	F. Cleon
pUNITATCC4TatC P210C	pUNITATCC4with *tatC* P210 substituted with cysteine	Amp^R	F. Cleon
pUNITATCC4TatC D211C	pUNITATCC4with *tatC* D211 substituted with cysteine	Amp^R	F. Cleon

pUNITATCC4TatC V212C	pUNITATCC4with *tatC* V212 substituted with cysteine	Amp^R	F. Cleon
pUNITATCC4TatC F213C	pUNITATCC4with *tatC* F213 substituted with cysteine	Amp^R	F. Cleon
pUNITATCC4TatC S214C	pUNITATCC4with *tatC* S214 substituted with cysteine	Amp^R	F. Cleon
pUNITATCC4TatC Q215C	pUNITATCC4with *tatC* Q215 substituted with cysteine	Amp^R	F. Cleon
pUNITATCC4TatC T216C	pUNITATCC4with *tatC* T216 substituted with cysteine	Amp^R	F. Cleon
pQE60 AΔBCC- TatC M205C	pQE60 AΔBCC- with *tatC* M205 substituted with cysteine	Amp^R	F. Cleon
pQE60 AΔBCC- TatC L206C	pQE60 AΔBCC- with *tatC* L206 substituted with cysteine	Amp^R	F. Cleon
pQE60 AΔBCC- TatC L207C	pQE60 AΔBCC- with *tatC* L207 substituted with cysteine	Amp^R	F. Cleon
pQE60 AΔBCC- TatC T208C	pQE60 AΔBCC- with *tatC* T208 substituted with cysteine	Amp^R	F. Cleon
pQE60 AΔBCC- TatC P209C	pQE60 AΔBCC- with *tatC* P209 substituted with cysteine	Amp^R	F. Cleon
pQE60 AΔBCC- TatC P210C	pQE60 AΔBCC- with *tatC* P210 substituted with cysteine	Amp^R	F. Cleon
pQE60 AΔBCC- TatC D211C	pQE60 AΔBCC- with *tatC* D211 substituted with cysteine	Amp^R	F. Cleon
pQE60 AΔBCC- TatC V212C	pQE60 AΔBCC- with *tatC* V212 substituted with cysteine	Amp^R	F. Cleon
pQE60 AΔBCC- TatC F213C	pQE60 AΔBCC- with *tatC* F213 substituted with cysteine	Amp^R	F. Cleon
pQE60 AΔBCC- TatC S214C	pQE60 AΔBCC- with *tatC* S214 substituted with cysteine	Amp^R	F. Cleon
pQE60 AΔBCC- TatC Q215C	pQE60 AΔBCC- with *tatC* Q215 substituted with cysteine	Amp^R	F. Cleon
pQE60 AΔBCC- TatC T216C	pQE60 AΔBCC- with *tatC* T216 substituted with cysteine	Amp^R	F. Cleon
pTAT101 ABCC- TatC M205C	pTAT101 ABCC- with *tatC* M205 substituted with cysteine	Kan^R	F. Cleon
pTAT101 ABCC- TatC L206C	pTAT101 ABCC- with *tatC* L206 substituted with cysteine	Kan^R	F. Cleon
pTAT101 ABCC- TatC P209C	pTAT101 ABCC- with *tatC* P209 substituted with cysteine	Kan^R	F. Cleon
pTAT101 ABCC- TatC P210C	pTAT101 ABCC- with *tatC* P210 substituted with cysteine	Kan^R	F. Cleon
pTAT101 ABCC- TatC D211C	pTAT101 ABCC- with *tatC* D211 substituted with cysteine	Kan^R	F. Cleon
pTAT101 ABCC- TatC V212C	pTAT101 ABCC- with *tatC* V212 substituted with cysteine	Kan^R	F. Cleon

pTAT101 ABCC- TatC F213C	pTAT101 ABCC- with *tatC* F213 substituted with cysteine	Kan^R	F. Cleon
pTAT101 ABCC- TatA L9C	pTAT101 ABCC- with *tatA* L9 substituted with cysteine	Kan^R	This work
pTAT101 ABCC- TatA L10C	pTAT101 ABCC- with *tatA* L10 substituted with cysteine	Kan^R	This work
pTAT101 ABCC- TatA L11C	pTAT101 ABCC- with *tatA* I11 substituted with cysteine	Kan^R	This work
pUNITATCC4TatA L9C, TatC M205C	pUNITATCC4with *tatA* L9 and *tatC* M205 substituted with cysteine	Amp^R	This work
pUNITATCC4TatA L9C, TatC L206C	pUNITATCC4with *tatA* L9 and *tatC* L206 substituted with cysteine	Amp^R	This work
pUNITATCC4TatA L9C, TatC L207C	pUNITATCC4with *tatA* L9 and *tatC* L207 substituted with cysteine	Amp^R	This work
pUNITATCC4TatA L9C, TatC T208C	pUNITATCC4with *tatA* L9 and *tatC* T208 substituted with cysteine	Amp^R	This work
pUNITATCC4TatA L9C, TatC P209C	pUNITATCC4with *tatA* L9 and *tatC* P209 substituted with cysteine	Amp^R	This work
pUNITATCC4TatA L9C, TatC P210C	pUNITATCC4with *tatA* L9 and *tatC* P210 substituted with cysteine	Amp^R	This work
pUNITATCC4TatA L9C, TatC D211C	pUNITATCC4with *tatA* L9 and *tatC* D211 substituted with cysteine	Amp^R	This work
pUNITATCC4TatA L9C, TatC V212C	pUNITATCC4with *tatA* L9 and *tatC* V212 substituted with cysteine	Amp^R	This work
pUNITATCC4TatA L9C, TatC F213C	pUNITATCC4with *tatA* L9 and *tatC* F213 substituted with cysteine	Amp^R	This work
pUNITATCC4TatA L9C, TatC S214C	pUNITATCC4with *tatA* L9 and *tatC* S214 substituted with cysteine	Amp^R	This work
pUNITATCC4TatA L9C, TatC Q215C	pUNITATCC4with *tatA* L9 and *tatC* Q215 substituted with cysteine	Amp^R	This work
pUNITATCC4TatA L9C, TatC T216C	pUNITATCC4with *tatA* L9 and *tatC* T216 substituted with cysteine	Amp^R	This work
pUNITATCC4TatA L10C, TatC M205C	pUNITATCC4with *tatA* L10 and *tatC* M205 substituted with cysteine	Amp^R	This work

pUNITATCC4TatA L10C, TatC L206C	pUNITATCC4with *tatA* L10 and *tatC* L206C substituted with cysteine	Amp^R	This work
pUNITATCC4TatA L10C, TatC L207C	pUNITATCC4with *tatA* L10 and *tatC* L207 substituted with cysteine	Amp^R	This work
pUNITATCC4TatA L10C, TatC T208C	pUNITATCC4with *tatA* L10 and *tatC* T208 substituted with cysteine	Amp^R	This work
pUNITATCC4TatA L10C, TatC P209C	pUNITATCC4with *tatA* L10 and *tatC* P209 substituted with cysteine	Amp^R	This work
pUNITATCC4TatA L10C, TatC P210C	pUNITATCC4with *tatA* L10 and *tatC* P210 substituted with cysteine	Amp^R	This work
pUNITATCC4TatA L10C, TatC D211C	pUNITATCC4with *tatA* L10 and *tatC* D211 substituted with cysteine	Amp^R	This work
pUNITATCC4TatA L10C, TatC V212C	pUNITATCC4with *tatA* L10 and *tatC* V212 substituted with cysteine	Amp^R	This work
pUNITATCC4TatA L10C, TatC F213C	pUNITATCC4with *tatA* I11 and *tatC* F213 substituted with cysteine	Amp^R	This work
pUNITATCC4TatA L10C, TatC S214C	pUNITATCC4with *tatA* I11 and *tatC* S214 substituted with cysteine	Amp^R	This work
pUNITATCC4TatA L10C, TatC Q215C	pUNITATCC4with *tatA* I11 and *tatC* Q215 substituted with cysteine	Amp^R	This work
pUNITATCC4TatA L10C, TatC T216C	pUNITATCC4with *tatA* I11 and *tatC* T216 substituted with cysteine	Amp^R	This work
pUNITATCC4TatA I11C, TatC M205C	pUNITATCC4with *tatA* I11 and *tatC* M205 substituted with cysteine	Amp^R	This work
pUNITATCC4TatA I11C, TatC L206C	pUNITATCC4with *tatA* I11 and *tatC* L206 substituted with cysteine	Amp^R	This work
pUNITATCC4TatA I11C, TatC L207C	pUNITATCC4with *tatA* I11 and *tatC* L207 substituted with cysteine	Amp^R	This work
pUNITATCC4TatA I11C, TatC T208C	pUNITATCC4with *tatA* I11 and *tatC* T208 substituted with cysteine	Amp^R	This work
pUNITATCC4TatA I11C, TatC P209C	pUNITATCC4with *tatA* I11 and *tatC* P209 substituted with cysteine	Amp^R	This work

pUNITATCC4TatA I11C, TatC P210C	pUNITATCC4with *tatA* I11 and *tatC* P210 substituted with cysteine	Amp^R	This work
pUNITATCC4TatA I11C, TatC D211C	pUNITATCC4with *tatA* I11 and *tatC* D211 substituted with cysteine	Amp^R	This work
pUNITATCC4TatA I11C, TatC V212C	pUNITATCC4with *tatA* I11 and *tatC* V212 substituted with cysteine	Amp^R	This work
pUNITATCC4TatA I11C, TatC F213C	pUNITATCC4with *tatA* I11 and *tatC* F213 substituted with cysteine	Amp^R	This work
pUNITATCC4TatA I11C, TatC S214C	pUNITATCC4with *tatA* I11 and *tatC* S214 substituted with cysteine	Amp^R	This work
pUNITATCC4TatA I11C, TatC Q215C	pUNITATCC4with *tatA* I11 and *tatC* Q215 substituted with cysteine	Amp^R	This work
pUNITATCC4TatA I11C, TatC T216C	pUNITATCC4with *tatA* I11 and *tatC* T216 substituted with cysteine	Amp^R	This work
pUNITATCC4TatA L9C, TatC V167C	pUNITATCC4with *tatA* L9 and *tatC* V167 substituted with cysteine	Amp^R	This work
pQE60 AΔBCC- TatA L9C, TatC M205C	pQE60 AΔBCC- with *tatA* L9 and *tatC* M205 substituted with cysteine	Amp^R	This work
pQE60 AΔBCC- TatA L9C, TatC L206C	pQE60 AΔBCC- with *tatA* L9 and *tatC* L206 substituted with cysteine	Amp^R	This work
pQE60 AΔBCC- TatA L9C, TatC L207C	pQE60 AΔBCC- with *tatA* L9 and tatC *L207* substituted with cysteine	Amp^R	This work
pQE60 AΔBCC- TatA L9C, TatC T208C	pQE60 AΔBCC- with *tatA* L9 and *tatC* T208 substituted with cysteine	Amp^R	This work
pQE60 AΔBCC- TatA L9C, TatC P209C	pQE60 AΔBCC- with *tatA* L9 and *tatC* P209 substituted with cysteine	Amp^R	This work
pQE60 AΔBCC- TatA L9C, TatC P210C	pQE60 AΔBCC- with *tatA* L9 and *tatC* P210 substituted with cysteine	Amp^R	This work
pQE60 AΔBCC- TatA L9C, TatC D211C	pQE60 AΔBCC- with *tatA* L9 and *tatC* D211 substituted with cysteine	Amp^R	This work
pQE60 AΔBCC- TatA L9C, TatC V212C	pQE60 AΔBCC- with *tatA* L9 and *tatC* V212 substituted with cysteine	Amp^R	This work

pQE60 AΔBCC- TatA L9C, TatC F213C	pQE60 AΔBCC- with *tatA* L9 and *tatC* F213 substituted with cysteine	Amp^R	This work
pQE60 AΔBCC- TatA L9C, TatC S214C	pQE60 AΔBCC- with *tatA* L9 and *tatC* S214 substituted with cysteine	Amp^R	This work
pQE60 AΔBCC- TatA L9C, TatC Q215C	pQE60 AΔBCC- with *tatA* L9 and *tatC* Q215 substituted with cysteine	Amp^R	This work
pQE60 AΔBCC- TatA L9C, TatC T216C	pQE60 AΔBCC- with *tatA* L9 and *tatC* T216 substituted with cysteine	Amp^R	This work
pQE60 AΔBCC- TatA L10C, TatC M205C	pQE60 AΔBCC- with *tatA* L10 and *tatC* M205 substituted with cysteine	Amp^R	This work
pQE60 AΔBCC- TatA L10C, TatC L206C	pQE60 AΔBCC- with *tatA* L10 and *tatC* L206 substituted with cysteine	Amp^R	This work
pQE60 AΔBCC- TatA L10C, TatC L207C	pQE60 AΔBCC- with *tatA* L10 and *tatC* L207 substituted with cysteine	Amp^R	This work
pQE60 AΔBCC- TatA L10C, TatC T208C	pQE60 AΔBCC- with *tatA* L10 and *tatC* T208 substituted with cysteine	Amp^R	This work
pQE60 AΔBCC- TatA L10C, TatC P209C	pQE60 AΔBCC- with *tatA* L10 and *tatC* P209 substituted with cysteine	Amp^R	This work
pQE60 AΔBCC- TatA L10C, TatC P210C	pQE60 AΔBCC- with *tatA* L10 and *tatC* P210 substituted with cysteine	Amp^R	This work
pQE60 AΔBCC- TatA L10C, TatC D211C	pQE60 AΔBCC- with *tatA* L10 and *tatC* D211 substituted with cysteine	Amp^R	This work
pQE60 AΔBCC- TatA L10C, TatC V212C	pQE60 AΔBCC- with *tatA* L10 and *tatC* V212 substituted with cysteine	Amp^R	This work
pQE60 AΔBCC- TatA L10C, TatC F213C	pQE60 AΔBCC- with *tatA* I11 and *tatC* F213 substituted with cysteine	Amp^R	This work
pQE60 AΔBCC- TatA L10C, TatC S214C	pQE60 AΔBCC- with *tatA* I11 and *tatC* S214 substituted with cysteine	Amp^R	This work
pQE60 AΔBCC- TatA L10C, TatC Q215C	pQE60 AΔBCC- with *tatA* I11 and *tatC* Q215 substituted with cysteine	Amp^R	This work
pQE60 AΔBCC- TatA L10C, TatC T216C	pQE60 AΔBCC- with *tatA* I11 and *tatC* T216 substituted with cysteine	Amp^R	This work

pQE60 AΔBCC- TatA I11C, TatC M205C	pQE60 AΔBCC- with *tatA* I11 and *tatC* M205 substituted with cysteine	Amp^R	This work
pQE60 AΔBCC- TatA I11C, TatC L206C	pQE60 AΔBCC- with *tatA* I11 and *tatC* L206 substituted with cysteine	Amp^R	This work
pQE60 AΔBCC- TatA I11C, TatC L207C	pQE60 AΔBCC- with *tatA* I11 and *tatC* L207 substituted with cysteine	Amp^R	This work
pQE60 AΔBCC- TatA I11C, TatC T208C	pQE60 AΔBCC- with *tatA* I11 and *tatC* T208 substituted with cysteine	Amp^R	This work
pQE60 AΔBCC- TatA I11C, TatC P209C	pQE60 AΔBCC- with *tatA* I11 and *tatC* P209 substituted with cysteine	Amp^R	This work
pQE60 AΔBCC- TatA I11C, TatC P210C	pQE60 AΔBCC- with *tatA* I11 and *tatC* P210 substituted with cysteine	Amp^R	This work
pQE60 AΔBCC- TatA I11C, TatC D211C	pQE60 AΔBCC- with *tatA* I11 and *tatC* D211 substituted with cysteine	Amp^R	This work
pQE60 AΔBCC- TatA I11C, TatC V212C	pQE60 AΔBCC- with *tatA* I11 and *tatC* V212 substituted with cysteine	Amp^R	This work
pQE60 AΔBCC- TatA I11C, TatC F213C	pQE60 AΔBCC- with *tatA* I11 and *tatC* F213 substituted with cysteine	Amp^R	This work
pQE60 AΔBCC- TatA I11C, TatC S214C	pQE60 AΔBCC- with *tatA* I11 and *tatC* S214 substituted with cysteine	Amp^R	This work
pQE60 AΔBCC- TatA I11C, TatC Q215C	pQE60 AΔBCC- with *tatA* I11 and *tatC* Q215 substituted with cysteine	Amp^R	This work
pQE60 AΔBCC- TatA I11C, TatC T216C	pQE60 AΔBCC- with *tatA* I11 and *tatC* T216 substituted with cysteine	Amp^R	This work
pQE60 AΔBCC- TatA L9C, TatC V167C	pQE60 AΔBCC- with *tatA* L9 and *tatC* V167 substituted with cysteine	Amp^R	This work
pTAT101 ABCC- TatA L9C, TatC M205C	pTAT101 ABCC- with *tatA* L9 and *tatC* M205 substituted with cysteine	Kan^R	This work
pTAT101 ABCC- TatA L9C, TatC L206C	pTAT101 ABCC- with *tatA* L9 and *tatC L206* substituted with cysteine	Kan^R	This work
pTAT101 ABCC- TatA L9C, TatC V212C	pTAT101 ABCC- with *tatA* L9 and *tatC* V212 substituted with cysteine	Kan^R	This work

pTAT101 ABCC- TatA L9C, TatC F213C	pTAT101 ABCC- with *tatA* L9 and *tatC* F213 substituted with cysteine	Kan^R	This work
pTAT101 ABCC- TatA L10C, TatC M205C	pTAT101 ABCC- with *tatA* L10 and *tatC* M205 substituted with cysteine	Kan^R	This work
pTAT101 ABCC- TatA L10C, TatC L206C	pTAT101 ABCC- with *tatA* L10 and *tatC* L206 substituted with cysteine	Kan^R	This work
pTAT101 ABCC- TatA L10C, TatC V212C	pTAT101 ABCC- with *tatA* L10 and *tatC* V212 substituted with cysteine	Kan^R	This work
pTAT101 ABCC- TatA L10C, TatC F213C	pTAT101 ABCC- with *tatA* L10 and *tatC* F213 substituted with cysteine	Kan^R	This work
pTAT101 ABCC- TatA I11C, TatC M205C	pTAT101 ABCC- with *tatA* I11 and *tatC* M205 substituted with cysteine	Kan^R	This work
pTAT101 ABCC- TatA I11C, TatC L206C	pTAT101 ABCC- with *tatA* I11 and *tatC* L206 substituted with cysteine	Kan^R	This work
pTAT101 ABCC- TatA I11C, TatC V212C	pTAT101 ABCC- with *tatA* I11 and *tatC* V212 substituted with cysteine	Kan^R	This work
pTAT101 ABCC- TatA I11C, TatC F213C	pTAT101 ABCC- with *tatA* I11 and *tatC* F213 substituted with cysteine	Kan^R	This work
pTAT101 ABCC- TatA L9C, TatC V167C	pTAT101 ABCC- with *tatA* L9 and *tatC* V167 substituted with cysteine	Kan^R	This work
pQE60 $TatABC_{His}$	*tatABC* operon with His_6-tagged *tatC* in pQE60 vector	Amp^R	Buchanan *et al.,* 2002
pQE60 $TatAC_{His}$	*tatAC* operon with *tatB* deleted and His_6-tagged *tatC* in pQE60 vector	Amp^R	Fritsch *et al*., 2012
pQE60 $TatBC_{His\ (pFAT75\Delta A)}$	*tatBC* operon with *tatA* deleted and His_6-tagged *tatC* in pQE60 vector	Amp^R	G. Buchanan Tarry *et al.*, 2009
pQE60 $TatABC_{His}$D211A	*tatABC* operon with His_6-tagged *tatC* containing the D211A subsitution in pQE60 vector	Amp^R	Buchanan *et al.,* 2002
pTat101 $TatABC_{His}$	*tatABC* operon with His_6-tagged *tatC* in $pTh19K^R$ vector	Kan^R	This work
pHASoxYZ	pSU20 with *tat* promoter controlling production of N-terminally HA-tagged SoxY and SoxZ, both from *Paracoccus panthotrophus.*	$Chlor^R$	Koch *et al.,* 2012

2.3.5 DNA Quantification

A nanodrop ND-1000 system (Thermo Scientific) spectrophotometer was used to calculate the concentration of DNA by measuring absorbance at 260 nm, with 1.5 µL of DNA solution pipetted onto the pedestal for quantification. Using the extinction coefficient of 0.020 ng μL^{-1} cm^{-1} for double stranded DNA and of 0.030 ng μL^{-1} cm^{-1} for single stranded, a nucleic acid concentration in ng μL^{-1} was calculated.

2.3.6 DNA amplification using Polymerase Chain Reaction (PCR)

DNA sequences of interest from plasmids were amplified using PCR. Herculase II DNA polymerase (Agilent) was used as to amplify the DNA in a thermocycler (Eppendorf Mastercycler personal). Forward and reverse primers flanking the DNA to be amplified were added to the reaction mixture, along with HercII reaction buffer (Agilent), dNTPs, dimethylsulfoxide (DMSO) and template DNA, according to Table 2.7. The thermocycler programme used to amplify the *tat* operon from plasmids is outlined in Table 2.8.

Table 2.7) The steps programmed in the PCR cycle during the QuikChange experiment.

Component	Volume (µL)	Final Concentration
MilliQ ultrapure H_2O	33	
5x conc. Herc II reaction buffer	10	1x
dNTP mix (10 mM of dATP, dCTP, dGTP and dTTP)	1.0	0.2 mM
100 µM For Primer	1	2 µM
100 µM Rev Primer	1	2 µM
DNA Template (100 ng)	2.0	2 ng/µL
Dimethyl sulfoxide	2.5	5% v/v
Herc II DNA Polymerase	1	5 units

Table 2.8) -The composition of the QuikChange PCR mix used- with the volume of each reagent and the final concentration noted

Reaction Step	Parameter
Preheating	1 min at 95ºC
Denaturation	30 sec at 95ºC
Annealing	1 min at 55ºC
Elongation	2 min at 68ºC
Cycles	16

2.3.7 QuikChange site directed mutagenesis

To construct plasmids encoding single amino acid codon substitutions in *tatA, tatB* and *tatC*, primers were designed that included an altered codon flanked either side by 15 nucleotides directly complementary to the template strand (a comprehensive list of primers is given in Table 2.9). A polymerase chain reaction (PCR) was then performed, identical to that in Table 2.7 but with an elongation time of 15 mins, to yield the mutated plasmid product, and the methylated template DNA was removed by adding 1 unit of *Dpn*I (Roche) before incubating for 1 hour at 37^{o}C. The PCR mix was used to transform competent DH5 α cells (or DH5α pRep4 for pQE60-based plasmids). A single colony following transformation was grown overnight at 37^{o}C with agitation at 200 rpm, before isolating plasmid DNA using a Qiagen miniprep plasmid preparation kit and confirmation of the presence of the introduced mutation by DNA sequence analysis (DNA Sequencing Service, University of Dundee).

2.3.8 Agarose gel electrophoresis of DNA

Plasmids and DNA products from PCR were analysed using gel electrophoresis to check the mobility, and therefore get an approximation of size in base pairs (bp). The sample DNA was mixed with loading dye (ratio of 1:4) and loaded onto a 1% (w/v) agarose gel containing GelRed stain (Biotem). The gel was placed in a tank containing TAE buffer and 200V was applied to drive migration of the DNA. Once complete, the gel was imaged using UV light at 302 nm in a Gel Doc XR+ camera (BioRad). A ladder corresponding to DNA bp sizes was used to estimate side of the product DNA.

Table 2.9) Primers used in this work,-noted forward and reverse.

Primer	5'-3' sequence
TatA L9C For	AATTTGGCAGTTATTGTGTATTGCCGTCATGTT
TatA L9C Rev	AACATGACGGCAATACACAATAACTGCCAAATT
TatA L10C For	AGTATTTGGCAGTTATGCATTATTGCCGTCATC
TatA L10C Rev	GATGACGGCAATAATGCATAACTGCCAAATACT
TatA I11C For	AACGATGACGGCAATACACAATAACTGCCAAAT
TatA I11C Rev	AATTTGGCAGTTATTGTGTATTGCCGTCATGTT
TatB L9C For	ATCGGTTTTAGCGAATGTCTATTGGTGTTCATC
TatB L9C Rev	GATGAACACCAATAGACATTCGCTAAAACCGAT
TatB L10C For	GGTTTTAGCGAACTGTGTTTGGTGTTCATCATC
TatB L10C Rev	GATGATGAACACCAAACACAGTTCGCTAAAAC
TatB L11C For	TTTAGCGAACTGCTATGCGTGTTCATCATCGGC
TatB L11C Rev	GCCGATGATGAACACGCATAGCAGTTCGCTAAA
TatC M205C For	GCATTCGTTGTCGGGTGTTTGCTGACGCCGCCG
TatC M205C Rev	CGGCGGCGTCAGCAAACACCCGACAACGAATGC
TatC F94A For	TATCAGGTGTGGGCAGCTATCGCCCCAGCGCTG
TatC F94A Rev	CAGCGCTGGGGCGATAGCTGCCCACACCTGATA
TatC E103A For	TGTATAAGCATGCGCGTCGCCTGGTG
TatC E103A Rev	CCACCAGGCGACGCGCATGCTTATAC
TatC V167C For	TTTATGGCGTTTGGTGTCTCCTTTGAAGTGCCG
TatC V167B Rev	CGGCACTTCAAAGGAGACACCAAACGCCATAAA
TatC E170C For	TTTGGTGTCTCCTTTGAAGTGCCGGTAGCAATT
TatC E170C Rev	AATTGCTACCGGCACTTCAAAGGAGACACCAAA
TatC M163C For	GTTATGGCGCTGTTTATGGCGTTTGGTGTCTCC
TatC M163C Rev	GGAGACACCAAACGCCATAAACAGCGCCATAAC

2.3.9 DNA Digestion

DNA was digested or fragmented using restriction endonucleases, which cleave DNA at specific sequences of base pairs. Restriction with endonucleases (NEB or Roche) was performed according to manufacturer's instructions. Reactions were performed in a 50 µL volume with 4 U of enzyme at 37^{o}C for between 1-3 hours depending on the enzyme. After restriction of plasmid DNA, it was treated with rAPID alkaline phosphatase (AP) (Roche), according to manufacturer's instructions, to prevent self-ligation. Linearised vectors and DNA fragments were purified using a QIAgen PCR Purification Kit according to manufacturer's instructions.

2.3.10 DNA ligation

Ligation was performed using T4 DNA ligase (Roche) to ligate insert (amplified form PCR or purified following digestion from another vector) into the linearised vector (which was AP treated as in Section 2.3.9). The reaction was performed in 10 µL with 50 ng of linearised vector and insert at a ratio of 1:3 with 1 U of T4 DNA ligase for three hours at room temperature. Of the reaction mix, 5 µL was used to transform DH5α competent cells as in Section 2.3.2. Clones from the subsequent transformation were screened for presence of the insert by PCR (Section 2.3.6), with primers flanking the insert and agarose gel electrophoresis was utilised (Section 2.3.8) to check the presence of a DNA fragment corresponding to the insert. Vectors which harboured the insert were confirmed by DNA sequencing.

2.4 Protein methods

2.4.1 SDS PAGE

Proteins were separated according to their molecular weight using SDS polyacrylamide gel electrophoresis (SDS PAGE). SDS PAGE gels were prepared using the Mini-PROTEAN II System (BioRad) according to instructions. Resolving gel (see Table 2.10) was poured until it was ~2 cm from the top of the glass plate and absolute ethanol layered on top, before the acrylamide was left to polymerise. Once the resolving gel was set, the ethanol was removed and stacking gel (see Table 2.10) was added to the top of the glass plate, a comb was then inserted and the gel allowed to set providing wells for the samples.

Table 2.10) Components of the resolving and stacking gel used to produce polyacrylamide gels for SDS-PAGE

Components of resolving gel
12.5% (v/v) of 30% (w/v) acrylamide
0.375 M Tris.HCl pH 8.8
0.1% (w/v) SDS
0.1% (w/v) Ammonium persulfate (APS)
0.1% (w/v) Tetramethylethylenediamine (TEMED)
Components of stacking gel
4% (v/v) of 30% (w/v) acrylamide
0.125 M Tris.HCl pH 6.8
0.1% (w/v) SDS
0.1% (w/v) Ammonium persulfate (APS)
0.1% (w/v) Tetramethylethylenediamine (TEMED)

A gel tank filled with SDS PAGE running buffer was used. Samples were mixed with an appropriate amount of 2x Laemmli buffer (with or without β-mercaptoethanol depending on whether it was desirable to maintain disulphide bonds) and mixed thoroughly before being loaded into the gel. Prestained protein marker (Precision plus, BioRad) was used as a protein standard on each gel after which 100 V was applied to the gel to separate the proteins in the stacking gel, before the voltage was increased to 200 V for migration through the resolving gel. Once complete, the gel was either used for Western blot or stained with Coomassie blue dye.

2.4.2 Western Blotting

Electroblotting was achieved by either dry or semi-dry transfer. Dry transfer was performed using an iBlot 2 device (Life Technologies) according to manufacturer's instructions. For semi-dry transfer gels following SDS PAGE were soaked in transfer buffer for 15 minutes, with a gel-sized piece of nitrocellulose membrane (Amersham Hybond, GE Healthcare) and four similarly sized blotting papers soaking separately. The transfer was performed using a transfer cell (Trans-Blot SD Semi-Dry Transfer Cell, BioRad) with 2 sheets of soaked filter paper placed on the positive electrode and the membrane placed on top, followed by the SDS PAGE gel. Two more filter papers were added and a roller was used to ensure the gel was fully in contact with the membrane, the transfer cell was then fully assembled, with the negative electrode in contact the surface of the top blotting paper. The transfer was performed at 10 V for 1 hour.

After the transfer, the nitrocellulose membrane was blocked by immediately placing it in TBS solution with 5% milk for 1 hour at room temperature, or 5^{o}C overnight, with gentle agitation. For the primary antibody incubation, the milk was removed and replaced with the primary antibody raised against the protein of interest, diluted suitably in TBS-Tween, before agitation at room temperature for 1 hour. The membrane was then washed twice for 15 minutes with TBS-Tween before the secondary antibody, that cross-reacted with the primary antibody, was diluted in TBS-Tween and applied for the secondary incubation. After a further hour with gentle agitation, the membrane was washed again twice for 15 minutes in TBS-Tween before detection. Antibodies used in this thesis are listed in Table 2.11.

The detection method utilised the catalytic activity of horse radish peroxidase (HRP) enzyme conjugated to the secondary antibody. When a chemiluminescent substrate containing luminol and H_2O_2 was applied to the membrane (chemiluminescent HRP

substrate, Millipore) HRP catalyses the oxidation of luminol, causing it to emit light and highlight bands on the membrane where the primary antibody has bound.

The light detection method used either X-ray film (Konica Minolta) developed in a SRX-101A film processor (Konoca Minolta) or a CCD camera in chemiluminescent detection system (GeneGnome, Syngene).

Table 2.11) List of antibodies in this study used for Western blots

Antibody	Organism	Dilution	Reference
E. coli anti-TatC antiserum (polyclonal)	Rabbit	1:10,000	Alami *et al.,* 2002
E. coli anti-TatA antiserum (polyclonal)	Rabbit	1:10,000	Sargent *et al.,* 2001
E. coli anti-TatB antiserum (polyclonal)	Rabbit	1:10,000	Sargent *et al.,* 2001
Tetra-His (monoclonal)	Mouse	1:20,000	Qiagen cat. 34670
GFP (monoclonal)	Mouse	1:5000	Roche cat. 11814460001

2.4.3 Cell fractionation and isolation of membranes

50 mL of LB was inoculated with a single colony of the strain of interest and grown overnight before cells were harvest and washed in 25 mL resuspension buffer. Cells were resuspended in 1 mL resuspension buffer after the washing step, and supplemented with 100 µL protease inhibitor cocktail (one Roche EDTA- free tablet in 500 uL resuspension buffer). Cells were then lysed by sonication for 5 sec with 5 sec breaks, 10 cycles, amplitude 20%, before pelleting the cell debris at 16000 x *g* for 5 mins and retaining the supernatant. The supernatant was centrifuged at 292500 x *g* for 30 mins at 4^{o}C in an Optima MAX-E benchtop ultracentrifuge (Beckman) with rotor TLA 120.2. The subsequent pellet, containing the membrane fraction, was resuspended in 100 µL buffer 1 and retained as the membrane fraction. This was used directly for further experiments or snap frozen in liquid nitrogen and stored at -80^{o}C

2.4.4 Periplasmic preparation of *E. coli*

5 mL of cells at OD_{600} 0.3 were harvested by centrifugation at 4000 x *g* for 10 min and resuspended in 200 µL ice cold sucrose buffer before incubation on ice for 10 min mixing at 1 min intervals. Cells were then harvested by centrifugation at 16000 x *g* for 1 min before resuspension in 100 µL ice cold 5 mM $MgCl_2$ with incubation on ice for 10 min, as previously. The sample was then centrifuged at 16000 x *g* for 10 min at 5^{o}C and the supernatant retained as the osmotic shock fluid containing periplasmic proteins.

2.4.5 Determining protein concentration of membrane fractions

Protein concentration of membrane fractions was obtained using a DC protein assay kit (BioRad) based around the Lowry assay. This involves the oxidation of amino acids in the protein and the subsequent reaction of amino acids (primarily tryptophan, tyrosine and cysteine) with Cu^{+} to form molybdenum/tungsten blue. The amount molybdenum/tungsten blue product, and therefore the amount of protein, can be detected in a spectrophotometer set at 750 nm.

In a 96-well plate, a standard curve was produced with triplicate samples of BSA (Sigma Aldrich), from 2-10 µg in 5 µL ultrapure water, along with a blank containing water only. Protein samples were diluted 1:10 and 1:100 in 5 µL ultrapure water. According the manufacturer's instructions, 25 µL of reagent A was added to each sample and incubated at room temperature for 5 mins, 200 µL of reagent B was then added before further incubation at room temperature for 15 minutes. Absorbance at 750 nM was obtained using an ELx808 absorbance microplate reader (BioTek).

2.4.6 Detergent solubilisation of membrane fractions

A single colony of the strain of interest was used to inoculate 5mL of LD medium and cultured overnight with shaking. This was used, at a 1:100 dilution, to inoculate a 1 L culture, which was grown overnight. Subsequently cells were harvested at 3000 x *g* for

20 mins before resuspension in 10 mL 20 mM MOPS/200 mM NaCl, pH 7.2 supplemented with 100 µL protease inhibitor cocktail (Roche) (1 tablet in 500 µL 20 mM MOPS/200 mM NaCl, pH 7.2) and lysed by sonication (as described in Section 2.4.1) Folowing ultracentrifugation, the final membrane pellet was resuspended in 4 mL 20 mM MOPS, 200 mM NaCl pH 7.4.

Protein concentration of the suspended membrane fraction was determined using a DC protein assay kit (BioRad) as in Section 2.4.4. For purification, resuspended membranes were diluted with wash buffer to a final concentration of 5 mg/mL and supplemented with either 1% digitonin/1% $C_{12}E_9$/1% Triton X-100 before the sample incubated on a rotating wheel (20 rpm) at 4^{o}C for 1 hour. After the incubation step, insoluble material was pelleted by centrifugation at 150000 x *g* for 1 hour at 4^{o}C with the supernatant retained as the solublised membrane protein.

2.4.7 Nickel affinity co-purification assay

Co-purification assays involved isolation of plasmid-encoded His_6-tagged TatC from solubilised membranes. During purification the His_6-tagged TatC should bind to the Ni-affinity resin, allowing unbound material to be washed away. Subsequently the tagged $TatC_{His}$ will be eluted and the eluent analysed using Western blotting with anti-TatA, TatB and TatC to identify proteins which co-elute with $TatC_{His}$.

Two 1 mL washes with ice- cold wash buffer was used to equilibrate 100 µL of IMAC Ni-charged resin (BioRad), pelleting the beads with centrifugation at 400 x *g* for 1 min after each wash and finally resuspending the resin using 1 mL solubilised membrane protein from Section 2.4.5. This was incubated at 4^{o}C with rotation on a wheel at 20 rpm for 1 hour before the resin was pelleted at 400 x *g* for 1 min with the supernatant removed and retained as the unbound fraction. The resin was then washed four times with 1 mL ice-cold wash buffer, pelleting as previously, and retaining the supernatant from the final wash as the wash fraction. The resin was then suspended in 100 µL elution buffer and incubated at 4^{o}C with rotation on a wheel at 20 rpm for 1 hour. A final

centrifugation was performed and the supernatant retained as the elution fraction. The retained samples were mixed with an appropriate amount of Laemmli buffer (BioRad) and analysed by SDS-PAGE and Western blotting.

2.4.8 *In vivo* disulphide crosslinking of proteins from a medium copy number construct

E. coli strain, DADE, harbouring the *lacI*-encoding plasmid, pRep4 (Qiagen) and pUNITATCC4/pQE60AΔBCCC- derivative was grown overnight and this was used at a 1:100 dilution to inoculate fresh LB which was cultured until an OD_{600} of 0.3 was reached. Three 2.5 mL aliquots were then withdrawn and made up to 5 mL with fresh LB. A control sample was left untreated, an oxidised sample had copper phenanthroline (360 mg phenanthroline monohydrate in 5 mL 50% ethanol freshly added to 150 mg $CuSO_4$ in 5 mL dH_2O) added to a final concentration of 1.8 mM and a reduced sample had 10 mM dithiothreitol added. After incubation at 37^{o}C for 1 minute with agitation at 200 rpm, the cells were harvested before resuspending in 100 µL resuspension buffer with 12 mM EDTA and 8 mM *N*-ethylmaleimide added and incubated at 37^{o}C for 10 mins. Cells were pelleted at 16000 x *g* for 1 minute before solubilising in 1 x Laemmli buffer (BioRad) for analysis by SDS-PAGE and Western blotting.

2.4.9 *In vivo* disulphide crosslinking from a medium copy number construct with overexpressed substrate

E. coli strain, DADE, harbouring the *lacI*-encoding plasmid, pRep4 (Qiagen) along with pUNITATCC4expressing *tatA* and *tatC* Cys substitutions and pTGS was grown overnight. This culture was used at a 1:100 dilution to inoculate fresh LB which was grown until an OD_{600} of 0.25 was reached, at which point L-arabinose at concentrations of 0.001-0.2% (v/v) was added to each sample as required before growth was continued for a further 20 minutes. The OD_{600} of each sample was normalised, if necessary, and made up to 5 mL with fresh LB. The crosslink and analysis stage was

identical to the normal crosslinking experiments *in vivo* at medium copy number in Section 2.4.8 from then onwards.

2.4.10 *In vivo* disulphide crosslinking at very low copy number with and without overexpressed substrate

E. coli strain, DADE, harbouring plasmid pTat101 ABCC- and in cases where substrate was required, pQE80 CueOH, was grown overnight. This culture was used at a 1:100 dilution to inoculate fresh LB and supplemented with 1 mM isopropyl β-D-1-thiogalactopyranoside (IPTG) to induce expression of plasmid-encoded His-tagged CueO, as required. The culture was grown until an OD_{600} of 0.3, at which point three 25 mL aliquots were withdrawn and made up to 50 mL with fresh LB. A control sample was left untreated, an oxidised sample had copper phenanthroline added to a final concentration of 1.8 mM and a reduced sample had 10 mM dithiothreitol added. After incubation at 37^{o}C for 1 minute with agitation at 200 rpm, the cells were harvested and resuspended in 1 mL resuspension buffer with 12 mM EDTA and 8 mM N-ethylmaleimide added. The cells were incubated at room temperature for 10 minutes before 100 µL protease inhibitor was added (one Roche cOmplete protease inhibitor cocktail tablet dissolved in 500 µL of resuspension buffer). Cells were then fractionated into soluble fraction and membrane fractions as in Section 2.4.3 with the membrane fraction resuspended in 50 µL Laemmli Buffer (BioRad) for analysis by SDS-PAGE and Western blotting.

2.4.11 *In vivo* disulphide crosslinking with indole as an uncoupler

In order to elucidate the role of PMF in TatA-TatC interactions, an uncoupler was used. Carbonyl cyanide *m*-chlorophenyl hydrazone (CCCP) has been used previously to examine the role of PMF *in vivo* (Alcock *et al*., 2013). During the oxidation step of crosslinking, however, CCCP precipitated out as a bright yellow solid. From this it was deduced that CCCP would not be an appropriate ionophore to use, and indole was identified as a viable alternative. Indole has been characterised extensively as an

uncoupler in bacteria and was found to have fewer precipitation problems than CCCP in this work (Chimerel *et al.*, 2013, Ismail et al., 2015).

Cells were grown to OD_{600} 0.3 as with previous *in vivo* crosslinking protocols before indole (stock 1 M in ethanol) was introduced by adding cells directly onto the appropriate amount of 1 M indole to give a final concentration of 5 mM in the reaction vessel and mixing quickly by inversion to prevent precipitation. Samples not incubated with indole had the equivalent amount of ethanol added at this stage. Incubation took place at room temperature for 5 minutes. To the oxidised samples, 3.6 mM copper phenanthroline was added directly before mixing the cells.

To show that the indole only dissipated the PMF and did not cause cell lysis, a control sample was washed twice in its volume with LB after indole incubation, centrifuging at 3000x *g* for 15 minutes to pellet the cells before crosslinking as above. This sample should be identical to cells not incubated at all with indole.

Chapter 3: TatA is loosely associated with the TatBC recognition complex

3.1 Introduction

3.1.1 Proposed interactions between TatA and TatBC

Several models for Tat transport assume a TatBC substrate recognition complex, initially devoid of TatA, which binds substrate and triggers TatA recruitment to the complex in a protonmotive force (PMF) dependent step (*e.g.* Palmer & Berks 2012) (see Chapter 1, Section 1.12). Past studies examining the purification of TatC-containing complexes yielded contradictory findings, with some supporting the presence of a low level of TatA in the recognition complex whilst others did not (Section 3.1.2). As mentioned in Chapter 1, Section 1.10.5 when TatA is found to co-purify with TatBC it is only present in very low amounts. However, crosslinking studies have observed a constitutively-bound Tha4 (the plant TatA equivalent) present on the TatBC complex in a manner unperturbed by PMF dissipation or substrate overexpression (Aldridge *et al*., 2014). Further to this, crosslinking experiments using *E. coli* inside-out inner membrane vesicles (INVs) observed that TatA can crosslink to TatC when a photoreactive amino acid was introduced into various positions in TatC, including the P3 loop and TM5 (Zoufaly *et al*., 2012, Blummel *et al*., 2015) (Chapter 1, Section 1.10.6), suggesting that TatA may be present as a regular component of the TatBC complex.

3.1.2 Previous purification of Tat complexes

One of the earliest studies examining the kinds of complexes formed by *E. coli* Tat subunits was undertaken by Bolhuis and co-workers (2001), who undertook affinity chromatography of overproduced strep-tagged TatC that had been solubilised from the membrane with digitonin. Subsequent gel filtration of the TatC-containing fractions identified a ~600 kDa complex in which, TatB and $TatC_{Strep}$ were both present, with a small amount of TatA also detected. Radio-labelling experiments confirmed the presence of all three Tat subunits in the purified complex, although it was noted that there was a gradual loss of TatA during the purification steps (Bolhuis *et al,* 2001).

Later studies found that digitonin-solubilised TatB and $TatC_{Strep}$ purified as a single complex during affinity purification trials, with a very small amount of associated TatA. This complex had a molecular mass of ~600 kDa, in accordance with calibrated gel chromatography (Oates *et al.,* 2003). An additional study using membranes solubilised with the same detergent found a TatBC complex of ~440 kDa from cells overproducing Tat components with a small amount of associated TatA (Behrendt *et al*., 2007).

Using the alternative technique of blue native polyacrylamide gel electrophoresis (BN-PAGE), the *E. coli* TatABC complex purified in digitonin was shown to migrate with a mass of ~370 kDa. Later it was shown by direct BN-PAGE analysis of digitonin-solubilised membrane fractions that bulk of TatB and essentially all of the TatC is found in this single 370kDa TatABC complex (Oates *et al.,* 2005). In the same study it was seen that the vast majority of TatA was not present in this complex but was present as a separate series of complexes ranging in size from 100-500 kDa (Oates *et al.,* 2005).

However, one criticism of these early studies is that they worked with Tat proteins that were heavily overproduced from plasmid vectors. A subsequent study analysing the Tat proteins at native level using immunoprecipitation found that while TatB and TatC could be isolated together, no TatA purified with TatC (McDevitt *et al*., 2006). Indeed, further purification trials found that digitonin-solubilised $TatBC_{His}$ migrated at ~430 kDa on BN-PAGE whether or not TatA was present in the cells (Orriss *et al*., 2007). Further to this, Tarry *et al.* (2009) were able to purify a stable complex of TatBC associated with the SufI substrate precursor, using affinity chromatography with a His-tag on either SufI or TatC itself, from strains lacking both TatA and TatE. The TatBC-SufI complex migrated as two discrete bands with estimated molecular weights of 540 and 580 kDa on BN-PAGE, with subsequent negative stain electron microscopy suggesting that the complexes had different numbers of SufI molecules bound.

More recently, co-purification trials have been performed using His-tagged TatC produced from a very low copy number plasmid construct (approximately four times

above native level). Here it was seen that a low level of TatA co-eluted with TatB and TatC during Ni affinity purification (Cleon *et al*., 2015).

Early studies on TatA-containing complexes were performed by Sargent and co-workers (2001), where untagged TatA was purified from membranes solubilised in the detergent CHAPS. Following anion exchange, gel filtration of TatA-containing fractions identified a TatA-containing complex at ~600 kDa (Sargent *et al.,* 2001). This complex was found to contain mostly TatA, with a small amount of associated TatB. Another study by Porcelli and co-workers found that when using digitonin in the solubilisation step, a TatA complex, separate to TatB and TatC, could be purified and was approximately 460 kDa in size (Porcelli *et al*., 2002). Indeed further studies observed TatA oligomers purified in detergents $C_{12}E_9$ or digitonin that varied in size from ~100 kDa to over 700 kDa, and that migrating as a distinct ladder of bands on BN-PAGE (Gohlke *et al*., 2005, Oates *et al*., 2005).

Finally, it should be noted that when TatA was overproduced with $TatC_{His}$ in the absence of TatB, a heterogeneous mix of complexes containing TatA and TatC were observed, unlike the homogeneous complex formed between TatB and TatC (Fritsch *et al.*, 2012).

From these findings it is unclear whether TatA is always associated with the TatBC complex, or whether it transiently associates with the complex only during Tat transport, and can be detected during purification as an artefact due to overexpression of Tat proteins. The work described in this chapter seeks to build on prior affinity purification trials performed to decipher the effect of protein overexpression and detergent choice on the association of TatA with TatC.

3.1.3 Detergents used in this work

Digitonin is a steroidal saponin (Fig 3.1) which has detergent properties and has been utilised to purify Tat components throughout most of the prior literature due to its ability to maintain the integrity of TatB-TatC interactions (Oates *et al*., 2003, Richter *et al*.,

2007). Outside the Tat field, digitonin has successfully been used to purify higher-order oligomers of ATP synthase from mitochondrial membranes (noted for their similarity to bacterial membranes) (Schagger & Pfeiffer, 2000).

$C_{12}E_9$ (nonaethylene glycol monododecyl ether) is a non-ionic polyethylene detergent (Fig 3.1), which has been harnessed previously in the purification of TatA oligomers of various sizes (Porcelli *et al*., 2002, Gohlke *et al*., 2005). In addition, McDevitt *et al.*, (2005) observed a TatBC complex purified in $C_{12}E_9$ using sedimentation equilibrium trials, which in this case was void of detectable TatA, as observed again subsequently in McDevitt *et al*., (2006) where Tat proteins purified at native level in $C_{12}E_9$ yielded a stable TatBC complex with no associated TatA. DeLeeuw *et al*., (2002) on the other hand observed small amounts of TatA associated with $TatBC_{His}$ using $C_{12}E_9$ when the Tat proteins were overproduced. Outside the Tat field $C_{12}E_9$ has been used to successfully isolate complex II from phototrophic *Rhodoferax fermentans*, where it was demonstrated to have a superior ability to preserve the catalytic activity over several other non-ionic detergents tested.

Apart from these two detergents, several other detergents have been used in Tat studies. Triton X-100 (Fig 3.1) has been utilised previously in the purification of $TatC_{His}$ whereby TatB and TatC were found to co-elute in Ni affinity purification trials, though in this instance the elution of TatA was not examined (Buchanan *et al*., 2002). It should also be noted that 3-[(3-cholamidopropyl)dimethylammonio]-1-propanesulfonate (CHAPS) (Fig 3.1) has also been utilised successfully in Sargent *et al*. (2001) and DeLeeuw *et al*. (2001) to purify TatA(B) complexes. In addition to this, detergent Lauryl Maltose Neopentyl Glycol (LMNG) (Fig 3.1) was used to purify TatC from *A. aeolicus* prior to crystallisation (Rollauer *et al*., 2012).

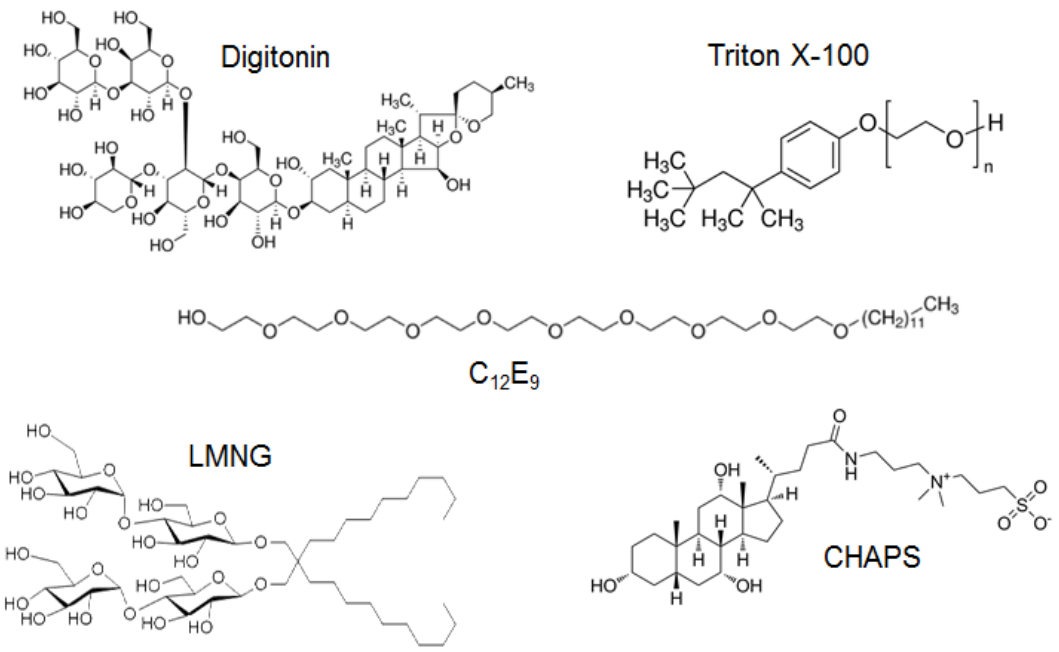

Fig. 3.1 Detergents used in this work- Chemical structures of digitonin, Triton X-100, $C_{12}E_9$ (Nonaethylene glycol monododecyl ether), LMNG (2,2-didecylpropane-1,3-bis-β-D-maltopyranoside), CHAPS (3-[(3-cholamidopropyl)dimethylammonio]-1-propanesulfonate) obtained from the Sigma Aldrich website.

3.2 Aims:

The work described in this Chapter aims to build on previous co-purification studies by using a Ni-affinity based approach to determine if there is co-elution of TatA and TatB with $TatC_{His}$. Potential artefactual TatA-TatC interactions caused by a result of protein overexpression will be explored by studying these components at high copy number and at close to native levels, and the role of selected detergents in TatA-TatC interactions, along with any potential effect of the presence of TatB will be investigated.

3.3 Results

3.3.1 A Tat(A)BC$_{His}$ complex can be purified after solubilisation in 1% digitonin,

E. coli strain DADE, which lacks chromosomally-encoded Tat components, overproducing TatA, TatB and TatC$_{His}$ from pQE60ABC$_{His}$ was used as an initial starting point for this study. Following solubilisation of membranes from this strain in 1% digitonin and purification of TatC$_{His}$ *via* Ni affinity chromatography, TatB was shown to co-purify, consistent with these proteins forming a stable complex, (Fig 3.2 Top). No TatB or TatC bound to the resin when TatC was produced without a His-tag, indicating that the interaction with the affinity matrix was specific to tagged TatC (Fig 3.2 Bottom). Some TatA was associated with the TatBC$_{His}$ complex as a faint band which cross-reacts with the TatA antibodies, detected in the elution fraction (Fig. 3.2 Top). However, this appeared to be only a very small fraction of the total amount of TatA present in the solubilised membranes (compare the unbound with the elution fractions in Fig 3.2). Some TatC$_{His}$ and TatB was also detected in the unbound fraction, however under these conditions it is clear that the majority of each has bound to the Ni^{2+} resin.

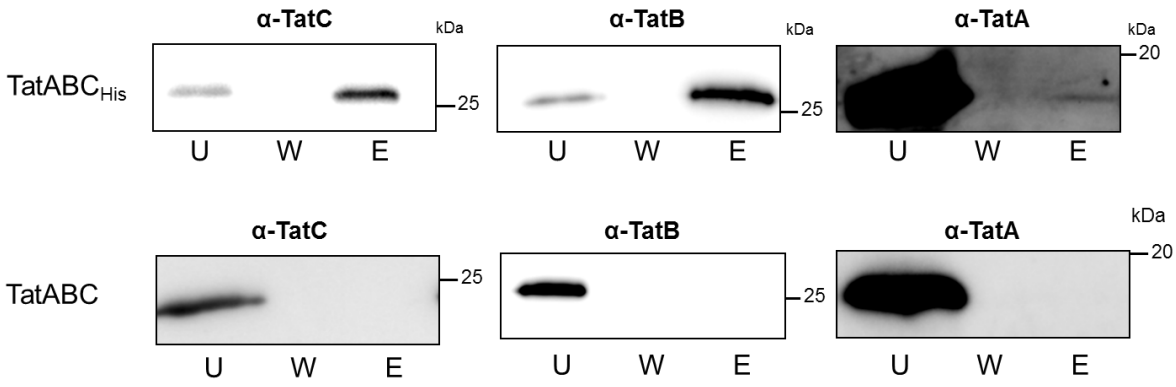

Figure 3.2) Western blot analysis of Ni^{2+} affinity-purified TatABC$_{His}$. Following solubilisation of membranes in 1 % digitonin, the solubilised material was incubated with Ni^{2+}-affinity resin, the unbound fraction (U) was retained, the resin was washed (W) and bound material eluted with imidazole (E). Each fraction was analysed via Western blotting for the presence of TatA, TatB or TatC, as indicated, with 5µL of sample loaded into each well. **Top-** Membranes from *E. coli* strain DADE expressing TatABC$_{His}$ **Bottom-** Membranes from strain DADE expressing TatABC as a negative control.

3.3.2 TatA-TatC$_{His}$ interactions are potentially enhanced in the absence of TatB when analysed using digitonin as detergent

To explore the types of TatC$_{His}$-containing complexes that might be present in the absence of either TatA or TatB, similar experiments were undertaken using digitonin-solubilised membranes of strain DADE expressing either pQE60A(ΔB)C$_{His}$ (*i.e*. TatAC$_{His}$ without TatB) or pFAT75ΔA (a pQE60-based vector encoding TatBC$_{His}$, *i.e.* lacking TatA).

As expected, in the absence of TatA, a TatBC$_{His}$ complex could be isolated (Fig 3.3 Top), in accord with the previous findings of Orriss *et al*. (2007). In the absence of TatB, TatA clearly co-eluted with TatC (Fig 3.3 Bottom), confirming the prior observations of Fritsch *et al*. (2012) and indicating that the likely binding site for TatA on the TatBC complex is the TatC rather than the TatB protein. Interestingly, it appeared qualitatively that more TatA may co-elute with TatC$_{His}$ in the absence of TatB than in its presence (compare anti-TatA in Fig. 3.2 and 3.3) suggesting that in the absence of TatB, TatA-C interactions are promoted. This could potentially be explained by additional TatA molecules moving in to occupy the now vacant TatB site on TatC$_{His}$ perhaps representing a step in the Tat cycle which TatB modulates.

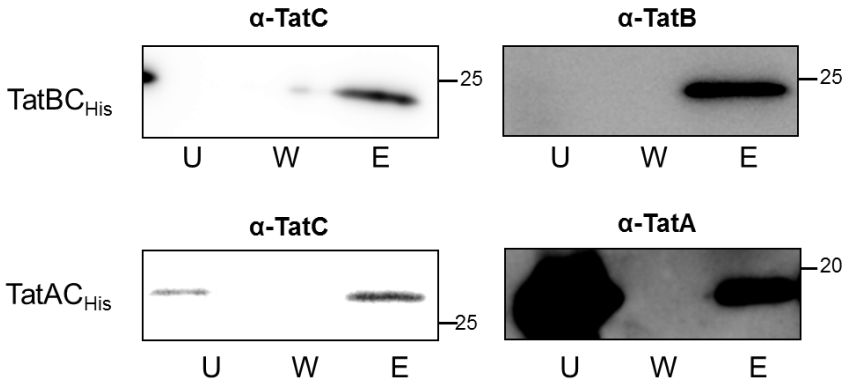

Figure 3.3) Western blot analysis of Ni^{2+} affinity-purified TatAC$_{His}$ and TatBC$_{His}$. Following solubilisation of membranes in 1 % digitonin, the solubilised material was incubated with Ni^{2+}-affinity resin, the unbound fraction (U) was retained, the resin was washed (W) and bound material eluted with imidazole (E). Each fraction was analysed *via* Western blotting for the presence of TatA, TatB or TatC, as indicated, with 5μL of sample loaded into each well. **Top**- Membranes from *E. coli* strain DADE expressing TatBC$_{His}$ **Bottom-** Membranes from strain DADE expressing TatAC$_{His}$

3.3.3 A TatB and $TatC_{His}$ complex can be purified after solubilisation in 1% $C_{12}E_9$, with no associated TatA

When $TatC_{His}$-containing complexes were purified from membranes of *E. coli* strain DADE harbouring $pQE60ABC_{His}$ using 1% $C_{12}E_9$ as detergent, a different elution pattern was observed (Fig 3.4 Top). Most notable was the lack of any detectable TatA in the elution fraction, suggesting that, unlike digitonin, solubilisation in $C_{12}E_9$ causes TatA to dissociate from the $TatBC_{His}$ complex. TatB and $TatC_{His}$ still appeared to form a stable complex in $C_{12}E_9$ (Fig. 3.4 Top) consistent with prior observations (DeLeeuw *et al.*, 2002, McDevitt *et al*., 2005, McDevitt *et al*., 2006, Behrendt & Bruser, 2014). Again control experiments using untagged Tat proteins showed that there was no non-specific binding of TatA, B or C to the Ni resin.

This discrepancy between detergents may reflect differences between the chemistry of digitonin and $C_{12}E_9$ with the latter perhaps having an ability to dissociate the more weakly bound TatA (this is expanded on in detail in Section 3.4.1). Interestingly, the conditions used to purify native levels of $TatC_{His}$ in McDevitt *et al.* (2006), where TatA was found not to co-elute with TatC, utilised $C_{12}E_9$ in the solubilisation step, suggesting that the choice of detergent rather than the copy number of Tat components may be the reason for the lack of co-purifying TatA.

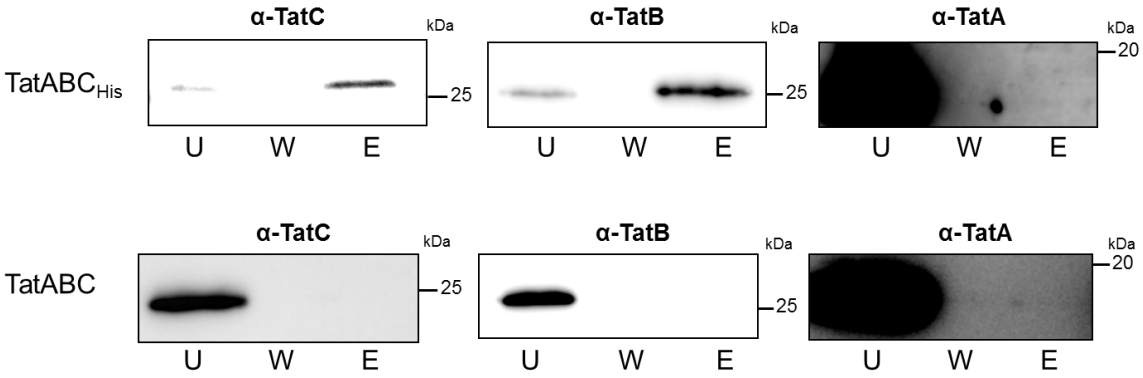

Figure 3.4) Western blot analysis of Ni^{2+} affinity-purified $TatABC_{His}$. Following solubilisation of membranes in 1 % $C_{12}E_9$, the solubilised material was incubated with Ni^{2+}-affinity resin, the unbound fraction (U) was retained, the resin was washed (W) and bound material eluted with imidazole (E). Each fraction was analysed *via* Western blotting for the presence of TatA, TatB or TatC, as indicated, with 5µL of sample loaded into each well. **Top-** Membranes from *E. coli* strain DADE expressing $TatABC_{His}$ **Bottom-** Membranes from strain DADE expressing TatABC as a negative control.

3.3.4 Trace amounts of TatA can be co-purified with $TatC_{His}$ after $C_{12}E_9$ solubilisation when TatB is absent

Although TatA could not be purified with $TatC_{His}$ after solubilisation with $C_{12}E_9$ when TatB was present (Section 3.3.3), it was hypothesised that the absence of TatB may modify TatA-TatC interactions, as was observed above after solubilisation with digitonin.

It can be seen that the use of $C_{12}E_9$ as detergent instead of digitonin made little difference to the elution of TatB with $TatC_{His}$ from $TatBC_{His}$ expressing constructs, as expected (Fig. 3.5 Top). In the absence of TatB, a very low level of TatA was found to co-elute with $TatC_{His}$ (Fig 3.5 Bottom), suggesting that there may potentially be some modulation of TatA-TatC interaction in the absence of TatB. However, the enhancement of TatA-$TatC_{His}$ interactions was much more notable when using digitonin, whereby a weak TatA-$TatC_{His}$ association in the presence of TatB became much stronger in its absence (compare Fig. 3.2 and 3.3). It therefore appears that TatA-TatC interactions are destabilised when $C_{12}E_9$ is used as detergent.

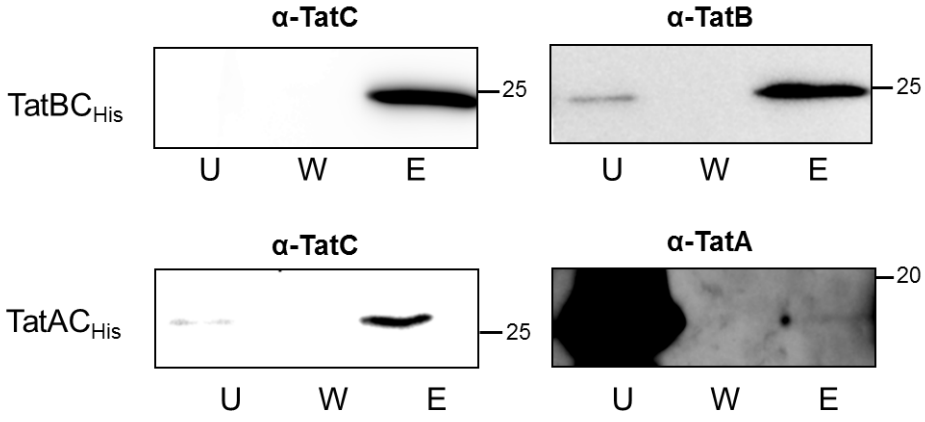

Figure 3.5) Western blot analysis of Ni^{2+} affinity-purified $TatAC_{His}$ and $TatBC_{His}$. Following solubilisation of membranes in 1 % $C_{12}E_9$, the solubilised material was incubated with Ni^{2+}-affinity resin, the unbound fraction (U) was retained, the resin was washed (W) and bound material eluted with imidazole (E). Each fraction was analysed *via* Western blotting for the presence of TatA, TatB or TatC, as indicated, with 5µL of sample loaded into each well. **Top**- Membranes from *E. coli* strain DADE expressing $TatBC_{His}$ **Bottom-** Membranes from strain DADE expressing $TatAC_{His}$

3.3.5 Using the TatC D211A substitution as a tool to examine TatA-TatC interactions

The D211 residue in the short periplasmic loop 3 of TatC is highly conserved and has been hypothesised to have an important role in Tat transport. Buchanan *et al.* (2002) found that substitution of D211 with alanine could not be tolerated, shown by subsequent analysis of Tat activity, while Kneuper *et al*. (2012) and Cleon *et al*. (2015) both found that the D211R substitution abolished Tat transport (the position of D211 is shown in Fig. 3.6A).

In addition to data showing the negative impact of D211 TatC substitutions on Tat activity, Buchanan *et al*. (2002) is the only study to have observed the effect of D211A on subunit interactions where it was reported that the substitution caused an abolishment of TatB co-elution with $TatC_{His}$. This was shown through Ni^{2+}-affinity purification experiments using the detergent Triton X-100, the only report for which this detergent has been used for the study of Tat components (Buchanan *et al.,* 2002). Currently this observation has yet to be confirmed using any other detergents, and the effect of the TatC D211A substitution on TatA-TatC interactions has not been examined. It was hypothesised in this work that if TatB-TatC interactions are impaired, this may promote TatA-TatC interactions as was observed in the absence of TatB seen in Sections 3.3.2 and 3.3.4. In support of this proposal, crosslinks to TatA have been observed through residues in the TatC P3 loop in *E. coli* (Zoufaly *et al*., 2012) and plants (Aldridge *et al*., 2014). Indeed, performing co-purification experiments using $TatC_{His}$ D211A would allow the investigation of TatA-$TatC_{His}$ interactions when TatB is present but presumably not tightly associated with TatC and in turn reveal whether D211 may also modulate TatA interactions.

3.3.6 The $TatC_{His}$ D211A substitution impairs Tat transport

To test the Tat transport activity of TatC containing the D211A substitution (Fig. 3.6A), the export of Tat substrates was analysed by growth assays on two types of selective

media, (i) screening for growth in the presence of 2% SDS assesses whether two Tat-dependent cell wall amidases, AmiA and AmiC, have been exported to the periplasm (Stanley *et al.*, 2001, Ize *et al.*, 2003), whereas (ii) screening for growth on minimal media containing TMAO/glycerol under anaerobic conditions would identify cells able to export Tat-dependent TMAO and DMSO reductases that collectively support anaerobic respiration using TMAO as the final electron acceptor (Santini *et al*., 1998) (Fig 3.6B).

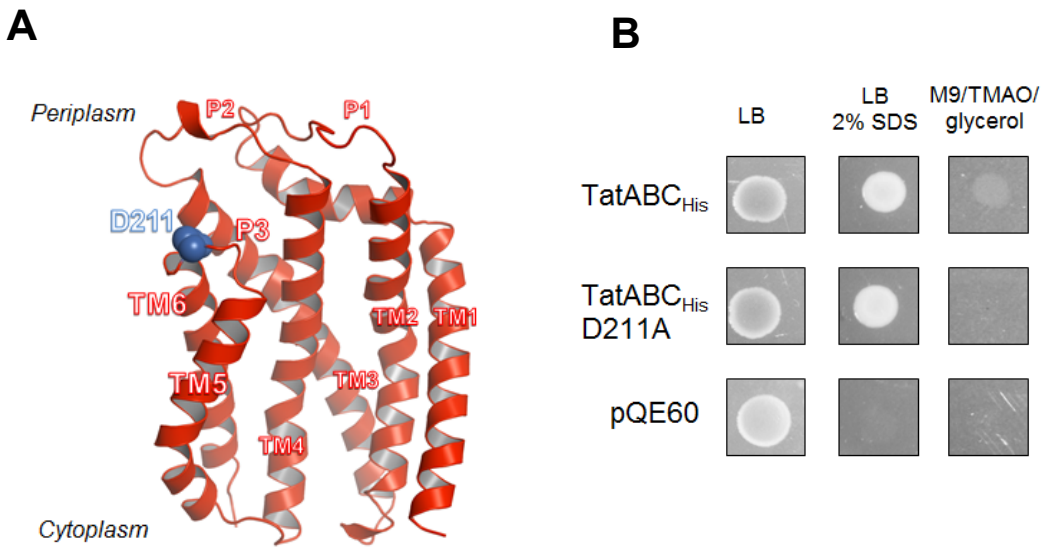

Figure 3.6) Growth assays to test for the presence of an active Tat system with the TatC substitution D211A- A- shows the position of the D211A substitution in TatC**, B-** DADE (a Δ*tatABCDE* strain) was transformed with medium copy number pQE60 based vectors encoding *tatABC$_{His}$/tatABC* and spotted onto media to test standard anaerobic growth on LB, with detergent stress (2% SDS) and anaerobically on minimal media containing glycerol with TMAO as the final electron acceptor. Proteins expressed are noted with the top denoting the conditions of growth.

It can be seen, as expected, that the strain harbouring pQE60ABC$_{His}$ could grow on both types of selective media. However, cells harbouring pQEABC$_{His}$D211A showed no detectable anaerobic growth on minimal TMAO medium, although the strain was able to grow in the presence of 2% SDS (Fig. 3.6B). This is consistent with the findings of Buchanan *et al*. (2002) who also observed growth of TatABC D211A expressing strains on SDS but not M9/TMAO/glycerol. Further to this, the latter work observed negligible periplasmic TorA activity in strains expressing TatABC$_{His}$D211A. While the discrepancy in the export of substrates is curious, it is clear that the D211A substitution in TatC severely impairs Tat function.

3.3.7 The $TatC_{His}$ D211A substitution causes detergent-dependent dissociation of TatB and stabilisation of TatA-TatC interactions

It was reported by Buchanan *et al*. (2002) that the TatB-TatC interaction was disrupted when TatC harboured the D211A substitution, using Triton X-100 as detergent. However, as discussed above, Triton X-100 has not been used routinely as a detergent for the purification of Tat complexes. Therefore, it was essential to first determine the amount of TatA that co-purifies with $TatC_{His}$ (without the D211A substitution) when membranes were solubilised in Triton X-100. Fig. 3.7 demonstrates that, while TatB and TatC form a stable complex in this detergent, no detectable TatA is found in the elution fraction. Thus, the Tat(A)BC complex appears to behave the same way in Triton X-100 as it does in $C_{12}E_9$, with a loss of TatA from the complex.

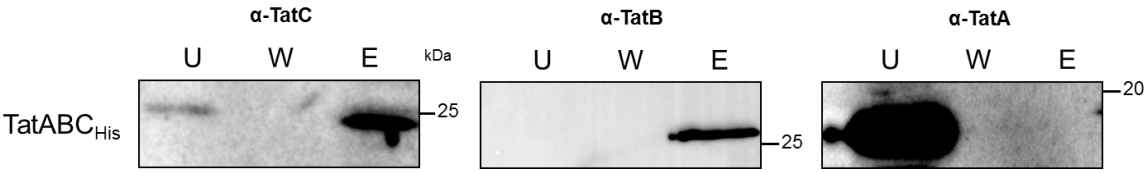

Figure 3.7) Western blot analysis of Ni^{2+} affinity-purified $TatABC_{His}$. Following solubilisation of membranes in 1 % Triton X-100 the solubilised material was incubated with Ni^{2+}-affinity resin, the unbound fraction (U) was retained, the resin was washed (W) and bound material eluted with imidazole (E). Each fraction was analysed *via* Western blotting for the presence of TatA, TatB or TatC, as indicated, with 5µL of sample loaded into each well.

Next, to confirm the prior findings of Buchanan *et al*. (2002), membranes of strain DADE expressing pQE60ABC_{His}D211A were solubilised using 1% Triton X-100 as detergent. Subsequent Ni-affinity purification demonstrated that while $TatC_{His}$ was clearly present in the elution fraction, all of the TatB remained unbound (Fig. 3.8 Top panel). This, taken together with the small amount of TatA present in the elution fraction, indicates that TatB is no longer able to form a stable complex with $TatC_{His}$ and in its absence TatA-$TatC_{His}$ interactions are increased. This could be explained by TatA moving to occupy the vacated TatB site, as may also be the case when cells express TatA and TatC only (Sections 3.3.4 and 3.3.2).

Interestingly, when $C_{12}E_9$ was used as detergent to solubilise TatABC$_{His}$D211A proteins, the Tat proteins behaved essentially the same on Ni-affinity purification as they did in Triton X-100, *i.e*. the TatB-TatC interactions were disrupted and TatB was found solely in the unbound fraction (Fig 3.8, Middle panel). Again, a low level of TatA was seen to co-purify with TatC$_{His}$ in this experiment. By contrast, when TatABC$_{His}$D211A proteins were solubilised using digitonin, a stable TatBC complex was

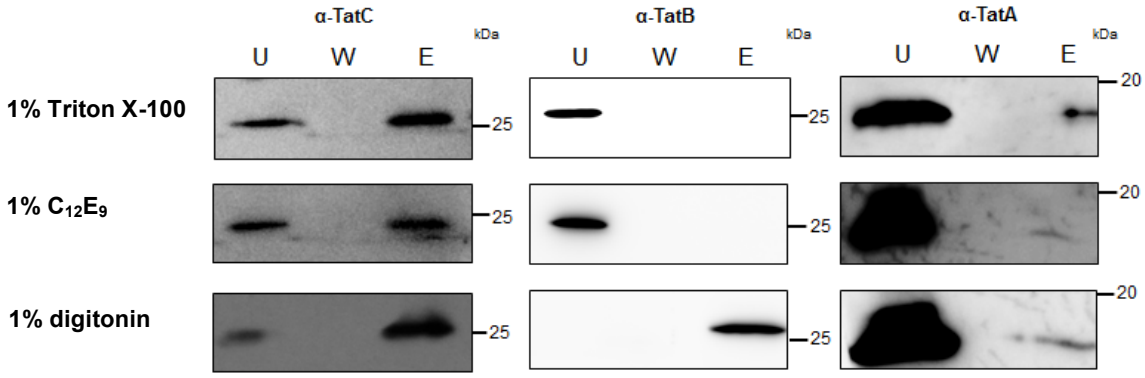

Figure 3.8) Western blot analysis of Ni^{2+} affinity-purified TatABC$_{His}$D211A. Following solubilisation of membranes in 1 % Triton X-100, 1% $C_{12}E_9$ or 1 % digitonin the solubilised material was incubated with Ni^{2+}-affinity resin, the unbound fraction (U) was retained, the resin was washed (W) and bound material eluted with imidazole (E). Each fraction was analysed *via* Western blotting for the presence of TatA, TatB or TatC, as indicated, with 5μL of sample loaded into each well.

still observed in the presence of the TatC D211A substitution, and no TatB was detected in the unbound fraction (Fig. 3.8, Bottom panel). The most plausible explanation for these findings is that the nature of the TatBC interaction is altered in the presence of the TatC D211A substitution and that this altered or more loosely bound TatB can be selectively stripped from its TatC binding site by some types of detergents. Since the co-elution of TatA with TatC seems unaffected by the TatC D211A substitution (for example compare Figs. 3.7 and 3.1), it would suggest that either the binding of TatA is remote from the TatC P3 loop and the D211 residue, or that it binds to the site in a different conformation to that of TatB.

3.3.8 Tat(A)BC$_{His}$ can be purified using 1% digitonin but not 1% C$_{12}$E$_9$ when proteins are expressed from a low copy number vector

To determine whether any of the co-purification results seen for the wild type Tat complexes in Figs 3.2 and 3.4 arose due to the relative overexpression of Tat components, similar experiments were repeated for Tat proteins produced at close to native copy number from plasmid pTat101 (estimated to be approximately four times native level; Kneuper *et al*., 2012). Figure 3.9 (Top panel) demonstrates that when membranes are solubilised with digitonin, TatA can still be co-purified with TatBC$_{His}$ when the subunits are present at low copy number. As expected, control experiments indicated that binding to the resin was specific to the His-tag present on TatC as Tat proteins expressed at a very low copy number without a His-tag did not bind to the Ni resin (Fig 3.9, Bottom panel).

When 1% C$_{12}$E$_9$ was used to solubilise Tat proteins from the membrane, TatB and TatC$_{His}$ could still co-elute from the Ni-charged resin, however TatA was not associated with the complex, which was also seen at medium copy number in this detergent (Fig. 3.4). Thus it appears that it is the nature of the detergent used for the purification experiments rather than the copy number of the Tat proteins that is critical for the types of TatC-containing complexes isolated.

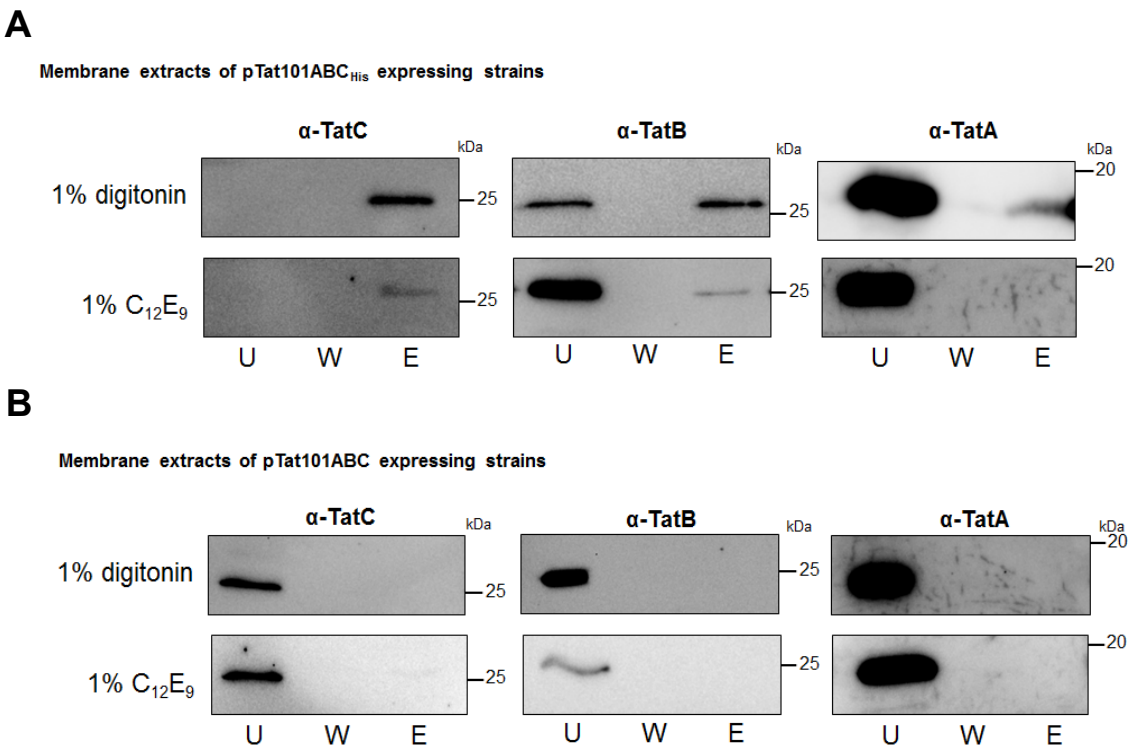

Figure 3.9) Western blot analysis of Ni^{2+i} affinity-purified TatABC$_{His}$ produced at a very low copy number. Following solubilisation of membranes in 1 % $C_{12}E_9$ or digitonin, as indicated, the solubilised material was incubated with Ni^{2+}-affinity resin, the unbound fraction (U) was retained, the resin was washed (W) and bound material eluted with imidazole (E). Each fraction was analysed *via* Western blotting for the presence of TatA, TatB or TatC, as indicated, with 5µL of sample loaded into each well. **A-** Membranes from *E. coli* strain DADE expressing TatABC$_{His}$ **B-** Membranes from strain DADE expressing TatABC as a negative control.

3.4 Discussion

3.4.1 TatA is weakly associated with TatC in the Tat(A)BC complex

The work presented in this Chapter, in combination with prior literature, makes a very strong case for the presence of at least a small amount of TatA in the TatBC recognition complex. As the experiments here were performed using isolated membranes, the complexes should be in the resting state, and any protonmotive force-dependent intermediate complexes (for example translocation intermediates where large assemblies of TatA are recruited to the TatBC complex) should not be present. Moreover, this work has clearly demonstrated that there is co-elution of TatB with TatC when either digitonin or $C_{12}E_9$ are used to solubilise the Tat components and at two different protein expression levels. This indicates a stable interaction between these two proteins. When using digitonin a low level of TatA is also clearly found associated with $TatC_{His}$, which is not seen when the $C_{12}E_9$ detergent is used

3.4.2 Choice of detergent is important: A Tat(A)BC complex can be purified with digitonin but not $C_{12}E_9$

Given that TatA has been found consistently to co-elute with affinity tagged TatC in the presence of digitonin, it may be the case that TatA is always associated with the TatBC complex, but the interaction is weak or transient, and therefore easily disrupted by harsher detergents (for example $C_{12}E_9$), or other buffer constituents (since Bolhuis *et al.* (2001) noticed successive loss of TatA associated with the TatBC complex during purification steps). The results presented here neatly account for the findings of McDevitt *et al.* (2006), who failed to co-purify TatA with $TatBC_{His}$ at native levels of protein production when membranes were solubilised in $C_{12}E_9$. An alternative explanation is that digitonin may somehow promote interactions that would not be observed in native membranes (for example by causing conformational change in the TatBC complex and driving TatA association). However, given that TatA association is still observed when protein is expressed from low copy number constructs, and

previous studies in plants have observed interactions between Tha4-cpTatC (TatA-TatC) interactions in thylakoid membranes which do not change in response to substrate (*i.e.* constitutive interactions; Aldridge *et al*., 2014) this seems less likely.

Interestingly, previous studies purifying ATP synthase from mitochondrial membranes (which have notable similarity to bacterial inner membranes) found that digitonin could stabilise higher order oligomers which could not be seen with other detergents (Schagger & Pfeiffer, 2000). Indeed, it could be the case that digitonin has properties that can facilitate extraction of membrane protein complexes in a more intact manner than with detergents that can more readily strip native membrane lipids away from or dissociate interactions between membrane proteins.

3.4.3 A potential step in the Tat cycle: TatB dissociation from TatC promotes TatA-TatC interactions

When $TatC_{His}$ purification was undertaken in the absence of TatB, it was seen that a low level of TatA could now co-elute with $TatC_{His}$ in $C_{12}E_9$ detergent, or that interaction was enhanced (for membranes solubilised with digitonin). There are a number of possible explanations that may account for this finding. It may be that TatB normally partly occludes TatA interaction with TatC, and its removal allows TatA to bind more tightly to its binding site. Alternatively, TatA could in addition be occupying the vacated TatB site on TatC TM5, given the homology between the two proteins, and the suggestion from crosslinking studies that both TatA and TatB can interact at TM5 (Blummel *et al*., 2015). In this context it is interesting to note that studies of the thylakoid Tat system suggest that TatA occupies a site at the P3 near TM5 loop constitutively (Aldridge *et al*., 2014) and this is supported by crosslinking studies in *E. coli* where crosslinks to TatA from TatC P3 residues 209 and 211 were observed (Zoufaly *et al*., 2012, Blummel *et al*., 2015). Importantly, Blummel *et al.* (2015) also observed that when TatB was absent TatA crosslinked to the TatC P3 loop, which may

account for the increased co-purification of TatA observed in this work in the absence of TatB.

Finally it is possible that TatA may be able to interact with the concave face of TatC in a step modulated by the presence of TatB. Indeed, crosslinks have been observed between TatA and this region of TatC in the thylakoid Tat system (Aldridge *et al.,* 2014), and Rollauer *et al*. (2012) proposed that TatA may interact at this region of TatC based on *in silico* models. Removal of TatB could allow TatA to interact with this site on TatC in a step that would normally only occur when TatB is triggered to move. Indeed, Blummel *et al*., (2015) also observed increased TatA crosslinks across TatC TM3 and TM4 in the absence of TatB.

3.4.4 The D211A substitution in TatC destabilises TatB-TatC interactions but still supports TatA-TatC interactions

Buchanan *et al.* (2002) concluded that the TatC D211A substitution impaired interactions with TatB based on the loss of TatB-$TatC_{His}$ co-elution after Ni affinity purification in Triton X-100 detergent solution. Here, the prior findings were confirmed and built upon showing that the TatC D211A mutation does not prevent interaction of TatC with TatA, on the contrary, in $C_{12}E_9$ and Triton X-100 solution TatA-$TatC_{His}$ interaction appeared to be enhanced. This is consistent with co-elution of TatA with $TatC_{His}$ observed when TatB was removed and is in support of the proposition that removal of TatB promotes TatA-TatC interactions.

By contrast, in digitonin solution all of the TatB remained bound to $TatC_{His}$D211A, a markedly different finding to the results when $C_{12}E_9$ and Triton X-100 were used as detergents. Taken at face value, the Triton X-100 and $C_{12}E_9$ purification results would suggest that the toxicity of the TatC D211A substitution is caused by dissociation of TatB from TatC, however in light of digitonin purification results, it seems more likely that TatB and TatC are still associated in the native *E. coli* membrane, but the interaction between the two is severely weakened. If this were the case it would be

reasonable to suggest that TatC D211 interacts with TatB and therefore crosslinks to TatB may be observed through residues in the TatC P3 loop. However of those P3 residues that were selected for photocrosslinking, residues 209 and 211 itself, neither formed a crosslink with TatB when substituted with Bpa (Zoufaly *et al*., 2012, Blummel *et al*., 2015). Those residues could, however, crosslink to TatA (and in plants Tha4, equivalent to TatA, was shown to interact at the P3 loop (Aldridge *et al.*, 2014). However, when Zoufaly *et al.* (2012) performed crosslinking using a D211-Bpa TatC variant, it was noted that Tat activity was severely impaired, perhaps consistent with a destabilisation of TatB-TatC interactions similar to those observed with D211A, which may lead to a loss of crosslinking to TatB. Indeed an alternative explanation could be a global effect on the Tat complex, whereby the D211A substitution causes an allosteric effect which favours TatA interaction over TatB. For example, perhaps D211 is responsible for the successful dissociation of TatA from the Tat complex, and its replacement causes aberrantTatA interactions which adversely affect TatB interactions.

In conclusion, the work in this Chapter strongly suggests that TatA is usually associated with the TatBC complex, and this complex will henceforth be called the Tat(A)BC complex.

Chapter 4: TatA interacts with TatC at the periplasmic facing region of TM6 *in vivo*

4.1 Introduction

4.1.1 Utilising crosslinking to dissect protein interactions in the Tat system

When deciphering protein-protein interactions, crosslinking-based methods provide an excellent indicator as to whether proteins are in proximity to each other. Interacting proteins can be identified from a reaction mixture as a covalently linked dimer, giving a change in molecular weight corresponding to the two proteins combined, and being responsive to antibodies raised to each protein. This covalent linkage is derived by chemical means, by adding crosslinking reagents to the reaction mixture containing proteins of interest, such as DSS (disuccinimidyl suberate), which can link proteins through lysine residues *via* an amine-reactive N-hydroxysuccinimide (NHS) ester. DSS itself consists of two NHS groups at either end of an eight carbon spacer, and therefore the amine groups on two proteins may be relatively far apart (Fig.4.1B).

The ability of DSS to traverse lipid bilayers means it lends itself well to analysing interactions between membrane proteins. Indeed, this method was used by Hicks *et al*. (2003) where TatA homo-oligomers were crosslinked together and in DeLeeuw *et al*. (2001) where TatA was also self-crosslinked. Dabney-Smith *et al.* (2006) also crosslinked Tha4 (the thylakoid TatA analogue) using DSS showing that it forms homo-oligomers in a similar manner to *E. coli* TatA.

Similarly, crosslinking can be performed with sulfhydryl-reactive groups separated by a spacer arm, as with DSS, however, instead of the amino-reactive NHS group, a maleimide can be used to couple with cysteine (Fig. 4.1A). To study interactions in the Tat system, Blummel *et al.* (2015) successfully utilised bismaleimidohexane (BMH), a compound with two maleimide groups separated by a 12 Å spacer arm, to link together two TatC proteins in the TatBC complex *via* cysteine residues incorporated into the periplasmic facing region of TatC. While in this instance, membrane-soluble BMH was used, a similar principle can also be used to label protein regions accessible to the periplasm by utilising molecules which cannot cross the lipid bilayer. For example,

Koch *et al.* (2012) utilised membrane-insoluble methoxypolyethylene glycol maleimide (MAL-PEG) to label cysteine groups accessible to the periplasm in TatA and TatB, identifying their N-out, C-in topology in cells.

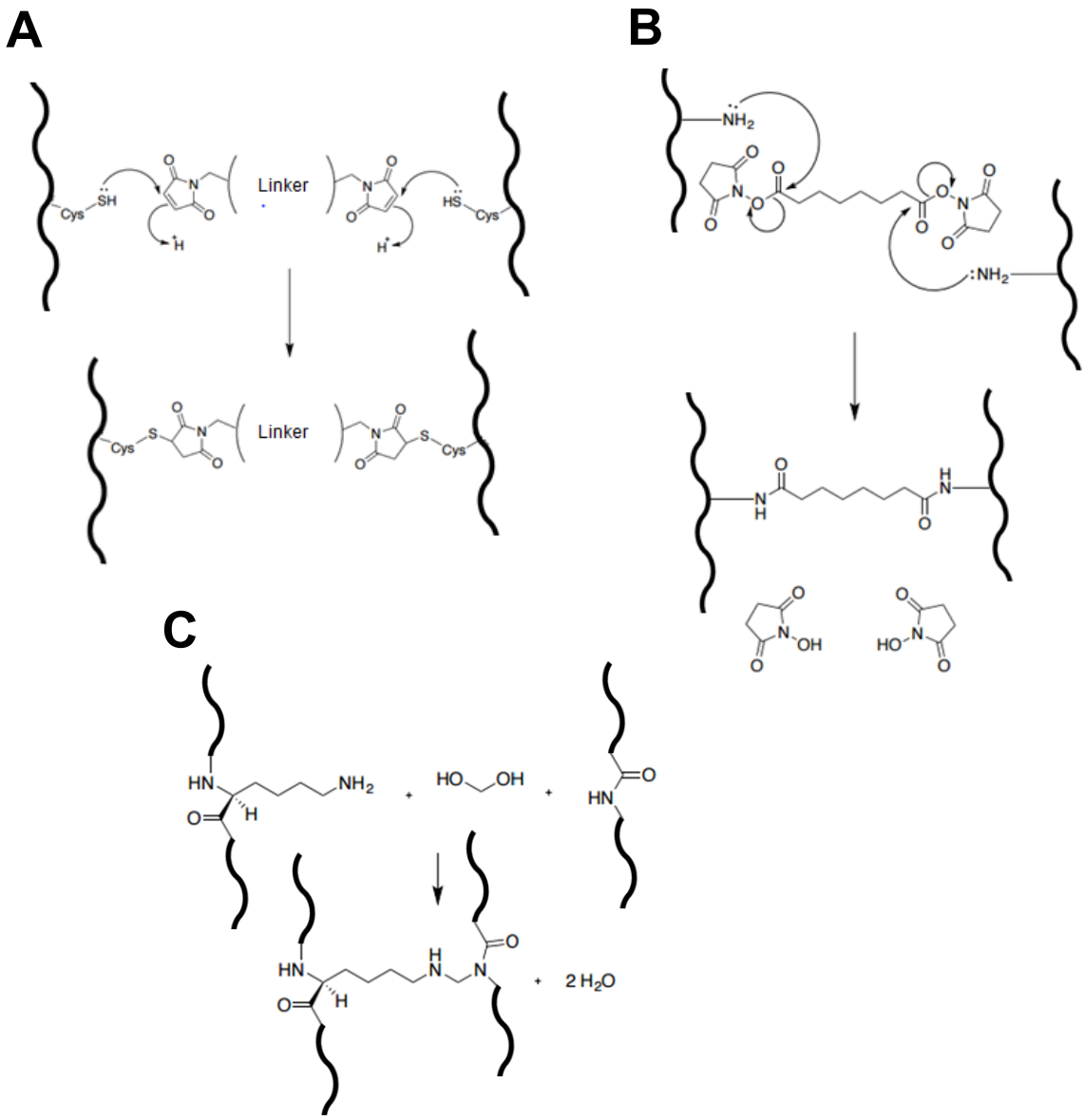

Fig. 4.1) Mechanisms behind maleimide, DSS and formaldehyde crosslinking- A- shows crosslinker molecule with two reactive maleimide groups, which is linked by a carbon chain of a variable length. The maleimide group reacts with free Cys residues on proteins, **B-** shows DSS crosslinking with an 8 carbon chain and two NHS groups at either side. These groups react with primary amines in lysine side chains to link two proteins together, **C-** shows formaldehyde crosslinking, whereby formaldehyde reacts with water to form glycol, which reacts with primary amines in proteins to link them to the backbone of another protein (protein backbone shown as black wavy line).

Formaldehyde can also be added to a reaction mixture to covalently link two proteins together. In water, formaldehyde reacts to form glycol, which is able to link a lysine

residue on one protein to the peptide backbone of an interacting partner (Fig. 4.1C). Unlike DSS/maleimide crosslinking, this only requires the functional group (a primary amine) to be present in one protein if the interacting partners are different, however, this slight convenience is offset by the fact the that no data can be derived about where on the interacting protein the primary amine is crosslinking, again allowing only the proximity of two proteins to be determined. Formaldehyde crosslinking was used by DeLeeuw *et al*. (2001) to identify TatA homo-oligomers.

Alternatively, crosslinking can be performed directly through residues incorporated into the protein without adding a crosslinking molecule to the reaction mixture, for example through Cys residues in disulphide crosslinking, or through a photo-reactive amino acid analogue in photo-crosslinking.

Disulphide crosslinking has been demonstrated to be a useful tool in dissecting Tat protein interactions. Essentially, this method can be used to elucidate protein interactions by engineering Cys-less variants of two proteins and re-engineering Cys residues back into them at sites which may be in contact. If these Cys residues are close to each other in the protein complex, a disulphide bond will form under oxidising conditions, linking the two proteins together covalently (Fig. 4.2) as a heterodimer (or homodimer if the proteins are the same). The subsequent molecular weight, corresponding to the combined weight of both proteins, can be analysed by Western blotting, whereby the heterodimer will respond to antibodies raised to both proteins in the dimer. Disadvantages to this method include the need for a protein which can function without native Cys residues, and in turn tolerate non-native Cys substitutions (for example, important residues may be involved in interaction sites, but sites may be disrupted by trying to analyse them with Cys substitutions). Interactions that are observed, however, are relatively reliable as Cys is a small amino acid, which requires close proximity to another Cys to form a disulphide bond, to an extent precluding non-specific crosslinks unless the proteins are interacting aberrantly.

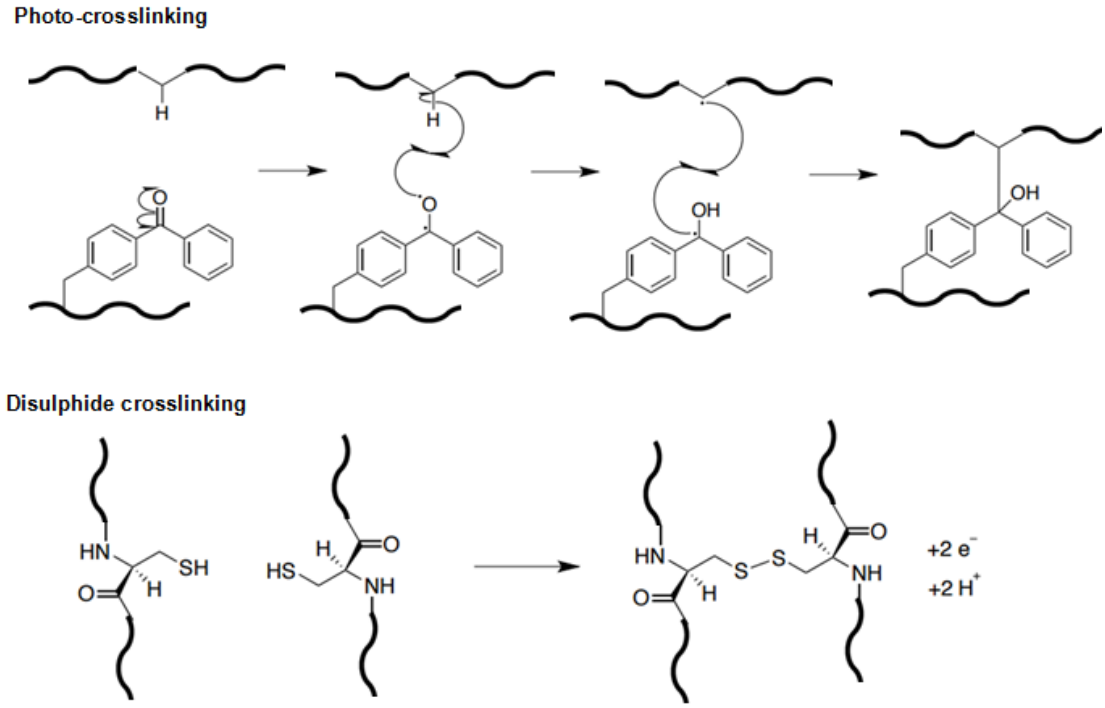

Fig. 4.2) Mechanisms behind disulphide and photo-crosslinking- Top- shows the mechanism behind photo-crosslinking with the radical formed *via* UV light in the first step, **Bottom-** shows a disulphide crosslink forming between to Cys residues under oxidising conditions, (wavy lines represent protein backbone)

Similarly, photo-crosslinking can be used to analyse protein interactions, for example using a benzoylphenylalanine (Bpa) photo-reactive amino acid analogue incorporated by genetic means into the protein of interest. Upon exposure to UV, the Bpa photo-reactive group, a benzophenone, is activated, causing it to couple covalently with nearby interacting proteins *via* the production of free radicals (Fig. 4.2). This allows crosslinking to be performed without the need for both removal of native Cys residues from proteins or exposure to oxidising agents. However, given that Bpa is significantly larger than Cys, issues around disrupting interaction faces caused by its incorporation into proteins may be exacerbated. In addition to this, photo-crosslinks require UV exposure, which may damage living cells, and furthermore this approach does not immediately reveal where on the interacting protein the Bpa group is crosslinking.

Photo-crosslinking and disulphide crosslinking are the most commonly used crosslinking approaches to study Tat complexes (Chapter 1, Sections 1.10.5 and

1.10.7) and this thesis uses disulphide crosslinking to analyse interactions between TatA and TatC. A Cys scanning region in TatC encompassing part of TM5, the P3 loop and part of TM6 was chosen to crosslink to the TatA transmembrane helix (the rationale for this choice and specific residues is detailed in Section 4.1.3). Given the small size of Cys, disulphide crosslinking lends itself well to performing Cys scanning mutagenesis with minimal disruption to Tat activity, while Cys substitutions in the TatA transmembrane helix (TM) and TatC TM5 have been previously demonstrated to be well tolerated (Rollauer *et al.,* 2012, Kneuper *et al.,* 2012, Greene *et al.,* 2007, Cleon *et al*., 2015). In addition, a disulphide crosslinking approach will also allow specific residues in both TatA and TatC to be directly identified as in close proximity.

4.1.2 Crosslinking the *E. coli* Tat subunits *in vitro* and *in vivo*

In the *E. coli* Tat system, *in vitro* disulphide crosslinking, whereby experiments are performed on isolated membrane fractions, has been used to identify a site at TM5 of TatC where TatB is proposed to bind constitutively (Rollauer *et al.,* 2012, Kneuper *et al.* 2012), while TatC self-interaction has been identified across all transmembrane helices of TatC using the same method (Punginelli *et al.,* 2007). In addition to this, a proposed arrangement of the TatBC complex has been put forward based on photo-crosslinking in *E. coli* inside-out inner membrane vesicles (INVs) (discussed in detail in Chapter 1, Section 1.10.5) with TatB occupying sites at TatC TM5 and TM2/4 (Blummel *et al.,* 2015). With regard to TatA, photo-crosslinking in *E. coli* INVs has shown interactions at TatC TM5/P3/P2 (Zoufaly *et al.,* 2012, Blummel *et al.,* 2015) and found that TatE, a functional homologue of TatA is associated with TatC in INVs (Eimer *et al.,* 2015).

In vivo disulphide crosslinking in living *E. coli* cells would allow an examination of protein-protein interactions in the presence of a PMF, delivering information as to the behaviour of membrane proteins in their native environment. Indeed, Cleon *et al*. (2015) published data showing that *in vivo,* the TatC homodimer that was Cys-linked through TM5 could not be observed unless overexpressed substrate was present,

apparently in disagreement with results using isolated *E. coli* membrane fractions in Rollauer *et al.* (2012) and Kneuper *et al.* (2012) which demonstrated TatC homodimerisation through M205C without the need for overexpressed substrate. From this, it is conceivable that crosslinking patterns observed between Tat subunits *in vitro* may not reflect those seen *in vivo*. Indeed, the role of PMF, which is not present *in vitro*, in modulating Tat subunit interactions has been explored extensively (Chapter 1, Section 1.10.5 and 1.10.7), which could feasibly translate to differential interactions detectable using disulphide crosslinking studies.

The work in this Chapter characterises TatA-TatC interactions further using *in vivo* disulphide crosslinking. This approach allows interactions to be mapped between the two subunits in the presence of the PMF and native lipid environment.

4.1.3 TatA and TatC Cys substitutions chosen in this work

Previous work has already identified TatC TM5 as a likely candidate for the TatB binding site (Chapter 1, Section 1.10.5), while other studies in plants and *E. coli* have identified both TatC TM5 and the P3 loop (or equivalent in chloroplast TatC) as a candidate for TatA interactions. Specifically, residue M205 in TatC TM5, when substituted with Bpa, was found to photo-crosslink to both TatA and TatB in *E. coli* INVs (Blummel *et al*., 2015) and when substituted with Cys was found to crosslink to Cys residues introduced at TatB L9, L10 I11 and I12 in isolated *E. coli* membrane fractions (Rollauer *et al*., 2012, Kneuper *et al*., 2012), The TM of the chloroplast TatA orthologue, Tha4, was also found to bind to the cpTatC TM5 (at the equivalent of TatC M205) in a manner enhanced by overexpression of Tat substrate, while a second Tha4 binding site at the equivalent of the TatC P3 loop, was found to be unaffected by both substrate overexpression and PMF dissipation and was proposed to be a constitutive binding site for Tha4 (Aldridge *et al*., 2014). The Tha4 interaction with the P3 loop is in agreement with data showing that an *E. coli* TatC D211 Bpa substitution resulted in photo-crosslinking with TatA, suggesting a potential TatA interaction site at TatC P3

(Zoufaly *et al.,* 2012). This Chapter explores this region further, thoroughly scanning the TatC TM5/P3/TM6 region for interactions with TatA using disulphide crosslinking experiments.

A scanning region on TatC covered the periplasmic facing part of TM5, including the residues found to crosslink TatB (TatC M205 and L206) (Rollauer *et al*., 2012, Kneuper *et al*., 2012, Blummel *et al*., 2015), the P3 loop and the periplasmic side of TM6 was selected for introduction of single Cys substitutions. The three residues chosen in TatA to mutate to Cys were L9, L10 and I11 – this region of TatA is most homologous to TatB, which has three leucines at these positions. The positions of the Cys mutations introduced into TatA and TatC shown in Fig. 4.3.

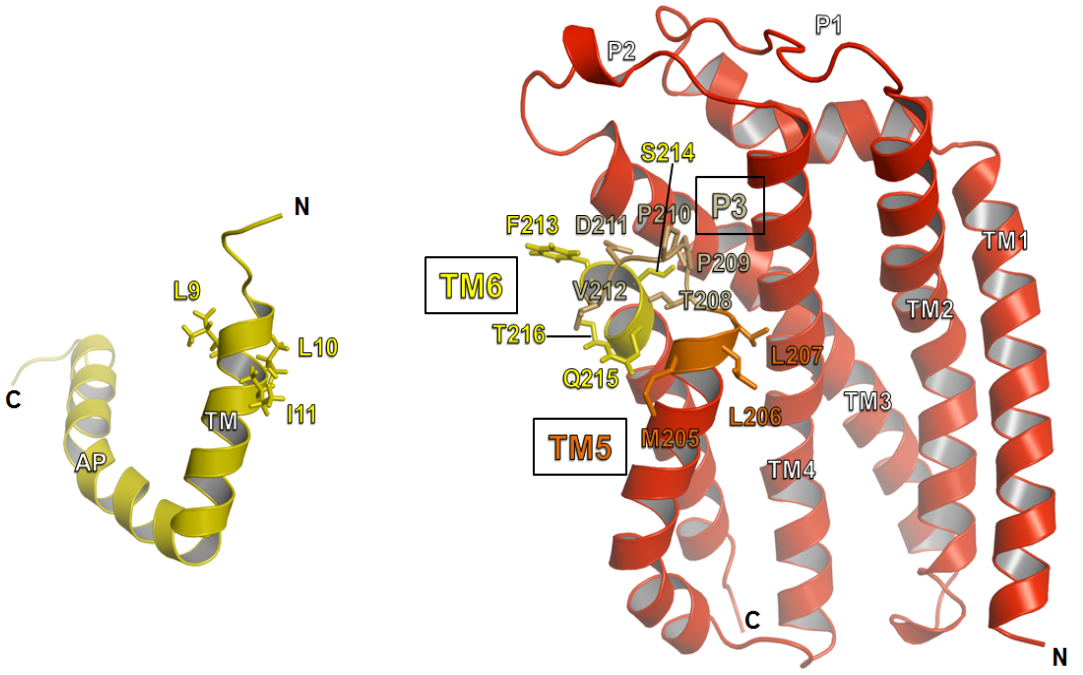

Figure 4.3) Residues substituted to Cys in TatA and TatC - Cys substitutions are shown as sticks in TatC (red) and TatA (yellow). Residues in the transmembrane helix of TatA are shown along with residues in the TM5 of TatC (orange M205-L207), the P3 loop (brown T208-V212) and TM6 (yellow F213-T216), images generated in PyMol using NMR structure of TatA (Rodriguez *et al*., 2013) and a homology model of *E. coli* TatC (Cleon *et al.,* 2015). TM- transmembrane helix, AP- amphipathic helix..

If Cys residues, engineered into TatA and TatC, are close to each other in the final complex (~5Å or less) they will form a disulphide bond under oxidising conditions. This will generate a covalent linkage between the two proteins, meaning that on subsequent SDS-PAGE they will migrate at the apparent molecular weight of both proteins combined. This heterodimer between TatA and TatC will also be responsive to both

anti-TatA and anti-TatC antibodies using Western blotting, and will disappear upon reduction. Homodimers, may also be detected based on previous data showing these proteins self-associate (See Sections 1.10.5 and 1.10.7).

4.2 Aims

The work described in this Chaper intends to elucidate TatA-TatC interactions occuring in living *E. coli* cells to potential identify Tat protein associations. This will include performing Cys scanning and crosslinking between the TatC region encompassing TM5/P3/TM6 to identify residues able to crosslink residues in the TatA transmembrane helix.

4.3 Results:

4.3.1 The *in vivo* disulphide cross-linking protocol used in this study is not lethal to *E. coli* cells

To induce Cys crosslinking it is necessary to expose *E. coli* cells to a membrane permeable oxidising reagent. In this work, copper phenanthroline was used. Work undertaken in collaboration with Johann Habersetzer resulted in development of a protocol whereby cells were treated with 1.8 mM copper phenanthroline for 1 minute, after which the reaction was quenched and the samples analysed. To analyse whether the copper phenanthroline concentration and incubation time used had any detrimental effect to *E. coli* cells, cell suspensions were treated with either 1.8mM copper phenanthroline for 1 minute, or mock treated with buffer, after which serial dilution and colony counting was performed. A comparison between the numbers of colony forming units (CFU) following copper phenanthroline treatment compared to the control showed that similar numbers of cells were recovered in both cases (Fig. 4.4). It can therefore be concluded that the 1 minute copper phenanthroline treatment of cells is not lethal.

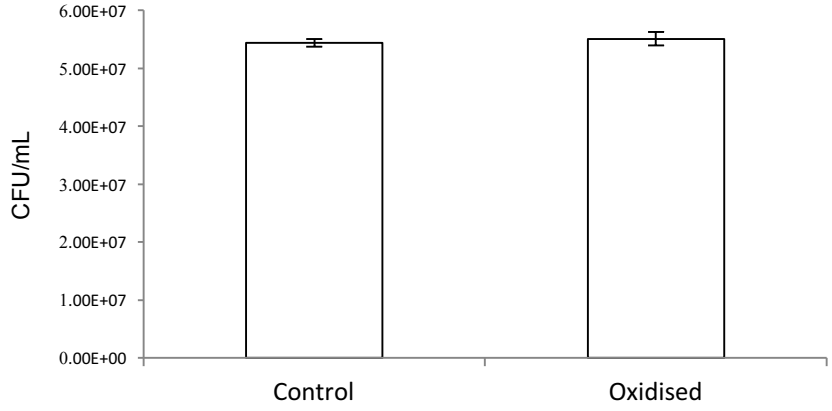

Figure 4.4) Colony forming units of *E. coli* recovered with and without copper phenanthroline exposure. *E. coli* strain DADE (Δ*tatABCD,* Δ*tatE*) *was* incubated with 1.8 mM copper phenanthroline or buffer only for one minute, after which dilution series were prepares and plated on LB-agar and scaling counts to give mean CFU/mL. The error bars represent standard error of the mean, *n* = 3.

4.3.2 Cys substitutions used in this work do not abolish Tat activity

As stated in Section 4.1.1, Cys substitutions of TatA and TatC could conceivably disrupt any potential interaction face/s between the proteins, preventing the Tat system from functioning. To determine whether any of the Cys substitutions abolished activity of the Tat system, Tat-dependent growth phenotypes were assessed for *E. coli* strain DADE (Δ*tatABCD,* Δ*tatE*) producing each of the Cys substitutions from the medium copy number pQE60 based vector, pUNITATCC4. Plasmid pRep4, which encodes *lacI*^{q}, was also present in the strain to reduce protein expression from the *lac* promoter on pUNITATCC4. Table 4.1 shows the results following screening for Tat transport activity

Table 4.1) Cys substitutions in TatA and TatC do not abolish Tat activity. *E. coli* strain DADE (Δ*tatABCD,* Δ*tatE*) harbouring pRep4 and pQE60-based vector, pUNITATCC4 encoding wild type TatB along with the indicated Cys substitutions in TatA and TatC was scored for growth by spotting 5 µL cells at OD_{600} 0.01 onto LB-agar containing 2% SDS or M9-glycerol-TMAO. The LB-SDS plates were incubated aerobically and the M9-glycerol-TMAO plates anaerobically for 24 hours before analysis. "+" denotes positive growth, "-" denotes no growth. DADE harbouring either pQE60 only or pQE60 encoding wild type TatABC was used as negative and positive controls, respectively.

Cys substitution				Cys substitution			
TatA	TatC	2% SDS	M9/TMAO/ Glycerol	TatA	TatC	2% SDS	M9/TMAO/ Glycerol
Wild type		+	+	L10C	P210C	+	+
Empty pQE60 vector		-	-	L10C	D211C	+	+
L9C	M205C	+	+	L10C	V212C	+	+
L9C	L206C	+	+	L10C	F213C	+	+
L9C	L207C	+	+	L10C	S214C	+	+
L9C	T208C	+	+	L10C	Q215C	+	+
L9C	P209C	+	+	L10C	T216C	+	+
L9C	P210C	+	+	I11C	M205C	+	+
L9C	D211C	+	+	I11C	L206C	+	+
L9C	V212C	+	+	I11C	L207C	+	+
L9C	F213C	+	+	I11C	T208C	+	+
L9C	S214C	+	+	I11C	P209C	+	+
L9C	Q215C	+	+	I11C	P210C	+	+
L9C	T216C	+	+	I11C	D211C	+	+
L10C	M205C	+	+	I11C	V212C	+	+
L10C	L206C	+	+	I11C	F213C	+	+
L10C	L207C	+	+	I11C	S214C	+	+
L10C	T208C	+	+	I11C	Q215C	+	+
L10C	P209C	+	+	I11C	T216C	+	+

by (i) testing for Tat-dependent export of cell wall amidases that confer resistance to 2% SDS added to the growth media (Stanley *et al.*, 2001, Ize *et al.*, 2003) and (ii) testing for anaerobic growth on M9 minimal medium with TMAO as sole electron acceptor, to identify the ability to export Tat-dependent TMAO and DMSO reductases (Santini *et al.*, 1998; Chapter 2, Section 3.3.6).

The results clearly indicate that all of the Cys constructs used in this work yield functional TatA and TatC proteins.

4.3.3 TatA-TatC disulphide crosslinking *in vivo*

Next, disulphide crosslinking was performed using suspensions of strain DADE (Δ*tatABCD, ΔtatE*) producing Cys-substituted TatA and TatC alongside wild type TatB from plasmid pUNITATCC4. The strain also routinely contained plasmid pRep4, in order to reduce protein expression from the *lac* promoter on pUNITATCC4.

Cells were grown until OD_{600} 0.3 was reached, whereupon three separate aliquots were withdrawn and diluted by addition of an equivalent volume of fresh LB. Oxidised samples had 1.8 mM copper phenanthroline added and incubated for 1 minute, while control cells were left untreated and reduced cells had 10 mM dithiothreitol (DTT) added before incubation for 1 minute. Subsequently all three samples were treated with N-ethylmaleimide to cap all remaining free disulphides and cells were lysed with Laemmli buffer and loaded onto SDS-PAGE for Western blotting.

4.3.3.1 TatA L9C crosslinks TatC F213C at TM6 *in vivo*

Fig. 4.5A presents an anti-TatC Western blot showing oxidised whole cell samples of strain DADE producing TatA L9C, wild type TatB and successive TatC Cys substitutions in the scanning region encompassing TatC M205C-T216C. It is apparent that for the TatA L9C - TatC M205C oxidised sample, no TatA-TatC heterodimer was detected, which would be expected to migrate at ~37 kDa (the combined SDS-PAGE molecular weight of TatA and TatC; monomeric TatC migrating just below 25 kDa on

the same blot in Fig. 4.5A). This implies that TatA L9C is not near to TatC M205C *in vivo*, despite studies showing that a position equivalent to TatA L9C in chloroplast Tha4 could crosslink to the cpTatC residue equivalent to TatC M205C (Aldridge *et al.,* 2014). It is also notable that no TatC M205C homodimer, expected to migrate just below 50 kDa, was detected under oxidising conditions. This lack of homodimer contrasts to previous crosslinking results with the same Cys-substituted TatC in isolated membranes (Rollauer *et al*., 2012, Kneuper *et al*., 2012, Punginelli *et al*., 2007) and *E. coli* INVs (Blummel *et al*., 2015). This seems to suggest that, *in vivo,* TatC homodimerisation is prevented at this position in *E. coli.* This conclusion is supported by results presented by Cleon *et al*. (2015), who also reported that there was no TatC-TatC dimerisation through M205C *in vivo* unless a Tat substrate was overexpressed.

Again, for position L206C in TatC (Fig. 4.5A), it can be seen that no TatA-TatC heterodimer or TatC-TatC homodimer can be detected under oxidising conditions. Rollauer *et al.* (2012) observed a prominent TatC homodimer linked through L206C in isolated membranes, again suggesting that *in vivo* TatC dimerisation may be prevented in this part of TatC. In contrast, Fig 4.5A shows that TatC L207C formed a weak homodimer after oxidation, but again there was a lack of any detectable TatA-TatC heterodimer formation. It should be noted that TatC homodimer, linked through L207C, was seen *in vitro* by Rollauer *et al.* (2012).

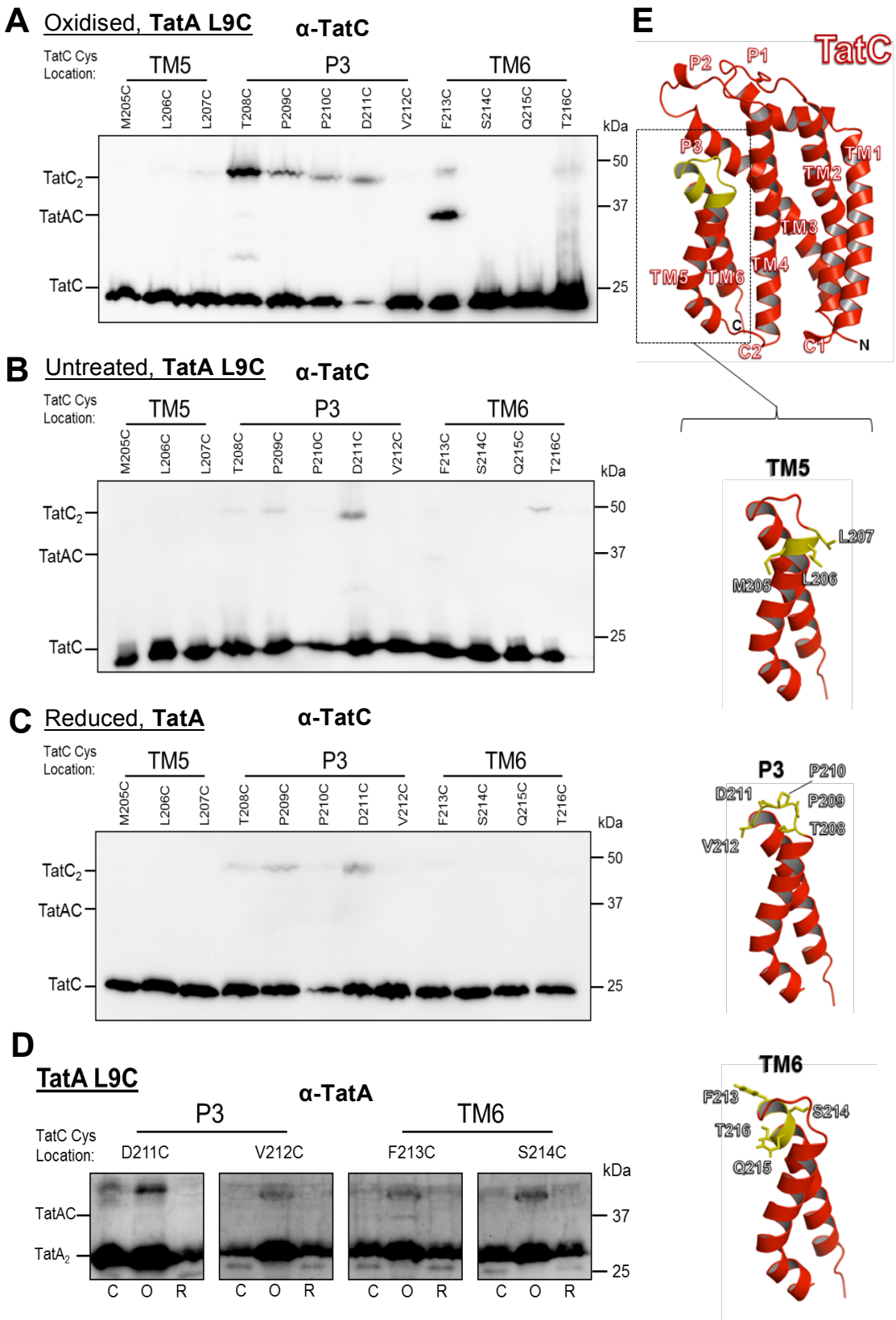

Figure. 4.5) TatA L9C interacts with TatC F213C *in vivo*. A-C Anti-TatC Western blots performed on whole cell samples of *E. coli* strain DADE (Δ*tatABCD,* Δ*tatE*) harbouring pREP4 and pUNITATCC4 producing wild type TatB along with the indicated Cys substitutions in TatA and TatC. **A** Cells were oxidised with 1.8 mM copper phenanthroline for 1 min, **B** Cells were left untreated, **C** cells were treated with 10 mM of the reductant DTT for 1 min. In each case the loading volume was 5 µL. The positions of the TatC monomer, TatC dimer and TatAC heterodimer are indicated. **D** Anti-TatA Western blots of selected samples from **A-C** to detect a corresponding TatA-TatC heterodimer band at ~37 kDa. "C", corresponds to control, untreated samples from **B**, "O" to oxidised samples from **A** and "R" to reduced samples from **C**. The positions of the TatA-TatC heterodimer and TatA homodimer are indicated and the overexposed TatA monomer band has been cropped for clarity. **E** denotes positions of Cys substitutions in TatC examined in this experiment.

Taken together, these results suggest that TatA does not interact through L9C with the periplasmic facing region of TatC TM5. Moreover, the distinct TatC homodimerisation through TM5 observed *in vitro* in previous studies is either completely absent or apparently greatly diminished *in vivo.*

Upon inspection of the crosslinking results between TatA L9C and Cys substitutions in the TatC P3 loop under oxidising conditions (Fig. 4.5A), again no TatAC heterodimer can be detected for any of the positions tested, from TatC T208C through to V212C. This conflicts with results from the thylakoid Tat system, where an interaction between the equivalent position of TatA L9C in the plant orthologue, Tha4 and a position at the centre of the L3 loop of cpTatC (analogous to the P3 loop of TatC) was found (Aldridge *et al*., 2014). Furthermore in *E. coli* INVs a Bpa incorporated into TatC position 211 (at the centre of the P3 loop) was able to crosslink to TatA. However in this latter case it is not known which region of TatA was crosslinked, and could potentially be the flexible N-terminal region (Zoufaly *et al.,* 2012).

The results presented here would suggest that in *E. coli* cells, TatA is not interacting through L9C in the TatC P3 loop. It can clearly be seen that there is strong TatC homodimerisation for cysteines within the P3 loop, this is particularly pronounced for positions T208C, P209C, P210C and D211C but not present for V212C. Existing data on TatC homodimer formation *via* residues in the P3 loop is conflicting, with Blummel *et al*. (2015) and Zoufaly *et al*. (2012) both reporting no self-crosslinks through Bpa residues incorporated into positions 211 and 209 in P3 (in the presence of TatB), whereas Aldridge *et al*. (2014) reported distinct cpTatC homodimers forming through Cys substitutions at the centre of the equivalent of the P3 loop in chloroplast TatC.

Finally, moving along to look at crosslinks between TatA L9C and residues in the TM6 region of TatC, strikingly, a clear TatA-TatC heterodimer band linked *via* TatA L9C and TatC F213C is apparent under oxidising conditions. This band appears to be notably stronger than the TatC F213C-linked homodimer that is also observed under oxidising

conditions migrating just below 50 kDa, suggesting TatA is more favourably interacting at this position *in vivo*. With the exception of weak TatC self-interactions through T216C (relative to the intensity of TatC homodimer bands formed through the P3 loop), no other homodimeric or heterodimeric crosslinks were detected for any of the other Cys substitutions tested in TatC TM6.

Interestingly, residues 213 and 216 are on the same face of TatC TM6, and this may represent a self-interaction face. Indeed, Punginelli *et al.* (2007) and Aldridge *et al.* (2014) both observed TM6-TM6 crosslinks in membrane fractions of *E. coli* and intact plant thylakoids, respectively, through residues at the centre of the fifth transmembrane helix.

Figs 4.5B and C are critical control experiments that serve to demonstrate that the TatA-TatC heterodimer formed through TatA L9C and TatC F213C under oxidising conditions in Fig 4.5A is not present under either untreated or reduced conditions indicating that it arises from a disulphide crosslink. Compared to the formation of TatC homodimers under oxidising conditions, relatively weak TatC homodimer bands can still be seen in the P3 loop at positions T208C, P209C and D211C along with a homodimer at T216C at TM6 under untreated conditions (Fig.4.5B). Upon reduction with DTT, interactions through T216C disappear while interactions in the P3 loop are still maintained (Fig. 4.5C). This suggests that associations through the P3 loop are very favourable in the absence of an oxidising agent to initiate the reaction and is likely due to the proximity of the loop to the oxidising periplasm. It may be that the periplasmic DsbAB system is responsible for some of this disulphide bond formation in the absence of externally-added oxidant as was suggested for TatA homodimerisation through Cys residues in TatA that are proximal to the periplasm (Greene *et al.*, 2007).

The TatA-TatC homodimer between TatA L9C and TatC F213C, detected under oxidising conditions, should also be responsive to anti-TatA antibodies. Fig. 4.5D shows that, indeed, a similar band at ~37 kDa can also be identified when probed with

an anti-TatA antibody. This indicates that the dimer is composed of both TatA and TatC proteins, and given its absence under control and reduced conditions, is demonstrated to be disulphide-linked. Furthermore the absence of such a band between TatA L9C and TatC D211C, V212C or S214C (Fig 4.5D) adds further support to the identification of this band in the TatA blot (Fig. 4.5A).

It should be noted that, in the native Tat system, TatA is produced at levels vastly in excess of TatC (Chapter 1, Section 1.10) and this native stoichiometry is very likely preserved for the plasmid-encoded proteins. As such, the population of TatA associated with TatC will be more difficult to detect on Western blots using anti-TatA antibodys as opposed to anti-TatC antibody, due to the large amount of unreacted TatA also present on the Western blot. This explains the relative weakness of the TatA-TatC heterodimer bands in Fig. 4.5D. It should be noted that the highly overexposed TatA monomer was cropped from anti-TatA Western blots in Fig 4.5D for clarity, with the full Western blots presented in the Supplementary Section.

Fig. 4.5D also demonstrates that TatA L9C itself can strongly self-associate, with intense TatA homodimer bands observed at around 30 kDa, in agreement with crosslinks observed for the same position of *E. coli* TatA *in vitro* (Greene *et al*., 2007). Remarkably, a higher molecular weight band is also observed in the oxidised samples on the anti-TatA blots, which may correspond to higher order oligomers of TatA which are somehow promoted through the creation of a Cys-linked dimer. Indeed, a band corresponding to a similar molecular weight was observed on some anti-TatA Western blots by Greene *et al.* (2007) after disulphide crosslinking of the same position *in vitro*.

4.3.3.2 TatA L10C crosslinks TatC V212C *in vivo*

Fig. 4.6A presents an anti-TatC Western blot showing oxidised whole cell samples of strain DADE producing TatA L10C, wild type TatB and successive TatC Cys substitutions in the scanning region encompassing TatC M205C-T216C. It can be seen that no TatA-TatC or TatC-TatC dimers form through TatC M205C, similar to what was

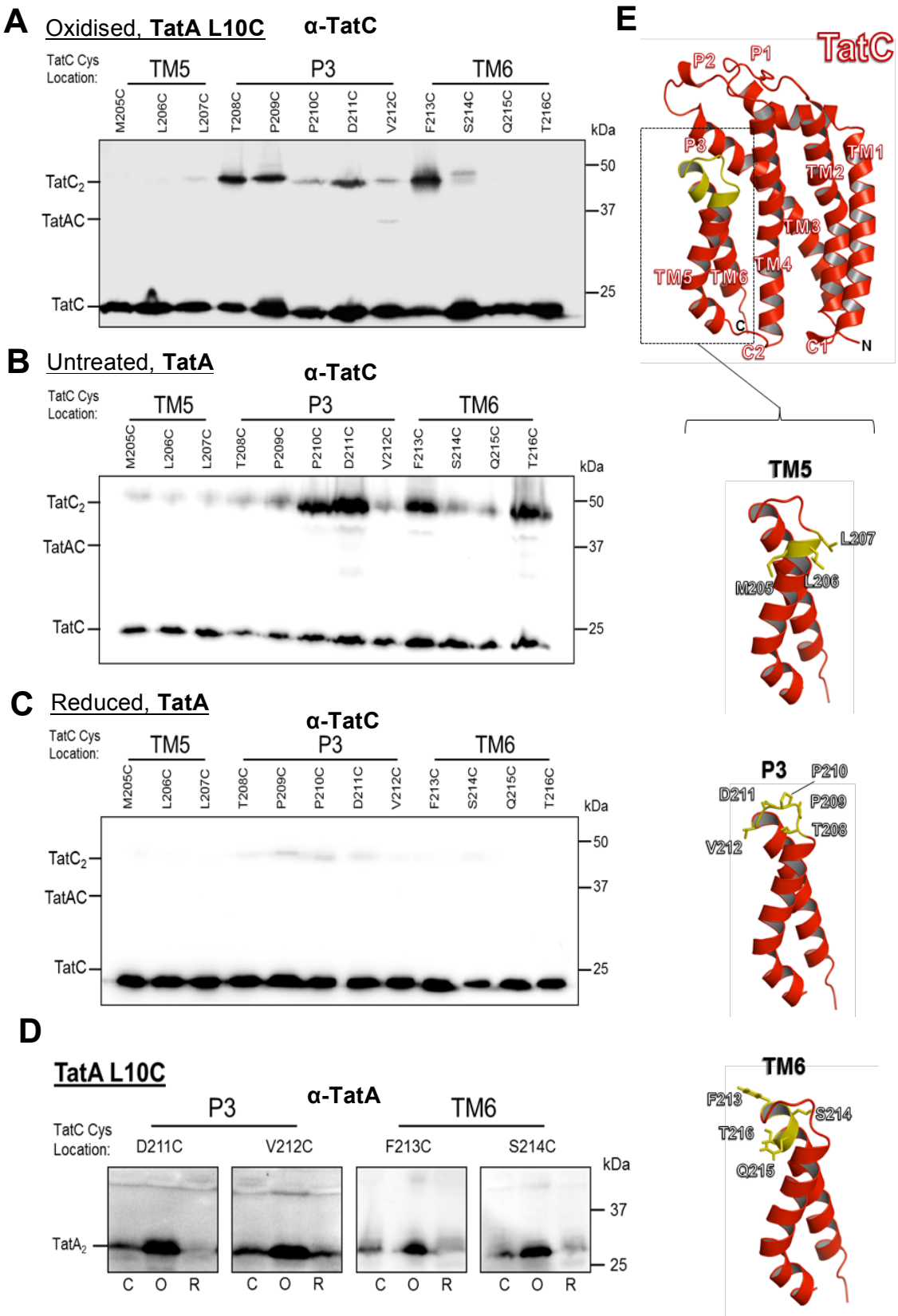

Figure. 4.6) TatA L10C interacts with TatC V212C *in vivo*. A-C Anti-TatC Western blots performed on whole cell samples of *E. coli* strain DADE (Δ*tatABCD,* Δ*tatE*) harbouring pREP4 and pUNITATCC4 producing wild type TatB along with the indicated Cys substitutions in TatA and TatC. **A** Cells were oxidised with 1.8 mM copper phenanthroline for 1 min, **B** Cells were left untreated, **C** cells were treated with 10 mM of the reductant DTT for 1 min. In each case the loading volume was 5 µL. The positions of the TatC monomer, TatC dimer and TatAC heterodimer are indicated. **D** Anti-TatA Western blots of selected samples from **A-C** to detect a corresponding TatA-TatC heterodimer band at ~37 kDa. Below each panel, "C", corresponds to control, untreated samples from **B**, "O" to oxidised samples from **A** and "R" to reduced samples from **C.** The positions of the TatA-TatC heterodimer and TatA homodimer are indicated and the overexposed TatA monomer band has been cropped for clarity. **E** denotes positions of Cys substitutions in TatC examined in this experiment.

seen for TatA L9C in Section 4.3.3.1. Again a similar result was seen for TatA L10C/TatC L206C, with no TatC homodimer or TatAC heterodimer detected. A faint TatC homodimer through TatC L207C, again identical to observations in Section 4.3.3.1 with the Cys substitution TatA L9C, was observed, but no detectable TatAC heterodimer was apparent.

Moving on to examine interactions between TatA L10C and cysteine substitutions in the P3 loop, a TatA-TatC heterodimer band was detected between TatA L10C and TatC V212C, which appears to be much fainter than that observed for TatA L9C and TatC F213C (compare the intensity of monomer and dimer forms of TatC relative to the TatA-TatC heterodimer in Section 4.3.3.1 Fig 4.5A), however, the placement of TatA L9C near F213C would allow TatA L10C on the same TatA to be near V212C, so this interaction is plausible. TatC self-interactions were also detected for Cys substitutions in the TatC P3 loop under oxidising conditions (Fig. 4.6A) and not surprisingly appear very similar to those observed for the TatA L9C crosslinking results in Fig 4.5A, for example with prominent TatC homodimer bands seen through positions T208C-V212C. It should be noted that homodimerisation through V212C was not observed in Section 4.3.3.1 with constructs expressing TatA L9C under oxidising conditions, although whether this is direct result of the different Cys substitution in TatA is not clear.

Crosslinks through TatA L10C to Cys residues in TatC TM6 are not present under oxidising conditions as shown in Fig. 4.6A, with TatC homodimers forming only through TatC F213C and S214C. With constructs expressing TatA L9C, TatC homodimers were observed through T216C, but not S214C, under oxidising conditions (Section 4.3.3.1, Fig. 4.5A). The reason for these differences is not clear.

Fig. 4.6B and 4.6C show that the weak TatA-TatC heterodimer band between TatA L10C and TatC V212C under oxidising conditions is not observed on anti-TatC Western blots under untreated or reducing conditions, suggesting it results from a disulphide linkage. As with constructs expressing TatA L9C, TatC homodimers under

oxidising conditions are still present under control conditions, though they seem more prominent in the P3 loop at positions P210 and D211 and in TM6 at F213C and T216C (Fig. 4.6B). Weaker TatC homodimer bands are present at all other positions tested, though these disappear, or are greatly diminished, under reducing conditions, with the exception of relatively faint TatC homodimer bands through P209C, P210C and D211C (Fig. 4.6C). As with constructs expressing TatA L9C alongside the TatC Cys substitutions, it indicates a propensity for TatC to form homodimers through the P3 loop.

TatC homodimer formation is seen through Q215C and T216C in TM6 under untreated conditions from TatA L10C expressing constructs (Fig. 4.6B) suggesting that TatC homodimerisation through TM6 residues in these experiments is favourable. This potential homodimerisation through TatC TM6 is supported by crosslinked homodimers that have have been observed through several positions in TatC TM6 (Punginelli *et al.,* 2007), along with cpTatC self-interactions at TM6 (Aldridge *et al*., 2014), these interactions may be present but occurring at a lower level under *in vivo* conditions.

Fig. 4.6D demonstrates that the TatA L10C crosslink to TatC V212C seen on the anti-TatC western blot under oxidising conditions (Fig. 4.6A), cannot be detected using the anti-TatA antibody. It is likely that the relatively small population of TatA associated with TatC is greatly outnumbered by free monomers or multimers of TatA in the membrane, making it more difficult to detect the TatA subpopulation associated with TatC. With regard to TatA homodimer formation, TatA L10C seems to self-crosslink less favourably than TatA L9C (Compare Fig. 4.5D and 4.6D), with less homodimer present in the control and reduced lanes than for TatA L9C. This is in agreement with the *in vitro* observations of Greene *et al.* (2007) who reported a reduced level of homodimer formation through TatA L10C than L9C.

4.3.3.3 TatA I11C crosslinks with TatC V212C and F213C *in vivo*

Fig. 4.7A shows an anti-TatC Western blot of oxidised whole cell samples of strain DADE producing TatA I11C, wild type TatB and successive TatC Cys substitutions in the scanning region encompassing TatC M205C-T216C. It can be seen that there is an absence of any TatA-TatC interaction through TatA I11C to Cys residues in TM5. Taken together with the absence of any interactions through TatA L9C and L10C with TatC M205C, L206C or L207C (Section 4.3.3.1, Fig 4.5A and Section 4.3.3.2, Fig 4.6A), this would suggest that TatA is unlikely to be associated with TatC TM5 *in vivo*. Though Blummel *et al.* (2015) observed that a Bpa substitution at position 205 in TatC could photo-crosslink TatA in INVs; this was much less favourable than the TatB-TatC heterodimer population that was able to form under identical conditions. Furthermore Kneuper *et al*. (2012) and Rollauer *at al*. (2012) both found residues in TatB (equivalent to those in homologous TatA) that formed disulphide crosslinks to TatC M205C *in vitro*. It is likely that TatB is occupying TatC TM5 *in vivo*, which probably prevents TatA association.

Notably, a clear TatC homodimer can be observed linked through position M205C under oxidising conditions (Fig. 4.7A). Though this was not seen under oxidising conditions with constructs expressing TatA L9C or L10C (Section 4.3.3.1, Fig. 4.5A and Section 4.3.3.2, Fig. 4.6A), it was seen in untreated conditions for L10C (Section 4.3.3.2, Fig. 4.6B). It should be noted that Cleon *et al*. (2015) reported this M205C homodimeric crosslink only formed *in vivo* after substrate binding, suggesting that there is some low level of interaction with native substrates during some of the experiments undertaken here. Comparatively weaker TatC homodimer bands through TatC L206C and L207C can also be seen (Fig 4.7A).

Moving to the P3 loop interactions under oxidising conditions in Fig 4.7A, no TatA-TatC interactions were detected except for a faint crosslink between TatA I11C and TatC

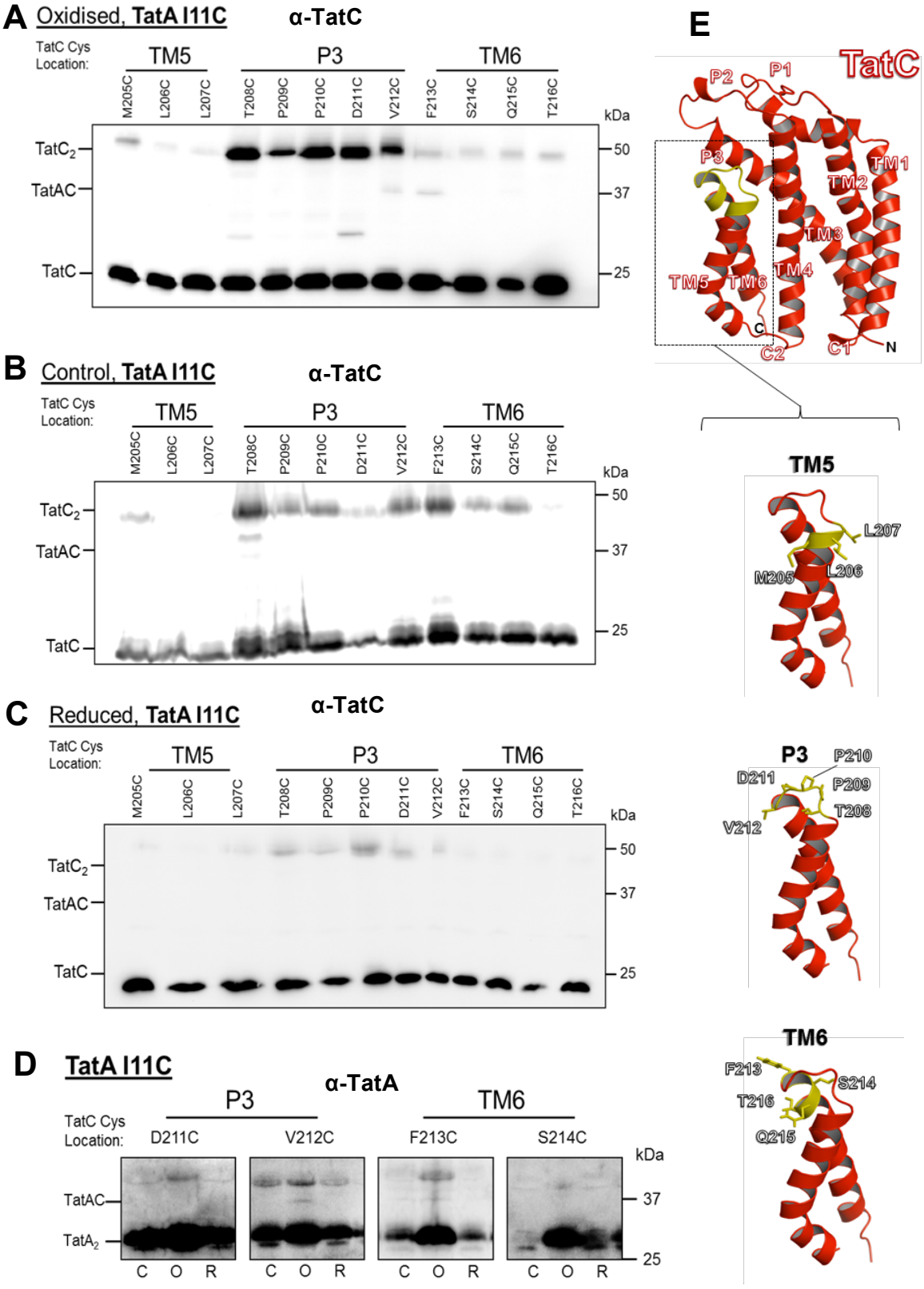

Figure. 4.7) TatA I11C interacts with TatC V212C and F213C *in vivo*. A-C Anti-TatC Western blots performed on whole cell samples of *E. coli* strain DADE (Δ*tatABCD,* Δ*tatE*) harbouring pREP4 and pUNITATCC4 producing wild type TatB along with the indicated Cys substitutions in TatA and TatC. **A** Cells were oxidised with 1.8 mM copper phenanthroline for 1 min, **B** Cells were left untreated, **C** cells were treated with 10 mM of the reductant DTT for 1 min. In each case the loading volume was 5 µL. The positions of the TatC monomer, TatC dimer and TatAC heterodimer are indicated. **D** Anti-TatA Western blots of selected samples from **A-C** to detect a corresponding TatA-TatC heterodimer band at ~37 kDa. Below each panel, "C", corresponds to control, untreated samples from **B**, "O" to oxidised samples from **A** and "R" to reduced samples from **C.** The positions of the TatA-TatC heterodimer and TatA homodimer are indicated and the overexposed TatA monomer band has been cropped for clarity. **E** denotes positions of Cys substitutions in TatC examined in this experiment.

V212C, that appeared to be much lower relative to the population of TatA L9C-TatC F213C linked heterodimer (Section 4.2.2.1, Fig 4.5A). It should be noted that TatA L10C crosslinking to TatC V212C was detected previously (Section 4.3.3.2, Fig 4.6A) which implies TatA L10C and I11C are close to TatC V212C, though it is not clear if these interactions are occurring on the same TatC protein through which F213C is able to crosslink TatC (Section 4.3.3.1, Fig 4.5) or whether the TatA transmembrane helix is simultaneously interacting with a separate TatC proteins through these residues. As expected, prominent TatC homodimer bands are detected through Cys substitutions in the P3 loop (T208C-V212C) under oxidising conditions (Fig. 4.7A), as was seen in Section 4.3.3.1 and 4.3.3.2.

Crosslinking TatA I11C to Cys substitutions in TatC TM6 reveals a TatA-TatC heterodimer band with F213C, which is of a similar intensity to that seen for V212C in the P3 loop. Indeed, the presence of TatA L9C interactions with F213C, TatA L10C interactions with V212C and TatA I11C interactions with both F213C and V212C would indicate that all three faces of the TatA transmembrane helix are able to interact with TatC at this site. Of these interactions, TatA L9C crosslinks to F213C appeared to be the strongest, and this could indicate either transient reactions through TatA L10C and I11C being detected relative to a much stronger TatA L9C crosslink to TatC F213C, or perhaps multiple TatC monomers interacting with one TatA, as is discussed further in Section 4.4.2. While no other TatA-TatC heterodimers are observed linked through TatA I11C at positions tested in the TatC TM6, fainter TatC homodimer bands appear at all positions under oxidising conditions, relative to Cys substitutions tested in the P3 loop (Fig. 4.7A). Fig. 4.7B and 4.7C demonstrate that no TatA I11C-mediated TatA-TatC heterodimers were detected under untreated or reducing conditions, while TatC homodimerisation can be seen strongly through all residues in the P3 loop relative to weaker interactions in the TM5, specifically at M205C (seen also under control conditions with TatA L10C in Section 4.3.3.2, Fig. 4.6B). TatC homodimerisation also occurs in TM6 through residues F213C, S214C and Q215C, with a relatively less

intense band found at T216C. Under reducing conditions TatC homodimer bands for Cys residues outside of the P3 loop are not detected (Fig. 4.7C).

Fig. 4.7D shows a band of ~37 kDa cross-reacts with anti-TatA antibodies and corresponds to positions where TatA I11C was crosslinked to TatC V212C and F213C (seen in Fig. 4.7A). The fact that this band was not detected under reducing and untreated conditions demonstrates this band is very likely to be a disulphide-linked TatAC heterodimer. TatA homodimerisation may be stronger through TatA I11C than L10C based on the intensity of bands around 30 kDa in Fig 4.6D compared to Fig. 4.7D. Greene *et al*. (2007) observed similar levels of homodimer formation for both of these substitutions, although as stated previously these experiments were performed *in vitro*, while this study analyses interactions *in vivo*, which may account for this noted difference as was discussed at length in Section 4.3.3.2.

4.4 Discussion

4.4.1 TatA interacts with TatC TM6 and the extreme N-terminus of the P3 loop *in vivo*

Disulphide crosslinking between TatA and TatC in Sections 4.3.3.1-4.3.3.3 suggests that residues tested in the transmembrane helix of TatA can interact with both F213C in the TM6 of TatC and V212C at the extreme N-terminal end of the P3 loop *in vivo*. Comparing crosslink intensity through TatA-TatC, it appears that the TatA L9C crosslink to F213C (Section 4.3.3.1, Fig 4.5A) is stronger than that of TatA L10C with TatC V212C (Section 4.3.3.2, Fig 4.6A) and TatA I11C with TatC V212C and F213C (Section 4.3.3.3, Fig 4.7A). This may indicate that the TatA-TatC interaction at this region of TatC is based around the association of TatA L9C with TatC F213C, with other crosslinks seen through TatA L10C and I11C forming at a lower level due to proximity. A diagram showing these crosslinks is presented in Fig. 4.8. Due to the strong association with TatC F213, this site will be hereby referred to as the TatA interaction site at TatC TM6.

Interactions between TatA and TatC TM6 have not been characterised previously - indeed the plant TatA homologue, Tha4, was found to interact with the cpTatC P3 loop

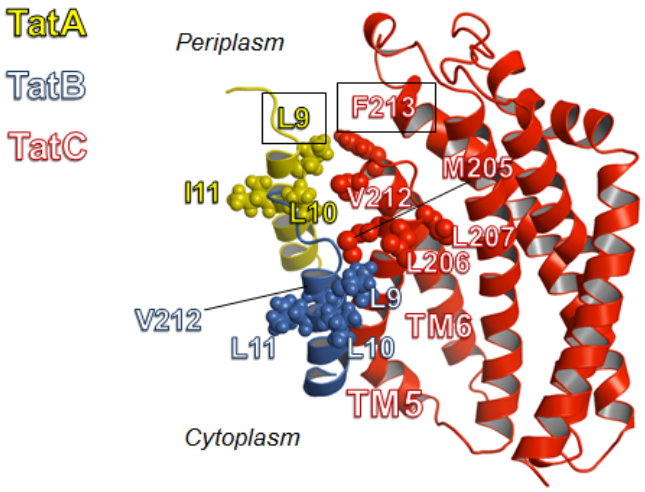

Figure 4.8) Diagram showing crosslinks between TatA and TatC in this work, along with the proposed placement of TatB from previous studies. TatA (yellow) is shown with near the TatC TM6 according to crosslinking data from Sections 4.3.3.1-4.3.3.3, with crosslinking residues shown as spheres. TatB is placed at TM5 with residues highlighted shown to interact with disulphide crosslinking *in vitro* (Rollauer *et al*. 2012, Kneuper *et al*., 2012)

through an equivalent residue in the transmembrane helix (P9C), however, at a more central position in the loop (Aldridge *et al*., 2014). Indeed the subsequent model presented in Aldridge *et al.* (2014) showed TatA at a position nearer the TatC TM5 than TM6. Crosslinks between TatA and TatC in this work are supported, however, by photo-crosslinks presented in Blummel *et al.* (2015) where residues at the periplasmic end of TatC TM3, which face TM6, could crosslink to TatA in *E. coli* inside-out inner membrane vesicles (INVs) suggesting a proximity of TatA in this region of TatC (See Chapter 1, Section 1.10.7. Blummel *et al*. (2015) did however find that photo-reactive residues incorporated at position 205 in the TM5 of TatC could crosslink to TatA in INVs, which was not seen with disulphide crosslinking in this work, and in addition Aldridge *et al.* (2014) found that residues in the TM5 cpTatC would interact with chloroplast TatA (Tha4). TatC TM5 has been proposed as a constitutive binding site for TatB (Rollauer *et al.,* 2012, Kneuper *et al*., 2012) but given the homology between TatA and TatB (Chapter 1, Section 1.10.1) it is conceivable that both TatA and TatB are able to differently occupy the same site at TatC TM5 at difference stages of the Tat cycle. It appears however that *in vivo* in *E. coli* this is not occurring and as such PMF may play a role in modulating these interactions.

Alcock *et al*. (2013) and Rose *et al.* (2013) both observed oligomerisation of fluorescently labelled TatA *in vivo* however this was only when Tat substrate was overexpressed. With endogenous substrate levels, as with crosslinking trials in this chapter, the TatA fluorescent clusters indicative of TatA oligomerisation were much less abundant. This would suggest that the interaction seen between TatA and TatC TM6 is not due to the presence of endogenous substrate *in vivo*, unless a low level of activation would promote this TatA-TatC association to the extent which it can be seen with crosslinking but not fluorescence microscopy. This seems unlikely however, given the amount of TatA-TatC heterodimer band on Western blots in Section 4.3.3.1, 4.5A relative to the amount of unreacted TatC monomer, would suggest this is a favourable interaction, coupled to fact that the Tat translocases expressed in these crosslinking

experiments are largely in excess of the native amount, and as such the effect of endogenous substrate would be mitigated.

Chapter 3 saw TatA association with TatC in affinity purification trials, where low levels of TatA were able to co-purify with His-tagged TatC in detergent-solubilised membrane fractions, and this is supported by *in vivo* observations in this Chapter where TatA crosslinked to TatC TM6. It is not known at this stage if this TatA association is constitutive or represents a transient interaction occurring at one or more stages of the Tat transport cycle. Chapter 5 will examine this in further detail.

Chapter 5: TatA occupies a constitutive binding site at TatC TM6, moving to occupy TatC TM5 in response to substrate overexpression

5.1 Introduction

5.1.1 Identifying further TatA interaction sites on TatC

The results presented in Chapter 4 identified a potential interaction site for TatA at the sixth transmembrane helix of TatC (TM6) and the extreme C-terminal part of the third periplasmic loop (P3), with *in vivo* disulphide crosslinking detected through Cys substitutions in the TatA transmembrane helix with TatC V212C and in particular F213C. As discussed in Chapter 4, other interactions between TatA and TatC within the TatC Cys scanning regions tested in this thesis (from M205C in TM5, through the P3 loop to TatC T216C at TM6), have been reported in the prior literature, including Cys crosslinks between P9C in Tha4 (the plant homologue of TatA) with the centre of the P3 loop of cpTatC (Aldridge *et al.,* 2014), and photo-crosslinks to TatA when a photoreactive Bpa was introduced at position 211 at the TatC P3 loop (Zoufaly *et al.,* 2012) or at position 205 in TM5 (Blummel *et al*., 2015). The conditions used for crosslinking analysis in Chapter 4, *i.e.* in living cells and in the presence of endogenous Tat substrates, could plausibly lead to differences in TatA-TatC interactions relative to the largely *in vitro* earlier studies. The work in this Chapter aims to explore these potential differences in greater detail.

5.1.2 Potential changes in TatA-TatC interactions in the absence of TatB

While the results described in Chapter 4 strongly indicate the presence of TatA near TatC TM6 *in vivo*, no TatA was found interacting at TM5, the presumed TatB constitutive binding site (Rollauer *et al.,* 2012, Kneuper *et al.,* 2012). This conflicts with previous studies suggesting that TatA has the ability to bind here in the thylakoid Tat system (Aldridge *et al.,* 2014) and in *E. coli* INVs (Blummel *et al*., 2015). Given the noted homology between the TMs of TatA and TatB, coupled to observations in Chapter 3 that the absence of TatB led to increased TatA-TatC associations in affinity-purification experiments, it seems likely TatA could occupy the TatB binding site. Indeed, it has been reported that in the absence of TatB, TatA association with TatC is

increased, as seen by enhanced photo-crosslinking with TatA through the TatC P3 loop and periplasmic facing regions of TM3 (Blummel *et al*., 2015). Therefore, is it conceivable that crosslinks between TatA and TatC TM5 may be present when TatB is absent.

5.1.3 The influence of substrate expression and PMF on TatA-TatC interactions

Aldridge *et al.* (2014) proposed that the Tha4 (TatA) interaction site at the equivalent of the P3 loop in cpTatC was constitutive, based on the finding that the intensity of the Tha4-cpTatC heterodimer did not change with either substrate overexpression or PMF dissipation. The work presented in Chapter 4 found no interaction of TatA with the TatC P3 loop in the presence of TatB *in vivo,* where the PMF was present, but instead, it was found that TatA occupied a site near TatC TM6. However, the experiments in Chapter 4 were carried out in the presence of native Tat substrates and it is unclear to what extent this influences the results obtained. Currently no *E. coli* strain exists where all of the genes encoding Tat substrates have been deleted. However, a substrate-free Tat system can be achieved *in vivo* by the combined introduction of F94A and E103A substitutions into TatC*.* Previously these substitutions have been shown to prevent Tat substrate binding, and the subsequent oligomerisation of TatA (Holzapfel *et al*., 2007, Alcock *et al*., 2013). Undertaking disulphide crosslinking in the presence of these substitutions will allow the determination of sites occupied by TatA in a resting, substrate-free state.

Aldridge *et al.* (2014) observed that although substrate overexpression did not alter interaction of Tha4 with the cpTatC P3 loop, it did result in increased association of Tha4 with cpTatC TM4 and TM5. It was proposed that this represented substrate gated Tha4 docking on cpTatC. Microscopy-based studies in living cells of *E. coli* have also observed recruitment of fluorescently labelled TatA to the TatBC complex in response to substrate overexpression (Alcock *et al*., 2013, Rose *et al*., 2013). While the *in vivo* conditions, through which disulphide crosslinking is performed in Chapter 4, allows

endogenous levels of substrate to bind the translocase, it is conceivable that overexpressed substrate could lead to a change in TatA-TatC interactions which would be reflected by a change in Cys crosslinking patterns.

Tat transport is powered by the PMF and Chapter 1, Section 1.11 has outlined in detail the known effect of PMF dissipation on the Tat system. Previous work examining the reliance of Tat subunit interactions on PMF found that it is required for TatA recruitment and oligomerisation in *E. coli* (Alcock *et al*., 2013, Rose *et al*., 2012) and plant thylakoids (Dabney-Smith *et al*., 2006, Mori & Cline, 2002). Undertaking disulphide crosslinking in a background where the PMF has been dissipated will report on whether any of the crosslinks observed in Chapter 4 are dependent on membrane energisation.

5.2 Aims

The work presented in this chapter aims to identify any potential sites on TatC which may be occupied by TatA when TatB is absent, using *in vivo* disulphide crosslinking. Potential constitutive TatA-TatC interactions will be analysed using disulphide crosslinking in a background where the Tat system cannot bind substrates. The effect of substrate overexpression will also be analysed in living cells by examining any potential change in TatA-TatC crosslinking. Finally, any potential change in TatA-TatC crosslinking will examined in response to PMF dissipation by performing crosslinking experiments on cells incubated with chemical ionophores.

5.3 Results

5.3.1 TatA L9C crosslinks both TatC TM5 and TM6 *in vivo* in the absence of TatB, with weaker interactions at P210C in the P3 loop.

To explore potential interactions between TatA and TatC when TatB was absent, disulphide crosslinking experiments were performed exactly as in Chapter 4, using pQE60-based constructs expressing Cys substituted TatA and TatC only.

Fig. 5.1A shows an anti-TatC Western blot of oxidised whole cell samples of strain DADE producing TatA L9C, and successive TatC Cys substitutions in the scanning region encompassing TatC M205C-T216C, in the absence of TatB. It can clearly be seen for TatA L9C and TatC M205C, a TatA-TatC heterodimer band has appeared which was not present when TatB was co-expressed (compare Chapter 4, Fig 4.5A with Fig 5.1A). TatC homodimer formation through M205C also appeared more prominent in the absence of TatB. A similar, but less pronounced effect was observed for crosslinking of TatA L9C to TatC L206C under the same conditions, with fainter hetero- and homodimer bands observed on anti-TatC blots (Fig. 5.1A). This crosslinking pattern between TatA and TatC is remarkably similar to that observed previously between TatB L9C and TatC M205C and L206C *in vitro* (Rollauer *et al*., 2012, Kneuper *et al*., 2012) suggesting that the homology between TatA and TatB could translate into the ability to differently occupy an interaction site on TatC. Crosslinking with TatA L9C and TatC L207C showed no notable difference in the absence of TatB, with a faint TatC homodimer detected and no TatA-TatC heterodimer. Taken together these results strongly imply that TatA is able to occupy the TatB constitutive site when TatB is absent.

Interestingly, when observing TatA-TatC interactions in the TatC P3 loop, a heterodimer band has appeared linking TatA L9C to TatC P210C when TatB is absent (Fig 5.1A). Crosslinking data from Zoufaly *et al*. (2012) observed an interaction with TatA through a Bpa substitution at TatC D211 and Aldridge *et al.* (2014) showed disulphide crosslinks between the equivalent of the TatA L9C residue (Tha4 P9C) and

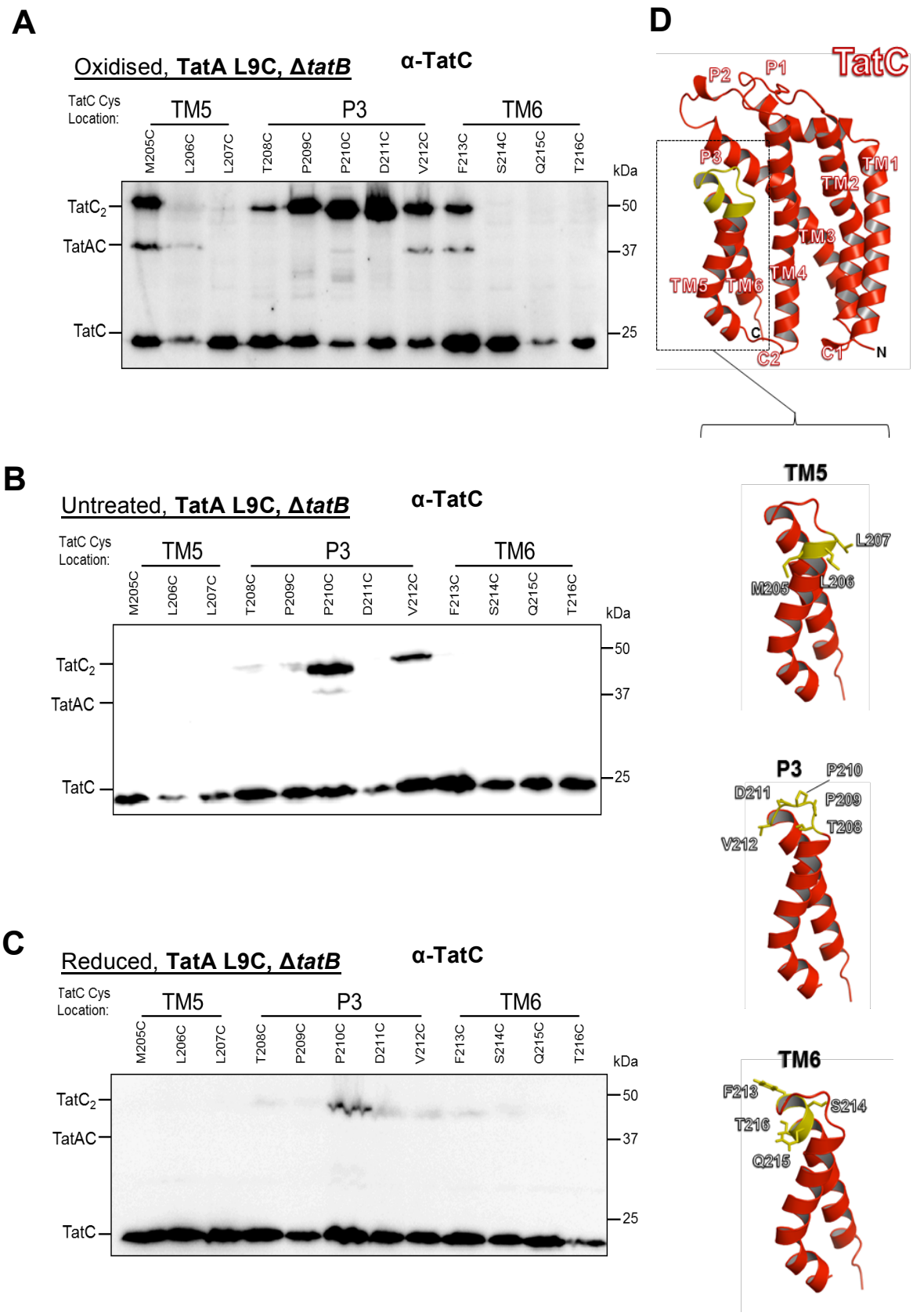

Figure 5.1) TatA L9C interacts with TatC TM5/TM6 and weakly at P3 in the absence of TatB *in vivo*-A-C Anti-TatC Western blots performed on whole cell samples of *E. coli* strain DADE (Δ*tatABCD,* Δ*tatE*) harbouring pREP4 and pQEA(ΔB)C producing the indicated Cys substitutions in TatA and TatC. **A** Cells were oxidised with 1.8 mM copper phenanthroline for 1 min, **B** Cells were left untreated, **C** cells were treated with 10 mM of the reductant DTT for 1 min. In each case the loading volume was 5 µL. The positions of the TatC monomer, TatC dimer and TatAC heterodimer are indicated. **D-** denotes positions of Cys substitutions in TatC examined in this experiment.

the cpTatC L3 (third luminal) loop (P3 loop in *E. coli*). Both of these studies were performed in the presence of TatB or the plant orthologue Hcf-106.

TatA-TatC crosslinks also appeared through TatC V212C in the absence of TatB, with a similar crosslink maintained at F213C at a weaker level (compare Chapter 4, Fig. 4.5A with Fig 5.1A). This implies that while the interactions between TatA and TatC through TM6 and the extreme N-terminal part of the P3 loop are preserved in the absence of TatB, the appearance of a new nearby crosslink between TatA L9C and V212C potentially suggests a greater degree of freedom experienced by the TatA TM, or perhaps another TatA monomer interacting nearby.

In Fig. 5.1A at the TatC P3 loop the intensity of the TatC homodimers linked through P209C-V212C seems stronger in the absence of TatB (compare Chapter 4, Fig. 4.5A and Fig. 5.1A). It appears that when TatB is not present, TatC monomers may rearrange or move closer to each other to facilitate further interactions in the P3 loop. It is of note that the residues nearer the centre of the P3 loop (P209C, P210C and D211C) all showed greater homodimer formation than other positions in the P3 loop. Increased TatC homodimerisation when TatB was absent was also observed with photo-crosslinking experiments in Blummel *et al*. (2012) where TatC self-crosslinks through T208C and P209C were increased when TatB was lacking.

Crosslinks between TatA L9C and TatC F213C in the TM6 have already been discussed above, however under oxidising conditions no further TatA L9C crosslinks to TatC were observed for TatC TM6, as in the presence of TatB (compare Chapter 4, Fig. 4.5A and Fig. 5.1A). Also no TatC homodimer interactions were seen in TatC TM6, comparable to the presence of TatB where only very faint homodimers were observed (Fig.5.1A).

Fig. 5.1B and 5.1C show that, as was the case in the presence of TatB, no TatA-TatC heterodimers were observed in untreated and reducing conditions, demonstrating the new heterodimer interactions through TatA L9C at TatC TM5 and V212C are

disulphide-linked. Under untreated conditions, all homodimer formation was confined to the P3 loop, in particular residues P210C and V212C (Fig. 5.1B) and in the presence of reductant, all TatC homodimers were greatly reduced (Fig. 5.1C).

Anti-TatA Western blots were performed to confirm whether the bands migrating at ~37 kDa in Chapter 4, Fig. 4.9A are responsive to anti-TatA antibodies. In Fig. 5.2, the characteristic band at ~37 kDa, was detected at corresponding positions, specifically between TatA L9C and TatC M205C/L206C, with no heterodimer through L207C and T208C as expected. Likewise, the TatA-TatC heterodimer band was detected in anti-TatA Western blots through TatC V212C and F213C. Because the ~37 kDa band was consistently detected with both anti-TatC and anti-TatA antibodies, and was not detected after untreated or reducing conditions, it can be concluded that it is a TatA-TatC disulphide-bonded heterodimer. No TatA-TatC heterodimer band between TatA L9C and TatC P210C was observed on Western blots using anti-TatA antibodies,

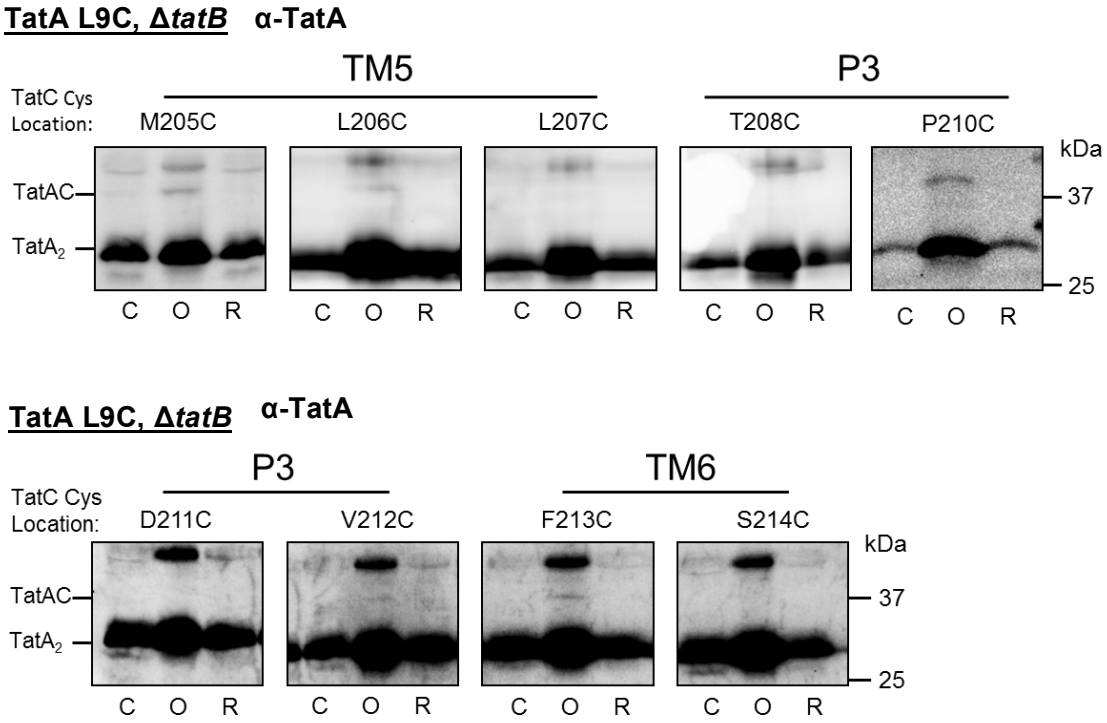

Figure 5.2) TatA-TatC heterodimer through TatA L9C and TatC TM5/TM6 can be detected on anti-TatA Western blots in the absence of TatB - Western blots performed on whole cell samples of *E. coli* strain DADE (Δ*tatABCD,* Δ*tatE*) harbouring pREP4 and pQE60AΔBC expressing Cys substituted TatA and TatC as noted. Cells were O- oxidised with 1.8 mM copper phenanthroline, C- cells were untreated, R- cells were treated with 10 mM of the reductant DTT for 1 min. In each case the loading volume was 5 µL. The positions of the TatA-TatC heterodimer and TatA homodimer are indicated and the overexposed TatA monomer band has been cropped for clarity.

suggesting that the population was very low, as expected given the low intensity seen on anti-TatC Western blots (Fig.5.1A). With regard to TatA homodimerisation through L9C in the absence of TatB, there seems to be little difference in the intensity, with an apparently strong interaction seen even under reducing or untreated conditions (Compare Chapter 4, Section 4.3.3.1, Fig. 4.5D and this Section, Fig. 5.2). The higher molecular weight band seen in the oxidised fractions in Chapter 4, Section 4.3.3.1-4.3.3.3 was also still present.

5.3.2 TatA L10C interacts with TatC TM5 in the absence of TatB

Fig. 5.3A shows an anti-TatC Western blot of oxidised whole cell samples of strain DADE producing TatA L10C, and successive TatC Cys substitutions in the scanning region encompassing TatC M205C-T216C, in the absence of TatB. No TatA-TatC heterodimer was detected between TatA L10C and TatC M205C, however, a heterodimer was detected with TatC L206C. This suggests that TatA L9C may interact with TatC M205C (shown in Chapter 4, Fig. 4.5A), while TatA L10C interacts with the adjacent L206C, as TatA occupies the TatB constitutive site. Interestingly, a similar result was observed for Cys crosslinking between TatB with TatC at equivalent positions *in vitro*, where the intensity of the TatB-TatC heterodimer linking TatB L10C to TatC L206C was higher than TatB L10C to TatC L205C and similarly the amount of TatB-TatC heterodimer linked through TatB L9C and TatC M205C was higher than that seen when crosslinking TatB L10C to the same TatC position (Rollauer *et al*., 2012).

As in Chapter 4, Sections 4.3.3.1-4.3.3.3, TatC homodimerisation appeared to be higher through TatC M205C and L206C in the absence of TatB (compare Chapter 4, Fig. 4.5A and Fig. 5.3A). No TatA-TatC homodimerisation was observed at L207C, with a faint TatC homodimer band relative to M205C and L206C seen in the absence of TatB (Fig. 5.3A).

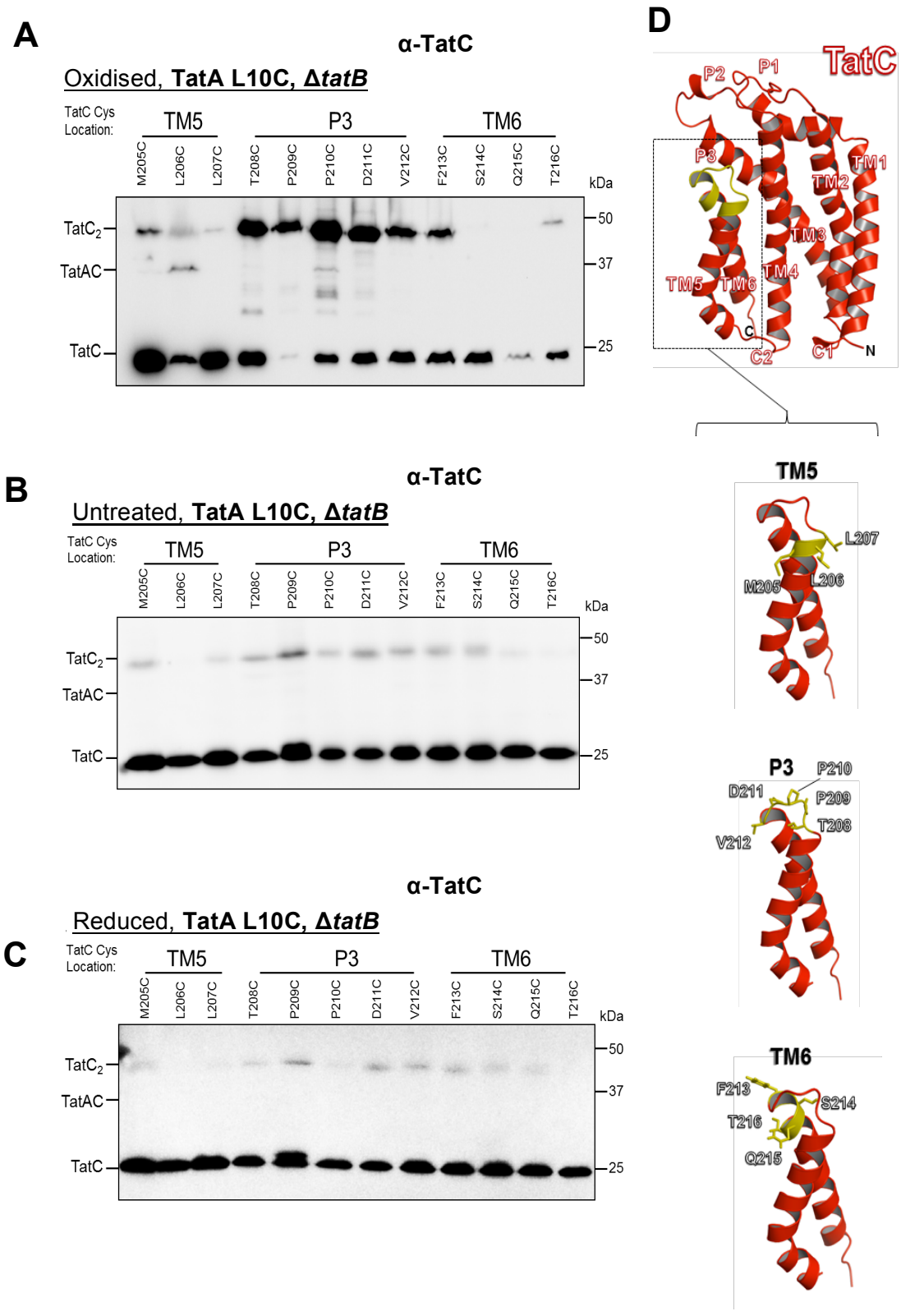

Figure 5.3) TatA L10C interacts with TatC TM5 and weakly at P3 in the absence of TatB *in vivo*- A-C Anti-TatC Western blots performed on whole cell samples of *E. coli* strain DADE (Δ*tatABCD,* Δ*tatE*) harbouring pREP4 and pQEA(ΔB)C producing the indicated Cys substitutions in TatA and TatC. **A** Cells were oxidised with 1.8 mM copper phenanthroline for 1 min, **B** Cells were left untreated, **C** cells were treated with 10 mM of the reductant DTT for 1 min. In each case the loading volume was 5 µL. The positions of the TatC monomer, TatC dimer and TatAC heterodimer are indicated. **D-** denotes positions of Cys substitutions in TatC examined in this experiment.

Moving on to examine interactions with the TatC P3 loop under oxidising conditions in the absence of TatB through TatA L10C, no TatA-TatC heterodimers were detected except for a faint interaction through TatC P210C at ~37 kDa (Fig. 5.3A). A similar interaction was observed through TatA L9C in Fig 4.5A, indicating interactions in the P3 loop occurring through both TatA L9C and L10C in the absence of TatB, which are not detected when TatB is present (Chapter 4, Sections 4.3.3.1-4.3.3.2). Interestingly, the interaction through TatA L10C and TatC V212C, seen in the presence of TatB in Chapter 4, was no longer detected when TatB was absent. This seems to support observations in Chapter 4, Section 4.3.4.2 whereby TatA L9C did not interact with TatC V212C in the presence of TatB but seemingly shifted to facilitate interactions with V212C in the absence of TatB seen in Fig. 5.3, in this case presumably moving TatA L10C away from V212C. Through all positions in the P3 loop, TatC homodimerisation was more pronounced in the absence of TatB, suggesting that TatC monomers are able to move into closer proximity through the P3 loops (compare Chapter 4, Fig. 4.6A and Fig. 5.3A). Fig. 5.3A also shows that, at positions tested in TatC TM6, no TatA-TatC heterodimers were detected under oxidising conditions, with an increased TatC homodimer band seen through F213C (relative to that in the presence of TatB) and a fainter TatC homodimer band through T216C (relative to interactions in the P3 loop on the same Western blot). An absence of TatA L10C interactions at this region of TatC is not surprising, as they were not present in the presence of TatB (Chapter 4, Fig. 4.6A).

As expected, no TatA-TatC homodimers were detected on anti-TatC Western blots under untreated and reducing conditions (Fig. 5.3B and 5.3C), while TatC homodimerisation was seen across all positions in TatC under untreated conditions with the exception of L206C in the TM5 and T216C in the TM6 (Fig. 5.3B). This may be due to the apparently increased favourability of TatC homodimerisation when TatB is absent. All homodimer interactions were diminished under reducing conditions, as expected (Fig. 5.3C).

On anti-TatA Western blots in Fig. 5.4, the TatA-TatC heterodimer formed through TatA L10C and TatC L206C in Fig. 5.3A was not detected, suggesting the crosslink itself is relatively weak, despite its presence on anti-TatC Western blots (Fig. 5.3A). Similarly, the fainter interaction in the P3 loop at P210C was not detectable on anti-TatA Western blots and TatA homodimerisation through TatA L10C in the absence of TatB, does not seem notably different (compare Fig. 4.6D and Fig. 5.4).

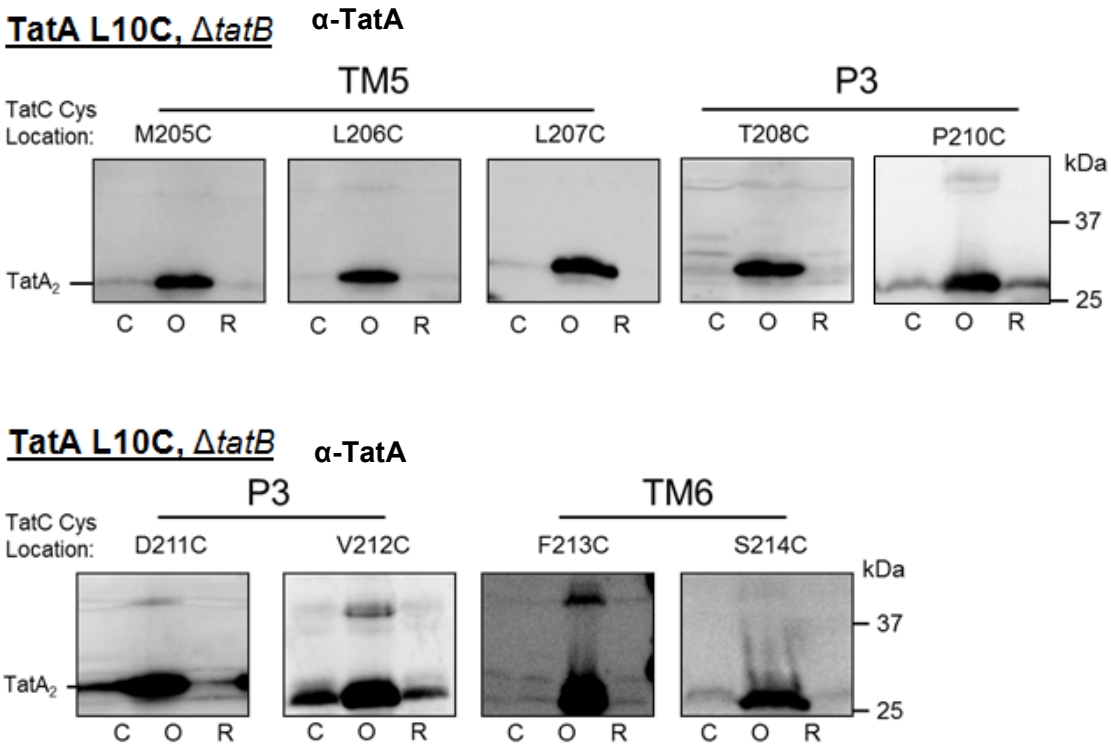

Fig. 5.4) TatA-TatC heterodimer formed through TatA L10C and TatC TM5 cannot be detected on anti-TatA Western blots in the absence of TatB- Western blots performed on whole cell samples of *E. coli* strain DADE (Δ*tatABCD,* Δ*tatE*) harbouring pREP4 and pQE60AΔBC expressing Cys substituted TatA and TatC as noted. Cells were O- oxidised with 1.8 mM copper phenanthroline, C- cells were untreated or R cells were treated with 10 mM of the reductant DTT for 1 min. In each case the loading volume was 5 µL. The positions of the TatA-TatC heterodimer and TatA homodimer are indicated and the overexposed TatA monomer band has been cropped for clarity.

This seems to suggest that interactions seen through TatA L10C with the scanning region of TatC are more difficult to detect, and as such may be weaker proximal interactions, with TatA L9C playing a more prominent role in the interface between TatA and TatC.

5.3.3 TatA I11C crosslinks TatC TM5, V213C and F213C in the absence of TatB *in vivo*

Fig. 5.5A shows an anti-TatC Western blot of oxidised whole cell samples of strain DADE producing TatA I11C, and successive TatC Cys substitutions in the scanning region encompassing TatC M205C-T216C, in the absence of TatB. TatA I11C crosslinked to both TatC M205C and L206C, in each case showing heterodimer bands migrating at ~37 kDa, indicating a similar interaction to that observed through TatA L9C (Fig. 5.1A), and demonstrating that all three faces of the TatA TM can interact at TatC TM5. A similar result was observed for the TatB TM (Rollauer *et al*., 2012), whereby TatB L9C, L10C and L11C could each crosslink TatC M205C *in vitro,* further indicating that these two proteins are both able to bind to this site on TatC.

TatC homodimers formed strongly through TatC M205C compared to the apparently weaker association through L206C and L207C. As with TatA L9C and L10C (Sections 5.3.1, Fig. 5.1A and 5.3.2, Fig. 5.3A), a TatA-TatC heterodimer appeared for Cys substitutions in the middle of the TatC P3 loop under oxidising conditions in the absence of TatB, however here it is at position P209C as opposed to P210C and as with TatA L9C and L10C, appears notably weaker than interactions seen with TM5 and TM6 (Fig. 5.5A). From the combination of crosslinks observing TatA L9C, L10C and I11C with the TatC P3 loop in the presence (Chapter 4, Sections 4.3.3.1-4.3.3.3) and absence (Sections 5.3.1-5.3.3) of TatB, it appears that low level interactions are present between the TM of TatA and the centre of the P3 loop when TatB is absent, and it may be that in the absence of TatB, the arrangement of the Tat subunits may be different from that observed in the native state. At the extreme C-terminal part of the P3 loop, V212C seems to more favourably associate with TatA I11C than P209C (Fig. 5.5A). Indeed, the interaction between TatA I11C and TatC V212C was also observed in the presence of TatB (Chapter 4, Section 4.3.3.3). As expected, prominent TatC homodimerisation was present through every position in the P3 loop and appears to be stronger than that observed in the absence of TatB (compare Fig. 4.7A with Fig. 5.5A.).

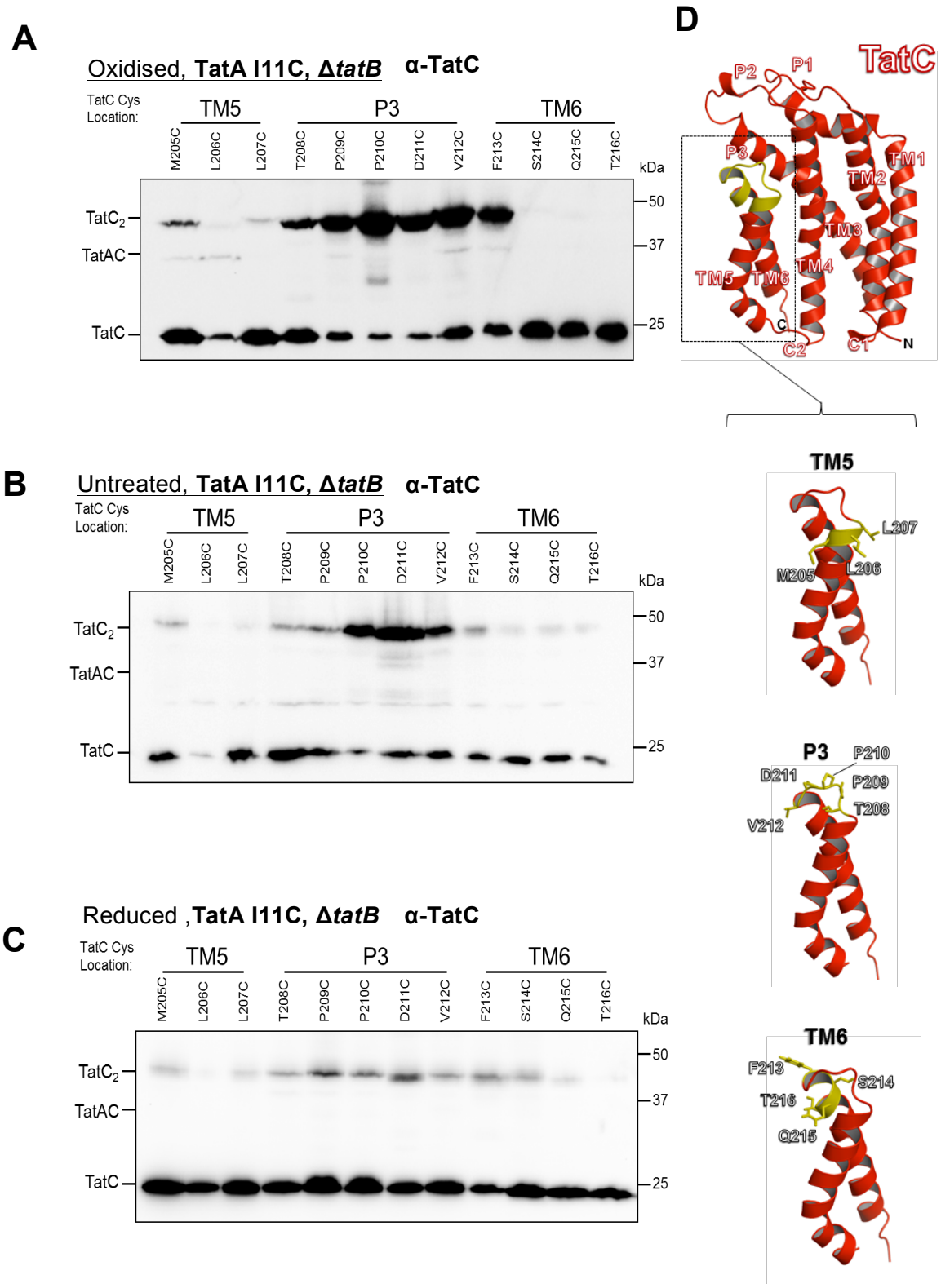

Figure 5.5) TatA I11C interacts with TatC TM5/TM6 and weakly at P3 in the absence of TatB *in vivo*- A-C Anti-TatC Western blots performed on whole cell samples of *E. coli* strain DADE (Δ*tatABCD,* Δ*tatE*) harbouring pREP4 and pQEA(ΔB)C producing the indicated Cys substitutions in TatA and TatC. **A** Cells were oxidised with 1.8 mM copper phenanthroline for 1 min, **B** Cells were left untreated, **C** cells were treated with 10 mM of the reductant DTT for 1 min. In each case the loading volume was 5 µL. The positions of the TatC monomer, TatC dimer and TatAC heterodimer are indicated. **D-** denotes positions of Cys substitutions in TatC examined in this experiment.

TatA-TatC interactions were also present through TatA I11C at the start of TM6, with a TatA-TatC heterodimer band forming though TatC F213C. Interestingly, the combination of an interaction at TatC V212C and F213C is shared by TatA L9C (Section 5.3.1) however they seem weaker through TatA I11C perhaps indicating that the L9C/I11C face of the TatA TM is in this vicinity on TatC, and TatA I11C can form transient interactions, while TatA L9C is interacting directly. TatC homodimerisation through TM6 under oxidising conditions was not detected, which is similar to observations made for TatA L9C and L10C under oxidising conditions (with the sole exception of a TatC T216C homodimer in the TatA L10C dataset; Section 5.3.1 and 5.3.2).

Fig. 5.5B and 5.5C shows that for untreated and reducing conditions, no TatA-TatC crosslinks were detected when constructs were expressing TatA I11C, and in addition the TatC homodimersation seen with oxidation was preserved in untreated conditions, with prominent TatC-TatC homodimers forming through M205C in the TM5 and all positions in the P3 loop, particularly P210C, D211C and V212C. Fainter interactions compared to those seen in the P3 loop were seen through residues in TM6, which were not present under oxidising conditions. The intensity of TatC homodimer bands through TatC P210C, D211C and V212C was notably decreased upon reduction (Fig. 5.5C), while still present at all positions observed under untreated conditions (Fig. 5.5B). Clearly based on this and control blots from all crosslinks performed thus far, TatC homodimerisation is very favourable, more so in the absence of TatB (compare all anti-TatC blots in Chapter 4, Section 4.3.3.1-4.3.3.3 with Sections, 5.3.1-5.3.3).

Corresponding anti-TatA blots demonstrate clearly the presence of a TatA-TatC heterodimer through TatA I11C and TatC M205C and L206C at ~37 kDa, which was absent in untreated or reducing conditions (Fig. 5.6). The weaker TatA I11C - TatC P209C heterodimer band (relative to those observed in TatC TM6; Fig. 5.5A) cannot be detected with anti-TatA antibodies, which was also the case for the TatA P3 loop interactions with TatA L9C and L10C, suggesting the interaction is weaker. In addition

to this, the interactions observed through TatA I11C and TatC V212C or F213C detected on anti-TatC blots under oxidising conditions cannot be seen with anti-TatA antibodies, again alluding to the weakness of this interaction in the absence of TatB, as they could be detected in Chapter 4, Section 4.3.3.3 (compare Chapter 4, Fig.4.7D and Fig. 5.5.) where TatB was present. TatA homodimerisation itself seems unchanged in the presence and absence of TatB (compare Chapter 4, Fig.4.7D and Fig. 5.5D). Indeed, based on this observation, it may be the case that lack of TatB decreased the intensity of TatA-TatC crosslinks through TatA I11C and V212C and F213C, as occurred through TatA L9C and F213C (Chapter 4, Section 4.3.3.1, Fig 4.5A compared to Section 5.3.1, Fig. 5.1).

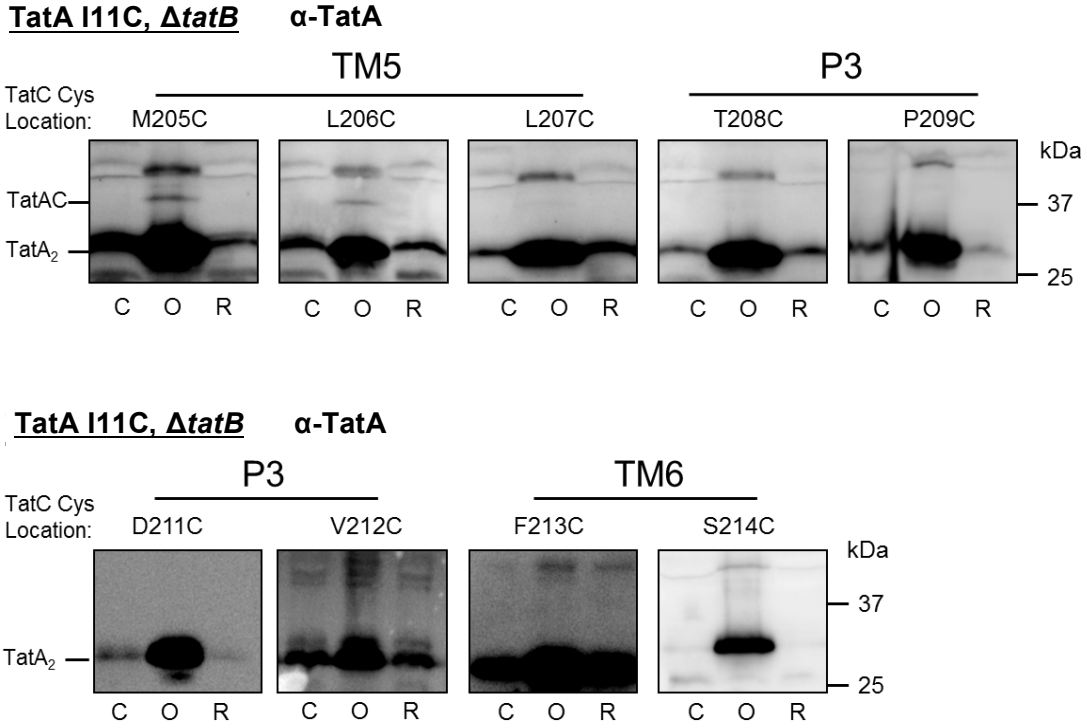

Fig. 5.6) TatA-TatC heterodimer through TatA I11C and TatC TM5 can be detected on anti-TatA Western blots in the absence of TatB- Western blots performed on whole cell samples of *E. coli* strain DADE (Δ*tatABCD,* Δ*tatE*) harbouring pREP4 and pQE60AΔBC expressing Cys substituted TatA and TatC as noted. Cells were O- oxidised with 1.8 mM copper phenanthroline, C**-** cells were untreated or R**-** cells were treated with 10 mM of the reductant DTT for 1 min. In each case the loading volume was 5 µL. The positions of the TatA-TatC heterodimer and TatA homodimer are indicated and the overexposed TatA monomer band has been cropped for clarity.

5.3.4 Mapping TatA-TatC interactions in the absence of TatB *in vivo*

The TatA-TatC crosslinking experiments in Chapter 4 demonstrated that TatA is able to interact at TatC TM6 when TatB is present. Here it was assumed that TatB was occupying its site at TM5 (Rollauer *et al*., 2012 and Kneuper *et al*., 2012), blocking any potential TatA-TatC interactions. Performing the same crosslinks between TatA and TatC *in vivo* in the absence of TatB found that while TatA could still occupy the site near TatC TM6, it could also crosslink to TM5 in a manner similar to TatB. Fig. 5.7 shows TatA TM interactions with TatC proposed to be present *in vivo* when TatB is absent. It should be noted that interactions between TatA and TatC TM6 may be slightly different in the presence and absence of TatB, as the TatA L9C and TatC V212C crosslink appeared in the absence of TatB, while the TatA L10C and V212C disappeared, but this may also be accounted for by further TatA monomers associating with TatC (only two are shown in Fig. 5.7). Indeed, as fluorescently labelled TatB has been demonstrated not to leave the TatBC complex (Alcock *et al*., 2013) it may relocate within the complex, therefore its removal may cause aberrant shifts within the whole complex.

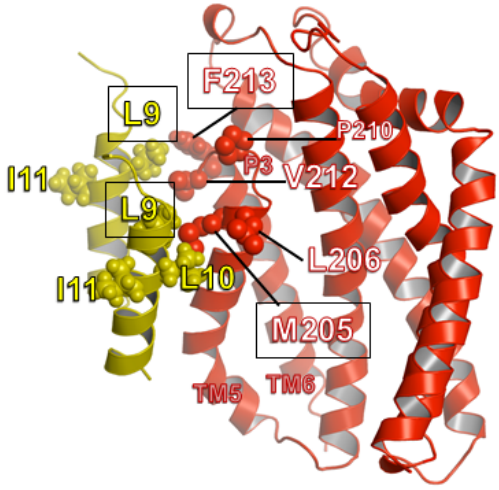

Figure 5.7) Diagram showing crosslinks between TatA and TatC in the absence of TatB- TatA (yellow) is shown with near the TatC TM6 and TM5 according to crosslinking data from Sections 4.3.4.1- to.3.4.3. With crosslinking residues shown as spheres. Residues selected to be further tested to examine both of the TatA sites on TatC shown with black boxes.

To further analyse these sites on TatC, found to be occupied by TatA in the presence and absence of TatB, the most prominent crosslinks for each of the proposed TatA interaction sites were taken forward for further study. Specifically, this included TatA L9C crosslinking to TatC F213C to study the proposed site at TatC TM6 and TatA L9C crosslinking to TatC M205C to analyse TatA occupying the TatB constitutive site at TM5.

5.3.5 The TatA interaction site at TatC TM6 *in vivo* is occupied in the absence of substrate binding

TatA has been found to interact at TatC TM6 when TatB is present (Chapter 4, Section 4.3.3.1), and is a candidate for a constitutive TatA-TatC interaction site. To determine whether TatA occupies this site in the absence of substrate binding, the crosslinking analysis described in Chapter 4, in the presence of TatB, was undertaken, in this case using TatC that harboured the combined F94A/E103A substitutions at the signal peptide binding site.

It can be seen that a clear heterodimer band at ~37 kDa, formed by TatA L9C crosslinking TatC F213C (TM6), was detected under oxidising conditions, that was responsive to both anti-TatA and TatC antibodies (Fig. 5.8A). The presence of this crosslink strongly suggests that TatA occupies this site in the absence of substrate interaction *(i.e*. the resting state) and is therefore constitutively bound. Furthermore, the homodimer formation between TatC F213C, which would usually migrate just below 50 kDa on anti-TatC Western blots, was not present in the resting state, supporting the inference of Cleon *et al*. (2015) that TatC dimerisation is a step in an activated Tat cycle. It should be noted that TatC homodimers were clearly observed in crosslinking experiments where endogenous substrate was able to bind (Chapter 4, Sections 4.3.3.1-4.3.3.3).

To examine whether the TatB constitutive site at TatC TM5, where TatA was found to bind in the absence of TatB (seen in Sections 5.3.1-5.3.3), could be occupied by TatA in the presence of TatB but the absence of substrate binding, crosslinking experiments

were performed between TatA L9C and TatC M205C in the presence of the TatC F94A/E103A substitutions. Fig. 5.8B demonstrates no bands migrating at a higher

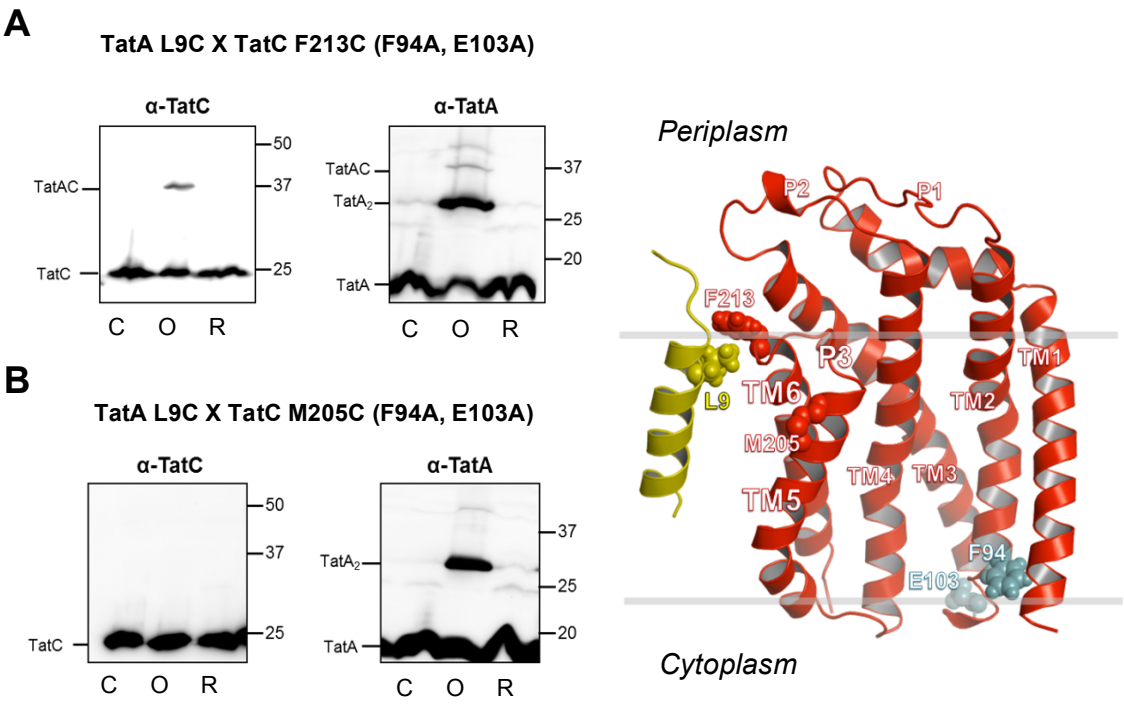

Figure 5.8) TatA L9C interacts with TatC F213C in the absence of substrate binding- A and **B** show anti-TatC/anti-TatA Western blots (as indicated) of whole cell samples of *E. coli* strain DADE (Δ*tatABCD*, Δ*tatE*) harbouring pRep4 and pUNITATCC4 expressing wild type TatB, TatA L9C and **A** TatC F213C with the F94A and E103A substitutions or **B** TatC M205C with the F94A and E103A substitutions. Cells were O- oxidised with 1.8 mM copper phenanthroline, C**-** untreated or R**-** treated with 10 mM of the reductant DTT for 1 min. Loading volume in each case was 5 µL. Diagramme of TatC (red) and the TatA transmembrane helix (yellow) is shown on the right with the positions of the Cys substitutions tested. The positions of F94 and E103 that were mutated to prevent signal peptide binding are shown in light blue.

molecular weight than the TatC monomer appeared on the anti-TatC Western blot under oxidising conditions, suggesting, as expected, that in the resting state there is no TatC dimerisation and that TatA does not interact at TatC TM5. It is likely that TM5 is occupied by TatB as outlined in Section 5.3.5.

The anti-TatA Western blots of the TatA L9C and TatC M205C crosslinking samples (Fig. 5.8B) are very similar to blots after crosslinking TatA L9C with TatC F213 (Fig. 5.8A), but as expected, no TatA-TatC heterodimer band was observed at ~37 kDa.

Observing both anti-TatA Western blots in Fig. 5.8, TatA homodimers linked through TatA L9C seem somewhat diminished in the resting state, comparing homodimer formation when co-expressed with TatC F94A/E103A in Fig 5.8 and or without the F94A/E103A substitutions in Fig 4.7D, with less homodimer present in the untreated or reduced conditions. A possible explanation for this is the lack of TatA oligomerisation due to the system being in the resting state (Alcock *et al*., 2013, Rose *et al*., 2013), causing a decrease in TatA homodimers, though it should be acknowledged that without comparing amounts of homodimer directly this is somewhat speculative. In addition to this, the higher molecular weight bands above 37 kDa still appeared on anti-TatA blots under oxidising conditions, as discussed in Section 4.3.3.1.

Given the strength of the TatA-TatC heterodimer formed through TatA L9C and TatC F213C in the resting state compared with the amount of unreacted TatC monomer (Fig 5.8A), it would suggest that a significant amount of TatA is associated with TatC under resting conditions *in vivo.* In light of this, henceforth this thesis will now refer to the TatA binding site at TM6 as the constitutive site.

5.3.6 TatA-TatC interactions during substrate binding/translocation

The effect of substrate overexpression on Tat subunit interactions has been explored previously in *E. coli* through fluorescence microscopy experiments in living *E. coli* cells, where it was found that disperse fluorescently-labelled TatA in the membrane formed clusters, presumed to correspond to TatA multimers, in response to overexpressed substrate (Rose *et al*., 2013, Alcock *et al*., 2013). It was proposed that this represents a step whereby TatA is recruited to the TatBC recognition complex and forms an oligomer which facilitates substrate translocation. Work examining specific crosslinking between Tat subunits in the presence of overexpressed substrate has been performed in *E. coli* where TatC M205C was found to self-crosslink only in the presence of overexpressed $CueO_{His}$ (Cleon *et al*., 2015) and plant thylakoids, whereby Tha4 (TatA) was found to more favourably associate with cpTatC TM5 and TM4, while interactions

at the proposed constitutive site in the equivalent of the P3 loop were unchanged (Aldridge *et al*., 2014). The plant studies utilised a modified OE17 precursor protein as the Tat substrate, which bound to the Tat complex but did not dissociate and was not translocated, in order to increase the lifetime of the complex.

It is conceivable that as Tat substrates are overexpressed in *E. coli*, TatA interactions on TatC may change, and that this could be detected using disulphide crosslinking. Thus, in the next Section, potential change/s in interactions through the TatA constitutive site at TatC TM6 and any potential TatA interactions at the TatB constitutive site at TM5 in the presence of overexpressed substrate were explored.

5.3.7 TatA moves from its constitutive site at TM6 to the TatB constitutive site at TM5 in response to overexpressed substrate

To identify whether TatA changed its crosslinking pattern to TatC in response to overexpressed substrate, crosslinking was performed in a background with an induced artificial Tat substrate, comprising green fluorescent protein fused to the signal sequence of the Tat substrate TorA and also harbouring a C-terminal SsrA tag, which targets the non-transported fusion protein for degradation by proteolytic ClpXP machinery in the cytoplasm. This construct, which is encoded on a pBAD33-based vector under the control of the arabinose-inducible P_{araBAD} promoter is named pTGS and was used previously by DeLisa *et al*. (2002) and was shown to be exported in a Tat-dependent manner.

It should be noted that the strain used for these experiments was DADE-P, which has the chromosomal *pcnB1* allele that substantially lowers the copy number of leaky *ColE1*-type plasmids such as pQE60 to 1-2 per cell (Lee *et al.,* 2006). This was necessary because pRep4, was previously used to repress expression from T4 promoter on pQE60, shares the same origin of replication with pTGS, and therefore would compete if co-transformed. It is not known whether the expression of the Tat

proteins from pQE60-based plasmids in strain DADE-P is higher or lower than in strain DADE/pREP4.

5.3.7.1 Induction of substrate expression with L-arabinose does not impair cell growth during 20 min incubation phase

As noted above, the substrate to be used was encoded on a pBAD33 based vector, pTGS, which requires induction with L-arabinose. L-arabinose is toxic to strains which contain the *araD* gene, such as DADE-P (Englesberg *et al.*, 1969) so a relatively short incubation time with this inducer was used to attempt to mitigate any potential damaging effect. Growth assays were performed to determine whether growth was impaired over the 20 minute incubation of the experiment (Fig. 5.9). The results show that over this time period, the propagation of the cells does not seem to be adversely affected by the presence of L-arabinose.

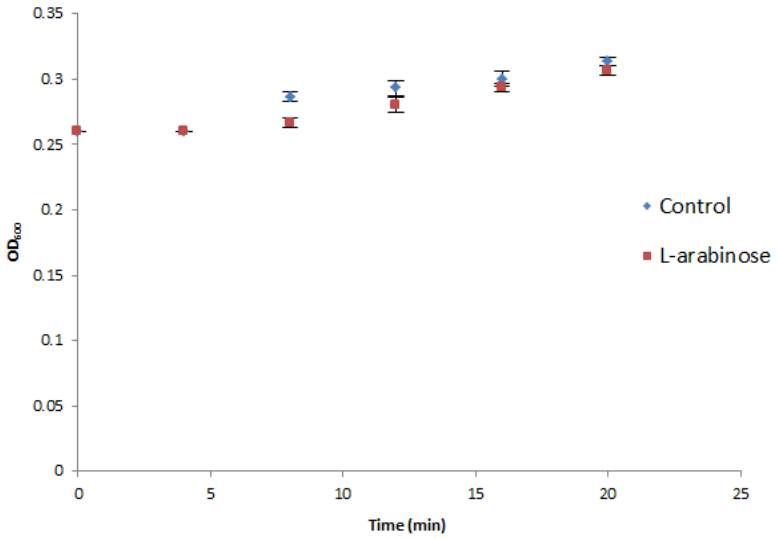

Figure 5.9) Growth of DADE-P is not affected during incubation with L-arabinose – DADE-P (Δ*tatABCD*, Δ*tatE, pcnB1 zad-981::*Tn*10d)* cells at OD_{600} of ~0.25 were either inoculated with L-arabinose (0.01% final concentration; red squares) for 20 mins, or mock inoculated (blue diamonds). Error bars show standard error of the mean, *n*=3.

5.3.7.2 TatA L9C crosslinks to TatC F213C at the proposed constitutive interactions site for TatA decrease with substrate overexpression

In order to elucidate the effect of substrate binding on TatA-TatC interactions, the artificial Tat substrate protein TorAss-GFP-ssrA was used. Plasmid pTGS was co-introduced along with the pUNITATCC4 vector encoding TatB along with Cys substituted TatA and TatC proteins, into DADE-P. To analyse any change in crosslinking pattern at the TatA constitutive site, the construct producing TatA L9C and TatC F213C alongside TatB was used. From Fig. 5.10 it can be seen that as the amount of L-arabinose was increased, and therefore the amount of translocated substrate, the intensity of the TatA-TatC heterodimer at ~37 kDa, linked through TatA L9C and TatC F213, appeared to decrease. This would indicate that TatA is vacating its constitutive site, or changing its association with TatC as the flux of substrate is increased through the Tat pathway. This observation is at odds with observations in

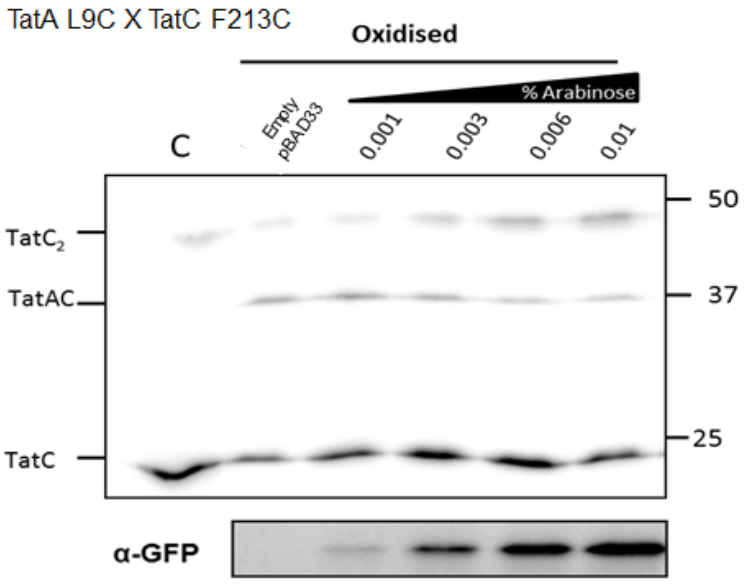

Figure 5.10) The TatA-TatC heterodimer intensity at TatC TM6 decreases as Tat substrate level is increased- Anti-TatC Western blot performed on whole cell samples of *E. coli* strain DADE-P (Δ*tatABCD*, Δ*tatE, pcnB1 zad-981::*Tn*10d*) harbouring plasmid pUNITATCC4 expressing wild type TatB and Cys-substituted TatA L9C and TatC F213C along with pTGS, which encodes the artificial Tat substrate TorAss-GFP-ssrA. These are shown with "C" untreated conditions, or after oxidation with 1.8 mM copper phenanthroline following induction of TorAss-GFP-ssrA production with the indicated concentration of L-arabinose. DADE-P harbouring pUNITATCC4 alongside empty pBAD33 was also oxidised, noted by "empty pBAD33". Bottom panel shows an anti-GFP Western blot performed on the periplasmic fraction of an aliquot of cells taken from each sample after incubation with L-arabinose but before oxidation.

plant thylakoids where Tha4 (TatA) interactions at the constitutive site at the P3 loop in cpTatC appeared unaffected by substrate overexpression (Aldridge *et al*., 2014). It is important to note, however, that Aldridge *et al.* (2014) utilised a substrate which binds irreversibly to the TatC complex, and is not transported, therefore steps involving the movement of TatA may be missed.

The intensity of the TatC homodimer crosslinked through F213C increased in response to substrate, suggesting that dimerisation is induced by substrate overexpression (Fig. 5.10), as was observed previously through M205C (Cleon *et al*., 2015). A possible explanation for this is that as TatA vacates TatC TM6, F213C of one TatC becomes free to interact with another F213C.

As a control to confirm that TorAss-GFP-ssrA was being produced and translocated in these experiments, aliquots of cells were withdrawn separately after incubation with each concentration of L-arabinose but prior to the crosslinking step, and the level of GFP assessed by Western blotting of periplasmic fractions (Fig. 5.10, lower panel). It can be seen that periplasmic substrate protein was clearly detectable, and increased with increasing arabinose concentrations.

5.3.7.3 TatA L9C crosslinks to TatC M205C at the TatB constitutive interactions site at TatC TM5 increase with substrate overexpression

Since TatA can occupy the TatB constitutive site on TatC (TM5) when TatB is absent (Section 5.3.1, Fig 5.1), it was hypothesised that during substrate overexpression TatA may be able to occupy the TatB site at TM5 even when TatB is present in cells, perhaps related to the apparent movement of TatA from its constitutive site. To analyse this, cells producing TatA L9C and TatC M205C alongside wild type TatB were oxidised in the presence of overexpressed substrate. It can clearly be seen that the intensity of the TatA L9C-TatC M205C heterodimer band increased as substrate level was increased by induction with L-arabinose (Fig. 5.11). Taken together with the decreased crosslinks seen at F213C, these findings suggest that TatA moves from its

constitutive site at TM6, to the TatB constitutive site at TM5 in response to substrate, and presumably after TatB has vacated TM5. As residues TatC M205C and F213C are ~15 Å apart the results cannot be explained by one TatA accounting for both interactions. Whether this movement of TatA is from one TatC to another, or occurs on the same TatC is unclear at this stage. Again, it should be noted that TatC homodimerisation through M205C increased with overexpressed substrate, in agreement with the findings of Cleon *et al*. (2015).

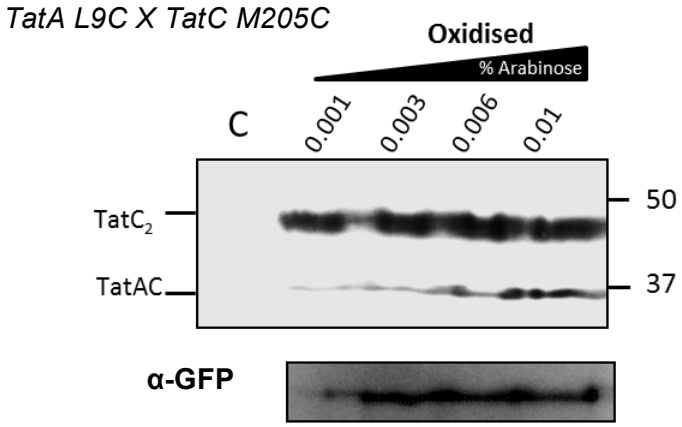

Figure 5.11) The TatA-TatC heterodimer intensity increases at TM5 as Tat substrate level is increased- Anti-TatC Western blot performed on whole cell samples of *E. coli* strain DADE-P (Δ*tatABCD*, Δ*tatE, pcnB1 zad-981::*Tn*10d*) harbouring plasmid pUNITATCC4 expressing wild type TatB and Cys-substituted TatA L9C and TatC M205C along with pTGS, which encodes the artificial Tat substrate TorAss-GFP-ssrA. These are shown with "C" untreated conditions, or after oxidation with 1.8 mM copper phenanthroline following induction of TorAss-GFP-ssrA production with the indicated concentration of L-arabinose. Bottom panel shows an anti-GFP Western blot performed on the periplasmic fraction of an aliquot of cells taken from each sample after incubation with L-arabinose but before oxidation.

5.3.7.4 TatA homodimerisation through TatA L9C increases in response to overexpressed substrate

Western blotting using anti-TatA antibodies also revealed a change in TatA homodimersation caused by overexpressed substrate. As demonstrated in Fig. 5.12 the level of TatA homodimer increased as L-arabinose was titrated in to induce substrate expression, in a similar manner to the increase in TatC homodimerisation through M205C and F213C seen in Figs. 5.10 and 5.11. These interactions may represent TatA monomers moving into the proximity of each other as they are recruited

to the Tat complex or perhaps more likely TatA interactions within transporting oligomers. In the Western blot shown in Fig. 5.12, no TatA-TatC heterodimer band was detected corresponding with those observed in Fig. 5.9 (expected migration is ~37 kDa). The reason for this is unclear.

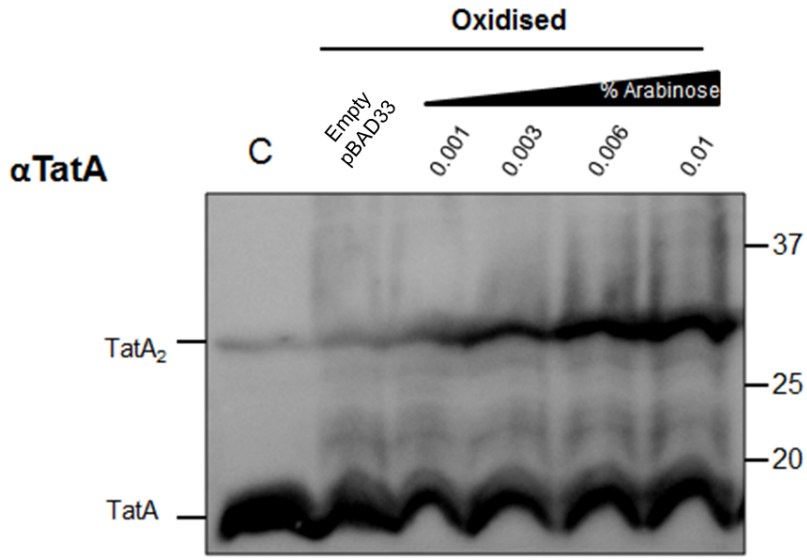

Figure 5.12) TatA homodimerisation through TatA L9C increases as Tat substrate level is increased- Anti-TatA Western blot performed on whole cell samples of *E. coli* strain DADE-P (Δ*tatABCD*, Δ*tatE, pcnB1 zad-981::*Tn*10d*) harbouring plasmid pUNITATCC4 expressing wild type TatB and Cys-substituted TatA L9C and TatC F213C along with pTGS, which encodes the artificial Tat substrate TorAss-GFP-ssrA. These are shown with "C" untreated conditions, or after oxidation with 1.8 mM copper phenanthroline following induction of TorAss-GFP-ssrA production with the indicated concentration of L-arabinose. DADE-P harbouring pUNITATCC4 alongside empty pBAD33 was also oxidised, noted by

5.3.7.5 The presence of substrate is linked to the decreased TatA interactions through L9C with TatC F213C

In order to to confirm that the presence of substrate as opposed to L-arabinose itself caused the change in crosslinking between TatA and TatC, similar crosslinking experiments were performed in the presence of empty pBAD33 (the vector from which pTGS is derived). It was observed that for the TatA L9C-TatC F213C samples, the intensity of the TatA-C heterodimer and TatC homodimer bands remained constant regardless of the L-arabinose concentration (Fig. 5.13). This is in clear contrast to Fig. 5.10, and thus links the movement of TatA directly to the presence of Tat substrate.

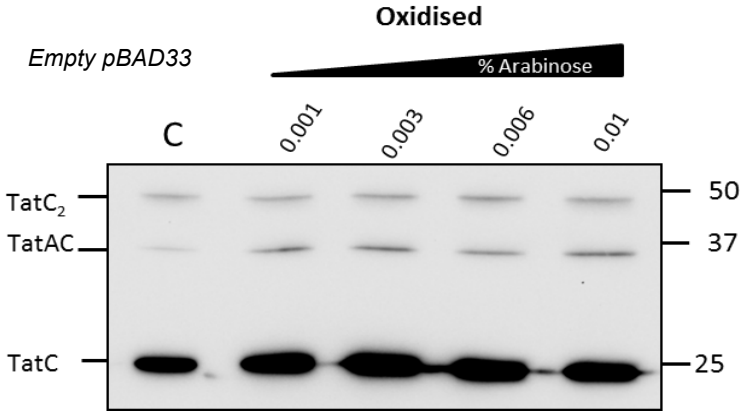

Figure 5.13) L-arabinose alone does not affect the TatA L9C TatC F213C crosslink - Anti-TatC Western blot of whole cell samples of *E. coli* strain DADE-P (Δ*tatABCD*, Δ*tatE, pcnB1 zad-981::*Tn*10d*) harbouring plasmid pUNITATCC4 expressing wild type TatB, TatA L9C and TatC F213C along with empty plasmid vector pBAD33. Varying concentrations of L-arabinose, as indicated, were added to the cells, prior to oxidation with 1.8 mM copper phenanthroline for 1 min. C- whole cells of the same strain and plasmid combination treated with 0.01% L-arabinose but without addition of copper phenanthroline.

5.3.8 TatA-TatC crosslinks at TatC TM6 are not detected *in vivo* when the PMF is dissipated

As outlined in Chapter 1, Section 1.11, translocation through the Tat system is driven by the PMF, and as such it is reasonable to assume that once the PMF is dissipated this may influence TatA-TatC interactions. If this is the case, changes in crosslinking patterns between TatA and TatC, associated with PMF dissipation may be revealed.

In order to dissipate the PMF, initially the uncoupler carbonyl cyanide *m*-chlorophenyl hydrazine (CCCP) was used, as has been employed in previous studies analysing the PMF dependence of Tat interactions in live *E. coli* cells (Alcock *et al*., 2013, Rose *et al*., 2013). However, in these crosslinking experiments it precipitated upon oxidation forming a bright yellow solid. Instead, indole was chosen as an uncoupler. Indole is composed of a benzene ring fused with a five membered pyrrole and is well distributed in the natural environment. It is utilised by both Gram-positive and Gram-negative bacteria for signalling purposes (Lee & Lee, 2010) but at high concentrations, in the region of 3 to 5 mM, it has been found to dissipate the PMF of *E. coli* (Chimerel *et al.*, 2012*)* and has been utilised in *E. coli* by Ismail *et al.* (2015) to characterise biphasic electrical forces during Sec translocation.

To analyse the effect of PMF dissipation on TatA-TatC interactions, crosslinking analysis of TatA L9C with either TatC F213C (the constitutive TatA binding site) or TatC M205C (the constitutive TatB binding site) was undertaken in the presence of 5 mM indole.

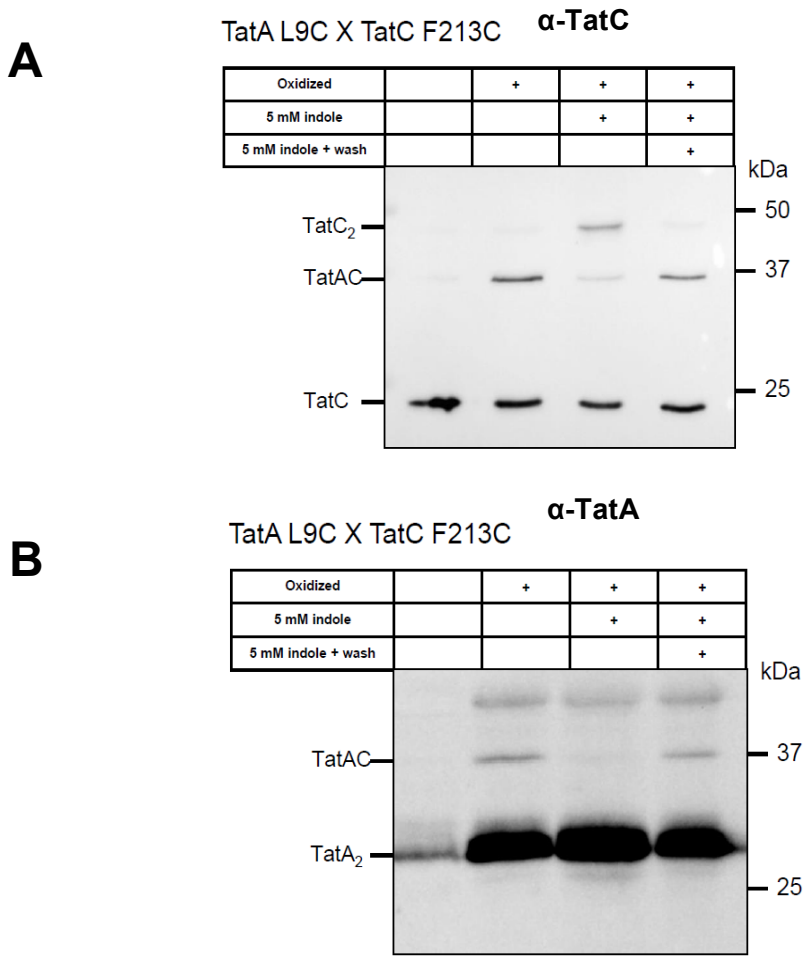

Figure 5.14) TatA vacates its constitutive site at TatC TM6 in response to PMF dissipation A Anti-TatC or **B-** Anti-TatA Western blot of whole cell samples from *E. coli* strain DADE (Δ*tatABCD*, Δ*tatE*) harbouring pRep4 and pUNITATCC4 expressing wild type TatB and Cys-substituted TatA L9C and TatC F213C. Samples were either untreated, oxidised with 1.8 mM copper phenanthroline for 1 min or incubated with 5 mM indole for 5 mins, followed by either a 1 min oxidation step or washed thoroughly to remove the indole followed by a 1 min oxidation step.

Fig 5.14A shows an anti-TatC blot for cells producing TatA L9C and TatC F213C alongside wild type TatB. Under oxidising conditions, in the absence of indole, the TatA-TatC heterodimer band was clearly detected at ~37 kDa. However, in the presence of indole, the TatA-TatC heterodimer was barely detectable and instead a

TatC homodimer was observed. To confirm that the effect of indole was reversible, a separate sample was loaded onto SDS-PAGE where the cells were first incubated with indole then washed thoroughly prior to oxidation. It can clearly be seen that upon indole removal the TatA-TatC heterodimer band was again detected and the TatC homodimer diminished. These results strongly suggest that a PMF is required to position TatA at its constitutive binding site on TM6 of TatC. Similar results were observed when the samples were analysed with anti-TatA antibodies, where the band migrating at ~37 kDa was not detected following indole incubation (Fig 5.14B). Interestingly PMF dissipation did not seem to impair TatA homodimerisation, with prominent TatA homodimer bands linked through TatA L9C detected in all of oxidised samples.

The increased homodimer formation through TatC F213C and decreased TatA-TatC heterodimer formation through TatA L9C and TatC F213C in response to PMF dissipation shows similarities to the findings in the presence of overexpressed substrate (Section 5.3.6). It was seen that overexpressed substrate caused TatA to move from its constitutive site at TatC TM6 to occupy the TatB constitutive site at TM5 (Section 5.3.6).

To investigate whether dissipation of the PMF resulted in the movement of TatA into the constitutive TatB binding site, similar experiments were repeated on cells producing TatA L9C and TatC M205C alongside wild type TatB. As can be seen in Fig. 5.15, under oxidising conditions TatA L9C did not crosslink with TatC M205C, as observed previously in Section 4.3.6.1. However, upon PMF dissipation using 5 mM indole, no TatA-TatC heterodimer band was detected, although a notable increase in TatC homodimer linked through M205C was seen. These findings were confirmed by blotting the same samples with an anti-TatA antibody (Fig 5.15B), however interestingly it appears that when constructs expressed TatA L9C alongside TatC M205C, TatA homodimerisation was increased upon incubation with 5 mM indole. This was not observed in Fig. 5.14B where TatA L9C was co-expressed TatC F213C, and may represent a discrepancy in protein amounts from different mutations in constructs used.

Taken together these findings suggest that as TatA moves away from its constitutive site at TatC TM6 when uncoupler is present it is not locating to TM5 as occurred with

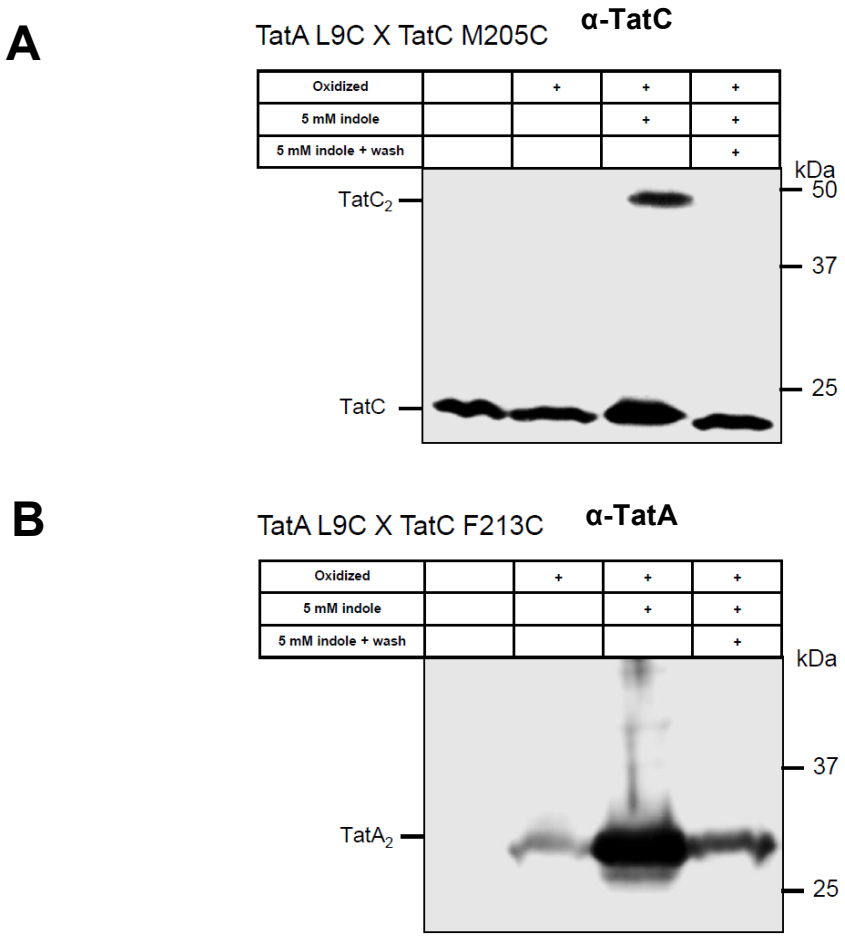

Figure 5.15) TatA L9C does not crosslink with TatC M205C when the PMF is dissipated- A- Anti-TatC or **B-** Anti-TatA Western blot of whole cell samples from *E. coli* strain DADE (Δ*tatABCD*, Δ*tatE*) harbouring pRep4 and pUNITATCC4 expressing wild type TatB and Cys-substituted TatA L9C and TatC M205C. Samples were either untreated, oxidised with 1.8 mM copper phenanthroline for 1 min or incubated with 5 mM indole for 5 mins, followed by either a 1 min oxidation step or washed thoroughly to remove the indole followed by a 1 min oxidation step.

overexpressed substrate, instead it is either interacting at an as yet unknown location on the Tat complex, or is leaving the complex completely. These findings have implications for experiments undertaken *in vitro* or after Tat protein extraction from native membranes, because it implies that once the PMF is dissipated TatA is no longer interacting in its constitutive site, found when the complex is in the resting state (Section 5.3.3). Indeed it may explain the discrepancy between the amount of TatA

crosslinking TatC in the resting state and the amount co-purified during affinity purification; this will be discussed further in Section 5.4.3.

5.3.9 TatA-TatC crosslinks at TatC TM6 are disrupted *in vitro* in isolated membrane fractions

Much of the prior disulphide crosslinking work was undertaken on isolated *E. coli* membrane fractions containing Tat proteins, where it was found that TatB could interact at TatC TM5, and TatC could self-associate extensively (Rollauer *et al*., 2012, Kneuper *et al.*, 2012, Punginelli *et al*., 2009). To examine whether the effect of indole as an uncoupler mirrors *in vitro* findings, experiments were performed examining the interaction of TatA at the constitutive site at TM6 and at the TatB constitutive site at TM5 in isolated membranes. Fig. 5.16A clearly shows that after cell lysis and extraction of membrane fractions, TatA L9C could no longer be crosslinked to TatC F213C at the constitutive TatA binding site. Additionally a clear TatC homodimer was observed through F213C *in vitro*, mirroring the observations seen after indole treatment (Section 5.3.8). Interestingly, the control conditions demonstrated that the TatC homodimer forms without favourable TatA L9C self-association, as was observed *in vivo* with ionophores (Section 5.3.8).

Strikingly, when isolated membranes containing TatA L9C and TatC M205C (alongside wild type TatB) were oxidised, a clear TatA-TatC heterodimer was observed that was not present under control or reducing conditions. This in contrast to the observation made *in vivo* in the presence of indole where no detectable TatA-TatC interaction was seen through the same Cys substitutions.

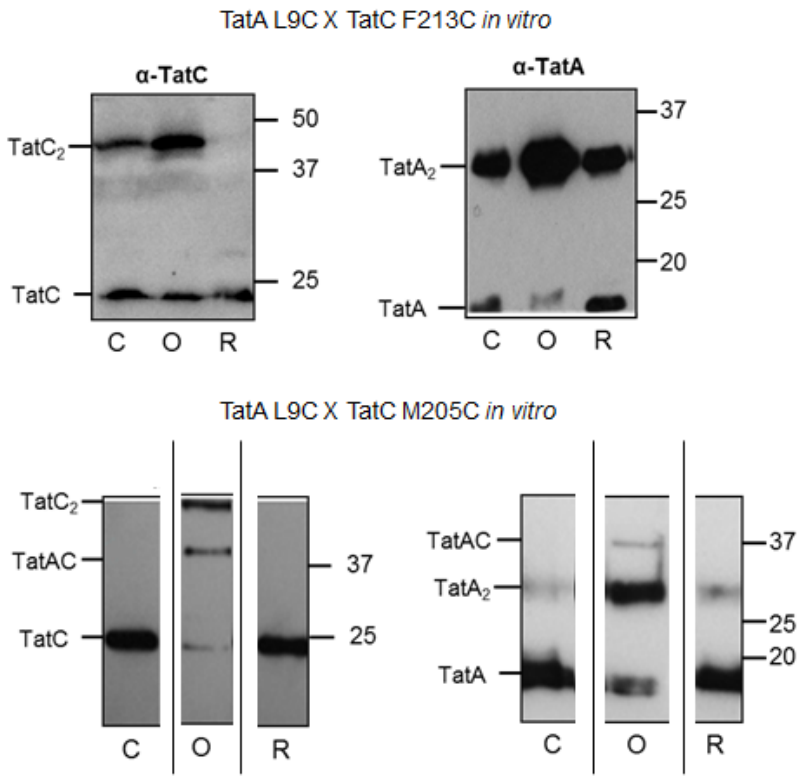

Figure 5.16) TatA L9C crosslinks to TatC M205C but not F213C *in vitro*- Anti-TatC and anti-TatA Western blots of membrane fractions isolated from *E. coli* strain DADE (Δt*atABCD,* Δ*tatE*) harbouring pRep4 and pUNITATCC4 encoding wild type TatB and Cys-substituted TatA L9C along with **A-** TatC F213C, or **B-** TatC M205C. Membrane fractions were C untreated, O oxidised with 0.6 mM copper phenanthroline for 1 hour or R treated with 10 mM of reductant DTT for 1 hour (following the protocol of Punginelli *et al*. (2009) Rollauer *et al*. (2012) and Kneuper *et al*. (2012)). Loading volume was 5 µL.

5.4 Discussion

5.4.1 TatA has constitutive binding site at TatC TM6 *in vivo*

Previous disulphide crosslinking experiments performed in plant thylakoids proposed that a constitutive binding site for Tha4 (the plant analogue of TatA) exists at the equivalent of the P3 loop in cpTatC. This was grounded in observations that a crosslink between Tha4 position 9 and cpTatC in this loop region was observed that was unchanged with overexpressed substrate, or PMF dissipation using the ionophores valinomycin and nigericin (Aldridge *et al*., 2014). Based on disulphide crosslinking between TatA and a Cys scanning region in TatC, covering the periplasmic end of TM5, the P3 loop and the periplasmic end of TM6, the work in this thesis identifies that a TatA constitutive site is also present on *E. coli* TatC encompassing the periplasmic region of TM6, which may include the extreme C-terminal end of the P3 loop. The placement of TatA here is based on TatA L9C crosslinking to TatC residue F213C in TM6 *in vivo* when the Tat system cannot interact with substrate and is therefore in the resting state (Section 5.3.3). It is also supported by the finding of weaker crosslinks through TatA L10C with V212C and TatA I11C with both V212C and F213C under conditions where the Tat system can bind only endogenous substrate (Chapter 4, Sections 4.3.3.1-4.3.3.3). Fig. 5.17 shows the proposed position of the TatA constitutive site on TatC identified in this work.

The discrepancy between the placement of Tha4/TatA in plants and *E. coli* could be explained by a number of factors. One reason may be that TatA and the plant orthologue, Tha4, occupy constitutive sites with slightly shifted positions, with *E. coli* TatA at TM6 on TatC and Tha4 at the equivalent of the P3 loop in plant cpTatC. It should be noted that the work in this thesis was able to detect TatA interactions in the TatC P3 loop in *E. coli*, but these were weak compared to interactions seen at TatC TM5 and TM6 and only occurred when TatB was not present (Sections 5.3.1-5.3.3). Interestingly, the nature of the crosslinking experiments in Aldridge *et al.* (2014) has

Tha4 in excess of the subunit Hcf-106 (TatB) relative to the native stoichiometry, as it requires importing into chloroplasts. Indeed the excess of Tha4 over Hcf-106 could potentially lead to interactions similar to those observed in this work where TatB is absent. It should also be noted that the equivalent of the periplasmic facing part of cpTatC TM6 was not tested for interactions with Tha4 by Aldridge *et al.* (2014), and it remains possible that Tha4 also interacts here in the plant Tat system.

The placement of TatA at TatC TM6 here is supported by prior photo-crosslinking in *E. coli* INVs whereby Bpa substitutions at positions at the periplasmic region of TatC TM3 (facing TM6) could photo-crosslink TatA (See Chapter 1, Section 1.10.7 for the positon of these Bpa substitutions in TatC TM3; Blummel *et al*., 2015). However, it should be noted that these photo-crosslinks were performed in *E. coli* INVs which may not have any PMF present, and as was observed in Section 5.3.8, this would have an impact on TatA-TatC interactions.

Aldridge *et al.* (2014) reported that the amount of heterodimer linked through Tha4 to the P3 loop of cpTatC was unchanged with substrate overexpression. However, the work in this thesis clearly shows that upon substrate overexpression, interactions at the proposed constitutive site at the TM6 of TatC decrease (Section 5.3.6). This discrepancy could, again, be due to native differences in the Tat translocase of plants and bacteria, or it could reflect the fact that Aldridge *et al.* (2014) used a Tat substrate which was able to irreversibly bind to the translocase in plants but was not exported. Indeed, interactions in the Tat translocase may be missed if the full translocation cycle is not occurring, as movement of TatA could conceivably occur during the transport event itself, or after the Tat substrate has moved into the periplasm.

5.4.2 TatA is able to occupy the TatB constitutive site when TatB is absent and during substrate binding and/or transport

The work in this Chapter demonstrated that TatA-TatC crosslinks at the constitutive TatA site were weakened in response to substrate overexpression, and were

accompanied by an increase in TatA-TatC interactions at TatC TM5 under the same conditions (Section 5.3.6). Further to this, in the absence of TatB it was found that TatA could form a crosslinking pattern remarkably similar to that found through TatB at TatC TM5 (Sections 5.3.1-5.3.3). Somewhat is support of this, Aldridge *et al*. (2014) demonstrated that Tha4 interactions at cpTatC TM5 and TM4 were increased in response to overexpressed substrate. This supports the hypothesis of a "gatekeeper" role for TatB, whereby it blocks TatA-TatC interactions associated with transport of substrate (in this case by interacting at its constitutive site at TatC TM5) until a point where substrate has bound the Tat complex. After transport is triggered by substrate binding, TatB may vacate its constitutive site and move to an as yet unknown location (based on fluorescence microscopy experiments it is unlikely to leave the complex; Alcock *et al*., 2013), whereby TatA moves in to occupy the TatB binding site. Indeed, Ni affinity purification trials in Chapter 3 observed that TatA-TatC associations were increased when TatB was not present and may be explained by TatA occupying the now vacant TatB sites on TatC further supporting this "gatekeeper" role of TatB.

If the data here is analysed in the context of Rodriguez *et al*. (2013), who observed two conformations of TatA, one relaxed and one with the TM and AP (amphipathic helix) positioned perpendicular to each other (L-Shaped; Chapter 1, Section 1.10.6), a representation of these is shown in Fig. 5.17 where it may be the case that interaction with TatC F213 (which is higher in the membrane, shown in Fig. 5.17) corresponds to the relaxed form of TatA, while interactions at M205C correspond to the more L-shaped conformation which is thought to pinch the membrane (Fig. 5.17). This step could initiate TatA oligomerisation whereby numerous TatA molecules adopt the L-shaped conformation, and large scale membrane disruption allows transport of the Tat substrate. Observing Fig 5.17, it is clear that when TatA moves from TM6 to TM5, it moves closer to the concave face of TatC. This may then include interactions at TM4, which have been observed in plant thylakoids (Aldridge *et al.*, 2014) and proposed in bacteria (Rollauer *et al.*, 2012).

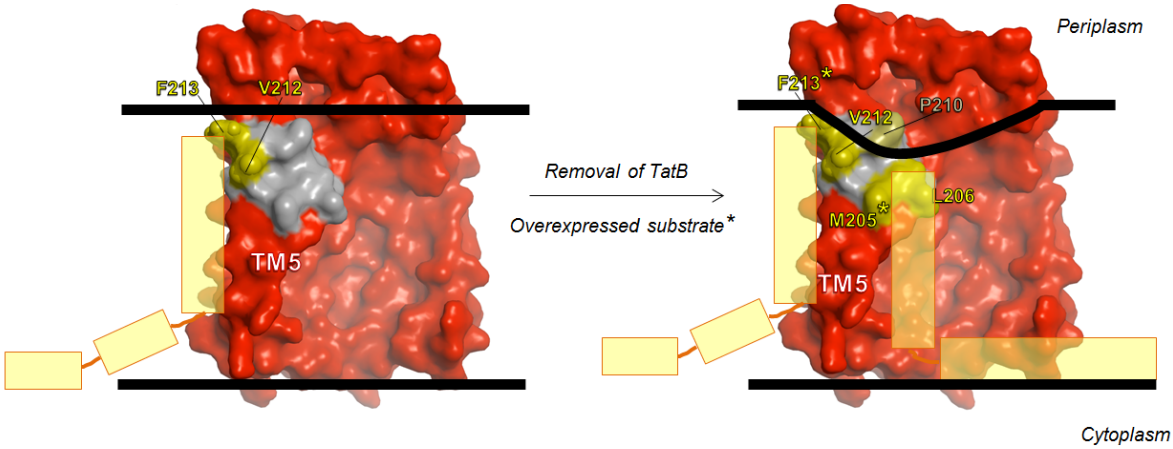

Figure 5.17) Proposed conformational change of TatA as it moves from TatC TM6 to TM5—Left- TatC (red) *in vivo* with TatA (yellow rectangles), and TatB (not shown for clarity but presumed to be occupying TatC TM5) with residues that were mutated to Cys but did not crosslink to TatA shown in grey, and those that formed heterodimers with TatA in yellow, indicating the constitutive TatA site. **Right-** TatA occupying the initial constitutive site on **Left-** as well as a site at TM5 which is occupied after substrate overexpression (shown *via* a change in TatA-TatC crosslink intensity to TatA L9C through residues with an asterisk). A weak interaction, relative to those at TM5 and TM6 is found at P210C which is shown in dark green. Membrane is shown as a black line, with distortion of the lipids on the periplasmic side of the membrane shown on the right.

It is not known whether TatA moves from the TM6 of one TatC to the TM5 of another (Fig. 5.18). Given the favourable homodimer formation through residues in this TM5/P3/TM6 region in TatC, it could be the situation that two TatC proteins are near to each other at this interface allowing a horizontal movement from one TatC to another (See Fig 5.18, which explores potential TatA-TatC and TatC-TatC interactions).

It was observed in Section 5.3.8 that PMF dissipation could be modulated in living *E. coli* cells using indole where these experiments in effect switch on and off TatA-TatC constitutive associations by altering the PMF, similar to experiments whereby TatA oligomerisation could be recovered after PMF disruption by CCCP, when the uncoupler was inactivated (Alcock *et al*., 2013). This has important implications for experiments performed on purified Tat components, since if TatA dissociates from TatC in the absence of a PMF, interactions would not be observed in subsequent affinity chromatography or gel filtration experiments. This may explain why so little TatA is observed co-purifying with TatC (Chapter 3, Section 3.3), despite the strong heterodimer band linking TatA to TatC TM6 in the resting state during crosslinking trials suggesting a favourable resting state TatA-TatC interaction.

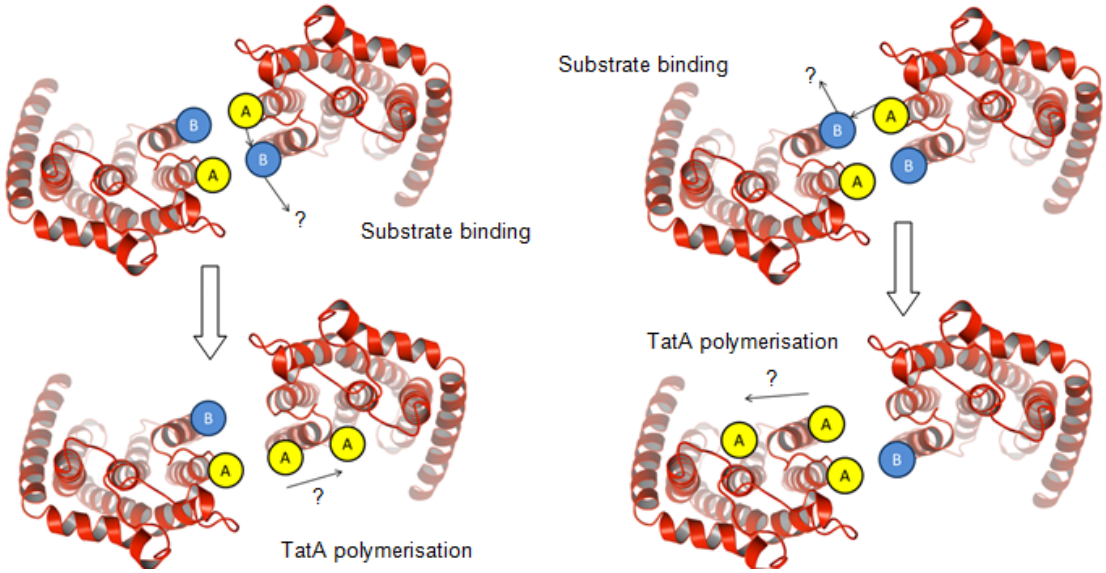

Figure 5.18) Proposed movements of TatA in response to substrate overexpression- A TatA (yellow) on TatC (red) moves from the constitutive site at TatC TM6 to the TatB (blue) constitutive site at TM5 on the same TatC protein. TatB moves to an as yet unknown location, denoted by "?", while TatA may oligomerise in the face of the same TatC protein. **Right-** TatA moves from its constitutive site at TatC TM6 to the TM5 of another TatC as TatB moves to an unknown location. TatA may then oligomerise in the concave face of the opposing TatC.

5.4.3 Elucidating the role of PMF in the Tat system

Though PMF dissipation using ionophores valinomycin and nigericin did not cause Tha4 to vacate its proposed constitutive site, at the equivalent of the P3 loop in cpTatC (Aldridge *et al*., 2014), this work found that *E. coli* TatA vacated its constitutive site at TatC TM in response to PMF dissipation with ionophore indole. However, it should be noted that during affinity purification studies in plant thylakoids, Cline & Mori (2001) observed no Tha4 (TatA) copurifying with the Hcf106-cpTatC complex, which may suggest that PMF dissipation does promote some changes between Tha4-cpTatC interaction. Despite this discrepancy, both this work and that of Aldridge *et al.* (2014) found that Tha4/TatA did not interact with TatC TM5 in the presence of PMF dissipation using ionophores, suggesting a PMF dependence on Tha4/TatA interactions here, or perhaps a PMF-dependent TatB dissociation step which would free TatC TM5 for interactions with TatA, which may explain increased TatA co-purification with affinity-tagged TatC in the absence of TatB (Chapter 3, Section 3.3).

Reasons as to why PMF may be important in maintaining constitutive TatA-TatC interactions could involve the ionisable conserved residue Q8 in the TM of TatA. Protonation (or deprotonation) of this residue may be mediated by an intact PMF. Additionally ionisable, conserved residues Q215 in the TM6 or D211 in the P3 loop of TatC may also be important in TatA-TatC interactions, though their substitution to Cys was tolerated by the Tat system.

Finally it should be noted that it is not clear whether PMF dissipation causes TatA to leave the Tat complex altogether or whether is moves to a different part of the Tat complex that has yet to be identified.

5.4.4 Linking the role of TatA to the TatA-TatC disulphide crosslinks observed in this Chapter

This work has identified a TatA constitutive site at the TM6 of TatC *in vivo* (Section 5.3.3). Interactions in this region require an intact PMF (Section 5.3.8 and 5.3.9) and were diminshed in response to overexpressed substrate (Section 5.3.6). This challenges previous dogma about the TatBC complex and the absence of constitutively-bound TatA based on purification experiments whereby no or very little TatA is found to co-purify with TatC (outlined in detail in Chapter 3, Section 3.3). Indeed, given that a significant amount of TatA was found to be associated with TatC in the resting state by crosslinking, it seems likely that TatA is a component part of the Tat complex in the absence of substrate binding, presumably before further TatA monomers are recruited to the activated Tat complex.

TatA rearrangement in response to substrate binding has been characterised by Rose *et al.* (2013) and Alcock *et al.* (2013) where fluorescently labelled TatA was found to form florescent clusters thought to correspond to the TatA oligomer which facilitates translocation of Tat substrates. Aldridge *et al.* (2014) were able to identify Tha4 (TatA) interacting at cpTatC TM5 and TM4 in a substrate-enhanced manner and this work may have identified movement of TatA to the TM5 in the early stages of translocation

of substrate, with movement of TatA from its constitutive site at TM6, towards TM5 and the concave face of TatC. Both these movements preface the start of TatA oligomerisation step in Tat export of proteins.

Two main models exist by which TatA polymerisation is mediated. As stated previously, work performed in plants suggests that the TatA transmembrane helix can occupy sites in the concave face of TatC upon substrate overexpression (Aldridge *et al*., 2014), and this could form a membrane disrupting oligomer at the centre of the Tat complex presented in Blummel *et al.* (2015) (See Chapter 1, Section 1.10.5). This is supported by *in silico* models proposing an interaction of *E. coli* TatA transmembrane helix with the concave face of TatC (Rollauer *et al*., 2012). Alternatively, TatA is proposed to form a separate ring-shaped oligomer on the outside of the TatBC complex which can vary in size depending on the size of the substrate to be translocated. This oligomer may have been characterised as a separate entity to the TatBC complex in detergent solution following purification (Sargent *et al.,* 2001), using Electron paramagnetic resonance (EPR) (White *et al.*, 2010) and electron microscopy (Gohlke *et al.,* 2005), with molecular modelling based on the monomer structure (Rodriguez *et al*., 2013) (Chapter 1, Section 1.10.6). However, data *in vivo* is currently lacking, with fluorescence-based studies unable to determine whether fluorescently-labelled TatA formed oligomers inside or outside the TatBC complex (Alcock *et al*., 2013, Rose *et al*., 2013). With regard to the crosslinking analysis in this work, the movement of TatA from TatC TM6 to TM5 could be compatible with either of these hypotheses. While the presumed direction of movement of TatA is towards the TatC concave face, this movement could also present the first step in TatA forming a separate oligomer, as further TatA monomers are perhaps recruited to form the membrane translocating oligomeric ring.

Chapter 6: TatA crosslinks to TatC are validated with low copy number expression, with TatA and TatB interactions observed in the presence of substrate

6.1 Introduction:

6.1.1 TatA-TatC crosslinks identified from disulphide crosslinking of TatA to a Cys scanning region of TatC

Chapters 4 and 5 were able to identify two proposed TatA interaction sites within TatC. Crosslinks between Cys-substituted residues in the TatA transmembrane helix, L9C and I11C, were found with TatC F213C in TM6, along with crosslinks to neighbouring V212C through TatA L10C and I11C (Chapter 4, Sections 4.3.3.1-4.3.3.3). Since the TatA L9C crosslink to TatC F213C is preserved in a resting Tat system, this suggests it is a constitutive interaction (Chapter 5, Section 5.3.5). Reduced interaction at this TatA constitutive site were also seen with overexpressed artificial Tat substrate (Chapter 5, Section 5.3.6), and interactions at the site were also shown to be PMF dependent (Chapter 5, Section 5.3.8). While the TatA L9C crosslink to TatC F213C was the most favourable observed in Cys scanning crosslinking of TatC in the presence of TatB, at this stage, the importance of weaker interactions through other residues in the TatA transmembrane helix with, TatC at this region, still remain to be deciphered. Cys substitutions in TatC at the proposed TatA constitutive site are shown in Fig. 6.1.

Interactions were also observed at a separate site in TatC, between TatA L9C and I11C with TatC TM5 through M205C and L206C when TatB was absent, with TatA L10C also shown to interact with the latter TatC Cys substitution under the same conditions (Chapter 5, Sections 5.3.1-5.3.3). Additional experiments showed TatA L9C crosslinks to M205C in the presence of an overexpressed artificial Tat substrate when TatB was present (Chapter 5, Section 5.3.7). TatB has previously been proposed to interact with TatC TM5 (Rollauer *et al.,* 2012, Kneuper *et al.,* 2012, Blummel *et al*., 2015) and this suggested a movement of TatA from its constitutive site to the TatB constitutive site during substrate transport, with TatA and TatB able to differentially occupy the same site at TatC TM5. Cys substitutions in TatC at the proposed TatA transport site are shown in Fig. 6.1.

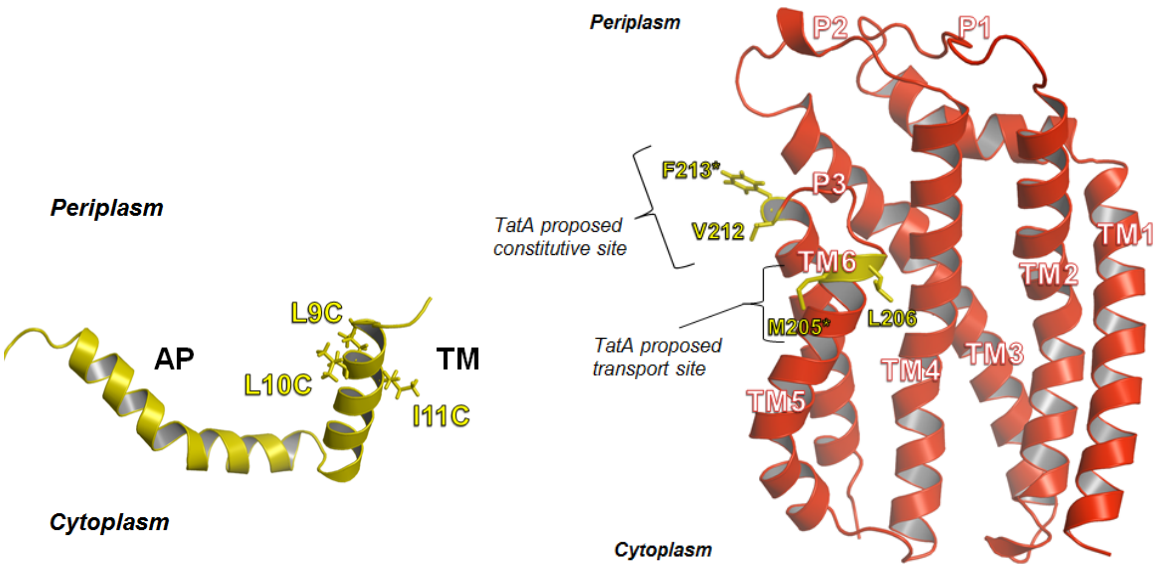

Figure 6.1) Residues on TatC proposed to interact with TatA through two different sites- Structure of TatC shows residues in yellow, F213 and V212 are near the proposed TatA constitutive site, while M205 and L206 are shown at the proposed transport site. TM-transmembrane helix. AP- amphipathic helix.

6.1.2 Copy number and substrate overexpression in studying the Tat system

In Chapters 4 and 5, disulphide crosslinking was performed using Cys-substituted proteins expressed from medium copy number plasmid constructs, producing protein amounts substantially higher than that found at native level. While this allows for clear mapping of subunit interactions because of ease of detection on Western blots, it may not reflect the situation with the Tat system in nature and such large amounts of protein, especially in the phospholipid bilayer, could present artefacts, such as aberrant protein associations, not seen with lower expression of Tat proteins.

Indeed, it has been observed previously that the TatB substitution E8C could support an active Tat system when expressed from medium copy number vectors only, while at low copy number the system was not functional when scoring for Tat activity (Johann Habersetzer, unpublished). From this it is conceivable that these growth defects may reflect a difference in interactions between the subunits- *i.e.* TatB interactions with TatC may be impaired or abolished due to the E8C substitution, but with overexpressed subunits, the interaction may be restored to an extent, raising questions about the use of medium copy number vectors.

In order to identify whether the TatA interactions with TatC observed with medium copy number expression in Chapter 4 and 5 are an accurate reflection of the state of the Tat system in nature, selected crosslinks (see Section 6.1.1) will be further examined in this Chapter with expression from a very low copy number vector, pTat101. This vector encodes the *tatABC* operon with the *tat* promoter, and has been shown to produce TatC four times in excess of native TatC, as determined by immunoblotting experiments (Kneuper *et al.*, 2012). The residues chosen to examine at a low copy number in TatC and TatA are those presented in Section 6.1.1, Fig. 6.1.

In addition to this, crosslinking performed in Chapter 5, Section 5.3.6 utilised GFP fused to a Tat signal sequence as an overexpressed Tat substrate. The substrate itself is not a native protein found in *E. coli* and in the experiments in this Chapter the overexpressed native Tat substrate, CueO, will be utilised.

6.1.3 Identifying TatA-TatB interactions

Results in Chapters 4 and 5 were able to identify TatA-TatC interactions *in vivo* which demonstrated that TatA interacts with two sites in close proximity. It is assumed that one of these sites is normally occupied by TatB. Given that the transmembrane helices of TatA and TatB are homologous (Chapter 1, Section 1.10.1) and each protein has a propensity to self-interact (Chapter 1, Sections 1.10.2 and 1.10.3), direct interactions between the two proteins may be expected at some points in the Tat transport cycle. Prior evidence would support this - for example TatB has been shown to co-purify with affinity-tagged TatA in trace amounts (Sargent *et al.,* 2001). Blummel *et al.* (2015) also identified TatA-TatB crosslinks with a photo-reactive Bpa residue introduced into the flexible N-terminal region of TatB in *E. coli* inside-out inner membrane vesicles (INVs). Though these experiments suggest that TatB and TatA interact, it is difficult to derive information regarding residues near to each other in an attempt to map the interface between the two proteins.

This Chapter will analyse crosslinking between residues L9C, L10C and I11C in the TM of TatA with equivalent residues L9C, L10C and L11C in the TM of TatB with expression from low copy number vector, pTat101 (Fig. 6.2).

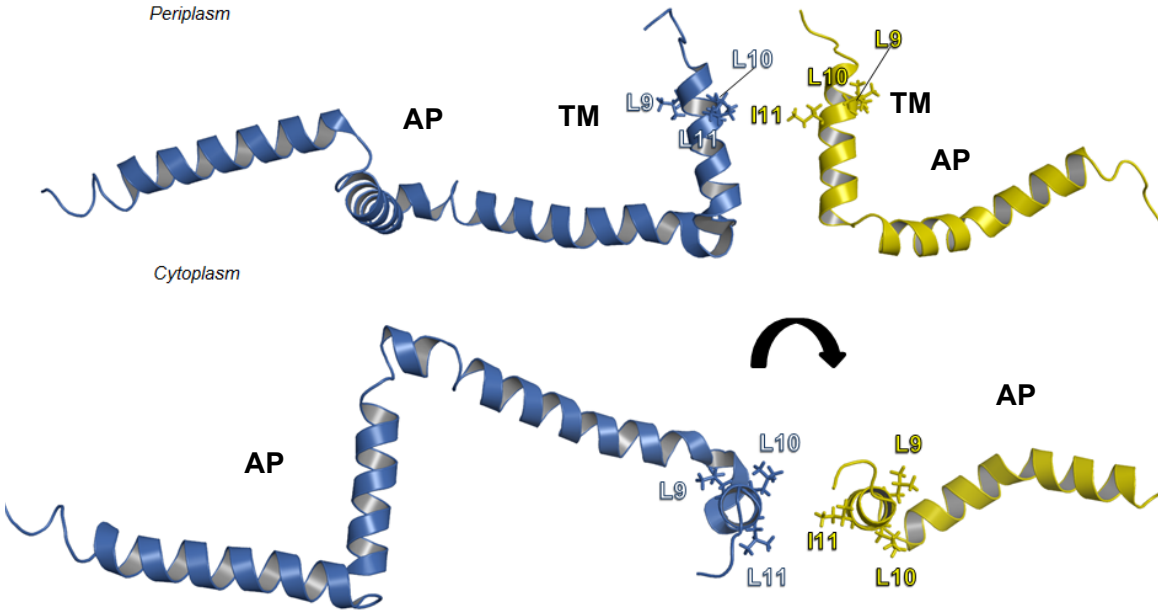

Figure 6.2) TatA and TatB residues which will be examined for interactions *via* disulphide crosslinking- TatB structure is shown in blue with residues L9C, L10C and I11C shown as sticks in the transmembrane helix, along with equivalent residues L9C, L10C and I11C in TatA (yellow). TM- transmembrane helix, AP- amphipathic helix.

6.2 Aims:

The aim of the work in this chapter is to build upon the TatA-TatC interactions observed *in vivo* with medium copy number expression levels by repeating the experiments with protein expressed from low copy number vectors under conditions much closer to that found in nature. The interaction of Tat with the constitutive site at TatC TM6 will be examined, along with the accompanying movement of TatA from TatC TM6 to TM5, in response to the overexpression of a native Tat substrate. The PMF dependence of TatA interacting at TatC TM6 will also be probed with expression at a low copy number. Finally, potential sites of TatA-TatB interaction will be investigated.

6.3 Results

6.3.1 Cys substitutions used in this work do not abolish Tat activity

In Chapter 4, Section 4.3.2, TatA and TatC Cys-substitutions were analysed to see whether they could support an active Tat translocase. Each of the substitutions yielded functional protein, however, as discussed above, the levels at which variant Tat proteins are produced can affect their activity. Therefore, the Tat-dependent growth assays performed in Chapter 4 were repeated for the Cys variants produced at low copy number. Table 6.1 shows that each of the constructs were able to support growth in the presence of 2% SDS and anaerobically on M9/TMAO minimal medium, indicating that they retained Tat function.

Table 6.1) Cys substitutions in TatA, TatB and TatC do not abolish Tat activity- *E. coli* strain DADE (Δ*tatABCD,* Δ*tatE*) harbouring pTH19 only, or pTH19 encoding TatA, TatB and TatC with the indicated Cys substitutions was scored for growth by spotting 5 µL cells at OD_{600} 0.01 onto LB-agar containing 2% SDS or M9-glycerol-TMAO. The LB-SDS plates were incubated aerobically and the M9-glycerol-TMAO plates anaerobically for 24 hours before analysis. "+" denotes positive growth, "-" denotes no growth.

Cys substitution		2% SDS	M9/TMAO/ Glycerol	Cys substitution		2% SDS	M9/TMAO/ Glycerol
TatA	TatC			TatA	TatB		
Wild type		+	+	L9C	L9C	+	+
Empty pTH19 vector		-	-	L9C	L10C	+	+
L9C	M205C	+	+	L9C	L11C	+	+
L9C	L206C	+	+	L10C	L9C	+	+
L9C	V212C	+	+	L10C	L10C	+	+
L9C	F213C	+	+	L10C	L11C	+	+
L10C	M205C	+	+	I11C	L9C	+	+
L10C	L206C	+	+	I11C	L10C	+	+
L10C	V212C	+	+	I11C	L11C	+	+
L10C	F213C	+	+				
I11C	M205C	+	+				
I11C	L206C	+	+				
I11C	V212C	+	+				
I11C	F213C	+	+				

6.3.2 TatA maintains interactions at TatC TM6 with protein expression at a low copy number

Chapter 4, Section 4.3.3.1 demonstrated that residue L9C in TatA could crosslink to TatC F213C, and weaker interactions were also observed through TatA L10C with TatC V212C and through TatA I11C with both TatC F213C and V212C (Chapter 4, Section 4.3.3.1 and 4.3.3.2). To validate these findings with low copy number protein expression, Cys substitutions in the TatA transmembrane helix L9C, L10C and I11C were crosslinked separately with TatC F213C and V212C. Cys substituted TatA and TatC proteins were encoded with wild type TatB on pTat101 vectors described in Section 6.1.2. To compensate for a reduced amount of protein using vectors with low copy number expression, 25 mL cultures of cells were used for crosslinking (as opposed to 2.5 mL with medium copy number expression). As in Chapter 4, cells were grown until OD_{600} 0.3 and three separate aliquots were withdrawn and diluted by addition of an equivalent volume of fresh LB, one of which was treated with 1.8 mM copper phenanthroline and one with 10 mM DTT each for one minute, while the third aliquot was left untreated. Samples were subsequently incubated with N-ethylmaleimide to cap all remaining free disulphides. Unlike crosslinking protocols with medium copy number protein expression, in which whole cell samples were loaded directly onto SDS-PAGE, for low copy expression, membrane fractions were isolated from cells after crosslinking occurred to enrich samples and obtain a better signal on Western blots.

6.3.2.1 TatA L9C interacts with TatC F213C at TatC TM6 *in vivo* with expression from low copy number constructs

Firstly, crosslinking of TatA L9C, L10C and I11C with TatC F213C in cells containing endogenous substrate was examined. Fig. 6.3A clearly demonstrates that on anti-TatC Western blots, a heterodimer band at ~37 kDa was detected for TatA L9C crosslinked through TatC F213C. As a band migrating ~37 kDa was not observed under control or reducing conditions, this indicates that it represents a disulphide link. A direct comparison of the relative intensity between the TatA-TatC heterodimer band linked

through TatA L9C with TatC F213C and TatC homodimer band linked through F213C, with medium copy number expression (Chapter 4, Fig 4.5A) and with low copy number expression in Fig 6.3A demonstrates that from low copy number vectors, the TatA-TatC crosslink is weaker than the TatC homodimer. This may be explained by a higher fraction of Tat translocases at low copy number interacting with endogenous substrates produced by the cell.

With expression from medium copy number constructs a crosslink through TatA L10C to TatC F213C could not be detected (Chapter 4, Section 4.3.3.2), and this is also the case with low copy number expression in Fig 6.3A. Notably however, a crosslink through TatA I11C to TatC F213C which was weaker than that observed through TatA

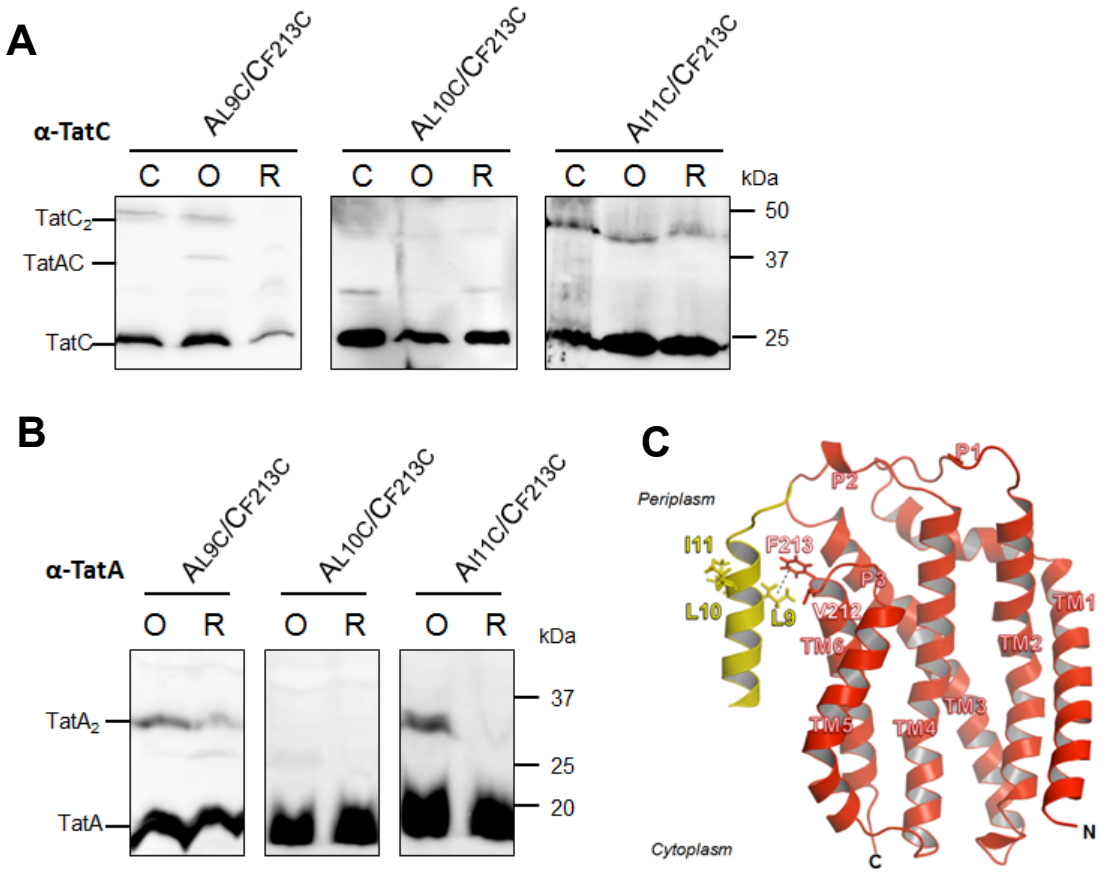

Figure 6.3) TatA L9C interacts with F213C *in vivo* A- Anti-TatC Western blots performed on isolated membrane fractions from *E. coli* strain DADE (Δ*tatABCD,* Δ*tatE*) harbouring pTat101 producing wild type TatB along with the indicated Cys substitutions in TatA and TatC, after exposure to experimental conditions *in vivo* noted by "C"-corresponding to control cells which were untreated, "O"- cells were oxidised with 1.8 mM copper phenanthroline for 1 min and "R"- cells were treated with 10 mM of the reductant DTT for 1 min. The positions of the TatC monomer, TatC dimer and TatAC heterodimer are indicated. **B-** Anti-TatA Western blots of samples from "O" and "R" from **A**. Loading volume in each case was 5 µL. **C-** denotes positions of Cys substitutions in TatC examined in this experiment.

L9C to TatC F213C (Chapter 4, Section 4.3.3.3) could not be detected with low copy number expression in Fig. 6.3A, suggesting that the interaction is either too weak to be detected, or is artefactual due to the high levels of protein from medium copy number vectors.

TatC homodimerisation through F213C was present with all three Cys substitutions in TatA in Fig 6.3A, with a population present in all control, oxidised and reduced samples (with the exception of the reduced lane of TatA L9C crosslinked to TatC F213C). This self-interaction indicates the favourability of this disulphide linkage as seen throughout Chapter 4, when expressed from medium copy number constructs, which is unsurprising given the proximity of F213 to the oxidising periplasm (Section 6.1.1, Fig. 6.1).

Fig 6.3B shows that the TatA-TatC heterodimer linking TatA L9C and TatC F213C could not be detected with anti-TatA antibodies (TatA is in great excess of TatC, meaning subpopulations associated with TatC are much more difficult to detect as discussed in Chapter 4). Given that the band on anti-TatA Western blots denoting a TatA-TatC interaction linked through TatA L9C and TatC F213C at ~37 kDa can be seen weakly relative to the corresponding anti-TatC Western blots with expression at a medium copy number (Chapter, Section 4.3.3.1, Fig 4.5D), it is likely the absence of the band with low copy number expression is due to the sensitivity of the Western blotting method. It is notable that TatA homodimer bands were more intense with TatA self-crosslinks through TatA L9C and I11C, when compared to TatA L10C. A similar result was obtained with medium copy number expression (Chapter 4, Sections 4.3.3.1-4.3.3.3) and is in line with TatA crosslinks *in vitro* in Greene *et al*. (2007), who found more favourable TatA homodimer formation through L9C than L10C under oxidising conditions.

It should be noted that a band in the oxidised fractions on anti-TatA Western blots migrating at a higher molecular weight than the TatA-TatC heterodimer was observed

with medium copy number expression of the Tat proteins, and was proposed to be a TatA oligomer conserved on SDS PAGE (Chapter 4, Section 4.3.3.1). This was not detected at low copy number expression.

6.3.2.2 No crosslinks are observed through TatA L9C, L10C or I11C to TatC V212C *in vivo* with expression from low copy number constructs

In Chapter 4, weak crosslinks between Cys residues at L10 and I11 in the TatA transmembrane helix with TatC V212C were seen. At low copy number expression, no detectable interaction between TatA L10C and TatC V212C was observed (Fig. 6.4A).

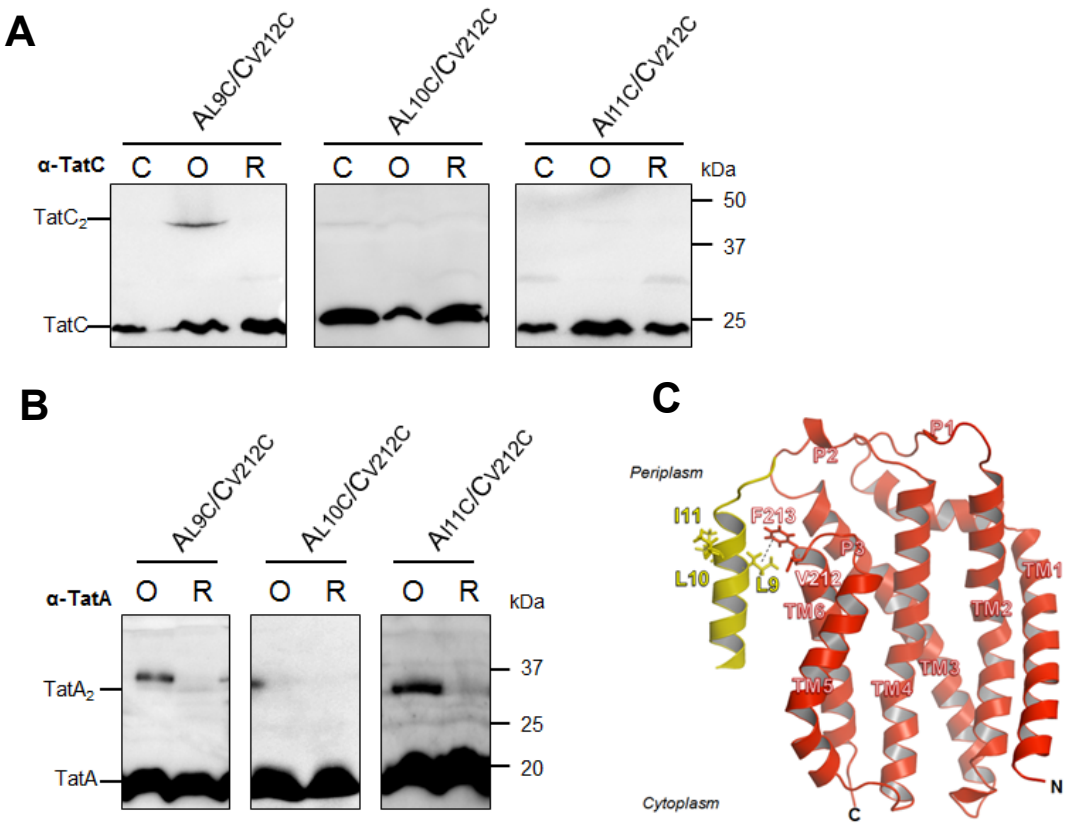

Figure 6.4) TatA L9C, L10 and I11 do not interact with V212C *in vivo*- A- Anti-TatC Western blots performed on isolated membrane fractions from *E. coli* strain DADE (Δ*tatABCD,* Δ*tatE*) harbouring pTat101 producing wild type TatB along with the indicated Cys substitutions in TatA and TatC, after exposure to experimental conditions *in vivo* noted by "C"-corresponding to control cells which were untreated, "O"- cells were oxidised with 1.8 mM copper phenanthroline for 1 min and "R"- cells were treated with 10 mM of the reductant DTT for 1 min. The positions of the TatC monomer, TatC dimer and TatAC heterodimer are indicated. **B-** Anti-TatA Western blots of samples from "O" and "R" from **A**. Loading volume in each case was 5 µL. **C-** denotes positions of Cys substitutions in TatC examined in this experiment.

Likewise, no crosslink between TatA I11C to TatC V212C was detected Fig. 6.4A. As expected, no TatA-TatC crosslink was detected through TatA L9C and TatC V212C, in agreement with the lack of crosslinking at these residues for medium copy number expression. No TatA-TatC heterodimer band at ~37 kDa was detected on the corresponding anti-TatA Western blots in Fig. 6.4B. It can be concluded that TatA-TatC interactions previously detected at the extreme C-terminal region of the P3 loop are either weak or artefactual due to high copy number expression.

6.3.3 TatA L9, L10 and I11 do not associate with M205C or L206C in TatC TM5 *in vivo* at low copy number expression

It was seen in Chapter 4 that no TatA-TatC crosslinks were detected between the transmembrane helix of TatA and TM5 of TatC when TatB was present. These previous findings are fully supported at low copy number expression level as Figs. 6.5 and 6.6 show no detectable crosslink between any of TatA L9C, L10C and I11C with TatC M205C or L206C in either the anti-TatC or the anti-TatA blots. It is interesting to note that TatC homodimers linked though M205C were detected in all conditions in anti-TatC formation through TatC M205C under similar conditions *in vivo* with wild type TatA was not seen. It cannot be ruled out that the NEM capping of free Cys residues was not complete, leaving TatC M205C free to self-crosslink, especially if TatA is lost from the complex Western blots in Fig. 6.5A yet Cleon *et al.* (2015) reported that homodimer during the membrane preparation stage (note that Chapter 5, Section 5.3.8 and 5.3.9 demonstrated no TatA crosslinking at TM5 or TM6 of TatC after PMF dissipation with indole). Given that the homodimer can be seen under reducing conditions this crosslink may form after DTT is removed in the cell fractionation step.

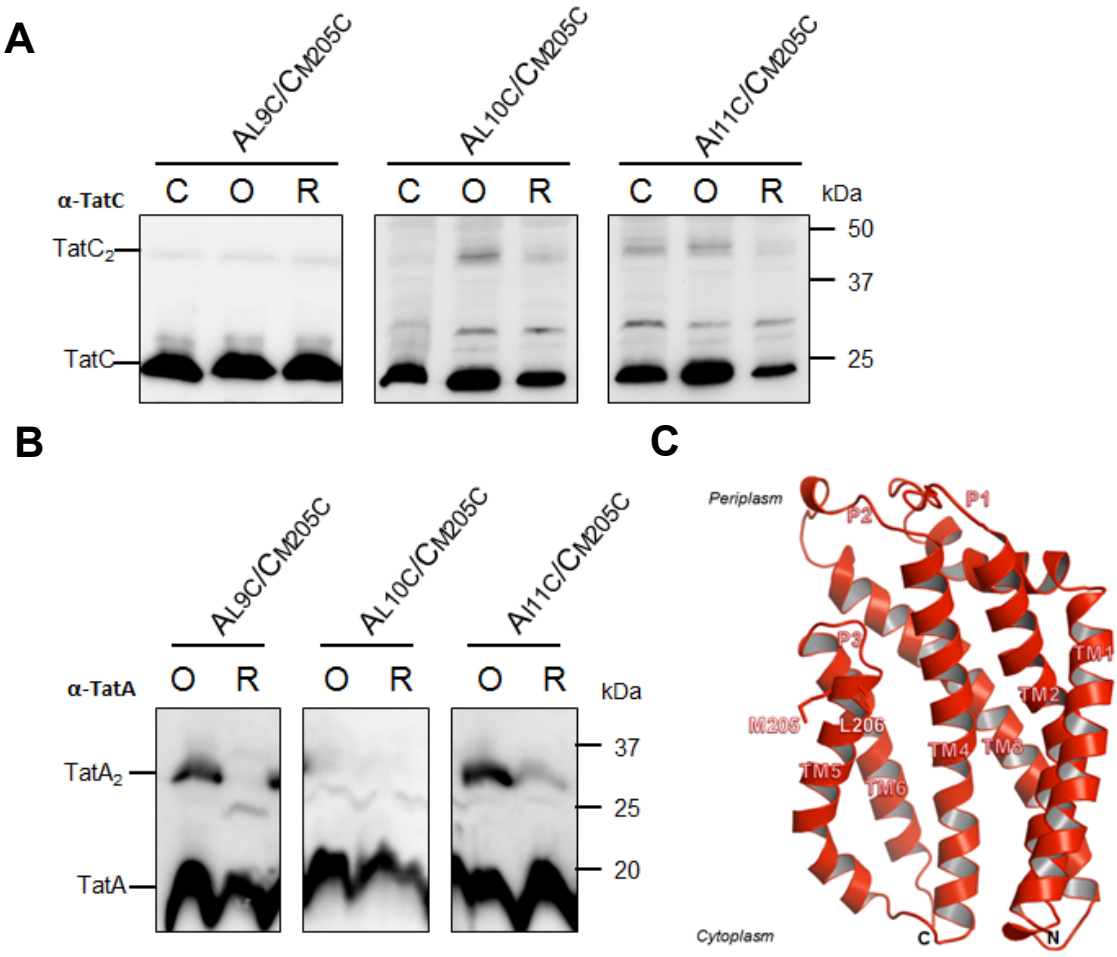

Figure 6.5) TatA L9C, L10 and I11 do not interact with M205C *in vivo*- A- Anti-TatC Western blots performed on isolated membrane fractions from *E. coli* strain DADE (Δ*tatABCD,* Δ*tatE*) harbouring pTat101 producing wild type TatB along with the indicated Cys substitutions in TatA and TatC, after exposure to experimental conditions *in vivo* noted by "C"-corresponding to control cells which were untreated, "O"- cells were oxidised with 1.8 mM copper phenanthroline for 1 min and "R"- cells were treated with 10 mM of the reductant DTT for 1 min. The positions of the TatC monomer, TatC dimer and TatAC heterodimer are indicated. **B-** Anti-TatA Western blots of samples from "O" and "R" from **A**. Loading volume in each case was 5 µL. **C-** denotes positions of Cys substitutions in TatC examined in this experiment.

Homodimerisation through TatC L206C is either not present or very weak (Fig. 6.6A) and may reveal that this residue is in less of a position to associate with equivalent residues in other TatC subunits, perhaps indicating an interaction with another component.

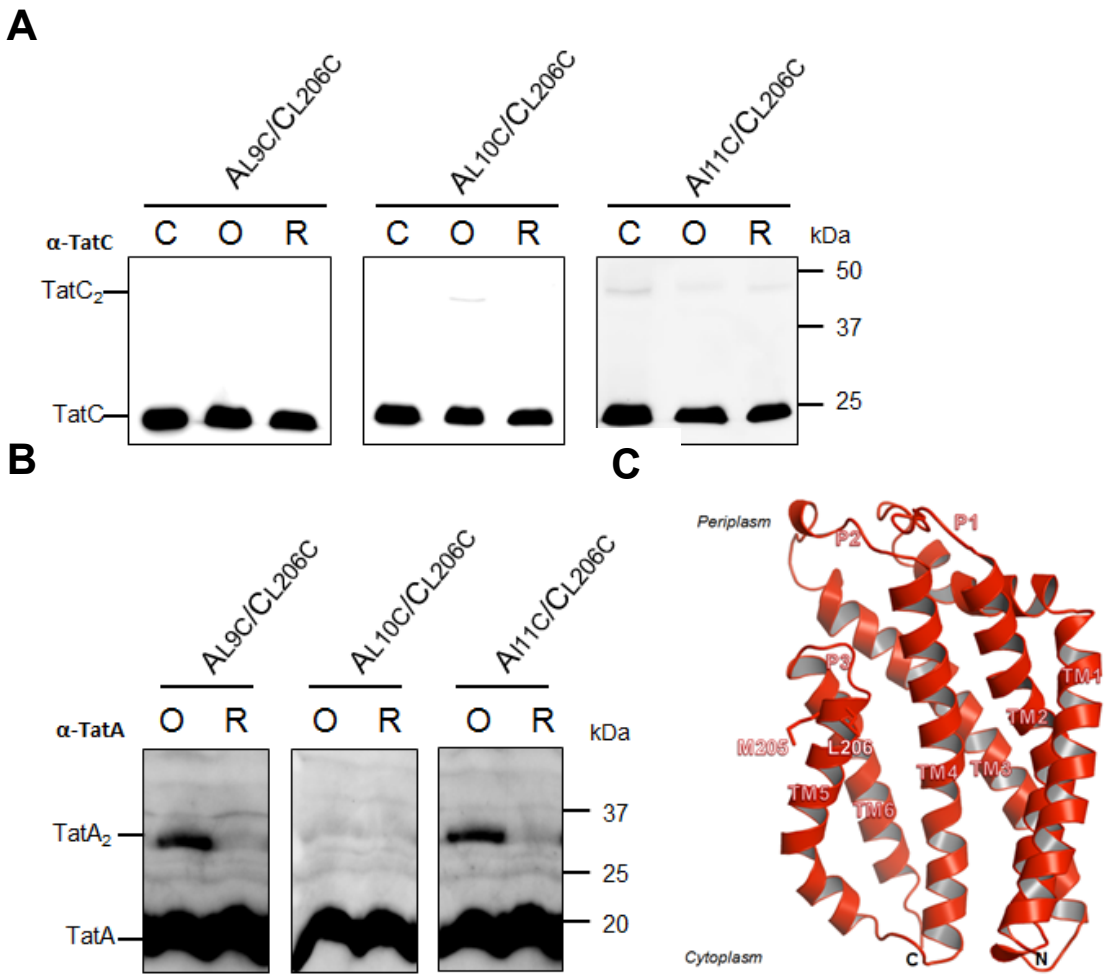

Figure 6.6) TatA L9C, L10 and I11 do not interact with L206C *in vivo*- A- Anti-TatC Western blots performed on isolated membrane fractions from *E. coli* strain DADE (Δ*tatABCD,* Δ*tatE*) harbouring pTat101 producing wild type TatB along with the indicated Cys substitutions in TatA and TatC, after exposure to experimental conditions *in vivo* noted by "C"-corresponding to control cells which were untreated, "O"- cells were oxidised with 1.8 mM copper phenanthroline for 1 min and "R"- cells were treated with 10 mM of the reductant DTT for 1 min. The positions of the TatC monomer, TatC dimer and TatAC heterodimer are indicated. **B-** Anti-TatA Western blots of samples from "O" and "R" from **A**. Loading volume in each case was 5 µL. **C-** denotes positions of Cys substitutions in TatC examined in this experiment.

6.3.4 TatA interacts constitutively with TatC TM6 with low copy number expression

Work in Chapter 5 demonstrated that the Cys crosslink between TatA L9C and TatC F213C at the periplasmic facing part of TM6 was maintained when TatC was unable to bind substrate, i.e. when the Tat system was in the resting state (Chapter 5, Section 5.3.5). Using the formation of this crosslink in the Tat resting state as a diagnosis for constitutive TatA interactions, the following section will examine whether the same

behaviour is seen at low copy number protein expression. Furthermore, interactions between TatA and TatC TM5 in the resting state will be also examined, where crosslinking at with medium copy number expression found no interaction (Chapter 5, Section 5.3.5).

6.3.4.1 TatA L9C crosslinks TatC F213C the TM6 in the resting state *in vivo*

To examine constitutive interactions in the Tat translocase, the mutations F94A and E103A were introduced into TatC to prevent substrate binding (as outlined in Chapter 5, Section 5.3.5). Crosslinking analysis of TatA L9C to TatC F213C at the proposed TatA constitutive site (Fig. 6.7) demonstrates a clear band migrating at ~37 kDa corresponding to a TatA-TatC heterodimer which was not present under control or reduced conditions and which is detectable on anti-TatC and, faintly, on anti-TatA Western blots. This is in full agreement with observations made with medium copy number expression (Chapter 5, Section 5.3.5).

Comparison of anti-TatC Western blots in Fig 6.3A with Fig 6.7 demonstrates that the ratio of TatA-TatC heterodimer and TatC-TatC homodimer changes to favour TatA-TatC interactions in the resting state (as opposed to Tat systems able to bind endogenous substrate) further showing that TatA movement away from its constitutive site and increasing TatC homodimerisation is influenced by substrate. It is also notable that the higher molecular weight band on anti-TatA Western blots, migrating above the TatA-TatC heterodimer (thought to correspond to TatA oligomers, Chapter 4, Section 4.3.3.1), was present, while it was either absent or extremely weak when crosslinking without the TatC F94A/E103A substitutions (Chapter 4, Section, 4.3.3.1-4.3.3.3 and Sections 6.3.2.1-6.3.2.2).

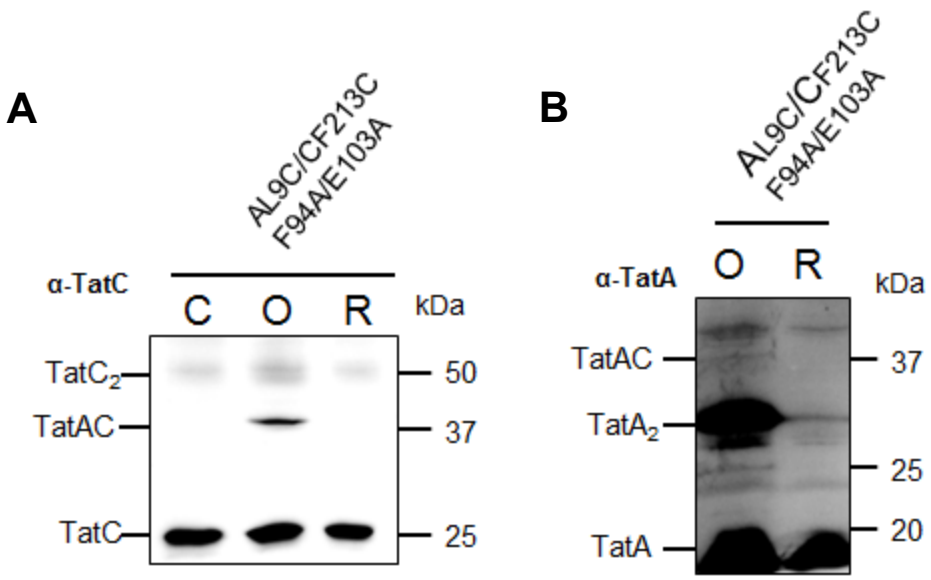

Figure 6.7) TatA L9C crosslinks with TatC F94A, E103A, F213C when expressed from low copy number vectors – A and **B** show anti-TatC/anti-TatA Western blots (as indicated) of isolated membrane fractions *E. coli* strain DADE (Δ*tatABCD*, Δ*tatE*) harbouring pTat101 expressing wild type TatB, TatA L9C and TatC F213C with the F94A and E103A substitutions. Prior to membrane fractionation, cells were O- oxidised with 1.8 mM copper phenanthroline, C- untreated or R- treated with 10 mM of the reductant DTT for 1 min. Loading volume in each case was 5 µL.

6.3.4.2 TatA L9C does not crosslink TatC M205C in TM5 *in vivo* in the resting state

Chapter 5, Section 5.3.5 demonstrated that TatA L9C could not crosslink TatC M205C also harbouring the F94A/E103A substitutions at medium copy number expression, indicating that TatA was unlikely to occupy the TatB constitutive site at TM5 in the resting state. Unsurprisingly, no interactions were observed with very low copy number expression when TatA L9C was oxidised alongside TatC M205C, with no bands corresponding to the size of a TatA-TatC heterodimer on anti-TatC or anti-TatA Western blots (Fig 6.8). As expected no TatC homodimers could be detected that formed through M205C the resting state, further confirming that homodimersation observed in Section 6.3.3 is likely due to endogenous substrate.

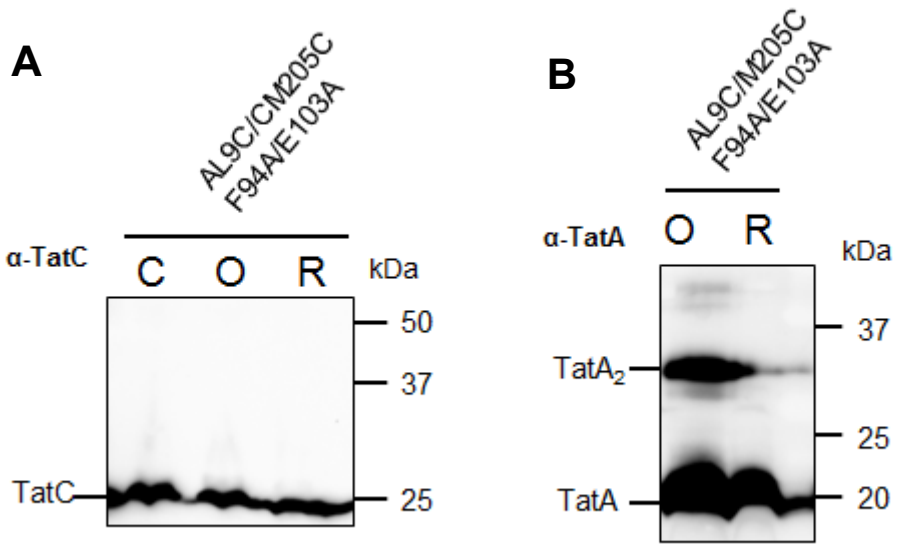

Figure 6.8) TatA L9C does not crosslink with TatC F94A, E103A, F213C at low copy number expression- A and **B** show anti-TatC/anti-TatA Western blots (as indicated) of isolated membrane fractions *E. coli* strain DADE (Δ*tatABCD*, Δ*tatE*) harbouring pTat101 expressing wild type TatB, TatA L9C and TatC M205C with the F94A and E103A substitutions. Cells were O- oxidised with 1.8 mM copper phenanthroline, C**-** untreated or R**-** treated with 10 mM of the reductant DTT for 1 min. Loading volume in each case was 5 µL.

6.3.5 TatA vacates its constitutive site at TatC TM6 and moves to TM5 at low copy number expression in the presence of overexpressed substrate

The work in Chapter 5, Section 5.3.6, found that the crosslink between TatA L9C and TatC F213C decreased in intensity on anti-TatC Western blots in response to substrate overexpression, indicating that TatA may be vacating this site. This was accompanied by an increase in TatA-TatC heterodimer intensity through TatA L9C crosslinked to TatC M205C at TM5 with overexpressed substrate, indicating a potential movement of TatA to occupy the TatB constitutive site. In those experiments, the Tat proteins were expressed from medium copy number vectors, and the substrate used was an artificial Tat substrate comprising GFP fused to the TorA signal sequence.

To validate these findings, low copy number expression of Tat proteins was used, alongside an overexpressed native Tat substrate. The substrate chosen was CueO, a multi-copper oxidase, which has been utilised previously in fluorescence microscopy experiments where TatA was found to form fluorescent clusters when it was

overexpressed (Alcock *et al.,* 2013), and in disulphide crosslinking experiments (Cleon *et al*., 2015). Crosslinking was performed as before using residues L9C, L10C and I11C in the transmembrane helix of TatA and each of; TatC F213C at TM6 to analyse potential constitutive TatA-TatC interactions, and TatC M205C to analyse interactions at the TatB constitutive site, each in the presence of overproduced His-tagged CueO (CueOH). For CueO expression, 1 mM IPTG was included during growth of cells and *in vivo* crosslinking was performed as in Section 6.3.2.1.

6.3.5.1 TatA L9C crosslinks to TatC F213C at TatC TM6 are greatly decreased with low copy number protein expression and overexpressed substrate

Fig. 6.9A demonstrates that when Tat substrate CueOH was overexpressed, the heterodimeric crosslink between TatA L9C and TatC F213C was extremely faint on the anti-TatC Western blots, accompanied by a large increase in the amount of TatC homodimer (compare Fig 6.9 with Figs. 6.3 and 6.7). With medium copy number expression in Chapter 5, TatA L10C and I11C crosslinks with F213C were not tested with overexpressed substrate, however, Fig. 6.9A demonstrates that with low copy number expression of Tat proteins and overexpressed CueOH, TatA-TatC heterodimers were not detected, though increased TatC homodimerisation was observed compared to conditions with endogenous substrate (Sections 6.3.2.2 and 6.3.2.3). Corresponding anti-TatA Western blots in Fig 6.9B demonstrate TatA homodimerisation was similar to that seen without overexpressed CueOH (Fig. 6.3B), with favourable homodimer interactions through TatA L9C and I11C and no TatA-TatC heterodimer band at ~37 kDa present, as expected.

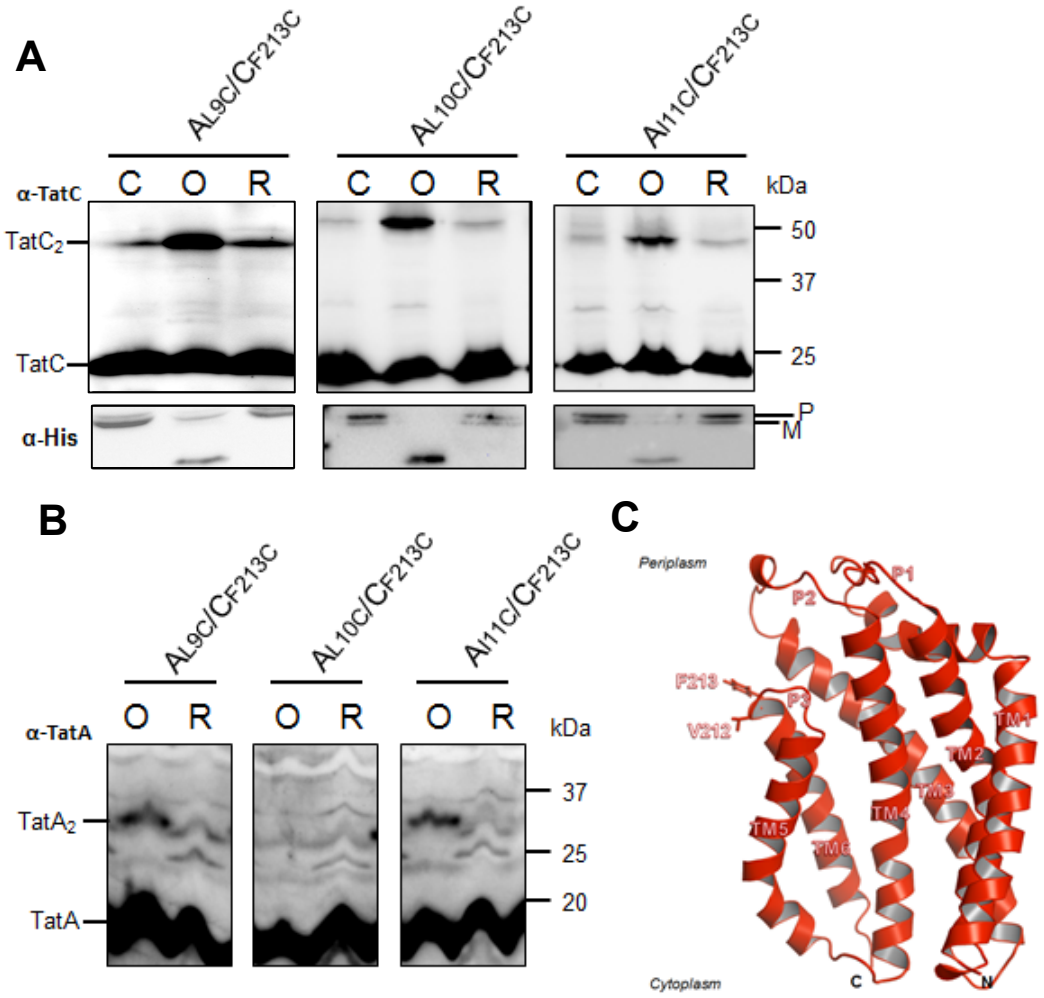

Figure 6.9) TatA L9C, L10 and I11 do not interact with F213C *in vivo* with overexpressed CueOH - A- Anti-TatC Western blots performed on isolated membrane fractions from *E. coli* strain DADE (Δ*tatABCD,* Δ*tatE*) harbouring pTat101 producing wild type TatB along with the indicated Cys substitutions in TatA and TatC alongside His-Tagged CueO produced from pQE80 after exposure to experimental conditions *in vivo* noted by "C"-corresponding to control cells which were untreated, "O"-cells were oxidised with 1.8 mM copper phenanthroline for 1 min and "R"- cells were treated with 10 mM of the reductant DTT for 1 min. The positions of the TatC monomer, TatC dimer and TatAC heterodimer are indicated. Anti-His Western blots are shown corresponding to the soluble fraction following the membrane fractionation of each sample, showing "p" precursor and "m" mature forms of CueOH. **B-** Anti-TatA Western blots of samples from "O" and "R" from **A**. Loading volume in each case was 5 µL. **C-** denotes positions of Cys substitutions in TatC examined in this experiment.

Anti-His Western blots (Fig. 6.9A, bottom panel) demonstrate that the signal sequence of CueOH (~3 kDa) was cleaved successfully, with the precursor and mature forms of the protein present. A clear band migrating at a lower molecular weight than both the precursor and mature forms of CueOH was found under oxidising conditions. This band was observed previously by Cleon *et al*. (2015) and is thought to result from an intra-disulphide link in the protein changing its migration pattern on SDS-PAGE.

These data support observations in Chapter 5, where overexpression of TorA-GFP

caused a similar decrease in interaction through TatA L9C and TatC F213C.

6.3.5.2 TatA L9C, L10C and I11C do not crosslink TatC V212C with low copy number in the presence of overexpressed substrate

Crosslinking of Cys residues in the TatA TM with TatC V212C at the C-terminal end of the P3 loop was not tested using medium copy number constructs in the presence of overexpressed substrate in Chapter 5, however TatA L10C and I11C were both found to crosslink this position TatC with endogenous substrate in Chapter 4, Sections 4.3.3.2 and 4.3.3.3. Fig 6.10A and B demonstrates that at low copy number expression, none of TatA L9C, L10C and I11C crosslinked with TatC V212C. TatC homodimerisation was clear with constructs expressing all three TatA Cys substitutions (Fig. 6.10A) indicating a propensity to homodimerise through V212C as was seen in Chapter 4, Sections 4.3.3.2-4.3.3.3. Again anti-His Western blots in Fig. 6.10A is indicative of CueO transport to the periplasm.

6.3.5.3 TatA crosslinks through L9C, L10C and I11C to M205C appear at low copy number in the presence of overexpressed substrate

Chapter 5, Section 5.3.7.3 demonstrated that TatA L9C - TatC M205C crosslinks appeared in response to overexpressed Tat substrate. From this, it was proposed that TatA was moving from its constitutive site to occupy the TatB constitutive site, presumably once TatB has moved, in response to Tat substrate overexpression. To confirm this interaction with low copy number expression of the Tat subunits and with a native Tat substrate, TatA L9C, L10C and I11C were crosslinked to TatC M205C with overexpressed CueOH as in Section 6.3.5.1. As clearly demonstrated in Fig 6.11A TatA-TatC interactions were detected in the presence of overexpressed CueOH through TatA L9C and I11C with TatC M205C, along with a weaker association through TatA L10C with a TatA-TatC heterodimer appearing at ~37 kDa under oxidising conditions. TatC homodimerisation was also notably increased through M205C with overexpressed CueOH (compare Fig. 6.5 with Fig. 6.11) as was observed by Cleon *et*

al. (2015) and in Chapter 5.

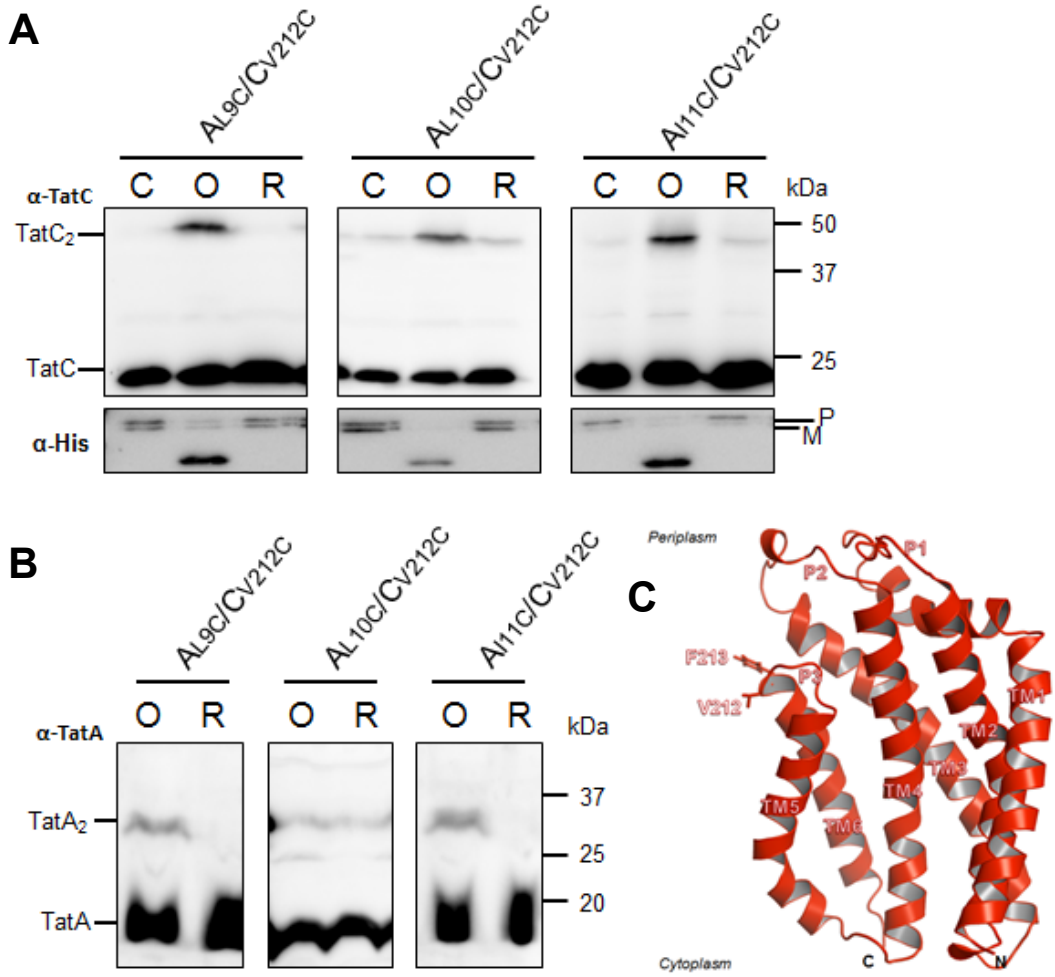

Figure 6.10) TatA L9C, L10 and I11 do not interact with V212C *in vivo* with overexpressed CueOH - A- Anti-TatC Western blots performed on isolated membrane fractions from *E. coli* strain DADE (Δ*tatABCD,* Δ*tatE*) harbouring pTat101 producing wild type TatB along with the indicated Cys substitutions in TatA and TatC alongside His-Tagged CueO produced from pQE80, after exposure to experimental conditions *in vivo* noted by "C"-corresponding to control cells which were untreated, "O"-cells were oxidised with 1.8 mM copper phenanthroline for 1 min and "R"- cells were treated with 10 mM of the reductant DTT for 1 min. The positions of the TatC monomer, TatC dimer and TatAC heterodimer are indicated. Anti-His Western blots are shown corresponding to the soluble fraction following the membrane fractionation of each sample, showing "p" precursor and "m" mature forms of CueOH. **B-** Anti-TatA Western blots of samples from "O" and "R" from **A**. Loading volume in each case was 5 µL. **C-** denotes positions of Cys substitutions in TatC examined in this experiment.

The corresponding TatA-TatC heterodimer band at ~37 kDa was not detected on anti-TatA Western blots in Fig 6.11B, which may be due to the sensitivity of the Western blotting method, as was found in Section 6.3.2.1 where the TatA-TatC heterodimer linked through TatA L9C and TatC F2123C could be detected on anti-TatC but not anti-TatA

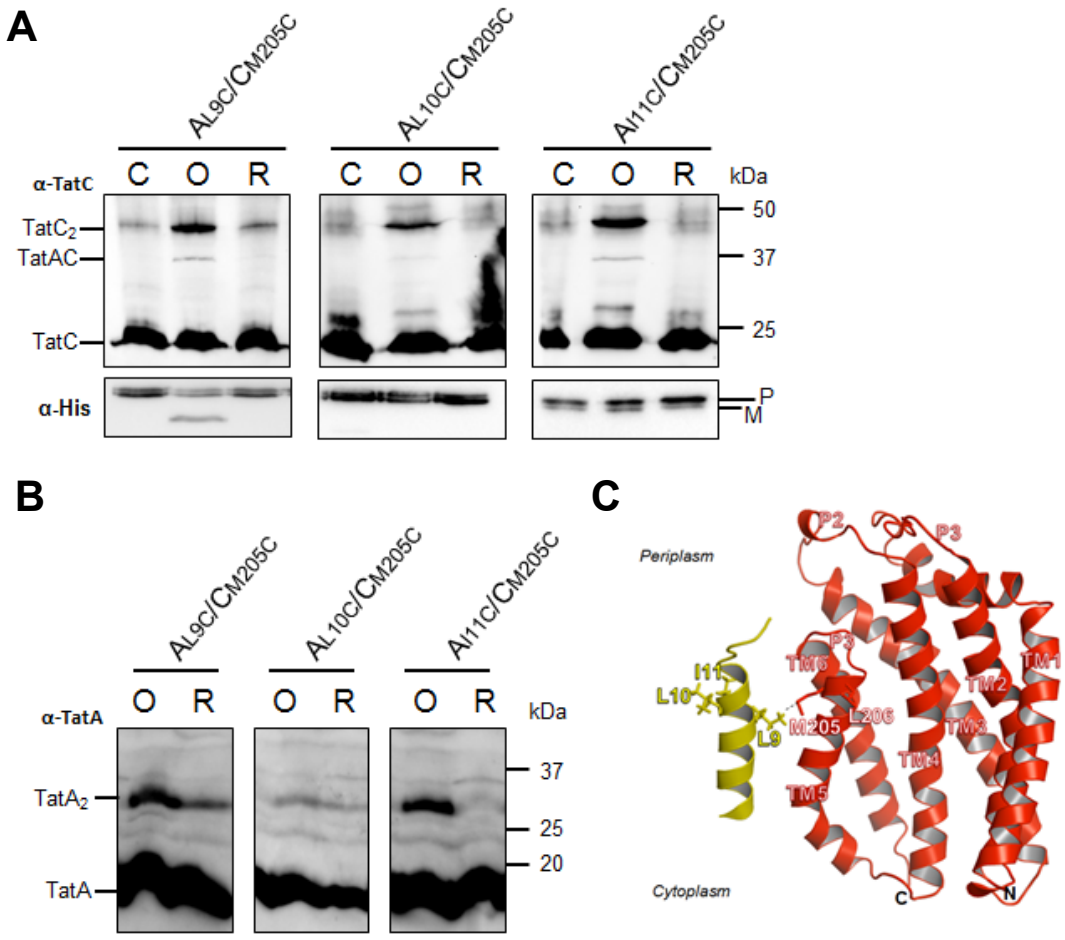

Figure 6.11) TatA L9C and I11 interact favourably with TatC M205C while TatA L10C interacts weakly *in vivo* with overexpressed CueOH- A- Anti-TatC Western blots performed on isolated membrane fractions from *E. coli* strain DADE (Δ*tatABCD,* Δ*tatE*) harbouring pTat101 producing wild type TatB along with the indicated Cys substitutions in TatA and TatC alongside His-Tagged CueO produced from pQE80, after exposure to experimental conditions *in vivo* noted by "C"-corresponding to control cells which were untreated, "O"- cells were oxidised with 1.8 mM copper phenanthroline for 1 min and "R"- cells were treated with 10 mM of the reductant DTT for 1 min. The positions of the TatC monomer, TatC dimer and TatAC heterodimer are indicated. Anti-His Western blots are shown corresponding to the soluble fraction following the membrane fractionation of each sample, showing "p" precursor and "m" mature forms of CueOH (His-tagged CueO) **B-** Anti-TatA Western blots of samples from "O" and "R" from **A**. Loading volume in each case was 5 µL. **C-** denotes positions of Cys substitutions in TatC examined in this experiment.

Western blots. Anti-His Western blots (Fig. 6.11A) demonstrated the presence of precursor and mature forms of CueOH.

The observations in this Section combined with data showing reduced crosslink intensity through TatA L9C and TatC F213C with overexpressed CueOH at the TM6 in Section 6.3.7.1, clearly demonstrates that at a low copy number with overexpressed substrate TatA may be moving from its constitutive site at TM6 to the TatB constitutive

site at TM5. Interestingly the crosslinking pattern between TatA L9C, L10C and I11C and TatC M205C is similar to that observed for disulphide crosslinking experiments with the equivalent conserved residues in TatB (L9, L10 and L11) crosslinking TatC M205C *in vitro* in Rollauer *et al*. (2012) suggesting it is differentially occupying the same site as TatB at TatC TM5.

6.3.5.4 TatA does not crosslink through L9C, L10C or I11C to L206C with low copy number expression and overexpressed substrate

Interactions between TatA L9C, L10C and I11C and TatC L206C were seen only when TatB was removed from the system and with medium copy number expression of the Tat proteins (Chapter 5, Sections 5.3.1-5.3.3). However TatA interactions were not tested at this position in TatC in the presence of overexpressed substrate, and given that Section 6.3.5.3 demonstrated TatA interactions with neighbouring TatC M205C in the presence of overexpressed substrate, it is conceivable that interaction may appear here under the same conditions.

Fig. 6.12 demonstrates that TatA L9C, L10C and I11C did not form detectable heterodimers with TatC L206C, indicating that TatA is not interacting here at low copy number expression and in the presence of overexpressed substrate. TatC homodimerisation through L206C (Fig. 6.12A) was weak compared to homodimerisation through M205C (Fig. 6.11), similar to observations at medium copy number expression in Chapter 4, and may allude to the presence of an interaction site which does not involve TatA or another TatC, which will be discussed further in Section 6.4.2. Multiple bands are present above the TatC homodimer on anti-TatC Western blots in Fig. 6.12A, especially in the presence of TatA I11C, which cannot be assigned. It is plausible that these correspond to non-specific interactions or perhaps different conformations of TatC.

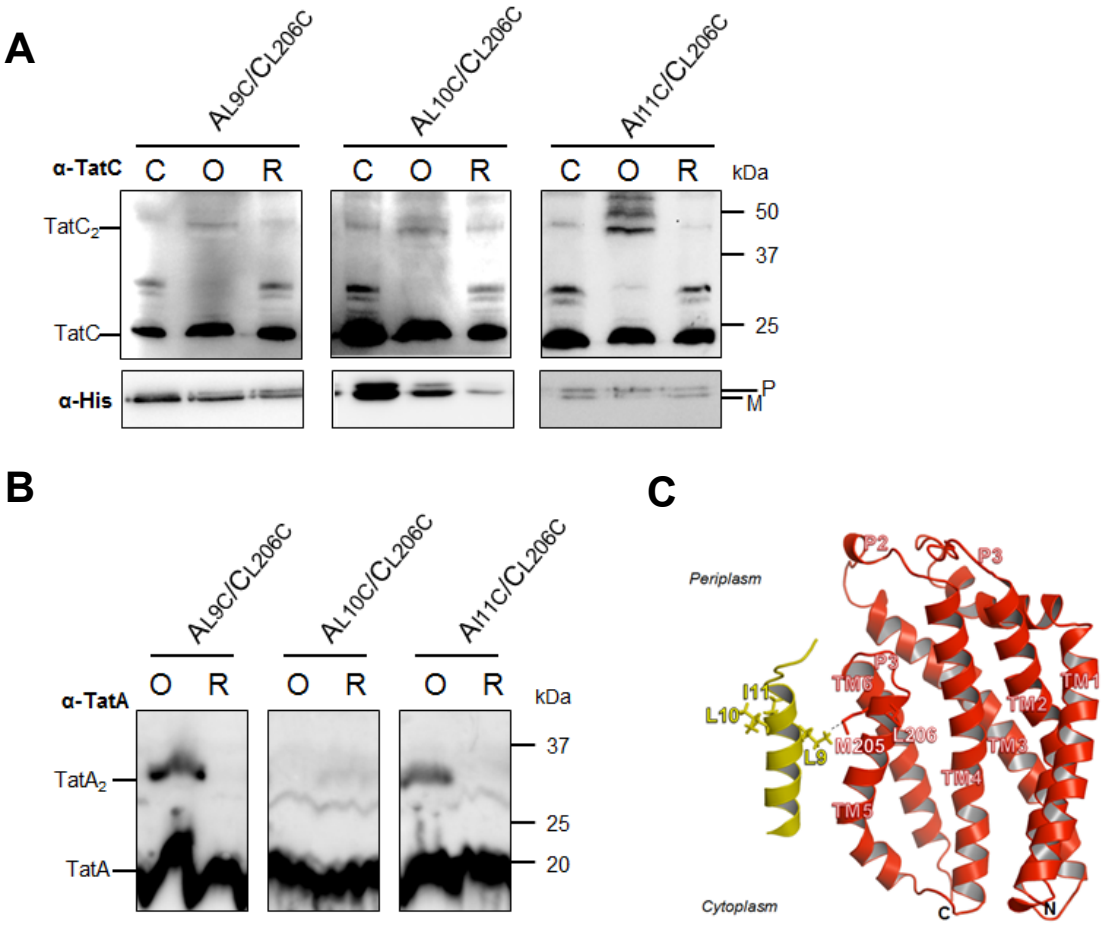

Figure 6.12) TatA L9C, L10 and I11 do not interact with TatCL206C *in vivo* with overexpressed CueOH- A- Anti-TatC Western blots performed on isolated membrane fractions from *E. coli* strain DADE (Δ*tatABCD,* Δ*tatE*) harbouring pTat101 producing wild type TatB along with the indicated Cys substitutions in TatA and TatC alongside His-Tagged CueO produced from pQE80, after exposure to experimental conditions *in vivo* noted by "C"-corresponding to control cells which were untreated, "O"- cells were oxidised with 1.8 mM copper phenanthroline for 1 min and "R"- cells were treated with 10 mM of the reductant DTT for 1 min. The positions of the TatC monomer, TatC dimer and TatAC heterodimer are indicated. Anti-His Western blots are shown corresponding to the soluble fraction following the membrane fractionation of each sample, showing "p" precurson and "m" mature forms of CueOH (His-tagged CueO) **B-** Anti-TatA Western blots of samples from "O" and "R" in **A-** to detect corresponding TatA-TatC heterodimer band at 37 kDa**.** Loading volume in each case was 5 µL. **C-** denotes positions of Cys substitutions in TatC examined in this experiment.

6.3.6 TatA vacates its constitutive binding site on TatC in response to PMF dissipation with indole with expression from low copy number vectors

Chapter 5, Section 5.3.8 previously demonstrated that with expression from medium copy number vectors, TatA may occupy its constitutive site at TatC TM6 in a PMF-dependent manner, as the TatA L9C crosslink to TatC F213C found *in vivo,* denoting interactions at the TatA constitutive site, was greatly diminished upon incubation with 5 mM of the uncoupler indole. TatA was also not found at TatC TM5 with dissipated

PMF,and it was therefore speculated to either change its interaction within the Tat complex or leave the Tat complex completely.

6.3.6.1 The TatA L9C crosslink to TatC F213C at TM6 is greatly diminished after PMF dissipation *in vivo*

Fig. 6.13 shows experiments similar to those performed with high copy number expression in Chapter 5, Section 5.3.8 with indole incubation, however here the Tat proteins are expressed at a low copy number as in Section 6.3.2.1. It can be seen on anti-TatC Western blots in Fig. 6.13A that the TatA-TatC heterodimer linked through TatA L9C and TatC F213C was present under oxidising conditions only, as was seen in Fig. 6.13A.

Upon PMF dissipation in the cells using 5 mM indole, the heterodimer was not seen after oxidation, as observed with medium copy number expression in Chapter 5. At medium copy expression this was accompanied by an increase in the amount of TatC homodimer (Section 5.3.8) and a similar pattern was also seen in Fig 6.13A. As expected, the TatA-TatC heterodimer band was restored after washing away the indole prior to oxidising. No corresponding heterodimer was observed on the anti-TatA Western blots with any of the conditions analysed (Fig. 6.13B), probably due to sensitivity issues.

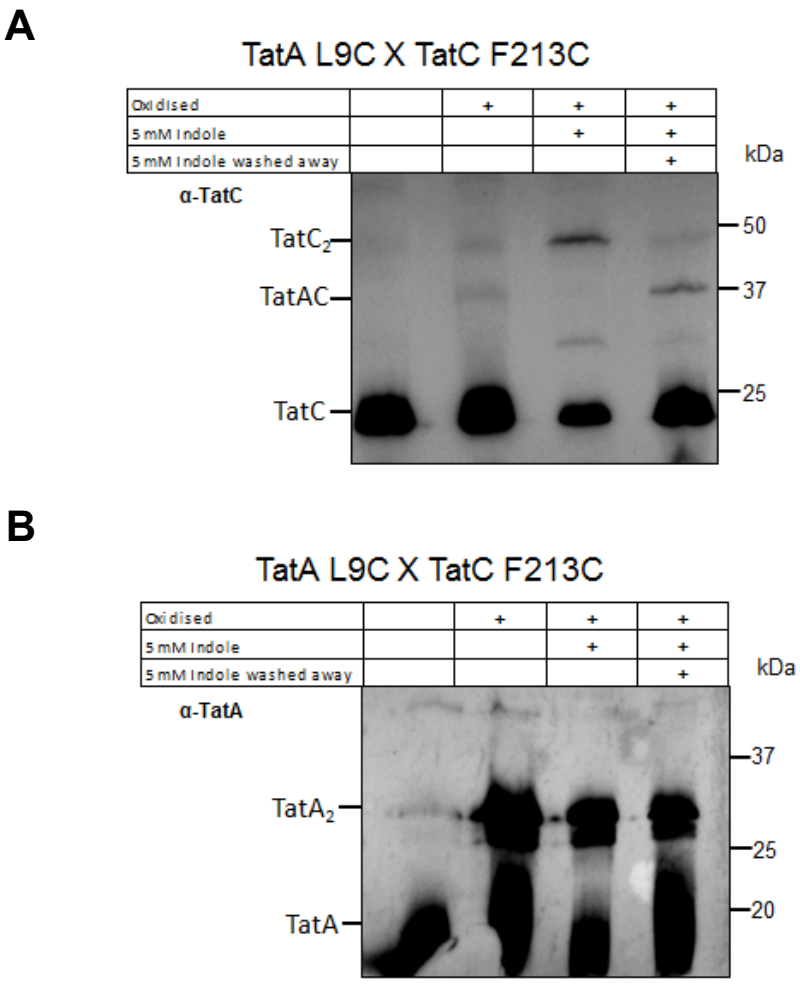

Figure 6.13) TatA vacates its constitutive site at TatC TM6 in response to PMF dissipation with 5 mM indole- A Anti-TatC or **B-** Anti-TatA Western blot of isolated membrane fractions from *E. coli* strain DADE (Δ*tatABCD*, Δ*tatE*) harbouring pTat101 expressing wild type TatB and Cys-substituted TatA L9C and TatC F213C. Cells, prior to isolation of the membrane fractions, were either untreated, oxidised with 1.8 mM copper phenanthroline for 1 min or incubated with 5 mM indole for 5 mins, followed by either a 1 min oxidation step or washed thoroughly to remove the indole followed by a 1 min oxidation step. Loading volume in each case was 5 µL.

6.3.6.2 TatA L9C does not crosslink TatC M205C after PMF dissipation *in vivo*

With expression from medium copy number constructs, TatA L9C did not crosslink with TatC M205C *in vivo* after PMF dissipation (Chapter 5, Section 5.3.8). At low copy number expression, no TatA L9C-TatC M205C heterodimer was detected, regardless of whether indole was present (Fig. 6.14). In the experiment in Fig 6.14A it was seen that the TatC homodimer appeared as a double band, in the presence of indole. This type of behaviour was not seen with TatC on other Western blots with indole incubation (*e.g.* Fig. 6.13) and it is difficult to determine whether it is merely a non-specific band or a manifestation of TatC behaviour.

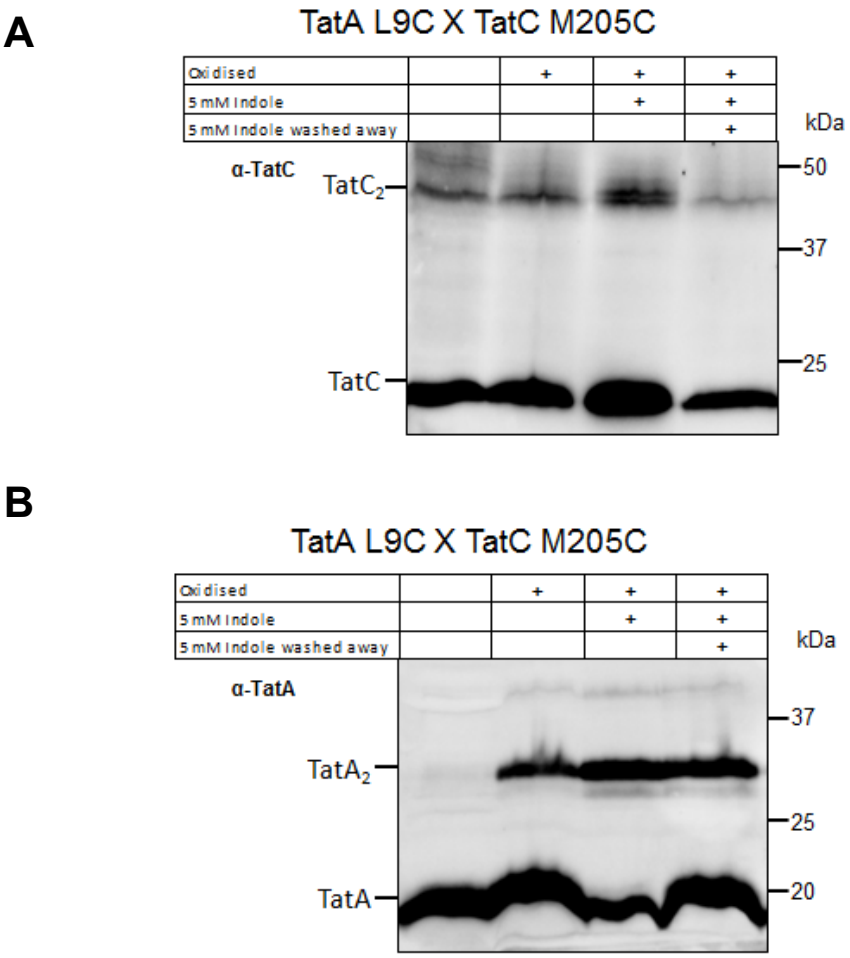

Figure 6.14) TatA does not interact with TatC TM5 in response to PMF dissipation with 5 mM indole- A Anti-TatC or **B-** Anti-TatA Western blot of isolated membrane fractions from *E. coli* strain DADE (Δ*tatABCD*, Δ*tatE*) harbouring pTat101 expressing wild type TatB and Cys-substituted TatA L9C and TatC M205C. Cells, prior to isolation of the membrane fractions, were either untreated, oxidised with 1.8 mM copper phenanthroline for 1 min or incubated with 5 mM indole for 5 mins, followed by either a 1 min oxidation step or washed thoroughly to remove the indole followed by a 1 min oxidation step. Loading volume in each case was 5 µL.

6.3.7 Assessing TatA-TatB interactions by disulphide crosslinking *in vivo*

As discussed in Section 6.1.3, to assess whether crosslinks could be detected between the transmembrane helices of TatA and TatB, crosslinking reactions were carried out using substitutions L9C, L10C and I11C in the TM of TatA with equivalent residues L9C, L10C and L11C in the TM of TatB as described in Sections 6.3.2.1, except in this case Western blot analysis used antibodies raised against TatA and TatB to identify potential heterodimer formation.

6.3.7.1 TatA L9C does not crosslink to TatB L9C, L10C or L11C *in vivo* with endogenous substrate levels

Examining anti-TatB Western blots in Fig. 6.15A, when TatA L9C is present alongside it would be expected to migrate just above 37 kDa (an estimation based on the combined apparent molecular weight of the monomers on SDS-PAGE). This is also the case when TatA L9C was present alongside TatB L10C or I11C in Fig. 6.15A.

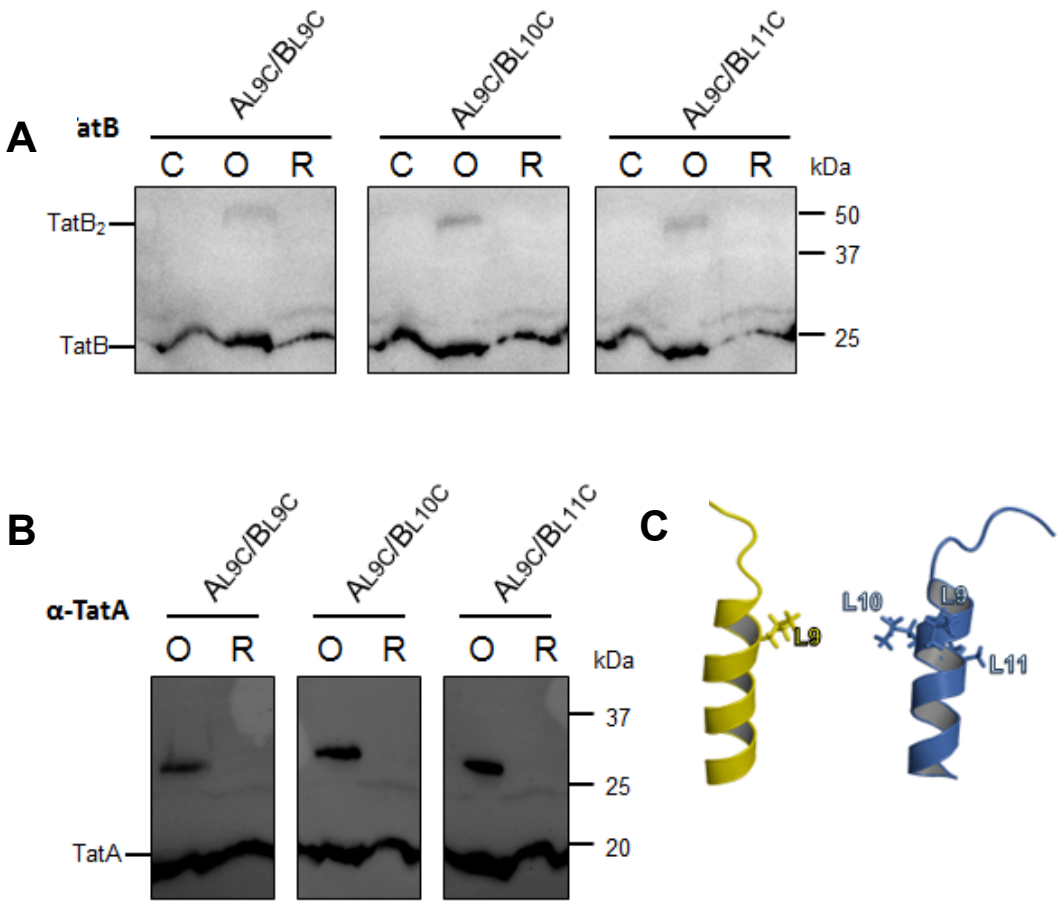

Figure 6.15) TatA L9C does not interact with TatB L9C, L10C or L11C *in vivo* with endogenous substrate– A- Anti-TatB Western blots performed on isolated membrane fractions from *E. coli* strain DADE (Δ*tatABCD,* Δ*tatE*) harbouring pTat101 producing Cysless TatC along with the indicated Cys substitutions in TatA and TatB, after exposure to experimental conditions *in vivo* noted by "C"- corresponding to control cells which were untreated, "O"- cells were oxidised with 1.8 mM copper phenanthroline for 1 min and "R"- cells were treated with 10 mM of the reductant DTT for 1 min. The positions of the TatB monomer and TatB homodimer are indicated. **B-** Anti-TatA Western blots of samples from "O" and "R" in **A**. Loading volume in each case was 5 µL. **C-** denotes positions of Cys substitutions in TatA and TatB examined in this experiment.

Faint TatB homodimer bands were seen under oxidising conditions at ~50 kDa through all Cys substitutions tested in TatB. This is consistent with observations in Lee *et al*.

(2006), whereby *in vitro* disulphide crosslinking of TatB gave homodimers through all three of these Cys substitutions. A double band was detected for the TatB monomer, with an upper fainter band that seems more prominent in untreated and reducing conditions and may reflect different conformations of TatB *in vivo*. As expected, TatA homodimers were detected under oxidising conditions for all samples (Fig 6.15B).

6.3.7.2 TatA L10C does not crosslink to TatB L9C, L10C or L11C *in vivo* with endogenous substrate levels

TatA L10C has been consistently shown to self-interact at a much lower level than TatA L9C and I11C and has demonstrated no interactions with TatC at any Cys positions examined at low copy number expression (Sections 6.3.2.1-6.3.2.2 and 6.3.3) and this may leave TatA L10C free to interact with TatB. However, anti-TatB Western blots in Fig. 6.16A show that no TatA-TatB heterodimer was detected through TatA L10C with any of the three Cys substitutions in TatB. TatB homodimers were detected, similar those seen in Fig 6.15A. Unsurprisingly, anti-TatA Western blots demonstrated no TatA-TatB crosslink band with only weak TatA homodimerisation (compared to TatA L9C).

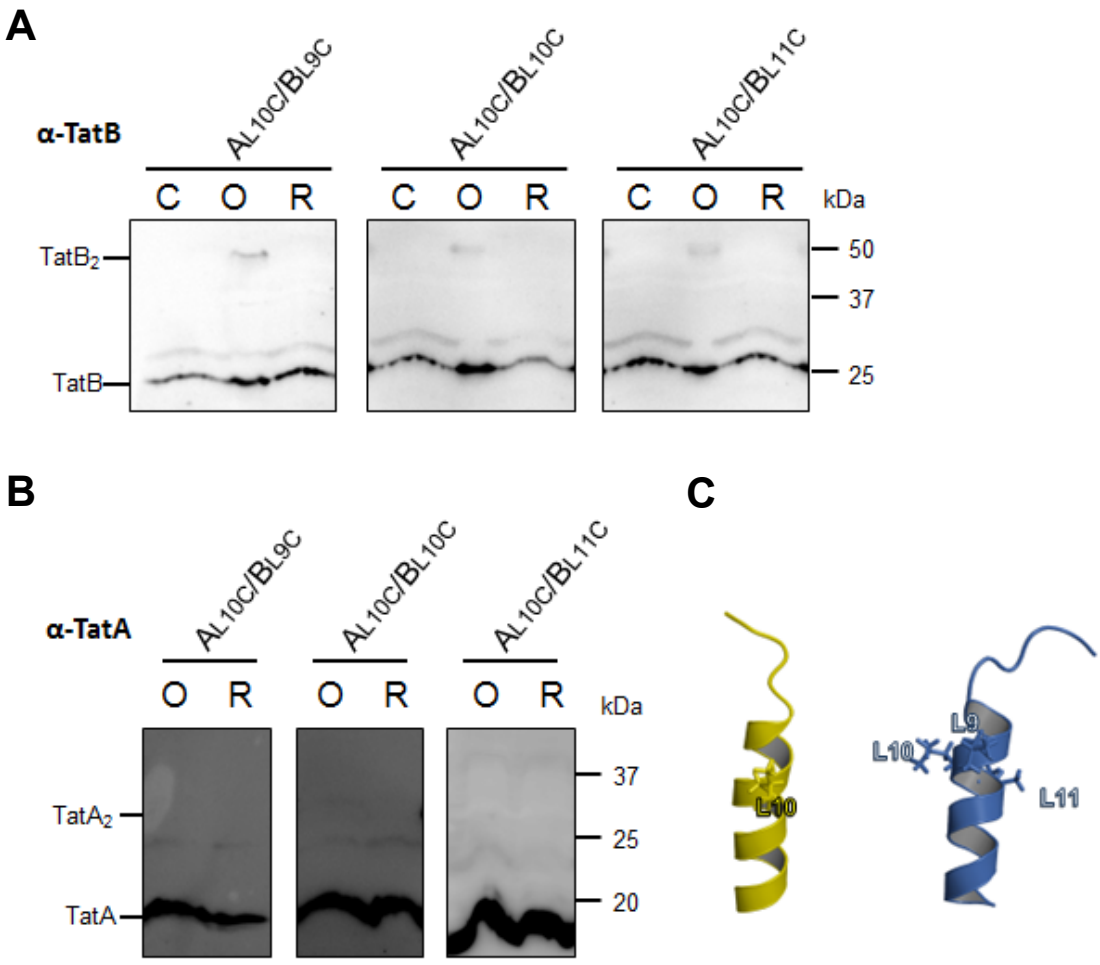

Figure 6.16) TatA L10C does not interact with TatB L9C, L10C or L11C *in vivo* with endogenous substrate–A- Anti-TatB Western blots performed on isolated membrane fractions from *E. coli* strain DADE (Δ*tatABCD,* Δ*tatE*) harbouring pTat101 producing Cysless TatC along with the indicated Cys substitutions in TatA and TatB, after exposure to experimental conditions *in vivo* noted by "C"- corresponding to control cells which were untreated, "O"- cells were oxidised with 1.8 mM copper phenanthroline for 1 min and "R"- cells were treated with 10 mM of the reductant DTT for 1 min. The positions of the TatB monomer and TatB homodimer are indicated. **B-** Anti-TatA Western blots of samples from "O" and "R" in **A**. Loading volume in each case was 5 µL. **C-** denotes positions of Cys substitutions in TatA and TatB examined in this experiment.

6.3.7.3 TatA I11C does not crosslink to TatB L9C, L10C or L11C *in vivo* with endogenous substrate levels

Given that TatA I11C did not interact with TatC at endogenous substrate levels, it was another potential interaction candidate for TatB. TatA I11C was examined for its ability to crosslink with the three consecutive Cys substitutions in TatB, however no TatA-TatB heterodimer was observed on anti-TatB Western blots (Fig 6.17A). TatB homodimerisation was similar to that observed in Figs 6.15 and 6.16 with a 50 kDa band forming with each TatB Cys substitution under oxidising conditions only. Anti-TatA alongside favourable TatA homodimerisation through I11C.

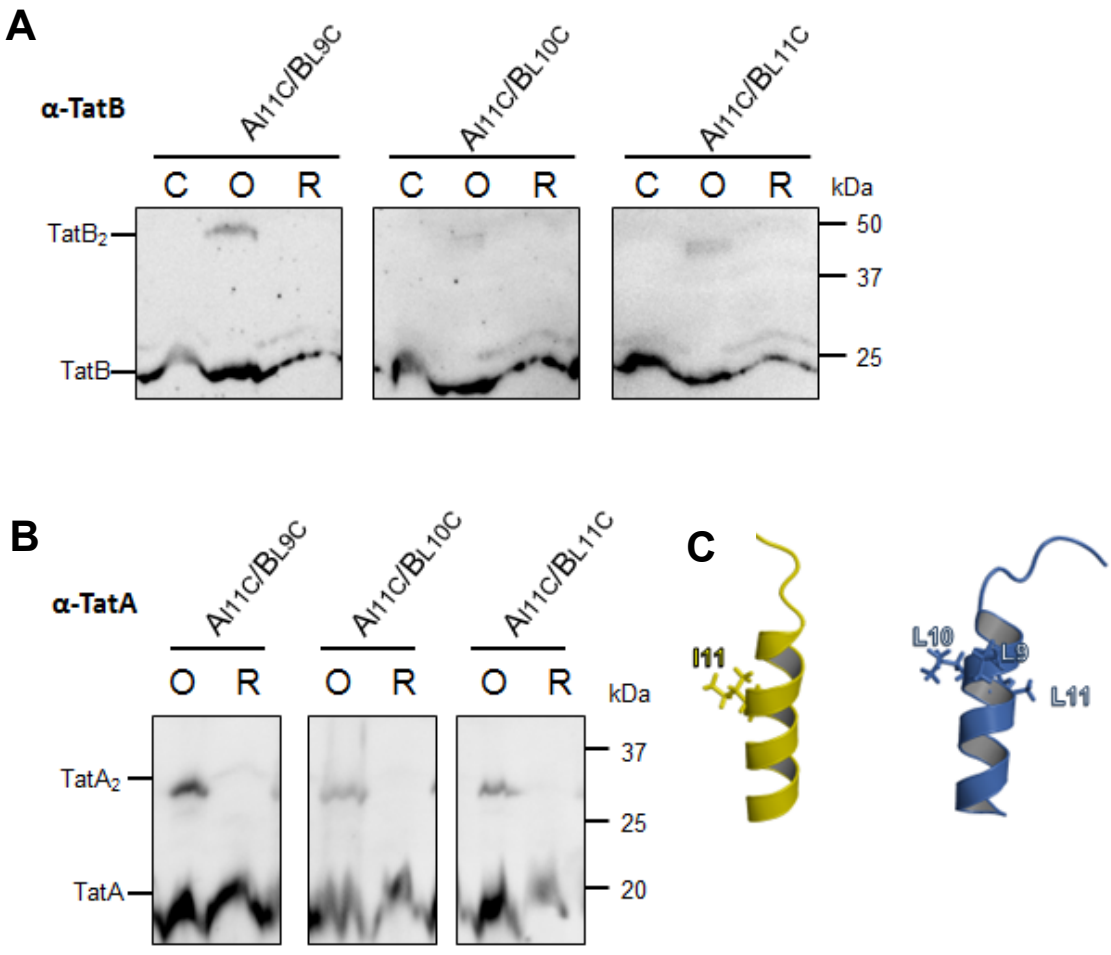

Figure 6.17) TatA I11C does not interact with TatB L9C, L10C or L11C *in vivo* with endogenous substrate–A- Anti-TatB Western blots performed on isolated membrane fractions from *E. coli* strain DADE (Δ*tatABCD,* Δ*tatE*) harbouring pTat101 producing Cysless TatC along with the indicated Cys substitutions in TatA and TatB, after exposure to experimental conditions *in vivo* noted by "C"-corresponding to control cells which were untreated, "O"- cells were oxidised with 1.8 mM copper phenanthroline for 1 min and "R"- cells were treated with 10 mM of the reductant DTT for 1 min. The positions of the TatB monomer and TatB homodimer are indicated. **B-** Anti-TatA Western blots of samples from "O" and "R" in **A**. Loading volume in each case was 5 µL. **C-** denotes positions of Cys substitutions in TatA and TatB examined in this experiment.

Western blots shown in Fig 6.17B also demonstrated a lack of TatA-TatB crosslinks

6.3.7.4 Summary of TatA-TatB crosslinks *in vivo* with low copy number expression and endogenous substrate

Based on the lack of TatA-TatB crosslinks in Section 6.3.7.1-6.3.7.3, it seems very unlikely that TatA and TatB are interacting at any significant level in the presence endogenous substrate. While it is feasible that the two proteins could be associated through residues at different heights to those tested in each transmembrane helix, or perhaps through the flexible N-terminal region or the amphipathic helices, it is also plausible that TatA and TatB can occupy TM6 and TM5 on TatC without being in contact with each other.

6.3.8 TatA-TatB interactions are observed *in vivo* with overexpressed substrate

To examine whether interactions between TatA and TatB appear at different stages of the Tat cycle, the crosslinking experiments described in Section 6.3.7.1-6.3.7.3 were repeated in the presence of overexpressed substrate CueOH.

6.3.8.1 TatA L9C crosslinks TatB L11C *in vivo* with overexpressed CueOH substrate

When crosslinking experiments from Section 6.3.7.1, Fig 6.15 were repeated in the presence of overexpressed CueOH, anti-TatB Western blots revealed no TatA-TatB heterodimerisation through TatA L9C with TatB L9C or L10C (Fig 6.18A). However, a distinct heterodimer band was detected, migrating just above 37 kDa, when TatA L9C was present with TatB L11C, suggesting that the presence of substrate brings TatB and TatA into close proximity. TatB homodimerisation was more pronounced through TatB L9C and L11C, in line with observations *in vitro* made Lee *et al*. (2006), whereby TatB L10C formed weaker self-crosslinks than TatB L9 or L11C. Interestingly there seems to be a lack of any TatB L10C homodimersation at all in Fig. 6.18 while in Fig. 6.16, without overexpressed substrate, it was present. However it is unclear whether

substrate overexpression decreases TatB homodimerisation through TatB L10C without a direct comparison between the two conditions using for Western blotting.

The corresponding TatA-TatB heterodimer band was not detected on anti-TatA Western blots (Fig. 6.18B), which may not be surprising given that the limit-of-detection of this Western blotting protocol did not allow the detection of TatA-TatC heterodimers on anti-TatA Western blots when proteins were expressed at a low copy number in Sections 6.3.2.1 and 6.3.5.1.

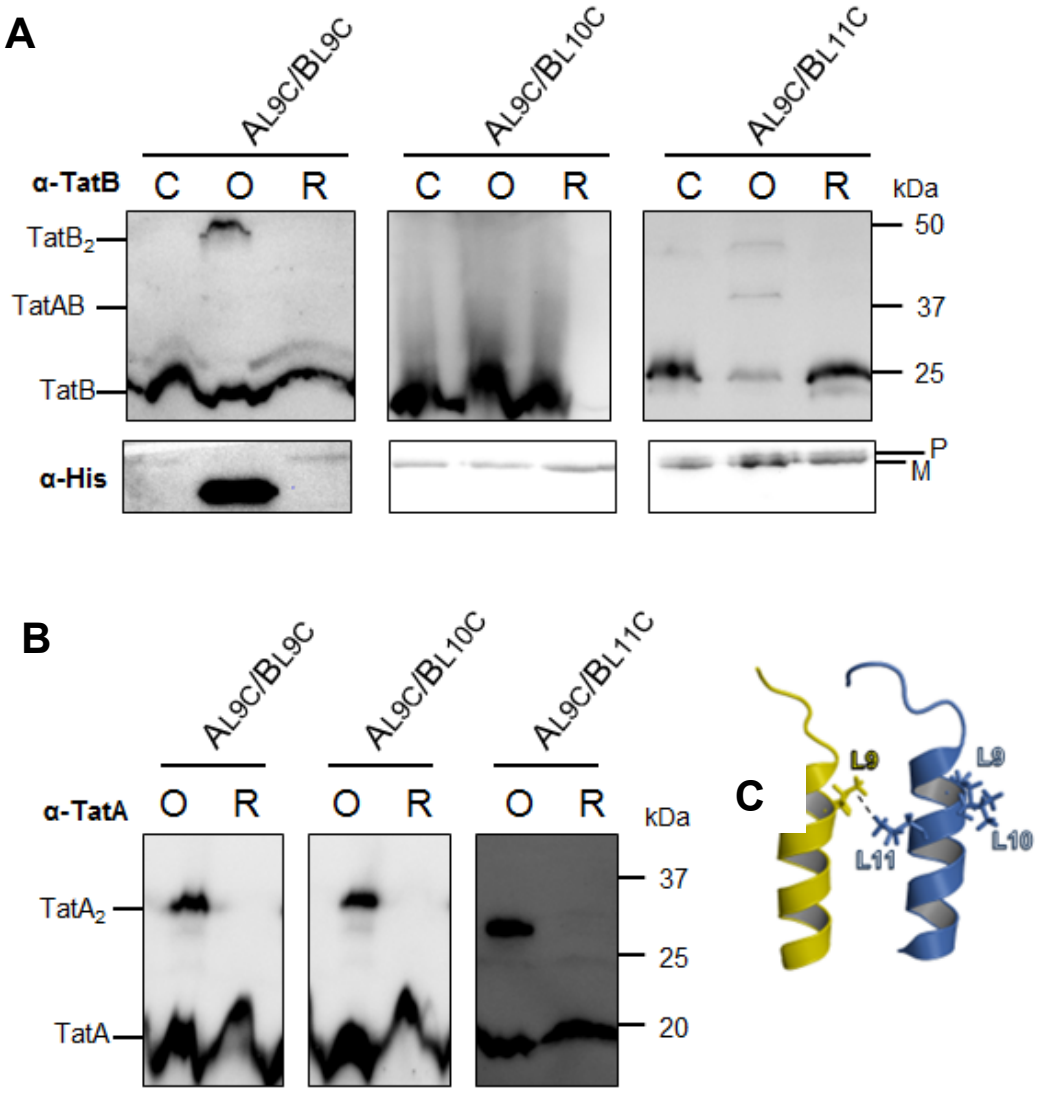

Figure 6.18) TatA L9C interacts with TatB L11C *in vivo* with overexpressed substrate - A- Anti-TatB Western blots performed on isolated membrane fractions from *E. coli* strain DADE (Δ*tatABCD,* Δ*tatE*) harbouring pTat101 producing Cysless TatC along with the indicated Cys substitutions in TatA and TatB alongside His-Tagged CueO produced from pQE80, after exposure to experimental conditions *in vivo* noted by "C"-corresponding to control cells which were untreated, "O"- cells were oxidised with 1.8 mM copper phenanthroline for 1 min and "R"- cells were treated with 10 mM of the reductant DTT for 1 min. The positions of the TatB monomer, TatB homodimer and TatAB heterodimer are indicated. Anti-His Western blots are shown corresponding to the soluble fraction following the membrane fractionation of each sample, showing "p" precursor and "m" mature forms of CueOH. **B-** Anti-TatA Western blots of

TatA homodimersation through TatA L9C was prominent, as it was when overexpressed substrate was not present, though it is unclear whether crosslinking with overexpressed substrate promoted TatA self-interactions, without comparing TatA homodimer intensity on the same Western blot

Anti-His Western blots (Fig.6.18A) confirmed the presence of precursor and mature forms of CueOH. For the oxidised TatA L9C - TatB L9C sample a very strong band migrating at a lower molecular weight was observed, which likely corresponds to an intra-disulphide linked form of CueOH (See Section 6.3.5.1). This form was not observed with constructs expressing TatA L9C and TatB L10C or L11C. It is not clear why CueOH behaves differently between these samples.

6.3.8.2 TatA L10C does not crosslink TatB L9C, L10C or L11C *in vivo* with overexpressed CueOH substrate

TatA L10C was discussed as a candidate for TatB interactions in Section 6.3.7.2 due to its lack of self-association or interaction with TatC, and it was seen that there was no interaction with the Cys residues in TatB that were tested. Similar results were also seen in the presence of overexpressed substrate as no TatA-TatB heterodimer was detectable through TatA L10C and any of the Cys positions tested in TatB under oxidising conditions on anti-TatB Western blots (Fig 6.19A). TatB homodimerisation was seen, similar to that in Section 6.3.8.1 with stronger TatB homodimerisation through TatB L9C and L11C than L10C. Anti-TatA Western blots (Fig. 6.19B) demonstrated, as expected, no TatA-TatB heterodimer band, and that TatA homodimerisation was not present or was very weakly detected. Anti-His Western blots (Fig. 6.19A) confirmed the presence of CueOH, in all of these experiments, with the protein migrating faster in all of the oxidised samples, as explained in Section 6.3.5.1.

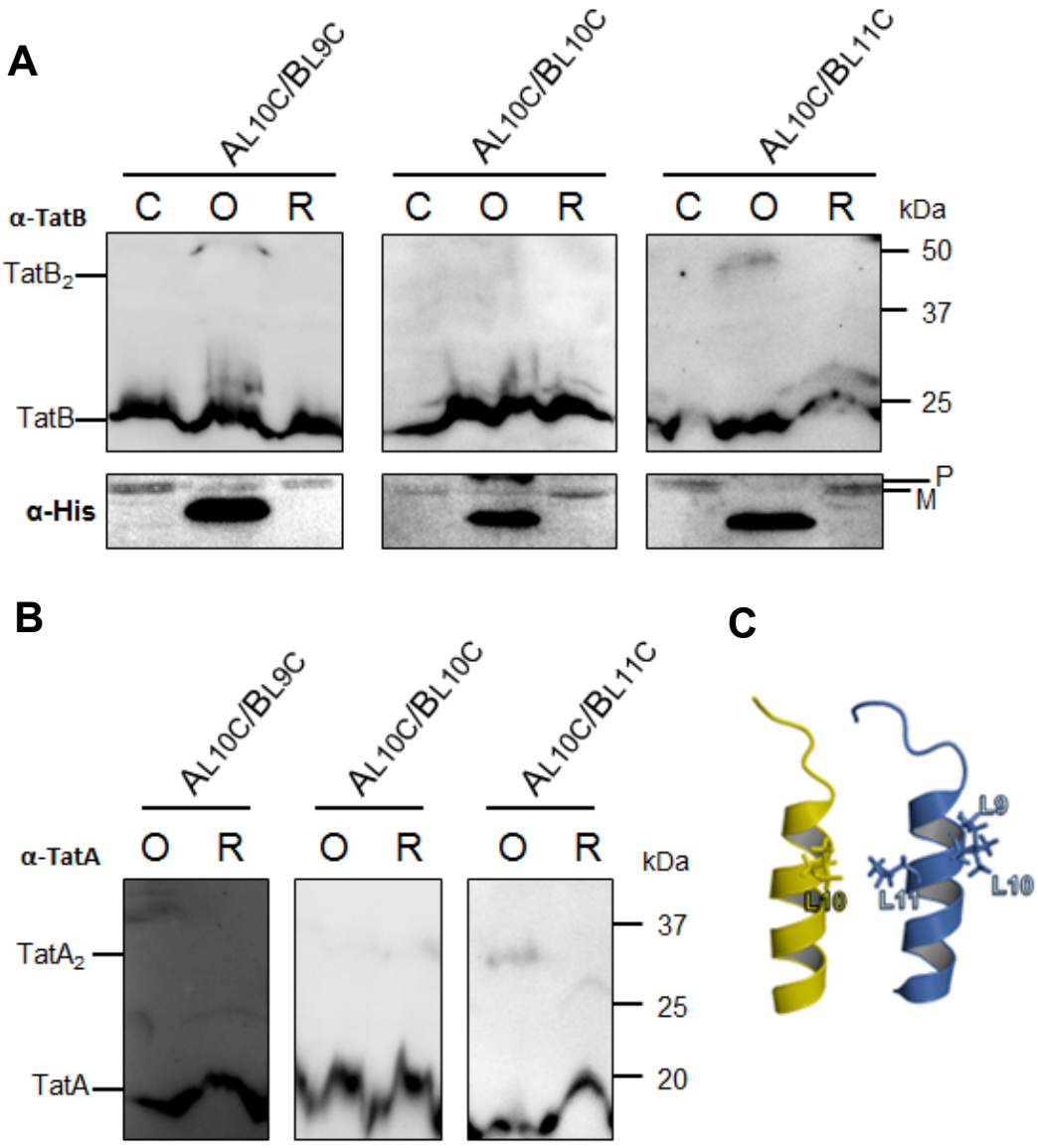

Figure 6.19) TatA L10C does not interact with TatB L9C, L10C or L11C *in vivo* with overexpressed substrate - A- Anti-TatB Western blots performed on isolated membrane fractions from *E. coli* strain DADE (Δ*tatABCD,* Δ*tatE*) harbouring pTat101 producing Cysless TatC along with the indicated Cys substitutions in TatA and TatB alongside His-Tagged CueO produced from pQE80, after exposure to experimental conditions *in vivo* noted by "C"-corresponding to control cells which were untreated, "O"- cells were oxidised with 1.8 mM copper phenanthroline for 1 min and "R"- cells were treated with 10 mM of the reductant DTT for 1 min. The positions of the TatB monomer and TatB homodimer are indicated. Anti-His Western blots are shown corresponding to the soluble fraction following the membrane fractionation of each sample, showing "p" precursor and "m" mature forms of CueOH. **B-** Anti-TatA Western blots of samples from "O" and "R" in **A**. Loading volume in each case was 5 µL. **C-** denotes positions of Cys substitutions in TatA and TatB examined in this experiment.

6.3.8.3 TatA I11C crosslinks TatB L11C *in vivo* with overexpressed CueOH substrate

Crosslink analysis between TatA I11C and TatB L9C demonstrated no detectable TatA-TatB heterodimer on anti-TatB Western blots in Fig. 6.20A, as was the case with TatA I11C oxidised alongside TatB L10C. However a distinct heterodimer band just above 37 kDa was seen through TatA I11C and TatB L11C with overexpressed substrate indicating that, as with TatA L9C and TatB L11C in Section 6.3.8.1, substrate overexpression brings TatB and TatA into close proximity.

A TatA-TatB heterodimer band above 37 kDa is seen through TatA I11C and TatB L11C with overexpressed substrate indicating that, as with residues TatA L9C and TatB L11C in Section 6.3.8.1 substrate overexpression is bringing these two residues closer together.

TatB homodimerisation seems to be present through all Cys substitutions in TatB, at a somewhat higher level than those performed without overexpressed substrate (Fig. 6.18), likely due to the sensitivity of the Western blotting method. TatA homodimerisation through I11C was distinct on anti-TatA Western blots in Fig. 6.20B. Anti-His Western blots demonstrate CueOH is produced in all of the samples tested.

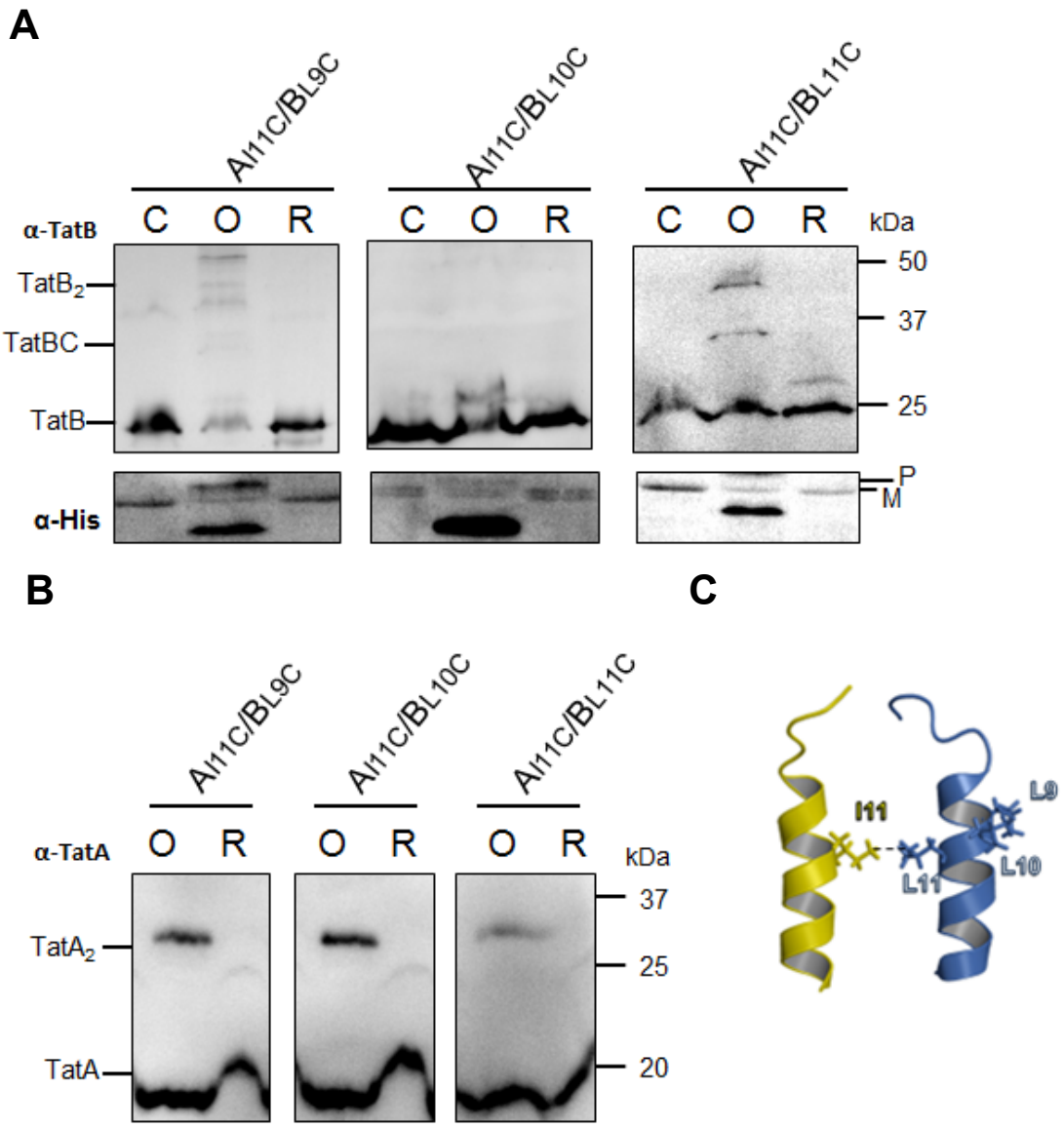

Figure 6.20) TatA I11C interacts with TatB L11C *in vivo* with overexpressed substrate - A- Anti-TatB Western blots performed on isolated membrane fractions from *E. coli* strain DADE (Δ*tatABCD,* Δ*tatE*) harbouring pTat101 producing Cysless TatC along with the indicated Cys substitutions in TatA and TatB alongside His-Tagged CueO produced from pQE80, after exposure to experimental conditions *in vivo* noted by "C"-corresponding to control cells which were untreated, "O"- cells were oxidised with 1.8 mM copper phenanthroline for 1 min and "R"- cells were treated with 10 mM of the reductant DTT for 1 min. The positions of the TatB monomer, TatB homodimer and TatAB heterodimer are indicated. Anti-His Western blots are shown corresponding to the soluble fraction following the membrane fractionation of each sample, showing "p" precursor and "m" mature forms of CueOH. **B-** Anti-TatA Western blots of samples from "O" and "R" in **A**. Loading volume in each case was 5 µL. **C-** denotes positions of Cys substitutions in TatA and TatB examined in this experiment.

6.3.9 TatA and TatB are able to interact following PMF dissipation, suggesting that TatA does not leave the Tat complex

Chapter 5, Section 5.3.8 previously established that TatA was not present in its constitutive site at TatC TM6 nor in the TatB constitutive site at TatC TM5 after PMF dissipation. From this it was hypothesised that either TatA left the Tat complex completely in response to PMF dissipation or interacted at a different region of the complex. Interactions between TatA L9C and I11C were observed with TatB L11C in the presence but not in the absence of overexpressed substrate. To determine whether PMF dissipation (in the absence of overexpressed substrate) influenced TatA-TatB interactions, the TatA L9C - TatB L11C pair were chosen. As shown in Fig. 6.21 on anti-TatB Western blots under conditions of endogenous substrate no TatA – TatB crosslink was detected (as expected, since data in Sections 6.3.7.1 and 6.3.8.1 showed interactions were only seen with overexpressed Tat substrate). However, upon PMF dissipation with 5 mM indole, a characteristic band just above 37 kDa was detected, corresponding to TatA-TatB heterodimer formation. When cells were thoroughly washed following indole treatment, the crosslink was no longer seen, indicating that it is reversible and does not arise because indole is lethal to cells. From this finding, it seems that TatA does not leave the Tat complex in response to PMF dissipation, but rather associates with TatB, while losing or adjusting its association with TatC (lack of interactions between Cys positions tested with TatC with dissipated PMF is shown in Sections 6.3.6.1 and 6.3.6.2).

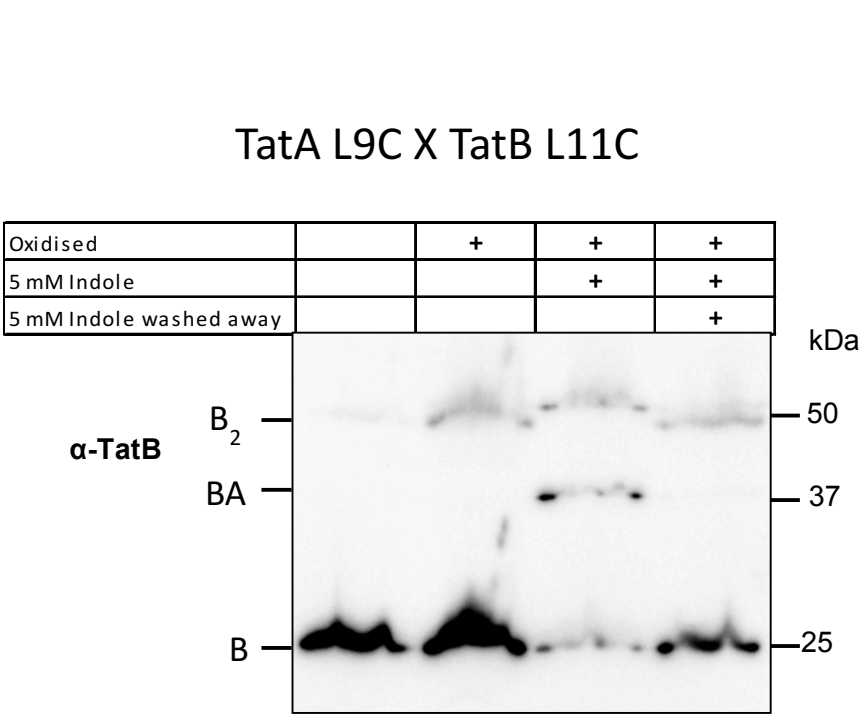

Figure 6.21) TatA L9C interacts with TatB L11C in response to PMF dissipation with 5 mM indole- Anti-TatB Western blot of isolated membrane fractions from *E. coli* strain DADE (Δ*tatABCD*, Δ*tatE*) harbouring pTat101 expressing Cysless TatC and Cys-substituted TatA L9C and TatB L11C. Cells, prior to isolation of the membrane fractions, were either untreated, oxidised with 1.8 mM copper phenanthroline for 1 min or incubated with 5 mM indole for 5 mins, followed by either a 1 min oxidation step or washed thoroughly to remove the indole followed by a 1 min oxidation step. Loading volume in each case was 5 µL.

6.4 Discussion

6.4.1 Mapping constitutive interactions between TatA and TatB with TatC informed by crosslinking proteins at low copy number expression

The aim of using low copy number constructs in the crosslinking experiments in this Chapter was to validate findings in Chapter 4 and 5, which were performed at medium copy number, due to concerns over artefacts caused by the large amount of Tat proteins present in the cell membrane. Medium copy number crosslinking in Chapter 5 identified a site on TatC where TatA interacted constitutively. This involved a crosslink through TatA L9C to TatC F213C at the periplasmic part of TatC TM6, which was preserved in the resting state of the Tat system. Comparatively weaker associations through TatA L10C and TatC V212C, at the extreme C-terminal region of the P3 loop and through TatA 11C and both TatC V213C and F213C, were also found with a Tat system able to bind endogenous substrate (Chapter 4, Sections 4.3.3.1-4.3.3.3). The results in this Chapter confirmed that the TatA L9C crosslink to TatC F213C was detected at low copy number expression, and replicated the preservation of this crosslink in the resting state (Section 6.3.4.1). The weaker interactions seen between TatA L10C/I11C with TatC F213C/V212C, in Chapter 4, were not seen with low copy number expression in Sections 6.3.2.1 and 6.3.2.2, and therefore may be too faint to detect at lower copy number, or could be explained as artefacts due to high copy number.

In addition to the constitutive site occupied by TatA at TatC TM6 being identified in this thesis, crosslinking experiments between TatB and TatC performed by Johann Habersetzer have produced data that supports the placement of a constitutive TatB at TatC TM5 (previously identified in Rollauer *et al*., (2012), Kneuper *et al*. (2012) and Blummel *et al.,* 2015) where a TatB-TatC crosslink was seen at native copy number expression *in vivo* through residues L9C in TatB and M205C in TatC TM5. This was preserved in a resting Tat system imparted by TatC mutations F94A and E103A which

prevent substrate binding (as was performed using TatA in Section 6.3.4.2). These data are shown in Fig. 6.22.

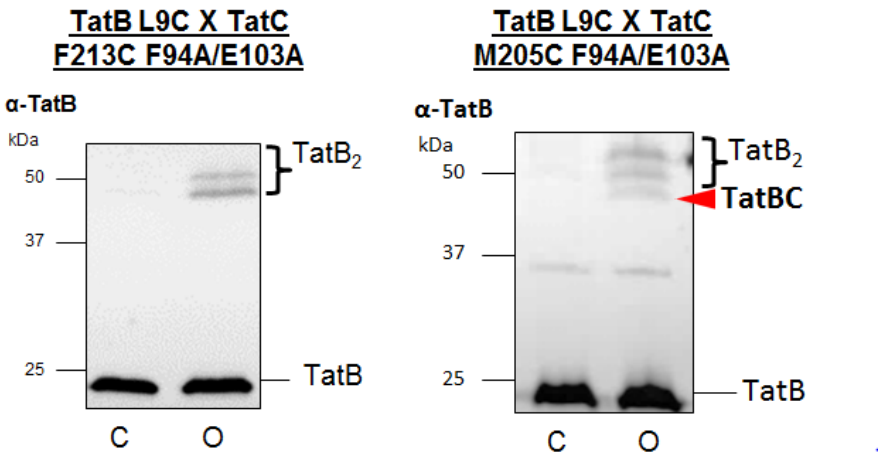

Figure 6.22) Crosslinking data from Johann Habersetzer shows TatB interacting with TatC TM5 in the resting state- anti-TatB Western blots produced by Johann Habersetzer (unpublished), *in vivo* disulphide crosslinking was performed on *E. coli* strain DADE (Δ*tat*ABCD, Δ*tatE*) harbouring pC*TatABC, a construct encoding wild type TatA with Cys substituted TatB and TatC as noted. "C" denotes untreated control and O denotes cells oxidised with 1.8 mM copper phenanthroline with membrane fractions of crosslinked cells loaded. TatC contained substitutions F94A and E103A to prevent substrate binding as in Section 6.3.6.1.

A model proposing interactions between TatA and TatB with TatC that may be occurring in a resting Tat system, based on the TatA-TatC crosslinking results generated in this thesis, is given in Fig 6.23. It should be noted that no TatA-TatB Cys crosslinks were detected in Sections 6.3.7.1-6.3.7.3 with only endogenous substrate present, therefore TatA and TatB are shown not to be in contact in Fig. 6.23. Indeed the TatA L9C crosslink to TatC F213C seen in the resting state could still be observed with endogenous levels of substrate present (Section 6.3.2.1, Fig. 6.3), meaning that it is largely constitutive Tat interactions being detected when endogenous substrates are being expressed by the cell.

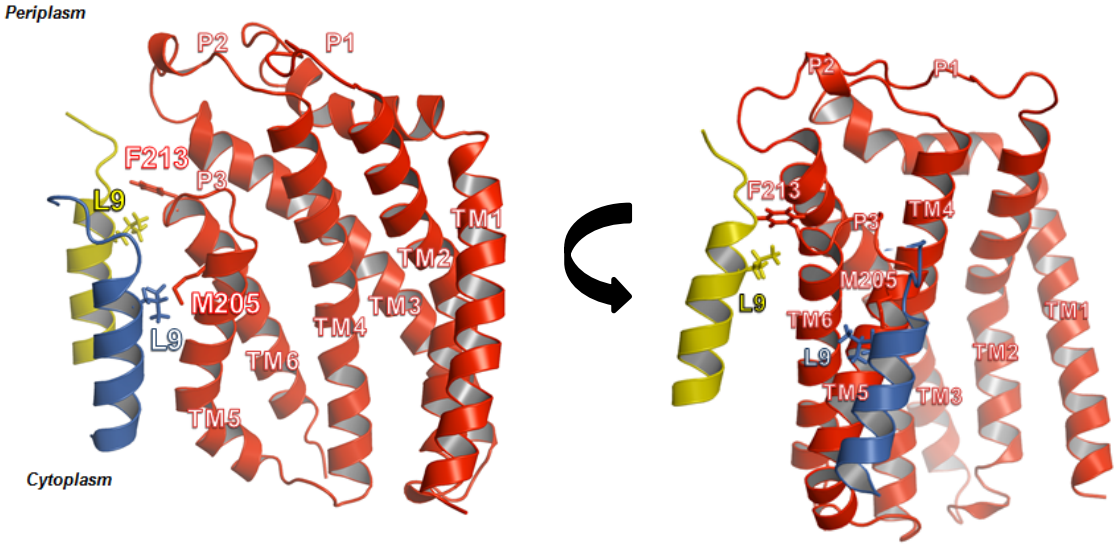

Figure 6.23) Proposed TatA and TatB interactions with TatC in the resting state based on crosslinking- Shows residue in TatC (red) F213 in contact with L9 of the TatA (yellow) TM, with M205C of TatC in contact with TatB (blue) L9C.

6.4.2 TatA and TatB swap sites during transport

The results presented here and in Chapter 5 both identified TatA movement from TatC TM6 to TM5 in response to the expression of two different Tat substrates; one artificial and one native, with Tat subunits expressed at both high and low copy number (Chapter 5, Sections 5.3.7.1-5.3.7.4 and this Chapter, Sections 6.3.5.1-6.3.5.4). This is again, supported by crosslinking from Johann Habersetzer (unpublished), who showed that *in vivo* TatB crosslinks at its constitutive site at TatC TM5 decrease in response to increasing amounts of substrate, CueOH (Fig. 6.24). Further to this, Johann Habersetzer also identified a crosslink of TatB at TatC TM6, the TatA constitutive site, in response to overexpression of the same substrate, through TatB L9C and TatC F213C (Fig. 6.24). This indicates that TatA and TatB are swapping sites in response to substrate overexpression and given the similarity of the residues found to crosslink (*i.e.* TatA L9C is conserved in homologous TatB), it is likely they are interacting with TatC in a similar manner. Indeed, while previous studies have identified TatB present at TM5 of TatC (Rollauer *et al.,* 2012, Kneuper *et al*., 2012, Blummel *et al*., 2015), with TatA

nearby (Aldridge *et al*., 2014, Blummel *et al*., 2015), the work presented in this thesis, combined with that of Johann Habersezter demonstrates that TatA and TatB interact at

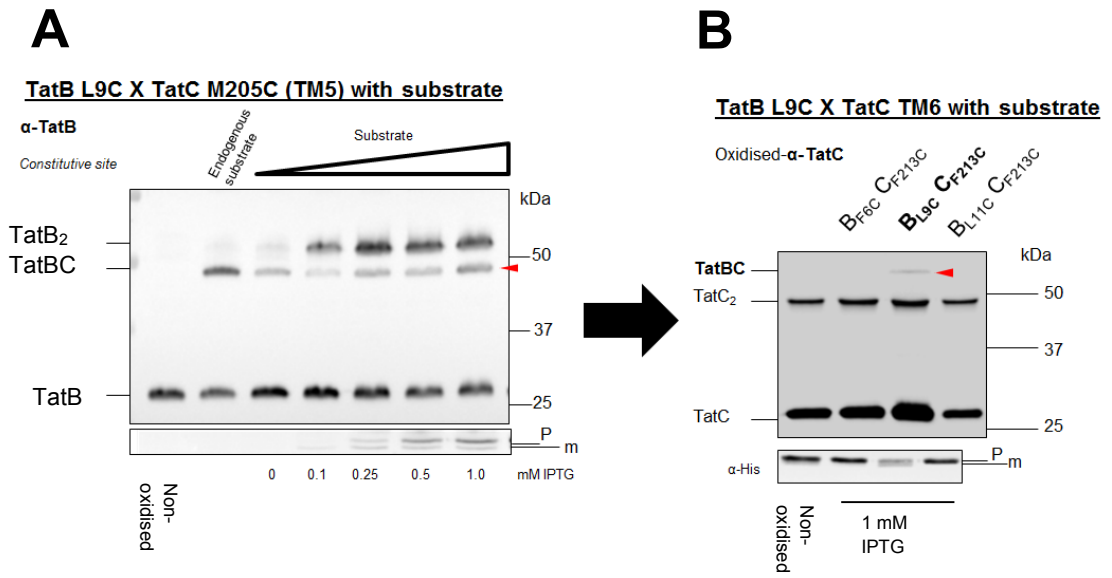

Figure 6.24) Western blots to show movement of TatB from TatC TM5 to TM6 in response to Tat substrate overexpression-A- anti-TatB Western blot produced by Johann Habersetzer (unpublished) showing *in vivo* disulphide crosslinking performed on isolated membrane fractions *E. coli* strain DADE (Δ*tat*ABCD, Δ*tatE*) harbouring pC*TatABC, a construct encoding wild type TatA with Cys substituted TatB and TatC as noted along with pQE80 expressing His-tagged Tat substrate CueO. Prior to membrane preparations, cells were treated as follows: "Non-oxidised" denotes the untreated control with remaining lanes all containing samples oxidised with 1.8 mM copper phenanthroline. Sample with endogenous substrate is noted, alongside cells expressing CueOH from pQE80 vector with increasing concentrations of the inducer, IPTG. The TatB monomer and homodimer are the TatBC heterodimer is noted with a red triangle. **B-** Shows anti-TatC Western blot produced by Johann Habersetzer showing TatB crosslinked to TatC at positions noted, in the same manner as in **A-,** however 1 mM IPTG only was used to induce expression of CueOH. TatBC heterodimer is noted with red triangle, while TatC homodimer and monomer are also noted.

TM6 and TM5 of TatC in the resting state with a subsequent swapping movement of TatA and TatB during translocation which has not been observed in the prior literature. This helps clarify data discussed previously in Chapter 5, Section 5.4.2 whereby TatB was hypothesised to move to an unknown location in the Tat complex to allow TatA to interact at TM5. Indeed Alcock *et al.* (2013) noted that fluorescently labelled TatB did not leave the Tat complex *in vivo* in response to overexpressed substrate and in these experiments a population of TatA may occupy TatC TM5 with a corresponding population of TatB at TM6.

This swapping movement strengthens the proposition that TatB acts as a "gatekeeper" controlling TatA access to TatC by demonstrating that TatB is moving away from its constitutive site in response to Tat substrate overexpression, allowing TatA to move in to interact with TM5. The purpose of this movement is discussed in Chapter 5, Section 5.4.4 and may facilitate further TatA polymerisation steps.

The stage of Tat transport subsequent to TatB dissociation from TatC TM5 may include polymerisation of TatA forming an oligomer through which the substrate can be translocated, perhaps through scaffolding of TatA in the TatC concave face as suggested by crosslinking in plant thylakoids (Aldridge *et al.,* 2014), or outside the complex (discussed previously in Chapter 5, Section 5.4.4). Indeed, TatA is proposed to exhibit membrane disrupting behaviour, which would otherwise be damaging to the cell unless coupled to Tat export, so therefore, control of this process is imperative. Further to this, these data may potentially explain why overexpression of TatB is toxic to the *E. coli* Tat system (Sargent *et al.,* 1999), if it is competing for interaction sites with TatA, TatB may block TatA-TatC interactions which are required to allow transport.

Interestingly, residue L206C in TM5 of TatC was not found to interact with any positions tested in the TatA TM. Indeed, homodimerisation through this residue was also very weak compared with neighbouring M205C (Section 6.3.3) this leaves open the question as to what, if anything, may be interacting here during the substrate transport stages of the Tat export cycle. Based on crosslinking studies in both bacteria (Blummel *et al*., 2015) and plants (Aldridge *et al.,* 2014) it is plausible that this is an interaction site for the Tat signal sequence, located deep in the Tat complex, perhaps representing a deeper binding site discussed in plant models (Gerard and Cline, 2007). This could involve interaction of the signal sequence with once face of TM5 in TatC, near L206, with TatA interacting at the other face near M205 after TatB has moved. Crosslinking could be performed between the Tat signal sequence and TatC *in vivo* to analyse a deeper binding site which may be near TatC TM5, using disulphide

crosslinking which would be informed by photo-crosslinks seen in Blummel *et al.* (2015).

Table 6.2 outlines crosslinks observed between Tat subunits seen in this Chapter and seen by Johann Habersetzer in the presence of overexpressed substrate, while Fig. 6.25 and Fig. 6.26 represent two potential Tat subunit organisations that satisfy these observations. Fig. 6.25A demonstrates an arrangement which attempts to satisfy TatA heterodimerisation through TatA I11C to TatB L11C, (Sections 6.3.8.3) along with TatA heterodimerisation through Tat L9C to TatC M205C (Section 6.3.5.3). The TatB L9C crosslink to TatC F213C, as demonstrated by Johann Habersetzer, in the presence of overexpressed substrate (Fig. 6.24), is also shown, along with TatC homodimerisation through TatC M205C increased in the presence of substrate (Section 6.3.5.3). Fig 6.25 A and B represents speculative TatA movement into the concave face of TatC (informed by crosslinked seen in plant thylakoids by Aldridge *et al.* (2014) and *in silico* data presented in Rollauer *et al.* (2012)) showing a TatA subunit satisfying the TatA L9C crosslink to TatB L11C in the presence of overexpressed substrate (Section 6.3.8.1). The Tat signal sequence is shown binding at TatC TM5.

Fig. 6.26A outlines a subunit arrangement which satisfies heterodimerisation of TatA L9C and I11C to TatB L11C (Sections 6.3.8.1 and 6.3.8.3), while also satisfying crosslinks between TatB L9C and TatC F213C (Fig. 6.24), along with TatA L9C to TatC M205C (Section 6.3.5.3). In this case, Fig. 6.26B demonstrates TatA I11C crosslinking to TatC M205C as a TatA subunit is proposed to move into the TatC concave face. As in Fig. 6.25 the Tat signal sequence is shown binding to TatC TM5.

Table 6.2) Cys positions of residues which form heterodimers between TatA, Tat and TatC- Cys substitution combinations are listed between each protein which were able to form significant heterodimers between the proteins with low copy number protein expression and overexpressed Tat substrate, CueOH.

Heterodimer crosslinks observed with overexpressed substrate					
Cys Substitutions					
TatA	**TatC**	**TatB**	**TatC**	**TatA**	**TatB**
L9C	M205C	L9C	F213C	L9C	L11C
I11C	M205C			L11C	L11C

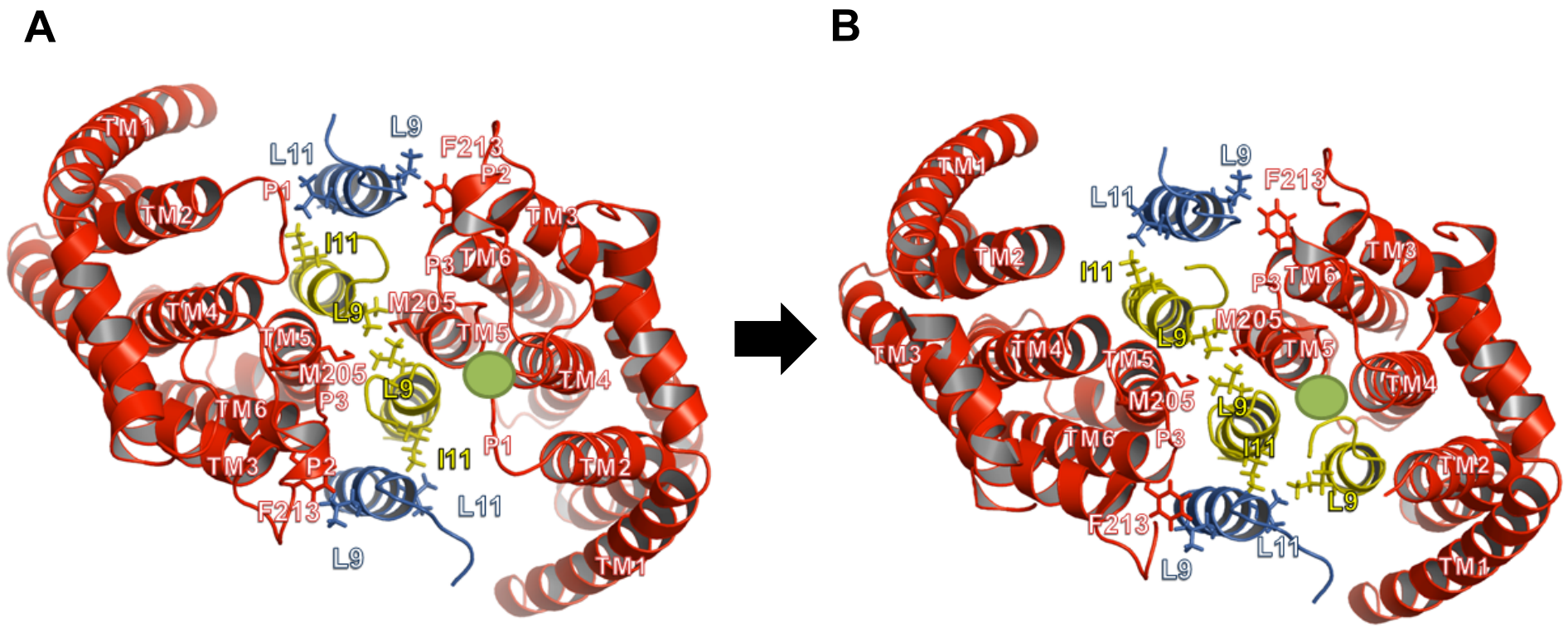

Fig. 6.25) A proposed arrangement of Tat subunits to satisfy heterodimerisation of Tat subunits through *in vivo* crosslinking experiments performed with overexpressed substrate –**A-**Two TatC monomers (red) are shown linked through M205C at TM5. TatA (yellow) is shown interacting at TatC M205C while simultaneously interacting through I11C with TatB L11C. TatB is shown interacting at TatC F213C at TM6 through L9C.The signal peptide binding a proposed interaction site near TatC TM5 is shown as a green circle. **B-** shows another TatA monomer in the concave face of TatC interacting with TatB L11C *via* L9C.

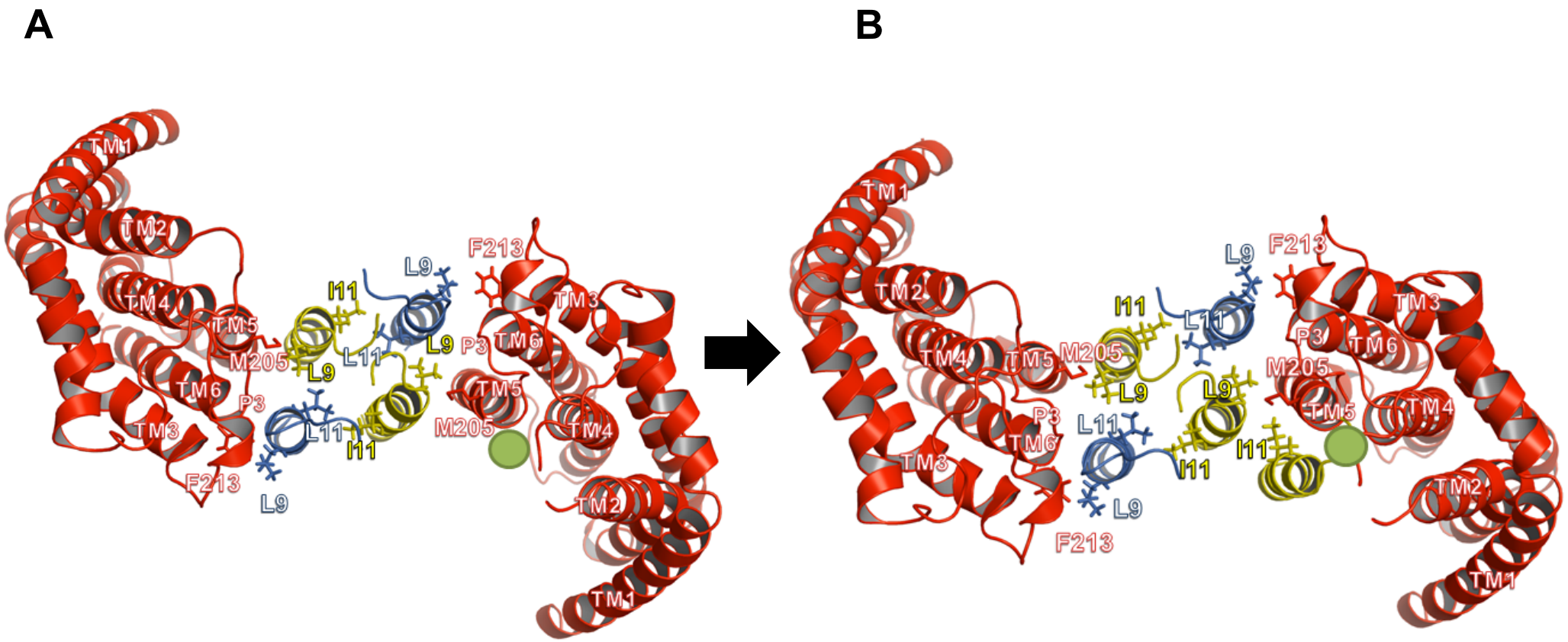

Fig. 6.26) A proposed arrangement of Tat subunits to satisfy heterodimerisation of Tat subunits through *in vivo* crosslinking experiments performed with overexpressed substrate –**A-**Two TatC monomers (red) are shown with residues M205C in the TM5 and F213C in the TM6 noted. The TatA transmembrane helix (TM) (yellow) is shown at TatC TM5 interacting with M205C *via* L9C, while L9C is simultaneously in contact with TatB L11C (blue). TatB L9C is shown in contact with TatC F213C at TM6. L1C-L11C crosslinks between TatA-TatB form between subunits interacting with the adjacent TatC monomer. The signal peptide binding a proposed interaction site near TatC TM5 is shown as a green circle. **B-** shows another TatA monomer in the concave face of TatC interacting with TatC M205C *via* I11C.

It should be noted that Fig. 6.25 and Fig. 6.26 both assume movement of TatA into the TatC concave face, which, as stated previously, is informed through crosslinks in the plant Tat system (Aldridge *et al.,* 2014) and *in silico* data presented in Rollauer *et al.* (2012) however, no crosslinks to the concave face of TatC have been attempted in this Chapter. Furthermore it is not known whether TatA is moving from TatA TM6 to TM5, then to the concave face of TatC with another TatA monomer filling the space as each TatA vacates its site, essentially ratcheting a TatA polymer into the face of TatC, or whether the subunit arrangement allows TatA subunits to be recruited to the concave face of TatC to form an oligomer directly. It should be noted that neither Fig. 6.25 nor 6.26 accounts for TatC homodimerisation observed through F213C in the presence of substrate, which may occur at another stage of the Tat cycle.

A drawback of performing crosslinks *in vivo* in the presence of overexpressed substrate is that a "snapshot" of the protein arrangement in all stages of Tat transport is captured. Although the bias will be towards steps involved in the binding and/or export of substrates, if multiple steps are occurring in this process, it is difficult to assign specific interactions to specific stages. All the crosslinks observed in this Chapter could be occurring during Tat transport, but at different stages of the Tat cycle, and therefore cannot be incorporated into one subunit arrangement. Alternatively, an asymmetric arrangement of Tat subunits may be able to explain all the crosslinks observed in this Chapter, with some TatC monomers associated through M205C and others through F213C for example.

To clarify this subunit arrangement further, crosslinking could be performed to analyse potential interactions between TatA and the TatC concave face in response to overexpressed substrate. Chapter 5, Section 5.4.3 outlined the two proposed models for TatA oligomerisation, one involving a separate TatA oligomer forming outside the Tat complex and another involving the transmembrane helices of TatA scaffolding in the concave face of TatC within the centre of the Tat complex (as was proposed in

Aldridge *et al.,* 2014). Crosslinking in the concave face of TatA would help shed light on this TatA arrangement.

6.4.3 PMF dissipation and the effect of Tat interactions

Chapter 5, Section 5.3.8 found that with medium copy number expression of Tat proteins, TatA vacated its constitutive site at TatC TM6 in response to PMF dissipation but did not move to the TatB constitutive site at TatC TM5. While this was confirmed with low copy number expression (Sections 6.3.6.1-6.3.6.2) it was further found that interactions between TatA and TatB could still be seen with PMF dissipation (Section 6.3.9). Indeed, this may correspond to residues such as Q8 in the TatA TM, or ionisable residues in TatC being required for interactions and adversely affected by PMF dissipation, with hydrophobic interactions between TatA and TatB not affected.

The above data sugguests that TatA was not leaving the Tat complex in response to PMF dissipation, but rather, either vacating its interaction sites with TatC or repositioning itself on TatC but still remaining in contact with TatB. Further to this, it seems that instead of vacating the TatB constitutive site at TM5, TatB remains there with PMF dissipation (based on crosslinks performed by Johann Habersetzer, unpublished and shown Fig. 6.27A) with TatA peripherally associated with TatB L11C through TatA L9C. Further to this, TatB crosslinking from Johann Habersetzer also observed TatB occupying the TatA constitutive site at TatC after incubation with uncoupler (Fig 6.27B), presumably after TatA has vacated the constitutive site. This has significant consequences with regard to Tat co-purification experiments (*i.e.* devoid of PMF) whereby TatB is found to strongly favour TatC interactions in detergent solution while TatA is co-eluted with TatC only in small amounts (Chapter 3, Section 3.3.1). Indeed it is tempting to propose that when the Tat subunits are purified with affinity-tagged TatC, TatB occupies both TatA and TatB constitutive sites on TatC with TatA only peripherally associated *via* an interaction with TatB. Though TatA has been shown to co-purify with TatC directly (Chapter 3, Section and Fritsch *et al*., 2012), this

is only when TatB is absent, and as such, the usual TatA sites may be blocked by TatB after PMF dissipation.

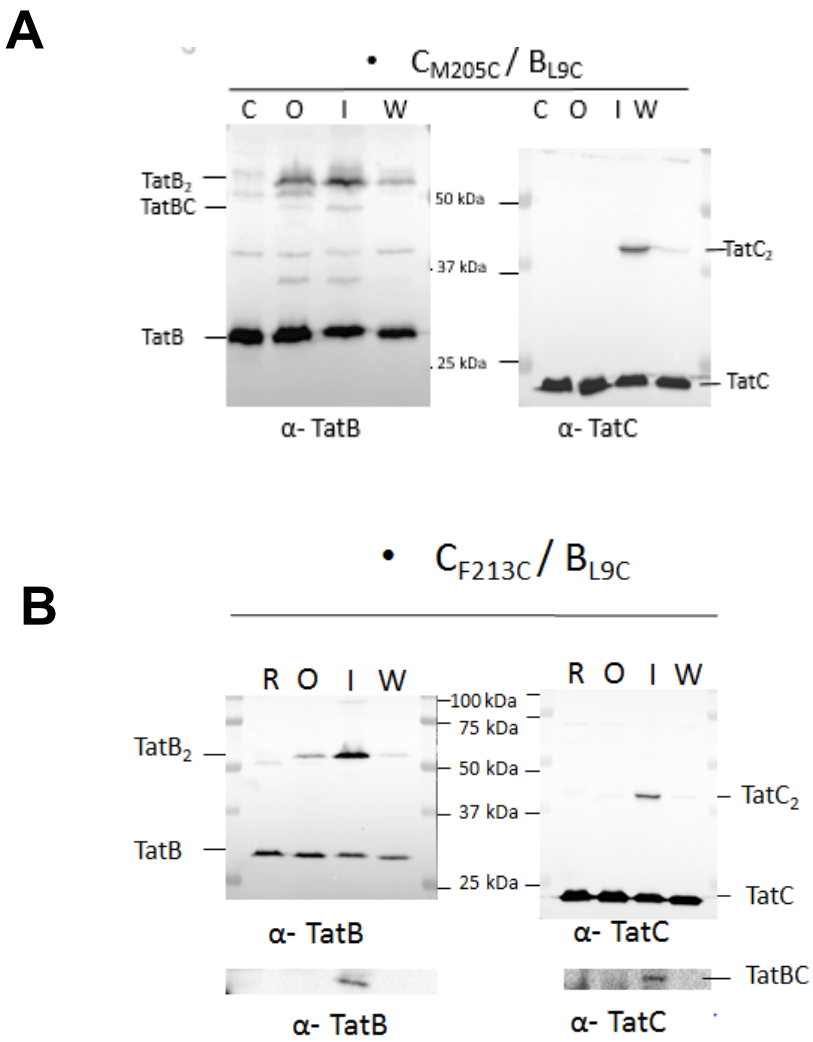

Figure 6.27) TatB occupies both TatC TM5 and TM6 after PMF dissipation with chemical uncouplers-A shows anti-TatB and TatC Western blots produced by Johann Habersetzer (unpublished) of isolated membrane fractions from *E. coli* strain DADE (Δ*tatABCD*, Δ*tatE*) harbouring pTat101 expressing wild type TatA and Cys-substituted TatBL9C and TatC M205C. Cells, prior to isolation of the membrane fractions, were either "C"- untreated, "R" reduced with 10 mM of reductant DTT, "O"- oxidised with 1.8 mM copper phenanthroline for 1 min or "I" incubated with 5 mM indole for 5 mins, followed by either a 1 min oxidation step or "W" washed thoroughly to remove the indole followed by a 1 min oxidation step. **B-** as with **A-** showing TatB Cys substitution L9C and TatC Cys substitution F213C. TatBC band was exposed separately in lower panels as it was difficult to detect.

Chapter 7: Conclusion and perspectives

7.1 Building a model of the membrane-bound resting Tat complex

Prior to the work performed in this thesis, the body of literature pointed to the TatBC complex playing a central role in the recognition of Tat substrates, with TatA having a peripheral or non-existent interaction with the complex in the resting state, being recruited only upon substrate binding. However, the work in this thesis has discovered a TatA-TatC interaction through TM6 of TatC, which is strongly detected when the Tat system is resting and diminished in the presence of overexpressed substrate (Chapters 5 and 6). Initially, this appeared to be incompatible with co-purification data presented in Chapter 3, which demonstrated only modest amounts of TatA co-purifying with affinity-tagged TatC (and only if digitonin was used to solubilise Tat components), however an explanation for this became apparent in further crosslinking experiments where the PMF was modulated. Indeed, dissipation of PMF using both chemical ionophores and *via* cell lysis (Chapter 5 and 6), caused TatA to vacate its constitutive site on TatC TM6, and be replaced with a weaker association with TatB and perhaps a reorientation on TatC. Co-purification experiments in Chapter 3 required Tat components to be solubilised, dissipating the PMF entirely, and likely explaining why so little TatA was found to be associated with TatBC in this context. Indeed, it appears that the constitutive TatA interaction at TatC TM6 requires an active PMF to be held in place.

It is conceivable that the experimental conditions where the Tat system was examined in de-energised membranes or detergent solution, as was the case in many of the early studies examining interactions between Tat subunits (See Chapter 3, Section 3.1.2), present a bias towards TatB-TatC interactions that would not necessarily be found *in vivo* with an intact PMF. Indeed, this work demonstrated that TatA required the PMF to interact with its constitutive site at TatC TM6, while crosslinking performed by Johann Habersetzer showed that TatB could still interact with its constitutive site at TatC TM5 with PMF dissipation, while also associating with the presumably vacated TatA constitutive site (Chapter 6, Section 6.4.3). Taking the discrepancy between *in vitro* and

in vivo experiments into account, in *E. coli* living cells with an intact PMF, it appears that TatA constitutively occupies a site at TatC TM6 (Chapters 5 and 6), while TatB constitutively occupies a site at TatC TM5 (data from Johann Habersetzer in Section 6.4.3).

A model proposed by Blummel *et al.* (2015) (here referred to as the Muller model) suggested a tetrameric state of TatC, based on the number of TatC linked *via* photo-crosslinking, with four TatB proteins associated at the centre of the complex (Chapter 1, Section 1.10.5), though the work acknowledges that the model would be compatible with further oligomeric states of TatC. The proposed schematic complex shown in Fig. 7.1 is compatible with dimeric, trimeric and tetrameric *etc.* states of the Tat complex and has taken the schematic diagram of the TatBC complex adapted from the Muller model and inserted TatA based on crosslinks seen in this work. A trimeric form of the complex is also shown alongside this.

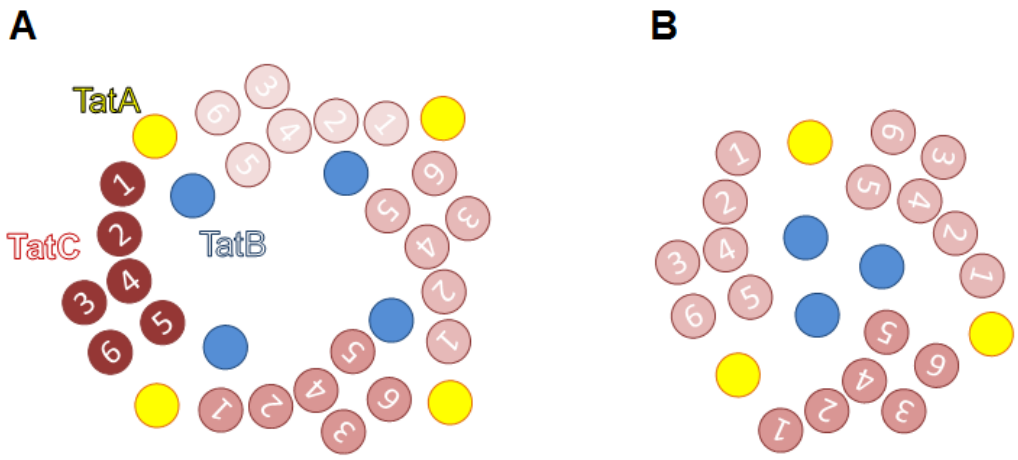

Figure 7.1) Schematic organisation of tetrameric and trimeric Tat complexes viewed from the periplasm- A- shows TatA (yellow), TatB (blue) and TatC (red) arranged with four TatC proteins, with TatB interacting with TatC TM5 and TM2. TatA is at TatC TM6. Based on a model presented by Blummel *et al.* (2015). **B**- a trimeric representation of **A**

No significant TatC homodimerisation has been observed through Cys substitutions F213C in TM6 and M205C in TM5 in this work in the resting state, and this is in agreement with the model presented in Fig. 7.1. Indeed, no other study to date has crosslinked *E. coli* TatC to itself *in vivo* in a Tat system unable to bind substrate, and as

such, it is difficult to incorporate what little data on TatC-TatC interactions seen under these conditions into the model in Fig. 7.1. While Cleon *et al.* (2015) did perform crosslinking *in vivo* observing TatC self-interactions through the periplasmic cap, given the presence of endogenous substrates binding the Tat system in these experiments, it is difficult to determine whether these would still be present in a Tat system unable to bind substrate.

Two models are proposed for a resting Tat system which were produced by Dr Phillip Stansfeld (University of Oxford) using HADDOCK (High Ambiguity Driven protein-protein DOCKing) software, informed by the crosslinks found in this study combined with those observed by Johann Habersetzer (presented in Chapter 6, Section 6.4.1). A tetrameric model (four of each Tat subunit) reminiscent of the Muller model, but incorporating TatA, is shown in Fig. 7.2. Here the transmembrane helix of TatA can be seen associated with TM6 of each TatC monomer in the complex, with TatB associated with TatC TM5 and relatively near the TM2 of another TatC monomer. The four TatC monomers arrange in a square-shape, leaning inwards slightly forming a dome with the TatB transmembrane helices inside. As in the Muller model, this arrangement leaves a groove between the TM6 of one TatC and the TM1/2 of another. Molecular modelling, performed by Dr Stansfeld, was able to place TatA in this groove based on crosslinks performed in this work, which is presented in Fig. 7.2. Notably, a cavity is present in the complex at the periplasmic facing part, which would allow access to the cytoplasm unless blocked. Regions proposed to be important in binding signal sequence are freely accessible at the cytoplasmic facing part of the complex. This includes the inner concave face, cytoplasmic parts of TM1 and TM2, the second cytoplasmic loop and part of TM5 of each TatC monomer where the Tat signal sequence has been proposed to bind in previous literature (Rollauer *et al.,* 2012, Zoufaly *et al*., 2012, Blummel *et al*., 2012, Alcock *et al*., 2012, Holzapfel *et al*., 2006). This would indicate that the Tat signal sequence interacts deep within the centre of the Tat complex, explaining extensive signal sequence-TatB crosslinks observed previously (Blummel *et al*., 2015).

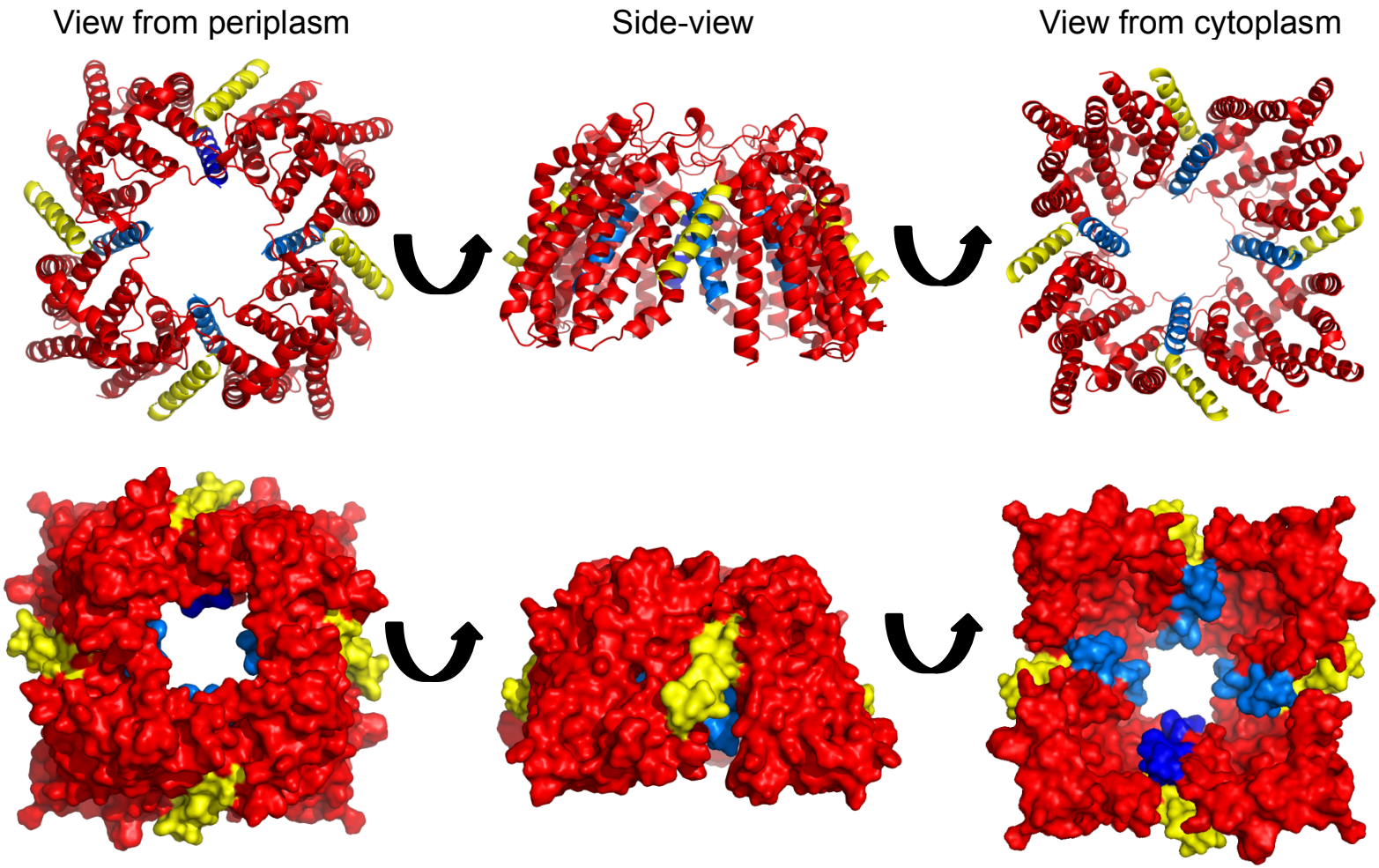

Figure 7.2) Model of tetrameric resting state Tat system- produced by Dr Phillip Stansfeld (University of Oxford) using HADDOCK (High Ambiguity Driven protein-protein DOCKing) software informed by the crosslinks found in this study. **Top-** cartoon representations of TatA (yellow), TatB (blue) and TatC (red) show three orientations of the complex. **Bottom**- shows surface representations of the proteins. Figures made using pyMOL.

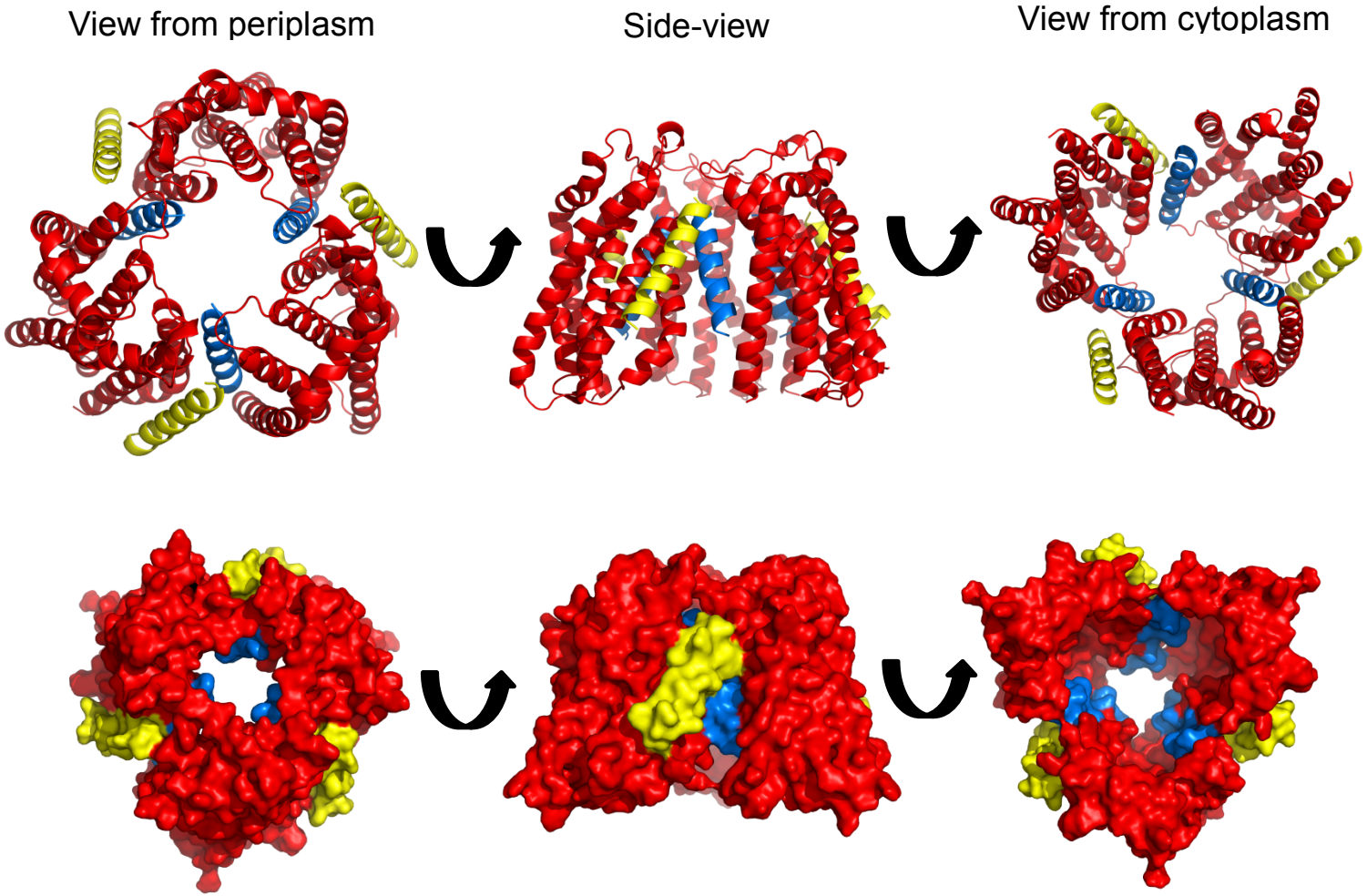

Figure 7.3) Model of trimeric resting state Tat system- produced by Dr Phillip Stansfeld (University of Oxford) using HADDOCK (High Ambiguity Driven protein-protein DOCKing) software informed by the crosslinks found in this study. **Top-** cartoon representations of TatA (yellow), TatB (blue) and TatC (red) show three orientations of the complex. **Bottom**- shows surface representations of the proteins. Figures made using pyMOL.

Fig. 7.3 shows a trimeric version of the model presented in Fig. 7.2, here the subunit arrangement is tighter, as expected, however, the proposed signal sequence binding sites on TatC are still freely accessible from the cytoplasm. The base of the complex is triangular, however, the dome shape is still retained. Although the 3-dimensional electron microscopy structures of the TatBC complex present a much larger structure, the hemicircular dome shape was shared with the complexes proposed in this study, along with a hollow inner cavity (Tarry *et al.,* 2009).

Indeed, the disparity between the reported or proposed sizes of the Tat resting complex (Chapter 1, Section 1.10.5) is a key factor that needs to be addressed in updating the proposed models. While they do not directly address the number of subunits in a resting Tat complex, the models presented in Fig. 7.2 and 7.3 provide a guideline for the development of crosslinking experiments to potentially link the complex together through Cys mutations. Future attempts at linking the complex together in this manner would benefit from having the complex in the resting state by blocking binding to substrate and preventing subunit rearrangement steps. Performing experiments *in vivo* would also remove any potential detergent effects or effects derived from PMF dissipation.

7.2 Subunit rearrangement during Tat export

Evidence presented in Chapter 6 indicates that TatA and TatB swap sites in response to substrate overexpression, implying that substrate binding causes TatB to vacate its constitutive site at TatC TM5, allowing TatA to move from TM6 to occupy TM5. While a simple remapping of TatA/B interactions with TatC can be performed to demonstrate an organisation of subunit in during this stage (as shown in Chapter 6, Section 6.4.2), it is difficult to factor in the increased TatC-TatC homodimerisation which occurs through Cys residues incorporated at TM5 and TM6. The presence of TatA and TatB on TatC would very likely preclude TatC self-interactions through this region (Dr Stansfeld, personal correspondence). Chapter 6, Fig. 6.25 attempted to factor in the TatC self-

interaction through M205C while accommodating TatB and TatA, however, this proposed arrangement was a diagram of crosslinks, as opposed to a model derived from a docking program, as used in this Section. Indeed, the diagram in Chapter 6, Fig 6.25 did not satisfy crosslinks between TatC TM6 and did not take into account the interaction energy between the proteins, so it is unknown how favourable this interaction would be. The difficulty in reconciling all crosslinks observed during substrate overexpression into one model may result from multi-step interactions occurring during Tat transport, or perhaps an asymmetry within the complex at this stage of the Tat cycle.

With regard to further TatA associations with the Tat recognition complex after substrate binding, the formation of TatA oligomers within the centre of the Tat complex, or as a separate entity is discussed in Chapter 5, Section 5.4.4. With regard to the models presented in Fig. 7.2 and 7.3, TatA may oligomerise in the centre of the Tat complex, scaffolding on the face of each TatC monomer to disrupt a localised area of membrane as a one-size-fits-all for each Tat substrate to be transported across the membrane. It should be noted, however, that this localised area of membrane disruption would be too small to transport all Tat substrates (*e.g.* Formate dehydrogenase), and as such the complex may expand outwards or accommodate further Tat subunits, though Alcock *et al.* (2013) found no evidence of an increase in TatB and TatC subunits within the Tat complex upon overexpression of substrate. An advantage of the hypothesis that TatA forms a separate oligomeric ring is that polymerisation can occur indefinitely until the ring size matches that of the substrate.

7.3 An updated Tat cycle

While many questions still remain to be addressed, the work presented in this thesis can inform a proposed updated Tat cycle. A comparison can be made between the proposed Tat cycle before this work was undertaken in Chapter 1, Section 1.12, and after in Fig. 7.4. This updated cycle begins with a TatABC recognition complex with the

TatA transmembrane helix further towards the periplasm unable to exert its membrane-disputing behaviour. Then the following steps occur: 1) The Tat signal sequence binds TatC within the concave face (as proposed in Blummel *et al.*, 2015, Ramasamy *et al.*, 2013, Aldridge *et al.*, 2014), which leads to TatA and TatB swapping sites on TatC (though, as discussed in Chapter 6, Section 6.4.2, this may involve movement across two TatC monomers, not shown for clarity). 2) TatA moves towards the concave face of TatC and begins to disrupt the membrane. 3) Further TatA monomers join the complex (Fig. 7.4 acknowledges that the TatA multimer may be scaffolding within the Tat complex as opposed to forming a discrete ring-shaped oligomer as discussed in Chapter 5, Section 5.4.4) forming a membrane-disrupting multimer. 4) Once the membrane is sufficiently disrupted the substrate is able to be translocated. 5) The signal sequence is cleaved and the substrate is released into the periplasm. 6) The system falls back into its resting state.

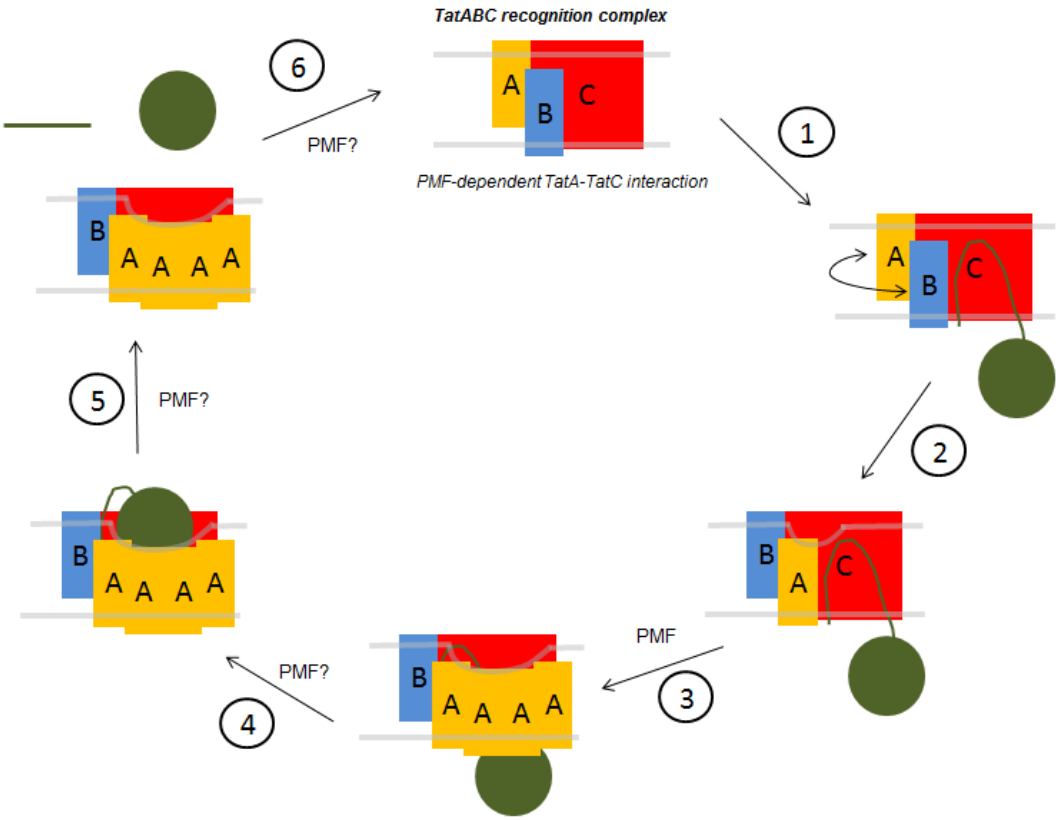

Figure 7.4) Updated Model of Tat transport- TatA (yellow), TatB (blue) and TatC (red) are shown in the membrane, with substrate (green) containing the twin arginine (RR) signal peptide.

7.4 Perspectives

When the work in this thesis began, a crystal structure of TatC from *Aquifex aeolicus* had just been published (Rollauer *et al*., 2012), while the latest Tat transport models assumed that TatA was primarily involved in forming an oligomeric pore which transported substrates bound to a discrete TatBC recognition complex. Over the course of this work, NMR structures of *E. coli* TatA (Rodrigues *et al.*, 2013) and TatB (Zhang *et al.*, 2014) emerged, which allowed for the detailed models presented in this Chapter. Not only have the crosslinks presented in this thesis built on previous literature (primarily Blummel *et al*., 2015 and Aldridge *et al*., 2014), leading to the modelling of proposed resting state Tat complexes, but the role of TatA has expanded beyond "pore-forming", taking on significance in the resting Tat complex which was previously thought to contain primarily/only TatBC. While the above represents significant steps taken in characterising the mechanism of Tat transport, many questions still remain. For example, the specific manner in which TatA oligomerises and how the substrate is translocated through the Tat system is still unknown. Furthermore, precise oligomerisation states of TatC are still contentious, with models ranging from dimer to octamer, though with improvements in electron microscopy technology and a resting state Tat complex model to identify TatC self-interaction faces, there is well-placed optimism that this will be settled in the future. Finally, through a comparison of Tat protein interaction data in detergent solution and *in vivo*, the work presented in this thesis could perhaps serve as cautionary tale for studying any membrane protein interactions, providing a case study whereby removing membrane proteins from their native environment can drastically alter their properties.

Bibliography

Akiyama, Y. & K. Ito, (1993) Folding and assembly of bacterial alkaline phosphatase *in vitro* and *in vivo*. ***The journal of biological chemistry,* 268**: 8146-8150.

Alami, M., I. Luke, S. Deitermann, G. Eisner, H. G. Koch, J. Brunner & M. Muller, (2003) Differential interactions between a twin-arginine signal peptide and its translocase in *Escherichia coli*. ***Molecular cell,* 12**: 937-946.

Alcock, F., M. A. Baker, N. P. Greene, T. Palmer, M. I. Wallace & B. C. Berks, (2013) Live cell imaging shows reversible assembly of the TatA component of the twin-arginine protein transport system. ***Proceedings of the National Academy of Sciences of the United States of America,* 110**: E3650-3659.

Alder, N. N. & S. M. Theg, (2003) Energetics of protein transport across biological membranes a study of the thylakoid DeltapH-dependent/cpTat pathway. ***Cell,* 112**: 231-242.

Aldridge, C., X. Ma, F. Gerard & K. Cline, (2014) Substrate-gated docking of pore subunit Tha4 in the TatC cavity initiates Tat translocase assembly. ***The journal of cell biology,* 205**: 51-65.

Allen, S. C., C. M. Barrett, N. Ray & C. Robinson, (2002) Essential cytoplasmic domains in the *Escherichia coli* TatC protein. ***The journal of biological chemistry,* 277**: 10362-10366.

Angelini, S., S. Deitermann & H. G. Koch, (2005) FtsY, the bacterial signal-recognition particle receptor, interacts functionally and physically with the SecYEG translocon. ***EMBO Reports,* 6**: 476-481.

Bageshwar, U. K. & S. M. Musser, (2007) Two electrical potential-dependent steps are required for transport by the *Escherichia coli* Tat machinery. ***The journal of cell biology,* 179**: 87-99.

Barnett, J. P., R. T. Eijlander, O. P. Kuipers & C. Robinson, (2008) A minimal Tat system from a gram-positive organism: a bifunctional TatA subunit participates in discrete TatAC and TatA complexes. ***The journal of biological chemistry,* 283**: 2534-2542.

Barrett, C. M., D. Mangels & C. Robinson, (2005) Mutations in subunits of the *Escherichia coli* twin-arginine translocase block function via differing effects on translocation activity or tat complex structure. ***Journal of molecular biology,* 347**: 453-463.

Bauer, B. W. & T. A. Rapoport, (2009) Mapping polypeptide interactions of the SecA ATPase during translocation. ***Proceedings of the National Academy of Sciences of the United States of America,* 106**: 20800-20805.

Bechtluft, P., N. Nouwen, S. J. Tans & A. J. Driessen, (2010) SecB--a chaperone dedicated to protein translocation. ***Molecular Biosystems,* 6**: 620-627.

Beck, K., G. Eisner, D. Trescher, R. E. Dalbey, J. Brunner & M. Muller, (2001) YidC, an assembly site for polytopic *Escherichia coli* membrane proteins located in immediate proximity to the SecYE translocon and lipids. ***EMBO Reports,* 2**: 709-714.

Behrendt, J., U. Lindenstrauss & T. Bruser, (2007) The TatBC complex formation suppresses a modular TatB-multimerization in *Escherichia coli*. ***FEBS letters,* 581**: 4085-4090.

Behrendt, J., K. Standar, U. Lindenstrauss & T. Bruser, (2004) Topological studies on the twin-arginine translocase component TatC. ***FEMS Microbiology Letters,* 234**: 303-308.

Benoit, S. & R. J. Maier, (2003) Dependence of *Helicobacter pylori* urease activity on the nickel-sequestering ability of the UreE accessory protein. ***Journal of bacteriology,* 185**: 4787-4795.

Benoit, S. L. & R. J. Maier, (2011) Mua (HP0868) is a nickel-binding protein that modulates urease activity in *Helicobacter pylori*. ***MBio,* 2**: e00039-00011.

Berks, B. C., (1996) A common export pathway for proteins binding complex redox cofactors? ***Molecular microbiology,* 22**: 393-404.

Bernstein, H. D., D. Zopf, D. M. Freymann & P. Walter, (1993) Functional substitution of the signal recognition particle 54-kDa subunit by its *Escherichia coli* homolog. ***Proceedings of the National Academy of Sciences of the United States of America,* 90**: 5229-5233.

Blaudeck, N., P. Kreutzenbeck, M. Muller, G. A. Sprenger & R. Freudl, (2005) Isolation and characterization of bifunctional *Escherichia coli* TatA mutant proteins that allow efficient *tat*-dependent protein translocation in the absence of TatB. ***The journal of biological chemistry,* 280**: 3426-3432.

Blummel, A. S., L. A. Haag, E. Eimer, M. Muller & J. Frobel, (2015) Initial assembly steps of a translocase for folded proteins. ***Nature Communications,* 6**: 7234.

Bogsch, E., S. Brink & C. Robinson, (1997) Pathway specificity for a delta pH-dependent precursor thylakoid lumen protein is governed by a 'Sec-avoidance' motif in the transfer peptide and a 'Sec-incompatible' mature protein. ***The EMBO journal,* 16**: 3851-3859.

Bogsch, E. G., F. Sargent, N. R. Stanley, B. C. Berks, C. Robinson & T. Palmer, (1998) An essential component of a novel bacterial protein export system with homologues in plastids and mitochondria. ***The journal of biological chemistry,* 273**: 18003-18006.

Bolhuis, A., J. E. Mathers, J. D. Thomas, C. M. Barrett & C. Robinson, (2001) TatB and TatC form a functional and structural unit of the twin-arginine translocase from *Escherichia coli*. ***The journal of biological chemistry,* 276**: 20213-20219.

Briggs, M. S., D. G. Cornell, R. A. Dluhy & L. M. Gierasch, (1986) Conformations of signal peptides induced by lipids suggest initial steps in protein export. ***Science,* 233**: 206-208.

Brundage, L., J. P. Hendrick, E. Schiebel, A. J. Driessen & W. Wickner, (1990) The purified *E. coli* integral membrane protein SecY/E is sufficient for reconstitution of SecA-dependent precursor protein translocation. ***Cell,* 62**: 649-657.

Buchanan, G., E. de Leeuw, N. R. Stanley, M. Wexler, B. C. Berks, F. Sargent & T. Palmer, (2002) Functional complexity of the twin-arginine translocase TatC component revealed by site-directed mutagenesis. ***Molecular microbiology,* 43**: 1457-1470.

Buchanan, G., F. Sargent, B. C. Berks & T. Palmer, (2001) A genetic screen for suppressors of *Escherichia coli* Tat signal peptide mutations establishes a critical role for the second arginine within the twin-arginine motif. ***Archives of microbiology,* 177**: 107-112.

Chaddock, A. M., A. Mant, I. Karnauchov, S. Brink, R. G. Herrmann, R. B. Klosgen & C. Robinson, (1995) A new type of signal peptide: central role of a twin-arginine motif in transfer signals for the delta pH-dependent thylakoidal protein translocase. ***The EMBO journal,* 14**: 2715-2722.

Chang, C. Y., L. Hobley, R. Till, M. Capeness, M. Kanna, W. Burtt, P. Jagtap, S. Aizawa & R. E. Sockett, (2011) The *Bdellovibrio bacteriovorus* twin-arginine transport system has roles in predatory and prey-independent growth. ***Microbiology,* 157**: 3079-3093.

Chen, Y., B. W. Bauer, T. A. Rapoport & J. C. Gumbart, (2015) Conformational Changes of the Clamp of the Protein Translocation ATPase SecA. ***Journal of molecular biology***, **427**: 2348-2359.

Chimerel, C., C. M. Field, S. Pinero-Fernandez, U. F. Keyser & D. K. Summers, (2012) Indole prevents *Escherichia coli* cell division by modulating membrane potential. ***Biochimica et Biophysica Acta,* 1818**: 1590-1594.

Chimerel, C., A. J. Murray, E. R. Oldewurtel, D. K. Summers & U. F. Keyser, (2013) The effect of bacterial signal indole on the electrical properties of lipid membranes. ***Chemphyschem,* 14**: 417-423.

Cleon, F., J. Habersetzer, F. Alcock, H. Kneuper, P. J. Stansfeld, H. Basit, M. I. Wallace, B. C. Berks & T. Palmer, (2015) The TatC component of the twin-arginine protein translocase functions as an obligate oligomer. ***Molecular microbiology,* 98**: 111-129.

Cline, K., W. F. Ettinger & S. M. Theg, (1992) Protein-specific energy requirements for protein transport across or into thylakoid membranes. Two lumenal proteins are transported in the absence of ATP. ***The journal of biological chemistry,* 267**: 2688-2696.

Cline, K. & M. McCaffery, (2007) Evidence for a dynamic and transient pathway through the TAT protein transport machinery. ***The EMBO journal,* 26**: 3039-3049.

Cline, K. & H. Mori, (2001) Thylakoid DeltapH-dependent precursor proteins bind to a cpTatC-Hcf106 complex before Tha4-dependent transport. ***The journal of cell biology,* 154**: 719-729.

Collier, D. N., V. A. Bankaitis, J. B. Weiss & P. J. Bassford, Jr., (1988) The antifolding activity of SecB promotes the export of the *E. coli* maltose-binding protein. ***Cell,* 53**: 273-283.

Collinson, I., R. A. Corey & W. J. Allen, (2015) Channel crossing: how are proteins shipped across the bacterial plasma membrane? ***Philosphical Transactions of the Royal Soceity of London Biological Sciences,* 370:** 20150025

Cristobal, S., J. W. de Gier, H. Nielsen & G. von Heijne, (1999) Competition between Sec- and TAT-dependent protein translocation in *Escherichia coli*. ***The EMBO journal,* 18**: 2982-2990.

Dabney-Smith, C. & K. Cline, (2009) Clustering of C-Terminal Stromal Domains of Tha4 Homo-Oligomers during Translocation by the Tat Protein Transport System. ***Molecular biology of the cell.* 20(7)**: 2060–2069

Dabney-Smith, C., H. Mori & K. Cline, (2006) Oligomers of Tha4 organize at the thylakoid Tat translocase during protein transport. ***The journal of biological chemistry,* 281**: 5476-5483.

Dalbey, R. E., P. Wang & A. Kuhn, (2011) Assembly of bacterial inner membrane proteins. ***Annual review of biochemistry,* 80**: 161-187.

De Buck, E., E. Lammertyn & J. Anne, (2008) The importance of the twin-arginine translocation pathway for bacterial virulence. ***Trends in microbiology,* 16**: 442-453.

de Gier, J. W. & J. Luirink, (2001) Biogenesis of inner membrane proteins in *Escherichia coli*. ***Molecular Microbiology,* 40**: 314-322.

de Keyzer, J., E. O. van der Sluis, R. E. Spelbrink, N. Nijstad, B. de Kruijff, N. Nouwen, C. van der Does & A. J. Driessen, (2005) Covalently dimerized SecA is functional in protein translocation. ***The journal of biological chemistry,* 280**: 35255-35260.

de Leeuw, E., T. Granjon, I. Porcelli, M. Alami, S. B. Carr, M. Muller, F. Sargent, T. Palmer & B. C. Berks, (2002) Oligomeric properties and signal peptide binding by *Escherichia coli* Tat protein transport complexes. ***Journal of molecular biology,* 322**: 1135-1146.

De Leeuw, E., I. Porcelli, F. Sargent, T. Palmer & B. C. Berks, (2001) Membrane interactions and self-association of the TatA and TatB components of the twin-arginine translocation pathway. ***FEBS letters,* 506**: 143-148.

DeLisa, M. P., P. Samuelson, T. Palmer & G. Georgiou, (2002) Genetic analysis of the twin arginine translocator secretion pathway in bacteria. ***The journal of biological chemistry,* 277**: 29825-29831.

DeLisa, M. P., D. Tullman & G. Georgiou, (2003) Folding quality control in the export of proteins by the bacterial twin-arginine translocation pathway. ***Proceedings of the National Academy of Sciences of the United States of America,* 100**: 6115-6120.

Dilks, K., M. I. Gimenez & M. Pohlschroder, (2005) Genetic and biochemical analysis of the twin-arginine translocation pathway in halophilic archaea***. Journal of bacteriology,* 187**: 8104-8113.

Dow, J. M., F. Gabel, F. Sargent & T. Palmer, (2013) Characterization of a pre-export enzyme-chaperone complex on the twin-arginine transport pathway. ***The Biochemical journal,* 452**: 57-66.

Dow, J. M., S. Grahl, R. Ward, R. Evans, O. Byron, D. G. Norman, T. Palmer & F. Sargent, (2014) Characterization of a periplasmic nitrate reductase in complex with its biosynthetic chaperone. ***The FEBS journal,* 281**: 246-260.

Drew, D., D. Sjostrand, J. Nilsson, T. Urbig, C. N. Chin, J. W. de Gier & G. von Heijne, (2002) Rapid topology mapping of *Escherichia coli* inner-membrane proteins by prediction and PhoA/GFP fusion analysis. ***Proceedings of the National Academy of Sciences of the United States of America,* 99**: 2690-2695.

Duong, F. & W. Wickner, (1997) Distinct catalytic roles of the SecYE, SecG and SecDFyajC subunits of preprotein translocase holoenzyme. ***EMBO Journal,* 16**: 2756-2768.

Eimer, E., J. Frobel, A. S. Blummel & M. Muller, (2015) TatE as a Regular Constituent of Bacterial Twin-arginine Protein Translocases. ***The journal of biological chemistry,* 290**: 29281-29289.

Englesberg, E., C. Squires & F. Meronk, Jr., (1969) The L-arabinose operon in *Escherichia coli* B-r: a genetic demonstration of two functional states of the product of a regulator gene***. Proceedings of the National Academy of Sciences of the United States of America,* 62**: 1100-1107.

Esko J. D., D. T. L., Raetz C. R. H., (2009) Eubacteria and Archea. In: Essentials of Glycobiology. R. D. C. A. Varki, J. D. Esko, H. H. Freeze, P. Stanley, C. R. Bertozzi, G. W. Hart & M. E. Etzler (ed). Cold Spring Harbor (NY): Cold Spring Harbor Laboratory Press, pp, 2009.

Facey, S. J., S. A. Neugebauer, S. Krauss & A. Kuhn, (2007) The mechanosensitive channel protein MscL is targeted by the SRP to the novel YidC membrane insertion pathway of *Escherichia coli*. ***The journal of molecular biology,* 365**: 995-1004.

Fritsch, M. J., M. Krehenbrink, M. J. Tarry, B. C. Berks & T. Palmer, (2012) Processing by rhomboid protease is required for *Providencia stuartii* TatA to interact with TatC and to form functional homo-oligomeric complexes. ***Molecular Microbiology,* 84**: 1108-1123.

Frobel, J., P. Rose, F. Lausberg, A. S. Blummel, R. Freudl & M. Muller, (2012) Transmembrane insertion of twin-arginine signal peptides is driven by TatC and regulated by TatB. ***Nature Communications,*** **3**: 1311.

Frobel, J., P. Rose & M. Muller, (2011) Early Contacts between Substrate Proteins and TatA Translocase Component in Twin-arginine Translocation. ***The journal of biological chemistry*** **286**: 43679-43689.

Gannon, P. M., P. Li & C. A. Kumamoto, (1989) The mature portion of *Escherichia coli* maltose-binding protein (MBP) determines the dependence of MBP on SecB for export. ***Journal of bacteriology,*** **171**: 813-818.

Gerard, F. & K. Cline, (2006) Efficient twin arginine translocation (Tat) pathway transport of a precursor protein covalently anchored to its initial cpTatC binding site. ***The journal of biological chemistry,*** **281**: 6130-6135.

Gerard, F. & K. Cline, (2007) The thylakoid proton gradient promotes an advanced stage of signal peptide binding deep within the Tat pathway receptor complex. ***The journal of biological chemistry,*** **282**: 5263-5272.

Gohlke, U., L. Pullan, C. A. McDevitt, I. Porcelli, E. de Leeuw, T. Palmer, H. R. Saibil & B. C. Berks, (2005) The TatA component of the twin-arginine protein transport system forms channel complexes of variable diameter. ***Proceedings of the National Academy of Sciences of the United States of America,*** **102**: 10482-10486.

Gold, V. A., S. Whitehouse, A. Robson & I. Collinson, (2013) The dynamic action of SecA during the initiation of protein translocation. ***Biochemical Journal,*** **449**: 695-705.

Grahl, S., J. Maillard, C. A. Spronk, G. W. Vuister & F. Sargent, (2012) Overlapping transport and chaperone-binding functions within a bacterial twin-arginine signal peptide. ***Molecular microbiology,*** **83**: 1254-1267.

Grant, S. G., J. Jessee, F. R. Bloom & D. Hanahan, (1990) Differential plasmid rescue from transgenic mouse DNAs into *Escherichia coli* methylation-restriction mutants. ***Proceedings of the National Academy of Sciences of the United States of America,*** **87**: 4645-4649.

Greene, N. P., I. Porcelli, G. Buchanan, M. G. Hicks, S. M. Schermann, T. Palmer & B. C. Berks, (2007) Cysteine scanning mutagenesis and disulfide mapping studies

of the TatA component of the bacterial twin arginine translocase. ***The journal of biological chemistry,* 282**: 23937-23945.

Hanada, M., K. Nishiyama & H. Tokuda, (1996) SecG plays a critical role in protein translocation in the absence of the proton motive force as well as at low temperature. ***FEBS Letters,* 381**: 25-28.

Hanada, M., K. I. Nishiyama, S. Mizushima & H. Tokuda, (1994) Reconstitution of an efficient protein translocation machinery comprising SecA and the three membrane proteins, SecY, SecE, and SecG (p12). ***The journal of biological chemistry,* 269**: 23625-23631.

Hatzixanthis, K., D. J. Richardson & F. Sargent, (2005) Chaperones involved in assembly and export of N-oxide reductases. ***Biochemical Society transactions,* 33**: 124-126.

Hicks, M. G., E. de Leeuw, I. Porcelli, G. Buchanan, B. C. Berks & T. Palmer, (2003) The *Escherichia coli* twin-arginine translocase: conserved residues of TatA and TatB family components involved in protein transport. ***FEBS letters,* 539**: 61-67.

Hicks, M. G., P. A. Lee, G. Georgiou, B. C. Berks & T. Palmer, (2005) Positive selection for loss-of-function tat mutations identifies critical residues required for TatA activity. ***Journal of bacteriology,* 187**: 2920-2925.

Hitchcock, A., S. J. Hall, J. D. Myers, F. Mulholland, M. A. Jones & D. J. Kelly, (2010) Roles of the twin-arginine translocase and associated chaperones in the biogenesis of the electron transport chains of the human pathogen *Campylobacter jejuni*. ***Microbiology,* 156**: 2994-3010.

Hizlan, D., A. Robson, S. Whitehouse, V. A. Gold, J. Vonck, D. Mills, W. Kuhlbrandt & I. Collinson, (2012) Structure of the SecY complex unlocked by a preprotein mimic. ***Cell Reports,* 1**: 21-28.

Holzapfel, E., G. Eisner, M. Alami, C. M. Barrett, G. Buchanan, I. Luke, J. M. Betton, C. Robinson, T. Palmer, M. Moser & M. Muller, (2007) The entire N-terminal half of TatC is involved in twin-arginine precursor binding. ***Biochemistry,* 46**: 2892-2898.

Hu, Y., E. Zhao, H. Li, B. Xia & C. Jin, (2010) Solution NMR structure of the TatA component of the twin-arginine protein transport system from gram-positive

bacterium *Bacillus subtilis*. ***Journal of the American Chemical Society,*** **132**: 15942-15944.

Hunt, J. F., S. Weinkauf, L. Henry, J. J. Fak, P. McNicholas, D. B. Oliver & J. Deisenhofer, (2002) Nucleotide control of interdomain interactions in the conformational reaction cycle of SecA. ***Science,*** **297**: 2018-2026.

Ismail, N., R. Hedman, M. Linden & G. von Heijne, (2015) Charge-driven dynamics of nascent-chain movement through the SecYEG translocon. ***Nature structural and molecular biology,*** **22**: 145-149.

Ize, B., N. R. Stanley, G. Buchanan & T. Palmer, (2003) Role of the *Escherichia coli* Tat pathway in outer membrane integrity. ***Molecular microbiology,*** **48**: 1183-1193.

Jack, R. L., G. Buchanan, A. Dubini, K. Hatzixanthis, T. Palmer & F. Sargent, (2004) Coordinating assembly and export of complex bacterial proteins. ***The EMBO journal,*** **23**: 3962-3972.

Jack, R. L., F. Sargent, B. C. Berks, G. Sawers & T. Palmer, (2001) Constitutive expression of *Escherichia coli* tat genes indicates an important role for the twin-arginine translocase during aerobic and anaerobic growth. ***Journal of bacteriology,*** **183**: 1801-1804.

Jilaveanu, L. B. & D. Oliver, (2006) SecA dimer cross-linked at its subunit interface is functional for protein translocation. ***Journal of bacteriology,*** **188**: 335-338.

Jongbloed, J. D., U. Grieger, H. Antelmann, M. Hecker, R. Nijland, S. Bron & J. M. van Dijl, (2004) Two minimal Tat translocases in Bacillus. ***Molecular microbiology,*** **54**: 1319-1325.

Kihara, A., Y. Akiyama & K. Ito, (1999) Dislocation of membrane proteins in FtsH-mediated proteolysis. ***EMBO Journal,*** **18**: 2970-2981.

Kneuper, H., B. Maldonado, F. Jager, M. Krehenbrink, G. Buchanan, R. Keller, M. Muller, B. C. Berks & T. Palmer, (2012) Molecular dissection of TatC defines critical regions essential for protein transport and a TatB-TatC contact site. ***Molecular microbiology***, **85(5)**:945-61

Koch, S., M. J. Fritsch, G. Buchanan & T. Palmer, (2012) The *Escherichia coli* TatA and TatB proteins have an N-out C-in topology in intact cells. ***The journal of biological chemistry***, **18**:14420-31

Koonin, E. V. & A. E. Gorbalenya, (1992) Autogenous translation regulation by *Escherichia coli* ATPase SecA may be mediated by an intrinsic RNA helicase activity of this protein. ***FEBS Letters,* 298**: 6-8.

Kreutzenbeck, P., C. Kroger, F. Lausberg, N. Blaudeck, G. A. Sprenger & R. Freudl, (2007) *Escherichia coli* twin arginine (Tat) mutant translocases possessing relaxed signal peptide recognition specificities. ***The journal of biological chemistry,* 282**: 7903-7911.

Kuhn, P., B. Weiche, L. Sturm, E. Sommer, F. Drepper, B. Warscheid, V. Sourjik & H. G. Koch, (2011) The bacterial SRP receptor, SecA and the ribosome use overlapping binding sites on the SecY translocon. ***Traffic,* 12**: 563-578.

Kumazaki, K., T. Kishimoto, A. Furukawa, H. Mori, Y. Tanaka, N. Dohmae, R. Ishitani, T. Tsukazaki & O. Nureki, (2014) Crystal structure of *Escherichia coli* YidC, a membrane protein chaperone and insertase. ***Scientific Reports,* 4**: 7299.

Lausberg, F., S. Fleckenstein, P. Kreutzenbeck, J. Frobel, P. Rose, M. Muller & R. Freudl, (2012) Genetic evidence for a tight cooperation of TatB and TatC during productive recognition of twin-arginine (Tat) signal peptides in *Escherichia coli*. ***PLoS One,* 7**: e39867.

Leake, M. C., N. P. Greene, R. M. Godun, T. Granjon, G. Buchanan, S. Chen, R. M. Berry, T. Palmer & B. C. Berks, (2008) Variable stoichiometry of the TatA component of the twin-arginine protein transport system observed by *in vivo* single-molecule imaging. ***Proceedings of the National Academy of Sciences of the United States of America,* 105**: 15376-15381.

Lee, J. H. & J. Lee, (2010) Indole as an intercellular signal in microbial communities. ***FEMS Microbiology Reviews,* 34**: 426-444.

Lee, P. A., G. Buchanan, N. R. Stanley, B. C. Berks & T. Palmer, (2002) Truncation analysis of TatA and TatB defines the minimal functional units required for protein translocation. ***Journal of bacteriology,* 184**: 5871-5879.

Lee, P. A., G. L. Orriss, G. Buchanan, N. P. Greene, P. J. Bond, C. Punginelli, R. L. Jack, M. S. Sansom, B. C. Berks & T. Palmer, (2006a) Cysteine-scanning mutagenesis and disulfide mapping studies of the conserved domain of the twin-arginine translocase TatB component. ***The journal of biological chemistry,* 281**: 34072-34085.

Lee, P. A., G. L. Orriss, G. Buchanan, N. P. Greene, P. J. Bond, C. Punginelli, R. L. Jack, M. S. Sansom, B. C. Berks & T. Palmer, (2006b) Cysteine-scanning mutagenesis and disulfide mapping studies of the conserved domain of the twin-arginine translocase TatB component. ***The journal of Biological Chemistry,* 281**: 34072-34085.

Li, H., D. Faury & R. Morosoli, (2006) Impact of amino acid changes in the signal peptide on the secretion of the Tat-dependent xylanase C from *Streptomyces lividan*s. ***FEMS microbiology letters,* 255**: 268-274.

Li, L., E. Park, J. Ling, J. Ingram, H. Ploegh & T. A. Rapoport, (2016) Crystal structure of a substrate-engaged SecY protein-translocation channel. ***Nature,* 531**: 395-399.

Liu, G., T. B. Topping & L. L. Randall, (1989) Physiological role during export for the retardation of folding by the leader peptide of maltose-binding protein. ***Proceedings of the National Academy of Sciences of the United States of America,* 86**: 9213-9217.

Luirink, J., G. von Heijne, E. Houben & J. W. de Gier, (2005) Biogenesis of inner membrane proteins in *Escherichia coli*. ***Annual Review of Microbiology,* 59**: 329-355.

Lycklama a Nijeholt, J. A., J. de Keyzer, I. Prabudiansyah & A. J. Driessen, (2013) Characterization of the supporting role of SecE in protein translocation***. FEBS Letters,* 587**: 3083-3088.

Ma, X. & K. Cline, (2010) Multiple precursor proteins bind individual Tat receptor complexes and are collectively transported. ***The EMBO journal,* 29**: 1477-1488.

Ma, X. & K. Cline, (2013) Mapping the signal peptide binding and oligomer contact sites of the core subunit of the pea twin arginine protein translocase. ***The Plant cell,* 25**: 999-1015.

Maier, T., F. Lottspeich & A. Bock, (1995) GTP hydrolysis by HypB is essential for nickel insertion into hydrogenases of *Escherichia coli*. ***European journal of biochemistry / FEBS,* 230**: 133-138.

Maldonado, B., G. Buchanan, M. Muller, B. C. Berks & T. Palmer, (2011) Genetic evidence for a TatC dimer at the core of the *Escherichia coli* twin arginine (Tat)

protein translocase. ***Journal of molecular microbiology and biotechnology,*** **20**: 168-175.

Matsuyama, S., Y. Fujita & S. Mizushima, (1993) SecD is involved in the release of translocated secretory proteins from the cytoplasmic membrane of *Escherichia coli.* ***The EMBO journal,*** **12**: 265-270.

Maurer, C., S. Panahandeh, A. C. Jungkamp, M. Moser & M. Muller, (2010) TatB functions as an oligomeric binding site for folded Tat precursor proteins. ***Molecular biology of the cell,*** **21**: 4151-4161.

McDevitt, C. A., G. Buchanan, F. Sargent, T. Palmer & B. C. Berks, (2006) Subunit composition and in vivo substrate-binding characteristics of *Escherichia coli* Tat protein complexes expressed at native levels. ***The FEBS journal,*** **273**: 5656-5668.

Mendel, S., A. McCarthy, J. P. Barnett, R. T. Eijlander, A. Nenninger, O. P. Kuipers & C. Robinson, (2008) The *Escherichia coli* TatABC system and a *Bacillus subtilis* TatAC-type system recognise three distinct targeting determinants in twin-arginine signal peptides. ***Journal of molecular biology,*** **375**: 661-672.

Mileykovskaya, E. & W. Dowhan, (2000) Visualization of phospholipid domains in *Escherichia coli* by using the cardiolipin-specific fluorescent dye 10-N-nonyl acridine orange. ***The journal of Bacteriology,*** **182**: 1172-1175.

Mori, H. & K. Cline, (2002) A twin arginine signal peptide and the pH gradient trigger reversible assembly of the thylakoid [Delta]pH/Tat translocase. ***The journal of cell biology,*** **157**: 205-210.

Mould, R. M. & C. Robinson, (1991) A proton gradient is required for the transport of two lumenal oxygen-evolving proteins across the thylakoid membrane. ***The journal of biological chemistry,*** **266**: 12189-12193.

Nishibori, A., J. Kusaka, H. Hara, M. Umeda & K. Matsumoto, (2005) Phosphatidylethanolamine domains and localization of phospholipid synthases in Bacillus subtilis membranes. ***Journal of Bacteriology,*** **187**: 2163-2174.

Nouwen, N. & A. J. Driessen, (2005) Inactivation of protein translocation by cold-sensitive mutations in the yajC-secDF operon. ***Journal of Bacteriology,*** **187**: 6852-6855.

Oates, J., C. M. Barrett, J. P. Barnett, K. G. Byrne, A. Bolhuis & C. Robinson, (2005) The *Escherichia coli* twin-arginine translocation apparatus incorporates a

distinct form of TatABC complex, spectrum of modular TatA complexes and minor TatAB complex. ***Journal of molecular biology,* 346**: 295-305.

Oates, J., J. Mathers, D. Mangels, W. Kuhlbrandt, C. Robinson & K. Model, (2003) Consensus structural features of purified bacterial TatABC complexes. ***Journal of molecular biology,* 330**: 277-286.

Or, E., D. Boyd, S. Gon, J. Beckwith & T. Rapoport, (2005) The bacterial ATPase SecA functions as a monomer in protein translocation. ***The journal of Biological Chemistry,* 280**: 9097-9105.

Or, E., A. Navon & T. Rapoport, (2002) Dissociation of the dimeric SecA ATPase during protein translocation across the bacterial membrane. ***EMBO journal,* 21**: 4470-4479.

Oresnik, I. J., C. L. Ladner & R. J. Turner, (2001) Identification of a twin-arginine leader-binding protein. ***Molecular microbiology,* 40**: 323-331.

Orriss, G. L., M. J. Tarry, B. Ize, F. Sargent, S. M. Lea, T. Palmer & B. C. Berks, (2007) TatBC, TatB, and TatC form structurally autonomous units within the twin arginine protein transport system of Escherichia coli. ***FEBS letters,* 581**: 4091-4097.

Osborne, A. R., W. M. Clemons, Jr. & T. A. Rapoport, (2004) A large conformational change of the translocation ATPase SecA. ***Proceedings of the National Academy of Sciences of the United States of America,* 101**: 10937-10942.

Osman, C., D. R. Voelker & T. Langer, (2011) Making heads or tails of phospholipids in mitochondria. ***The Journal of cell biology,* 192**: 7-16.

Palmer, T. & B. C. Berks, (2012) The twin-arginine translocation (Tat) protein export pathway. ***Nature Reviews Microbiology,* 10**: 483-496.

Palmer, T., F. Sargent & B. C. Berks, (2010) The Tat Protein Export Pathway. ***EcoSal Plus 4***. Washington, DC: ASM Press.

Panahandeh, S., C. Maurer, M. Moser, M. P. DeLisa & M. Muller, (2008) Following the path of a twin-arginine precursor along the TatABC translocase of Escherichia coli. ***The journal of biological chemistry,* 283**: 33267-33275.

Papanikolau, Y., M. Papadovasilaki, R. B. Ravelli, A. A. McCarthy, S. Cusack, A. Economou & K. Petratos, (2007) Structure of dimeric SecA, the *Escherichia coli*

preprotein translocase motor. ***The journal of molecular biology,*** **366**: 1545-1557.

Pickering, B. S. & I. J. Oresnik, (2010) The twin arginine transport system appears to be essential for viability in *Sinorhizobium meliloti.* ***Journal of bacteriology,*** **192**: 5173-5180.

Pogliano, J. A. & J. Beckwith, (1994) SecD and SecF facilitate protein export in Escherichia coli. ***EMBO Journal,*** **13**: 554-561.

Porcelli, I., E. de Leeuw, R. Wallis, E. van den Brink-van der Laan, B. de Kruijff, B. A. Wallace, T. Palmer & B. C. Berks, (2002) Characterization and membrane assembly of the TatA component of the *Escherichia coli* twin-arginine protein transport system. ***Biochemistry,*** **41**: 13690-13697.

Punginelli, C., B. Maldonado, S. Grahl, R. Jack, M. Alami, J. Schroder, B. C. Berks & T. Palmer, (2007) Cysteine scanning mutagenesis and topological mapping of the *Escherichia coli* twin-arginine translocase TatC Component. ***Journal of bacteriology,*** **189**: 5482-5494.

Raetz, C. R. & C. Whitfield, (2002) Lipopolysaccharide endotoxins. ***Annual Reviews Biochemistry,*** **71**: 635-700.

Ramasamy, S., R. Abrol, C. J. Suloway & W. M. Clemons, Jr., (2013) The glove-like structure of the conserved membrane protein TatC provides insight into signal sequence recognition in twin-arginine translocation. ***Structure,*** **21**: 777-788.

Richter, S., U. Lindenstrauss, C. Lucke, R. Bayliss & T. Bruser, (2007) Functional Tat transport of unstructured, small, hydrophilic proteins. ***The journal of biological chemistry,*** **282**: 33257-33264.

Rocco, M. A., D. Waraho-Zhmayev & M. P. DeLisa, (2012) Twin-arginine translocase mutations that suppress folding quality control and permit export of misfolded substrate proteins. ***Proceedings of the National Academy of Sciences of the United States of America,*** **109**: 13392-13397.

Rodrigue, A., A. Chanal, K. Beck, M. Muller & L. F. Wu, (1999) Co-translocation of a periplasmic enzyme complex by a hitchhiker mechanism through the bacterial tat pathway. ***The journal of biological chemistry,*** **274**: 13223-13228.

Rodriguez, F., S. L. Rouse, C. E. Tait, J. Harmer, A. De Riso, C. R. Timmel, M. S. Sansom, B. C. Berks & J. R. Schnell, (2013) Structural model for the protein-translocating element of the twin-arginine transport system. ***Proceedings of***

the National Academy of Sciences of the United States of America, **110**: E1092-1101.

Rollauer, S. E., M. J. Tarry, J. E. Graham, M. Jaaskelainen, F. Jager, S. Johnson, M. Krehenbrink, S. M. Liu, M. J. Lukey, J. Marcoux, M. A. McDowell, F. Rodriguez, P. Roversi, P. J. Stansfeld, C. V. Robinson, M. S. Sansom, T. Palmer, M. Hogbom, B. C. Berks & S. M. Lea, (2012) Structure of the TatC core of the twin-arginine protein transport system. ***Nature,*** **492**: 210-214.

Rose, P., J. Frobel, P. L. Graumann & M. Muller, (2013) Substrate-dependent assembly of the Tat translocase as observed in live *Escherichia coli* cells. ***PLoS ONE,*** **8**: e69488.

Sachelaru, I., N. A. Petriman, R. Kudva, P. Kuhn, T. Welte, B. Knapp, F. Drepper, B. Warscheid & H. G. Koch, (2015) YidC occupies the lateral gate of the SecYEG translocon and is sequentially displaced by a nascent membrane protein. ***The journal of biological chemistry,*** **290**: 14492.

Saint-Joanis, B., C. Demangel, M. Jackson, P. Brodin, L. Marsollier, H. Boshoff & S. T. Cole, (2006) Inactivation of Rv2525c, a substrate of the twin arginine translocation (Tat) system of *Mycobacterium tuberculosis*, increases beta-lactam susceptibility and virulence. ***Journal of bacteriology,*** **188**: 6669-6679.

Samuelson, J. C., M. Chen, F. Jiang, I. Moller, M. Wiedmann, A. Kuhn, G. J. Phillips & R. E. Dalbey, (2000) YidC mediates membrane protein insertion in bacteria. ***Nature,*** **406**: 637-641.

Sargent, F., E. G. Bogsch, N. R. Stanley, M. Wexler, C. Robinson, B. C. Berks & T. Palmer, (1998) Overlapping functions of components of a bacterial Sec-independent protein export pathway. ***The EMBO journal,*** **17**: 3640-3650.

Sargent, F., U. Gohlke, E. De Leeuw, N. R. Stanley, T. Palmer, H. R. Saibil & B. C. Berks, (2001) Purified components of the *Escherichia coli* Tat protein transport system form a double-layered ring structure. ***European journal of biochemistry / FEBS,*** **268**: 3361-3367.

Sargent, F., N. R. Stanley, B. C. Berks & T. Palmer, (1999) Sec-independent protein translocation in *Escherichia coli*. A distinct and pivotal role for the TatB protein. ***The journal of biological chemistry,*** **274**: 36073-36082.

Schagger, H. & K. Pfeiffer, (2000) Supercomplexes in the respiratory chains of yeast and mammalian mitochondria. ***EMBO Journal,*** **19**: 1777-1783.

Schiebel, E., A. J. Driessen, F. U. Hartl & W. Wickner, (1991) Delta mu H+ and ATP function at different steps of the catalytic cycle of preprotein translocase. ***Cell,*** **64**: 927-939.

Schulze, R. J., J. Komar, M. Botte, W. J. Allen, S. Whitehouse, V. A. Gold, A. N. J. A. Lycklama, K. Huard, I. Berger, C. Schaffitzel & I. Collinson, (2014) Membrane protein insertion and proton-motive-force-dependent secretion through the bacterial holo-translocon SecYEG-SecDF-YajC-YidC. ***Proceedings of the National Academy of Sciences of the United States of America,*** **111**: 4844-4849.

Scotti, P. A., M. L. Urbanus, J. Brunner, J. W. de Gier, G. von Heijne, C. van der Does, A. J. Driessen, B. Oudega & J. Luirink, (2000) YidC, the *Escherichia coli* homologue of mitochondrial Oxa1p, is a component of the Sec translocase. ***EMBO Journal,*** **19**: 542-549.

Settles, A. M., A. Yonetani, A. Baron, D. R. Bush, K. Cline & R. Martienssen, (1997) Sec-independent protein translocation by the maize Hcf106 protein. ***Science,*** **278**: 1467-1470.

Sharma, V., A. Arockiasamy, D. R. Ronning, C. G. Savva, A. Holzenburg, M. Braunstein, W. R. Jacobs, Jr. & J. C. Sacchettini, (2003) Crystal structure of *Mycobacterium tuberculosis* SecA, a preprotein translocating ATPase. ***Proceedings of the National Academy of Sciences of the United States of America,*** **100**: 2243-2248.

Sianidis, G., S. Karamanou, E. Vrontou, K. Boulias, K. Repanas, N. Kyrpides, A. S. Politou & A. Economou, (2001) Cross-talk between catalytic and regulatory elements in a DEAD motor domain is essential for SecA function. ***EMBO Journal,*** **20**: 961-970.

Stanley, N. R., T. Palmer & B. C. Berks, (2000) The twin arginine consensus motif of Tat signal peptides is involved in Sec-independent protein targeting in *Escherichia coli*. ***The journal of biological chemistry,*** **275**: 11591-11596.

Stanley, N. R., F. Sargent, G. Buchanan, J. Shi, V. Stewart, T. Palmer & B. C. Berks, (2002) Behaviour of topological marker proteins targeted to the Tat protein transport pathway. ***Molecular microbiology,*** **43**: 1005-1021.

Strauch, E. M. & G. Georgiou, (2007) *Escherichia coli tatC* mutations that suppress defective twin-arginine transporter signal peptides. ***The journal of molecular biology,*** **374**: 283-291.

Tani, K., K. Shiozuka, H. Tokuda & S. Mizushima, (1989) *In vitro* analysis of the process of translocation of OmpA across the *Escherichia coli* cytoplasmic membrane. A translocation intermediate accumulates transiently in the absence of the proton motive force. ***The journal of biological chemistry,* 264**: 18582-18588.

Tarry, M. J., E. Schafer, S. Chen, G. Buchanan, N. P. Greene, S. M. Lea, T. Palmer, H. R. Saibil & B. C. Berks, (2009) Structural analysis of substrate binding by the TatBC component of the twin-arginine protein transport system. ***Proceedings of the National Academy of Sciences of the United States of America,* 106**: 13284-13289.

Thomas, J. R. & A. Bolhuis, (2006) The *tatC* gene cluster is essential for viability in halophilic archaea. ***FEMS microbiology letters,* 256**: 44-49.

Thony-Meyer, L. & P. Kunzler, (1997) Translocation to the periplasm and signal sequence cleavage of preapocytochrome c depend on sec and lep, but not on the ccm gene products. ***European journal of biochemistry / FEBS,* 246**: 794-799.

Tottey, S., K. J. Waldron, S. J. Firbank, B. Reale, C. Bessant, K. Sato, T. R. Cheek, J. Gray, M. J. Banfield, C. Dennison & N. J. Robinson, (2008) Protein-folding location can regulate manganese-binding versus copper- or zinc-binding. ***Nature,* 455**: 1138-1142.

Urbanus, M. L., P. A. Scotti, L. Froderberg, A. Saaf, J. W. de Gier, J. Brunner, J. C. Samuelson, R. E. Dalbey, B. Oudega & J. Luirink, (2001) Sec-dependent membrane protein insertion: sequential interaction of nascent FtsQ with SecY and YidC. ***EMBO Reports,* 2**: 524-529.

van Dalen, A., A. Killian & B. de Kruijff, (1999) Delta psi stimulates membrane translocation of the C-terminal part of a signal sequence. ***The journal of biological chemistry,* 274**: 19913-19918.

Van den Berg, B., W. M. Clemons, Jr., I. Collinson, Y. Modis, E. Hartmann, S. C. Harrison & T. A. Rapoport, (2004) X-ray structure of a protein-conducting channel. ***Nature,* 427**: 36-44.

Vollmer, W. & J. V. Holtje, (2004) The architecture of the murein (peptidoglycan) in gram-negative bacteria: vertical scaffold or horizontal layer(s)? ***Journal of bacteriology,* 186**: 5978-5987.

Weiner, J. H., P. T. Bilous, G. M. Shaw, S. P. Lubitz, L. Frost, G. H. Thomas, J. A. Cole & R. J. Turner, (1998) A novel and ubiquitous system for membrane targeting and secretion of cofactor-containing proteins. ***Cell,* 93**: 93-101.

Wexler, M., F. Sargent, R. L. Jack, N. R. Stanley, E. G. Bogsch, C. Robinson, B. C. Berks & T. Palmer, (2000) TatD is a cytoplasmic protein with DNase activity. No requirement for TatD family proteins in sec-independent protein export. ***The journal of biological chemistry,* 275**: 16717-16722.

Whitaker, N., U. K. Bageshwar & S. M. Musser, (2012) Kinetics of precursor interactions with the bacterial Tat translocase detected by real-time FRET. ***The Journal of biological chemistry***, **14**:11252-60..

White, G. F., S. M. Schermann, J. Bradley, A. Roberts, N. P. Greene, B. C. Berks & A. J. Thomson, (2010) Subunit organization in the TatA complex of the twin arginine protein translocase: a site-directed EPR spin labelling study. ***The journal of biological chemistry,* 285**: 2294-2301.

Widdick, D. A., R. T. Eijlander, J. M. van Dijl, O. P. Kuipers & T. Palmer, (2008) A facile reporter system for the experimental identification of twin-arginine translocation (Tat) signal peptides from all kingdoms of life. ***Journal of molecular biology,* 375**: 595-603.

Winstone, T. L., M. L. Workentine, K. J. Sarfo, A. J. Binding, B. D. Haslam & R. J. Turner, (2006) Physical nature of signal peptide binding to DmsD. ***Archives of biochemistry and biophysics,* 455**: 89-97.

Xu, Z., J. D. Knafels & K. Yoshino, (2000) Crystal structure of the bacterial protein export chaperone secB. ***Nature Structural Biology,* 7**: 1172-1177.

Yahr, T. L. & W. T. Wickner, (2001) Functional reconstitution of bacterial Tat translocation in vitro. ***The EMBO journal,* 20**: 2472-2479.

Yen, M. R., Y. H. Tseng, E. H. Nguyen, L. F. Wu & M. H. Saier, Jr., (2002) Sequence and phylogenetic analyses of the twin-arginine targeting (Tat) protein export system. ***Archives of microbiology,* 177**: 441-450.

Zhang, Y., L. Wang, Y. Hu & C. Jin, (2014) Solution structure of the TatB component of the twin-arginine translocation system. ***Biochimica et biophysica acta,* 1838**: 1881-1888.

Zhou, J. & Z. Xu, (2003) Structural determinants of SecB recognition by SecA in bacterial protein translocation. ***Nature Structural Biology,* 10**: 942-947.

Zimmer, J., W. Li & T. A. Rapoport, (2006) A novel dimer interface and conformational changes revealed by an X-ray structure of B. subtilis SecA. ***The journal of molecular biology,*** **364**: 259-265.

Zimmer, J., Y. Nam & T. A. Rapoport, (2008) Structure of a complex of the ATPase SecA and the protein-translocation channel. ***Nature,*** **455**: 936-943.

Supplementary Material

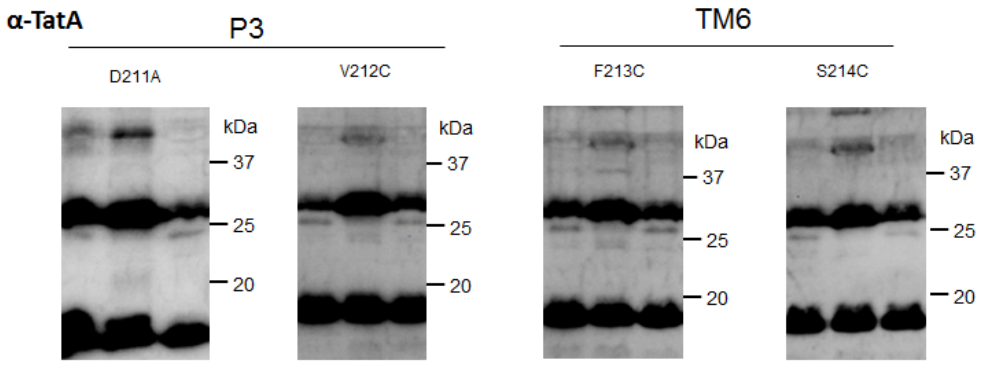

Figure S1- shows Figure 4.5D anti-TatA Western blots with TatA monomer

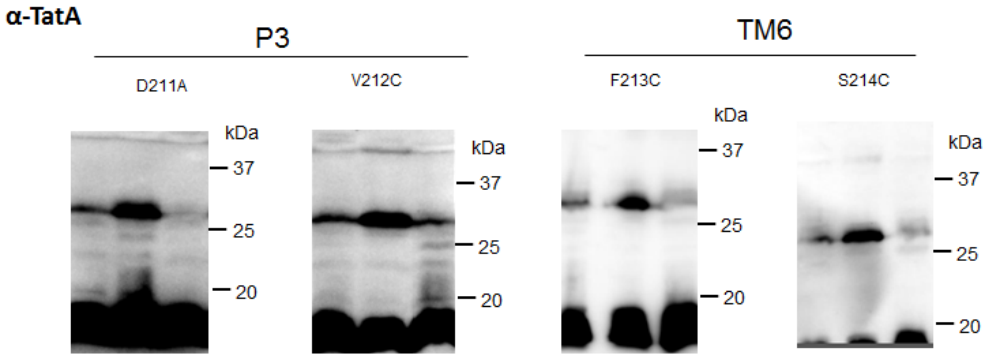

Figure S2- shows Figure 4.6D anti-TatA Western blots with TatA monomer

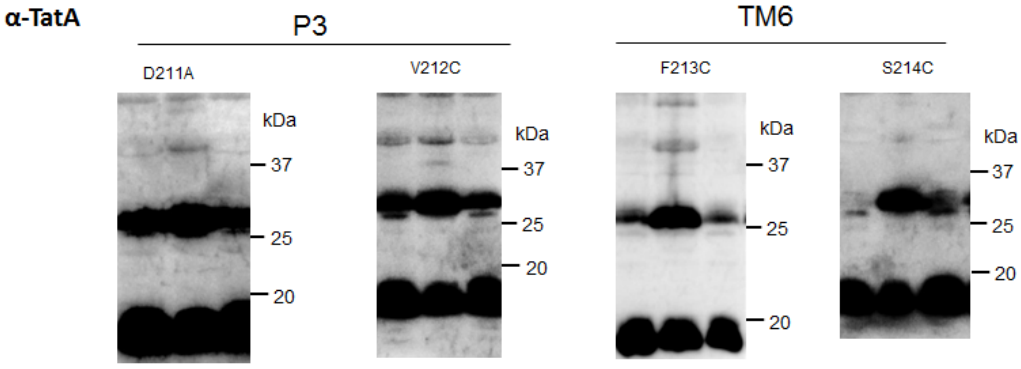

Figure S3- shows Figure 4.7D anti-TatA Western blots with TatA monomer

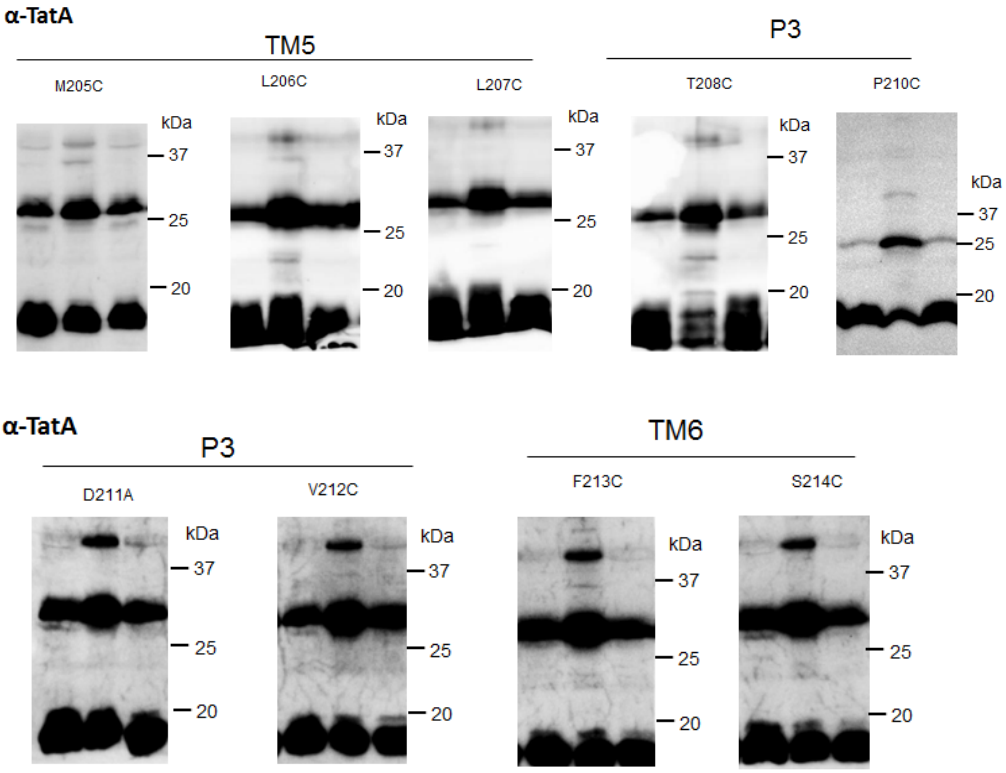

Figure S4- shows Figure 5.2 anti-TatA Western blots with TatA monomer

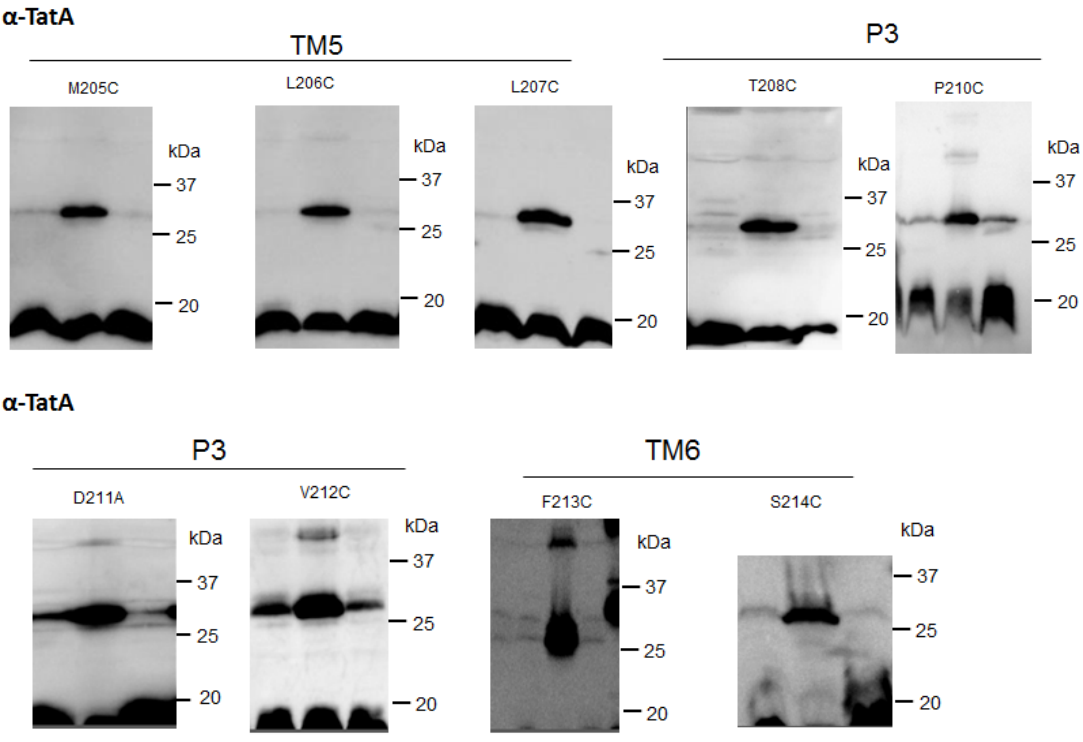

Figure S5- shows Figure 5.4 anti-TatA Western blots with TatA monomer

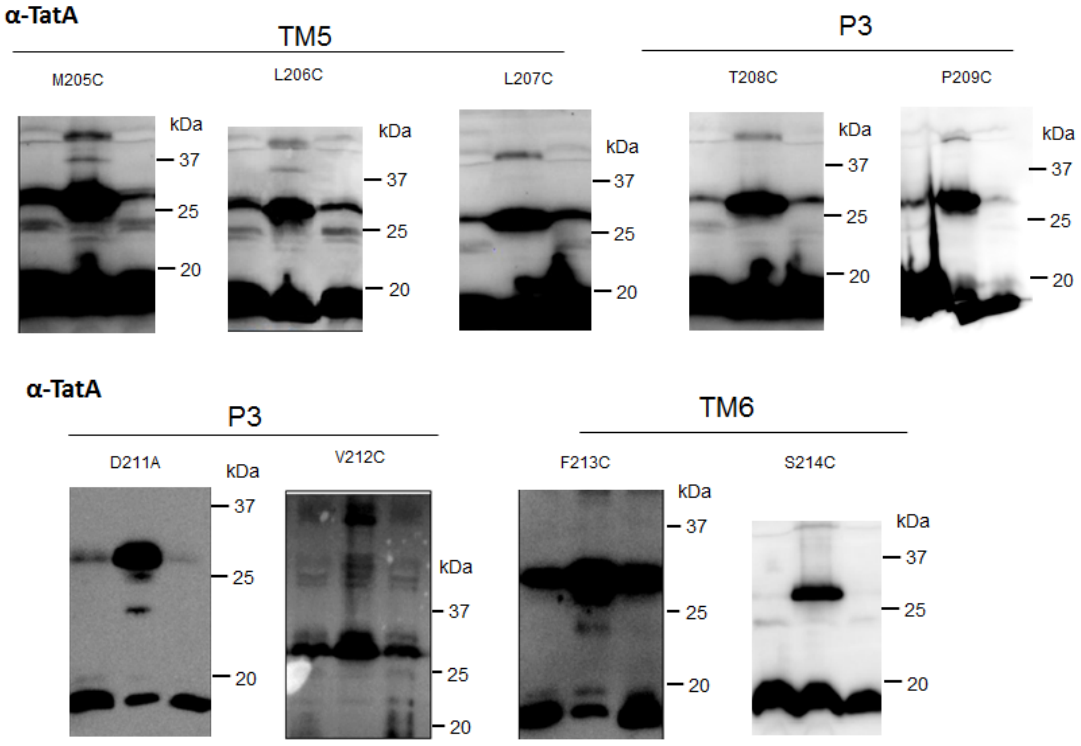

Figure S6-shows Figure 5.6 anti-TatA Western blots with TatA monomer